Fish growth, temperature, and life history: applying theory to improve fisheries research and management

A Dissertation
SUBMITTED TO THE FACULTY OF THE
UNIVERSITY OF MINNESOTA
BY

Andrew Edgar Honsey

IN PARTIAL FULFILLMENT OF THE REQUIREMENTS
FOR THE DEGREE OF
DOCTOR OF PHILOSOPHY

Advised by Paul A. Venturelli

December 2018

Acknowledgements

If there's one thing that I've learned during my time as a Ph.D. student, it's that I am not a self-sufficient scientist. I realize each and every day that I don't know it all and that I can't do it alone. I am greatly indebted to the following people, without whose help I would have been a rudderless ship.

First, I would like to thank my advisor, Paul Venturelli. When I was searching for a Ph.D. position, it was important to me to find an advisor who not only would push me to succeed in fish science, but who also cared about me and my well-being. I consider myself very lucky to have found someone who did just that. Thank you, Paul, for your instruction, advice, and guidance. Thank you for your support, encouragement, and understanding. Thank you for making time for me, even when you didn't have it. Thank you for the dad jokes. Most of all, thank you for being a good guy who respects and cares about his students. And hey, if this whole fish science thing doesn't work out, we've always got *Mortality Landscape* to fall back on.

I am also indebted to the members of my committee: Drs. Jacques Finlay, James Cotner, Przemek Bajer, and Gretchen Hansen. Thank you all for lending your expertise, showing your support, and sacrificing your time to help me throughout the past few years. Jacques – thank you for helping me navigate the EEB waters, challenging me with your questions, reminding me that there's more to aquatic science than just fish in lakes (there's also P in streams, and maybe some other stuff), and going out of your way to ease my teaching burden in my final semester. Jim – thank you for convincing me that stoichiometry is pretty cool, showing your support and excitement whenever I got some

interesting results or had a paper accepted, and getting fired up about Buckeye football with me. Oh, and thanks for the beer! Przemek – thank you for sharing your thoughts and advice on my work (especially related to bioenergetics modeling) and for encouraging me when I felt lost in the weeds. Gretchen – I can't thank you enough for agreeing to serve on my defense committee on such late notice. I owe you one, and I'm excited to be a founding member of the #hansenlab!

I would like to thank the coauthors on manuscripts in this dissertation: David Staples, Nigel Lester, Andrew Rypel, Robert Allman, and Gary Fitzhugh. Your help was absolutely instrumental to this work, and your input has greatly improved its quality. A special thank you to Nigel Lester, whose research and ideas provided the foundation for most of the work in this volume. Thank you, Nigel, for welcoming me into your home, organizing an entire workshop around my ideas when I was only a first-year graduate student, and showing me that you can put family first and still be successful in science.

I thank the members of the Venturelli Lab (Grace, Jason, Megan, Tim, Leslie, Erin, Maxime, Kirsten, Jit, Natnael, and Manu) for their valuable input, constant encouragement, and friendship. I also thank the members of the EEB graduate program (particularly the 2014 cohort), my former office mates in the 4-1-1, and many members of the EEB community for their support and guidance.

I am thankful to all who have helped along the way by providing ideas, insight, encouragement, and data: Cindy Chu, Henrique Giacomini, Brian Shuter, Richard Bruce, Daniel Nadeau, Sandra Orsatti, Mike Palmer, Beth Matta, David Deslauriers, Dan Dembkowski, Maggie Gorsuch, Alex Latzka, Jordan Read, and many others.

I would also like to thank my family and friends for their love and support. I am blessed to have all of you in my life. I am particularly grateful to my parents, Phil and Cindy, who encouraged me to become the first Honsey with a Ph.D.

Most importantly, I would like to thank my beautiful wife, Diana. I truly could not have done this without your undying love, support, and friendship. Thank you for sharing your life with me, picking me up when I'm feeling down, and challenging me to be the best version of myself. I can't imagine life without you, and I don't want to. Thank you for everything.

Finally, to my little Tadpole: I hope that we can read this together someday and talk about what your father was up to while you were busy gestating. It's a pretty dull read, but perhaps you'll indulge me. I love you, and I can't wait to meet you. See you soon, buddy.

Abstract

Ectotherm growth is inextricably linked to both temperature and other aspects of life history. In this dissertation, I leverage life history and bioenergetics theory to (1) justify and standardize the use of metrics that adequately describe the effect of temperature on ectotherm growth, and (2) develop and apply methods that leverage the links between ectotherm growth and life history to extract life history information from growth data. I focus on fishes as example ectotherms. Fish growth is driven by the amount of thermal energy accrued over time (i.e., the thermal integral). Accordingly, numerous studies have found strong linear relationships between fish growth and degree-days (DD), a thermal integral metric. Despite these findings, fish science lags behind other fields in the widespread adoption of DD, likely due to (1) a lack of theoretically-sound support for the observed linear relationships between fish growth and DD, and (2) insufficient justification for using DD derived from air temperatures in place of DD derived from water temperatures in fish science. Moreover, there is limited guidance for selecting the base temperature for growth (T_0), an important parameter for calculating DD, among fishes and scenarios. In Chapter 2, I combine empirical data and simulation modeling to provide bioenergetic and limnological foundations for the linear relationship between fish growth and DD, and I show that air-based DD can serve as an accurate proxy for water-based DD for describing fish growth. In Chapter 3, I provide estimates of T_0 for 82 fish species using approaches that are rooted in fish biology. Together, these analyses will help to justify and standardize the use of DD in fish science. Fish growth is also strongly correlated with other aspects of life history (e.g., maturity, mortality). Recent advances in

life history theory have led to the development of biphasic growth models that allow for the estimation of age-at-maturity, reproductive investment, and other life history traits from growth data. However, these models can be difficult to fit in the absence of maturity data. In Chapter 4, I develop a statistical framework for fitting biphasic growth models using only length-at-age data. I show that this approach can provide accurate estimates of age-at-maturity and other life history traits, and I evaluate the performance of the method across various species and data quality scenarios. In Chapter 5, I use a similar approach to investigate shifts in life history traits in an ecologically and economically important fish stock (Gulf of Mexico red snapper *Lutjanus campechanus*) from 1941-2005. This growth-based approach allows for the estimation of life history traits deeper into the past than would have been possible using traditional approaches and provides a more holistic understanding of how red snapper life histories have shifted in the face of fishing pressure and other stressors. Taken together, this work has the potential to improve fisheries research, promote sustainable fisheries management, increase global food security, and encourage similar advances in other fields.

Supplementary Files

Supplementary Data File 1 describes the fish length-at-age dataset used for the empirical growth analysis in Chapter 3. Supplementary Data File 2 describes the bioenergetics model parameters and settings used for the 10 ^{o}C rule approach, also in Chapter 3.

Table of Contents

List of Tables

Chapter 2

Chapter 3

Chapter 4

Appendix 1

Appendix 2

Appendix 3

Appendix 4

List of Figures

Chapter 2

Chapter 4

Chapter 5

Appendix 1

Appendix 3

Appendix 4

Chapter 1

General introduction: fish growth, temperature, and life history

Understanding individual growth is a central focus of modern biology and is key to a wide range of biological inquiry. Growth influences population dynamics (Lorenzen and Enberg 2002) and is strongly linked to evolutionary fitness (e.g., growth correlates with maturity, reproduction, and mortality; Stearns 1992, Bernardo 1993, Lester et al. 2004). In addition, growth and other aspects of life history often shift in response to environmental drivers (e.g., temperature) and human activities (e.g., fishing; Hutchings and Fraser 2008, Heino et al. 2015, Dunlop et al. 2018). These shifts can complicate management (Heino et al. 2013), reduce yields from harvested populations (Heino 1998), and increase the likelihood of population crashes (Anderson et al. 2008). Detecting and accounting for these shifts requires a thorough understanding of growth and is crucial for sustainable management (Hilborn and Walters 1992), particularly in the face of stressors such as climate change (IPCC 2014). Unfortunately, conventional methods for understanding growth are often limited both in their representation of important processes (e.g., the effect of temperature on ectotherm growth) and their ability to provide information on growth-correlated traits (e.g., maturity, mortality).

Ectotherm growth and other physiological processes are driven by ambient temperature (Hazel and Prosser 1974, Atkinson 1994, Diana 2003). More specifically, ectotherm metabolic processes and phenologies are closely linked with the amount of

thermal energy that is accrued over a given time period (i.e., the thermal integral; Charnov and Gillooly 2003, Neuheimer and Taggart 2007). The integrated nature of the effects of thermal energy on ectotherm metabolic processes also holds for many plant species; as a result, plant biologists have used thermal integrals to describe plant physiological processes for centuries (Réamur 1735). Some ectotherm-centered branches of biology (e.g., entomology) have also used thermal integrals for many years (Seamster 1950, Allen 1976). In contrast, fish science lags behind in the widespread adoption of thermal integrals despite the fact that they consistently outperform commonly-used temperature metrics (e.g., mean temperatures over a given time period) and calendar time in describing fish growth and other physiological processes (Neuheimer and Taggart 2007, Chezik et al. 2014a, 2014b). There are a number of potential reasons for this lag. For example, high-resolution water temperature data are relatively scarce, and, although air temperatures may serve as an accurate proxy for water temperatures in many cases, sufficient justification for using thermal integrals derived from air temperatures to describe fish growth is lacking. In addition, the appropriate value for the base temperature for growth, an important parameter for thermal integral calculation, is unknown for many fish species. As a result, fish scientists have used a variety of base temperatures to calculate thermal integrals with little or no justification (Chezik et al. 2014b), which can complicate inference and lead to erroneous conclusions (e.g., the apparent evolution of countergradient growth; Levins 1969, Conover and Present 1990). Among the most pressing challenges that remain are to (1) explore the validity of using air temperatures to calculate thermal integrals in fish science and (2) create an objective

and theoretically-sound framework for estimating base temperatures for growth for various fishes.

The lifetime growth of ectotherms is not only coupled with temperature, but it is also strongly correlated with other aspects of life history. For example, increases in growth rates typically lead to earlier maturity, increased investment in reproduction, and increased mortality rates (Stearns 1992). Moreover, growth rates often change throughout life based on life history. For example, although ectotherms grow indeterminately (i.e., they continue growing throughout life), their growth typically slows after maturity due to energetic investment in reproduction (Kozlowski 1996). Unfortunately, traditional approaches for modeling ectotherm growth (e.g., the von Bertalanffy growth model; von Bertalanffy 1938) smooth over these changes by describing lifetime growth as a single curve. In response to this issue, researchers have proposed growth models that account for changes in growth throughout life and include parameters that correspond with life history traits (e.g., age-at-maturity; Lester et al. 2004, Quince et al. 2008, Mollet et al. 2010, Boukal et al. 2014). Regrettably, the application of these models is limited due to their strict requirements for data on a variety of life history traits (but see Quince et al. 2008b, Mollet et al. 2013, Lester et al. 2014, Uusi-Heikkilä et al. 2015, Chavarie et al. 2016). However, because growth is correlated with many other life history traits, it should be possible to estimate multiple life history traits from growth data. The ability to do so accurately would provide a wealth of relevant knowledge from common growth data and allow us to address important questions related to life history plasticity and evolution.

My overarching goal is to improve our understanding of ectotherm growth and life history through the development and application of methods that leverage the inextricable links between temperature, growth, and life history. My first broad aim focuses on temperature and fish growth. In Chapter 2, I use theoretically-sound and well-supported models of both fish bioenergetics and annual lacustrine surface water temperature cycles to provide physiological and limnological foundations for using thermal integrals derived from air temperatures to describe fish growth. Specifically, I show that thermal integrals derived from both air and water temperature data are roughly linearly related to fish growth, highlighting their utility as metrics for describing fish growth and physiology. In Chapter 3, I meet the need for guidance in calculating thermal integrals by providing estimates of the base temperature for growth for 82 fish species using approaches that are rooted in fish biology. My results show that the appropriate value for the base temperature for growth varies across species and life stages and can also differ for calculating air- versus water-based thermal integrals within species. My second broad aim centers on estimating life history traits from fish growth data. In Chapter 4, I develop a statistical framework for estimating age-at-maturity and other life history traits solely from growth data. I show that this method provides accurate estimates of age-at-maturity in the absence of maturity data for fishes and other ectotherms. In addition, I use simulation modeling to explore the ability of the method to recover 'true' life history trait values across various data quality scenarios, thereby providing guidance to users. In Chapter 5, I use an approach similar to the one developed in Chapter 4 to track changes in life history traits over time for Gulf of Mexico red snapper *Lutjanus*

campechanus, an economically important and historically overexploited fish stock. By leveraging growth data, I provide otherwise unattainable estimates of life history traits for red snapper during the expansion of the fishery in the 1940s-1960s. Moreover, I show that red snapper life histories shifted dramatically toward a faster regime (i.e., faster growth, earlier maturity) in the mid-20th century, likely in response to fishing pressure.

Chapter 2 has been accepted for publication in the Canadian Journal of Fisheries and Aquatic Sciences and is currently in press (dx.doi.org/10.1139/cjfas-2018-0051). As such, Chapter 2 is referred to as Honsey et al. (in press) throughout this document. The publication of this chapter by the University of Minnesota is granted by the Canadian Journal of Fisheries and Aquatic Sciences Author Rights, which state the following: "Authors may reuse all or part of their manuscript in other works created by them for non-commercial purposes, provided the original publication in an NRC Research Press journal is acknowledged through a note or citation." Chapter 4 is published in Ecological Applications (https://doi.org/10.1002/eap.1421) and is referred to as Honsey et al. (2017) herein. A document granting permission to publish this material from John Wiley and Sons has been submitted to the University of Minnesota Graduate Student Services and Progress office alongside this dissertation. Chapters 3 and 5 are currently in preparation for publication in peer-reviewed scientific journals. Co-authors on these manuscripts are as follows: Chapter 2, Paul A.Venturelli and Nigel P. Lester; Chapter 3, Andrew L. Rypel and Paul A. Venturelli; Chapter 4, David F. Staples and Paul A. Venturelli; and Chapter 5, Robert J. Allman, Gary R. Fitzhugh, and Paul A. Venturelli. I use plural pronouns (i.e.,

"we" and "our" instead of "I" and "my") in Chapters 2-5 to reflect these authors' contributions to the work.

Chapter 2

Bioenergetic and limnological foundations for using degree-days derived from air temperatures to describe fish growth

Synopsis

Degree-days (DD) are an effective metric for quantifying the thermal opportunity for ectotherm growth. There is strong empirical evidence to suggest that DD are useful for describing fish growth, and that immature growth increases linearly with DD. However, fish ecology lags behind other disciplines in the widespread adoption of DD. We provide (1) a foundation for the observed linear relationship between immature fish growth and DD, and (2) justification for using DD derived from air temperatures as a proxy for DD derived from water temperatures in fish science. We use bioenergetics models and both simulated and empirical water temperatures to show that immature annual and interannual fish growth are approximately linear with water DD. We then use simulated and empirical data to show that air and surface water temperatures are often highly correlated, and that immature fish growth is also approximately linear with air DD. By connecting the dots among air temperature, water temperature, and fish growth, we lay the foundation for wider adoption of DD in fish science.

2.1 Introduction

There is an obvious link between ambient temperatures and physiological processes in ectotherms (Hazel and Prosser 1974; Atkinson 1994; van der Have and de Jong 1996). Less obvious is how one should measure temperature to best understand its influence on ectotherm growth and other metabolic processes. Instantaneous metrics (e.g., mean temperatures over a given time period; Pauly 1980; Doubleday *et al.* 2015) are often used to explain ectotherm growth. These metrics are easy to calculate but may not adequately index the effect of temperature on ectotherm growth and metabolism (Neuheimer and Taggart 2007).

Degree-days (DD) are a summation of the metabolically-relevant thermal energy that is experienced by an individual over time. As such, DD are a useful index of the thermal scope for ectotherm growth (Chezik et al. 2014a). Other fields (e.g., agronomy, entomology) have used DD extensively for decades to centuries (Neuheimer and Taggart 2007), and DD have been shown to outperform calendar time in describing ectotherm growth (e.g., Colby and Nepszy 1981). Moreover, because DD integrate time and temperature, they provide a physiologically-valid understanding of how growth responds to temperature that can be particularly useful when comparing growth rates among populations (e.g., for studies of countergradient variation in growth; Chezik et al. 2014b; Snover et al. 2015).

The application of DD in fish science has become increasingly common, as has the use of DD derived from air temperatures as a surrogate for DD calculated from water temperatures (e.g., Fig. 1.1 in Chezik 2013). In particular, DD have been shown to be

useful for describing fish growth, with multiple empirical studies finding strong linear relationships between DD and immature fish growth (e.g., Neuheimer and Taggart 2007; Venturelli et al. 2010; Chezik et al. 2014a). Although fish culturists have used DD for many decades (e.g., Wallich 1901; Soderberg 1992; Dumas et al. 2010), other fish sciences, such as fish ecology, have yet to adopt DD in a widespread manner. Likely reasons for this lack of widespread adoption include the relative scarcity of high-resolution water temperature data compared to air temperature data, and insufficient evidence to suggest that DD calculated from air temperatures can serve as an accurate proxy for DD derived from water temperatures. Moreover, researchers who are familiar with conventional, nonlinear fish growth models (e.g., the von Bertalanffy model; von Bertalanffy 1938; Beverton and Holt 1957) may not be convinced by the evidence for linear relationships between immature fish growth and DD (e.g., Malzahn et al. 2003; Neuheimer and Taggart 2007; Chezik et al. 2014a).

Our objectives were to provide (1) a bioenergetic foundation for the linear relationship between immature fish growth and DD that has been found in multiple empirical studies, and (2) justification for using DD derived from air temperatures as a proxy for DD derived from water temperatures. To accomplish these objectives, we review existing knowledge and use simulated and empirical data to connect the dots among air temperature, water temperature, and fish growth. First, we use bioenergetics models to demonstrate the effect of water temperature on fish growth at daily, annual, and interannual time scales. We then examine the relationships between air and surface water temperatures, and we assess whether air-based DD can serve as an accurate proxy

for water-based DD. Finally, we compare the performance of air- and water-based DD in describing fish growth, and we discuss the limits of using air-based DD to describe growth (e.g., for coldwater fishes in thermally stratified systems). By providing a theoretically-sound and empirically-supported basis for the expanded and appropriate use of DD, our analyses promote a more thorough understanding of the growth and physiology of fishes and other aquatic organisms.

2.2 Water temperature and fish growth

In this section, we use bioenergetics models to demonstrate the effects of water temperature on fish growth (Kitchell et al. 1977; Jobling 1995; Hanson et al. 1997). Bioenergetics models are based on an energy balance equation in which the potential for growth is governed by energy acquired via consumption minus metabolism (e.g., respiration, specific dynamic action) and waste. The functions that describe these processes often depend on water temperature. As a result, growth is also temperature-dependent, and the nature of the growth-temperature relationship is shaped by species-specific parameters (e.g., optimum temperature for consumption, upper lethal water temperature; Hanson et al. 1997).

We used bioenergetics models to simulate juvenile growth for three fishes: yellow perch *Perca flavescens*, brown bullhead *Ameiurus nebulosus*, and tiger muskellunge (northern pike *Esox lucius* X muskellunge *Esox masquinongy*). These models encompass diversity in two key areas. First, they use different combinations of model functions (i.e., equations) for the various model processes (Table 2.1). For instance, the brown bullhead

model uses a respiration function that is exponential with temperature, whereas the respiration function used in the other two models accounts for decreased respiration rates at high temperatures. Therefore, any similarities in model results are unlikely to be driven by similar functional response assumptions across model processes. Second, the thermal regimes differ for each model species, with the three models encompassing a fair amount of thermal diversity for cool- and warmwater species (thermal optima for consumption ranging from 24-29 ^{o}C). Parameters, equations, and sources for these models are given in Table 2.1. We excluded models for coldwater species because our analytical approaches assumed that the simulated fish experienced epilimnetic temperatures year-round (see below). As such, we chose models for cool- and warmwater fishes so that this assumption would likely not be meaningfully violated.

i) *Daily growth*

We begin by showing how daily growth in length varies with water temperature across levels of prey consumption and activity (a multiplier on respiration, with 1 = resting metabolism). We did this to establish a foundation for how growth responds to these factors over short time periods, which is an important first step in understanding how growth relates to DD over longer time periods. We set initial sizes to 100 mm for yellow perch and brown bullhead, and 150 mm for tiger muskellunge. We used geometric mean parameters for the length-weight relationship from FishBase (Froese and Pauly 2016) for length-weight conversions. We set the energy density of oxygen to 13556 $J \cdot g^{-1}$ here and

throughout (Elliott and Davison 1975). We conducted these and all additional calculations and simulations in R version 3.4.1 (R Core Team 2017).

Our bioenergetics simulations produced typical results showing the non-linear relationship between daily growth in length and temperature (Fig. 2.1). This relationship is positive for most water temperatures and approximately linear across a midrange of temperatures (e.g., 10-20 ^{o}C). The relationship appears to become more linear when either activity is higher than resting metabolism or consumption is below satiation (Fig. 2.1a,b). However, if we consider growth as a proportion of maximum growth for a given activity or consumption level (Fig. 2.1c,d), we see that the relationship is nonlinear for all scenarios examined, and among the most noticeable effects of increased activity or reduced consumption is a decrease in the optimum temperature for growth (see Kitchell et al. 1977). Fig. 2.1 shows results for the yellow perch bioenergetics model; results for the other two models are shown in Appendix 1, Figs. A1.1 and A1.2.

ii) *Annual growth*

In fish science and other disciplines, samples are often collected at a relatively coarse temporal resolution (e.g., once per year), and individual sizes across ages and/or sampling events are compared to approximate growth patterns (Lorenzen 2016). Therefore, we were primarily interested in examining the cumulative effect of water temperature on growth at annual and interannual time scales.

For this portion of the analysis, our goal was to examine the effect of varying temperature scenarios on the relationship between annual immature fish growth and DD

derived from water temperatures (WDD). We first simulated annual surface water temperature cycles using the Shuter water temperature model and empirical predictors for maximum daily surface water temperature (T_{max}) and the duration of the ice-free season (DR; Shuter et al. 1983):

$$T_{max} = 23.5 \cdot \bar{Z}^{-0.108} e^{0.0437 \cdot \overline{AT} - 0.002 \cdot \overline{AT}^2}$$

$$DR = 149 \cdot \bar{Z}^{0.073} e^{0.06 \cdot \overline{AT}}$$

$$T_t = 4 + (T_{max} - 4) \cdot \sin(\pi \cdot \frac{t - (365 - DR)}{DR})$$

where $\bar{Z}$ is mean lake depth (or mean thermocline depth for stratified systems), $\overline{AT}$ is mean annual air temperature, and T_t is mean surface water temperature on day t. We used simulated rather than empirical water temperatures for this portion of the analysis so that we could encompass a broad range of climatic scenarios in a relatively straightforward and analytically robust manner. We assumed that liquid water temperature did not fall below 4 ºC and that the year was 365 days long. Using these equations, the annual water temperature cycle can be defined as a function of $\bar{Z}$ and $\overline{AT}$. We fixed $\bar{Z}$ at 8 m for the sake of simplicity and because variation in $\bar{Z}$ generally has a smaller impact than variation in $\overline{AT}$ on the surface water temperature cycle (see Appendix 1, Section A1.1 and Fig. A1.3). We then simulated annual surface water temperature cycles from 0 to 10 ºC $\overline{AT}$ in increments of 0.5 ºC.

We used these simulated daily water temperatures to drive the yellow perch, brown bullhead, and tiger muskellunge bioenergetics models (Table 2.1). We assumed that fish experienced surface water temperatures, which approximate the temperature of the typically well-mixed epilimnion (e.g., Livingstone and Lotter 1998), throughout the

ice-free season. We then summed daily growth in length throughout the ice-free season, assuming that growth during winter was negligible (Pitcher and Macdonald 1973; García-Berthou et al. 2012). We subtracted initial length from final length to determine annual growth. We then compared annual growth to WDD above 5 ºC (WDD_5), calculated as

$$WDD_5 = \sum_{t=1}^{N} T_t - 5\,, \qquad T_t > 5 \tag{1}$$

where N is the number of days (in this case, 365) and T_t is the daily mean surface water temperature on day t. We used 5 ºC as a base temperature because it is highly correlated with the length of the ice-free season (Shuter et al. 1983; Venturelli et al. 2010) and has been used to describe growth in yellow perch and other fishes (e.g., Power and McKinley 1997; Purchase *et al.* 2005; Rennie *et al.* 2010).

We first simulated growth under the 'ideal' bioenergetic scenario in which individuals achieve satiation at resting metabolism. However, these results are unrealistic because empirical data suggest that activity costs are often higher than resting metabolism (e.g., Rowan and Rasmussen 1996). In addition, consumption can be highly variable (e.g., Schaeffer et al. 1999) and is typically estimated at roughly 40-60% of satiation in wild populations (Hartman and Margraf 1992; Petersen and Paukert 2005; Hartman and Cox 2008). To explore the nature of the relationship between WDD_5 and annual growth given reduced consumption and/or increased activity, we repeated the simulations for three additional bioenergetics scenarios: (1) satiation with increased activity (activity multiplier = 3); (2) lower consumption (50% of satiation) with resting metabolism; and (3) lower consumption (85% of satiation) with increased activity

(activity multiplier = 2). Our results show that the relationship between annual growth and WDD_5 is approximately linear for all of these bioenergetic scenarios (all $R^2 \geq 0.99$), with the most substantial change in the relationship among scenarios being a change in the slope of the line (Fig. 2.2).

iii) *Interannual growth*

We have shown that annual fish growth in length is roughly linear with WDD_5 across a variety of scenarios. Here, we test whether interannual immature growth (i.e., length-at-age) is also approximately linear with WDD_5 for many bioenergetic scenarios. We focus on immature growth because the linear approximation of the length-at-age versus DD relationship is typically only valid for growth leading up to maturity (Lester et al. 2004), whereas adult length-at-age is often nonlinear due to investment in reproduction and other factors (e.g., increasing activity costs with body size; Ware 1978; Kozlowski 1996; Andersen and Beyer 2015).

We included empirical water temperature in this portion of the analysis by retrieving five years of publicly-available daily mean water temperature data (1 m depth) from two lakes: Sparkling Lake, WI, USA (2000, 2002-2005) and Lake Lacawac, PA, USA (2010-2014; Fig. 2.3). The Sparkling Lake data were retrieved from the University of Wisconsin's North Temperate Lakes Long Term Ecological Research network (NTL LTER 1991a). These data were continuous apart from eight gaps (mean $\pm$ SD gap length = 2.875 $\pm$ 3.23 days; 1.3% of total sample size), which we filled using linear interpolation. The Lake Lacawac data were retrieved from an electronic database

maintained by Lehigh University (http://www.lehigh.edu/~brh0/pocono_mon/) and were continuous.

We used the empirical water temperature data to drive multi-annual bioenergetics simulations for each of our model species (Table 2.1). We summed growth throughout the ice-free seasons (i.e., when water temperatures at 1 m were > 4 ºC) and defined length-at-age as the length on the last day of each year. We carried out a factorial simulation to determine the effects of varying consumption (10-100% satiation in increments of 5%), activity (1-4 in increments of 0.2), and initial size (yellow perch = 25, 50, and 75 mm; brown bullhead = 50, 100, 150 mm; tiger muskellunge = 100, 150, 200 mm) on interannual growth. We fit a linear model to the length versus WDD_5 relationship and recorded the adjusted R^2 value after each simulation. We focused on R^2 because we were primarily interested in the explanatory power of a metric (WDD_5) in describing interannual fish growth in a linear model framework across a wide range of bioenergetic scenarios; we were not interested in, e.g., the relative performance of a given model, or whether a particular relationship was statistically significant. We disregarded R^2 values for scenarios in which individuals did not grow across all five years (e.g., fish losing weight from one year to the next) because these scenarios would likely result in death. Figure 2.4 shows example results from simulations with consumption set at 40% of satiation and the activity multiplier set at 1.2. We acknowledge that simulating immature growth across five years may be unrealistic because the model species may mature before age 5 (e.g., Trippel 1995; Feiner *et al.* 2015); however, we argue that these simulations are valid given our goal of better understanding how immature growth relates to DD, and

we note that the relationship should be approximately linear leading up to maturity regardless of age-at-maturity.

Our results suggest that immature interannual growth is approximately linear with WDD_5 for most bioenergetic scenarios across species (Fig. 2.5). The brown bullhead and tiger muskellunge models displayed nearly linear ($R^2 \geq 0.90$) growth for all scenarios examined. Simulated growth for the yellow perch model was less linear ($R^2 < 0.90$) in some cases; however, most of these cases occurred when activity was unrealistically high for immature yellow perch (e.g., ACT ≥ 2; Rowan and Rasmussen 1996). The yellow perch model was the most sensitive to initial fish size, with fewer cases of highly linear growth at smaller initial sizes. Importantly, growth was approximately linear ($R^2 \geq 0.90$) with WDD_5 for 95% of cases (n = 268) for which consumption was similar to empirical estimates (40-60% of satiation, or $p(C_{max}) = 0.4\text{-}0.6$; Hartman 2017). This percentage increased to 98% (n = 256) for realistic levels of activity (ACT ≈ 1-2.4 for immature fishes; Rowan and Rasmussen 1996). These summaries and Fig. 2.5 describe the simulations driven by Sparkling Lake water temperatures; results from the simulations driven by Lake Lacawac temperatures were nearly identical (Appendix 1, Fig. A1.4).

2.3 Air temperature and fish growth

i) *Air temperature as a proxy for water temperature*

Air temperatures and surface water temperatures are often highly correlated in lacustrine (Macan and Maudsley 1966; Livingstone and Lotter 1998; Livingstone and Dokuli 2001) and riverine (Pilgrim et al. 1998; Mohseni and Stefan 1999; Erickson and Stefan 2000)

systems during open water periods. For this reason, air temperatures have been used in place of surface water temperatures in fish science (e.g., Schlesinger and Regier 1982; Rypel 2012; Honsey et al. 2016). Moreover, because heat flux at the air-water interface is a major driver of lake temperatures (e.g., Edinger et al. 1968; Wetzel and Likens 2000; Read et al. 2014), air temperatures are commonly included as drivers in limnological models (e.g., Hondzo and Stefan 1993; Jacobson et al. 2010; Piccolroaz et al. 2017).

We first demonstrate the correlation between air and surface water temperatures in Sparkling Lake and Lake Lacawac. To do this, we retrieved mean daily air temperature data from weather stations near the two lakes that covered the same time periods as the water temperature data. For Sparkling Lake, we retrieved air temperature data from Woodruff Airport (-4.22 m elevation and 9.11 km from Sparkling Lake; NTL LTER 1991b). These data contained three gaps (mean $\pm$ SD gap length = 7.33 $\pm$ 10.12 days; 1.2% of total sample size). Because one of the gaps in these data was 19 days long and because mean daily air temperature data from other nearby sites were unavailable, we used a linear model to predict the unknown mean daily air temperatures as a function of daily minimum and maximum air temperatures from another nearby weather station (Minocqua Dam, -11.32 m elevation and 6.05 km from Woodruff Airport; Kratz 1983; n = 1805, $R^2 = 0.994$). For Lake Lacawac, we retrieved continuous mean daily air temperature data from the Wilkes Barre Scranton International Airport (-160.66 m elevation and 35.97 km from Lake Lacawac) using the National Oceanic and Atmospheric Administration Climate Data Online tool (https://www.ncdc.noaa.gov/cdo-web/). Air and surface water temperatures were highly correlated for both lakes

(Pearson's ρ = 0.87 and 0.91 for Sparkling and Lacawac, respectively; Fig. 2.3), suggesting that mean daily air temperatures can serve as a good proxy for mean daily surface water temperatures.

Our next goals were to examine the relationship between DD derived from air temperatures (ADD) and WDD, and to determine whether ADD can serve as an accurate proxy for WDD. Both the degree to which ADD correlates with WDD within lakes and the nature of the ADD versus WDD relationship among lakes have important implications for ADD applications (e.g., using ADD to describe fish growth and physiology within and/or among lakes, using ADD to drive limnological models, etc.). We used both simulated and empirical data to explore these relationships. For the empirical comparisons, we calculated ADD above 5 ºC (ADD_5) using eq. 1 and the air temperature data described above. We then calculated the Pearson correlation coefficient between ADD_5 and WDD_5 derived from the empirical water temperature data from each lake at both annual and cumulative (i.e., summed across years) time scales. For the simulations, we once again used the Shuter model (Shuter et al. 1983) to generate annual water temperature cycles across four values of $\bar{Z}$ (4, 8, 16, and 32 m) and with $\overline{AT}$ ranging from -10 to 15 ºC in increments of 0.5 ºC. We used these water temperature data and eq. 1 to calculate WDD_5. We then collected air temperature data from 107 weather stations in the United States and Canada using the National Oceanic and Atmospheric Administration Climate Data Online tool (see Appendix 1, Section A1.2 for details), and we used these data to generate an empirical relationship for predicting ADD_5 from $\overline{AT}$:

$$ADD_5 = 1346.8 \cdot e^{0.0729 \cdot \overline{AT}}.$$

We used this relationship to estimate ADD_5 for the simulated scenarios, and we compared annual ADD_5 to WDD_5 across simulations.

Our empirical results show that annual ADD_5 and WDD_5 are highly correlated for both the Sparkling Lake and Lake Lacawac datasets ($\rho = 0.97$ and 0.87, respectively; Fig. 2.6). Moreover, although WDD_5 is consistently higher than ADD_5 due to higher average water temperatures (Fig. 2.3), the two cumulative metrics are almost linearly related for both datasets ($\rho > 0.99$; Appendix 1, Fig. A1.7). These results suggest that ADD_5 can be an accurate surrogate for WDD_5 both within and across years. Our simulation results indicate that the relationship between WDD_5 and ADD_5 is nonlinear and not proportional (Fig. 2.6). However, the relationship for a given $\bar{Z}$ value is approximately linear across relatively broad ranges of temperatures (e.g., ~1300-3000 ADD_5), suggesting that the slope of the relationship (and therefore the utility of ADD_5 as a proxy for WDD_5) is not likely to change within a given lake due to annual variation in temperature.

ii) *Annual growth*

Our next aim was to investigate the relationship between annual growth and ADD across a variety of temperature scenarios. To do this, we used the Shuter model to generate water temperatures, with $\bar{Z}$ fixed at 8 m and with $\overline{AT}$ ranging from 0 to 10 ºC in increments of 0.5 ºC. We used these simulated temperatures to drive the three bioenergetics models (Table 2.1), summed daily growth throughout the ice-free season, and subtracted initial length from final length to determine annual growth (Δmm). We calculated ADD_5 using the empirical relationship described above. We then regressed

ADD_5 against annual growth for four bioenergetic scenarios: (1) the 'ideal' case of satiation at resting metabolism, (2) satiation with activity multiplier = 3, (3) 50% of satiation at resting metabolism, and (4) 85% of satiation with activity multiplier = 2. Our results show that annual growth is roughly linear with the empirically-derived ADD_5 for all bioenergetic scenarios examined (all $R^2 \geq 0.98$), suggesting that ADD_5 can be as effective as WDD_5 for describing annual growth within lakes (Fig. 2.7).

iii) *Interannual growth*

We have shown that ADD and WDD can have nearly equivalent power in explaining annual fish growth. Our final goal was to compare the performance of ADD to that of WDD in describing interannual growth (i.e., length-at-age). To do this, we again used five years of empirical water temperature data from Sparkling Lake and Lake Lacawac to drive bioenergetics simulations for the three model species (Table 2.1), and we employed the same factorial design used above to examine the effects of varying consumption, activity, and initial size on the growth versus DD relationship. In this case, we calculated ADD_5 using the empirical air temperature datasets collected near each lake and eq. 1 (substituting ADD_5 for WDD_5), and we fit linear models to the length versus ADD_5 relationship for each simulation. Our results closely mirrored those of the length versus WDD_5 comparisons for both Sparkling Lake (Fig. 2.8) and Lake Lacawac (Appendix 1, Fig. A1.8). In some cases, adjusted R^2 values were higher for the length versus ADD_5 regressions than they were for the length versus WDD_5 regressions (e.g., Fig. 2.8g,h,i).

These results suggest that immature fish length-at-age is approximately linear with ADD_5 across a wide range of bioenergetic scenarios.

2.4 Discussion

Our analysis provides bioenergetic foundations for the nearly linear relationship between DD and immature fish growth, as well as justification for using ADD as a proxy for WDD when describing growth. We show that, although daily growth rates are nonlinear with temperature, the nonlinear increase in DD through time explains the nonlinear nature of growth in a linear manner at annual and interannual time scales (Neuheimer and Taggart 2007). In other words, growth occurs intermittently, but always along a trajectory that is approximately linear with DD at relatively coarse (but highly relevant) time scales. The fact that ADD can serve as an accurate proxy for WDD should facilitate the use of DD and promote a more physiologically-valid understanding of how the growth of fishes and other aquatic organisms responds to thermal energy.

A number of factors can limit the ability of surface WDD or ADD to describe fish growth. For example, the growth versus ADD relationship may be nonlinear if ADD become disentangled from WDD (e.g., due to wind, groundwater, shade, etc.). We also assumed that our simulated fish experienced epilimnetic temperatures throughout the growing season. This assumption was reasonable for our three model species, but coldwater species in many stratified systems spend much of the growing season below the epilimnion. As such, ADD and surface WDD may not provide an adequate description of the thermal environments experienced by these fishes. We note that more

adequate DD metrics could be calculated for fishes that do not inhabit the epilimnion year-round, but that doing so would require both depth-specific water temperature data and knowledge of the depths that individuals inhabit throughout the year, which may render the calculation of such a metric impractical or impossible (although more complex water temperature models could facilitate such efforts; e.g., Read et al. 2014). We also note that any shortcomings of ADD in describing growth of coldwater fishes in stratified systems would likely extend to any air temperature-based metric due to the often poor correlation between air temperatures and meta- or hypolimnetic water temperatures (e.g., Robertson and Ragotzkie 1990). Importantly, Chezik et al. (2014a) showed that ADD can still have a high degree of explanatory power in describing length-at-age for a coldwater species (cisco *Coregonus artedi*), albeit a reduced amount compared to cool- and warmwater fishes. Furthermore, if surface water temperatures exceed growth optima and no refugia are present (e.g., in unstratified systems), then the growth versus surface WDD or ADD relationship may become nonlinear; however, we expect that nonlinearities due to this mechanism are relatively rare in nature because species seldom persist in systems in which temperatures regularly exceed growth optima and in which no refugia are present (e.g., coldwater species such as lake trout do not inhabit warm, unstratified lakes). That being said, individuals may spend some amount of time in temperatures that are above growth optima (e.g., Sellers et al. 1998), which can reduce the utility of DD metrics in describing growth and other physiological processes. Future work should address this shortcoming, perhaps by introducing an upper temperature limit for calculating DD or incorporating a 'penalty' (i.e., reduction in DD) if temperatures exceed

some (likely species-specific) value. Finally, growth may be nonlinear due to a variety of other biological factors, including factors that cause large changes in consumption rates or activity costs within or among years (e.g., substantial shifts in prey or predator density; ontogenetic diet shifts, especially in very early life; etc.; Lorenzen and Enberg 2002).

Although the adult fish growth versus DD relationship may be nonlinear due to investment in reproduction and other factors (e.g., Lester et al. 2004; Andersen and Beyer 2015; Honsey et al. 2017), using DD to describe lifetime growth is still useful, particularly when comparing growth among populations that experience different thermal regimes (Chezik et al. 2014b; Lester et al. 2014). That being said, daily growth for adult fishes is often a near-linear function of temperature over a midrange of temperatures, much as it is for immature fishes (see Appendix 1, Section A1.3). Indeed, many fish bioenergetics models are intended to apply to both juvenile and adult growth for a given species, as is the case for the brown bullhead model used herein (Hartman 2017; see also, e.g., Madon et al. 2001; Pääkkönen et al. 2003). As such, many of our results (particularly the linearity of annual growth versus DD) may also extend to adult fish growth.

Both our simulated and empirical comparisons of ADD and WDD highlight the potential for the ADD versus WDD relationship to vary among lakes. For instance, in Lake Lacawac, $WDD_5 \approx 1.2 \times ADD_5$. In contrast, $WDD_5 \approx 1.3 \times ADD_5$ for Sparkling Lake. This result is intuitive because water temperatures in lakes with different characteristics (e.g., Secchi depth, morphometry) will respond differently to air temperatures (e.g., Rose et al. 2016). These differences are important to consider for a

number of applications, including using ADD to (1) describe growth and other physiological processes among lakes and (2) drive limnological models of lake thermal regimes. Future work should examine the degree to which the ADD versus WDD relationship varies among lakes, and explore whether that variation introduces substantial error and/or bias in among-lake comparisons of growth and other physiological processes.

If DD are an accurate index for the thermal scope for growth, then growth should be proportional to DD given that they are calculated using the correct base temperature for growth, i.e., the temperature below which growth is negligible. This base temperature for growth (T_0) is a key parameter for calculating DD; incorrect T_0 values can bias growth rate estimates, which can be particularly problematic for among-population comparisons (Chezik et al. 2014b). Unfortunately, T_0 has not been estimated for most fish species. It may be possible to use bioenergetics models to estimate T_0 by finding the T_0 value for which the growth versus DD relationship is proportional (i.e., passes through the origin). We provide an example of this approach using the yellow perch bioenergetics model in the annual growth simulation framework described above (see Appendix 1, Section A1.4). Our results indicate that the appropriate T_0 value for yellow perch when using ADD is ~9 ºC (Fig. 2.9), which agrees with two other independent estimates for this species (Chezik et al. 2014b).

In our view, DD remain underutilized in fish science (but see, e.g., Rypel and David 2017; Ward et al. 2017). Our results suggest that the empirically-observed, linear relationship between DD and immature fish growth is rooted in bioenergetics. As such,

DD are an effective metric for quantifying the thermal scope for growth in fishes. In addition, ADD can serve as an accurate proxy for WDD. Given that high-resolution air temperature data are more common than water temperature data, this result provides a foundation for expanding the use of DD in fish science and other aquatic disciplines. This expanded use of DD should, in turn, promote a better understanding of the growth and physiology of aquatic organisms and may be particularly useful for assessing and predicting the impacts of global change. In addition to the suggestions mentioned above, future work should focus on (1) standardizing DD calculation (e.g., by estimating T_0 for many fishes) and (2) assessing whether ADD can serve as an accurate proxy for WDD in lotic and marine systems.

Table 2.1 Bioenergetics equations and parameters used for simulation. All models follow the Wisconsin bioenergetics framework; see Hanson *et al.* (1997) for equations and details. Sources are listed in footnotes.

Model component	**Model species**		
	Yellow perch[1]	**Brown bullhead[2]**	**Tiger muskellunge[3]**
Consumption equation	2	3	2
CA	0.25	0.12	0.2215
CB	-0.27	-0.225	-0.18
CQ	2.3	15	2.53
CTO	29	24	26
CTM	32	26	34
CTL	-	30	-
CK1	-	0.473	-
CK4	-	0.55	-
Respiration equation	2	1	1
RA	0.0108	0.0007	0.00246
RB	-0.2	-0.271	-0.18
RQ	2.1	0.0915	0.055
RTO	32	0.4055	0
RTM	35	0	0
RTL	-	0	0
RK1	-	1	0
RK4	-	0	0
ACT	variable	variable	variable
BACT	-	0	0
SDA	0.172	0.172	0.14
Egestion-excretion equation	2	1	1
FA	0.158	0.2	0.13
FB	-0.222	-	-
FG	0.631	-	-
UA	0.0253	0.07	0.07
UB	0.58	-	-
UG	-0.299	-	-
Energy density equation	1	1	1
Predator energy density ($J \cdot g^{-1}$)	4186	6700	3600
Prey energy density ($J \cdot g^{-1}$)	3770[4]	4392[5]	3874[6]

[1]Hanson et al. (1997)
[2]Hartman (2017)
[3]Schoenebeck et al. (2008)
[4]Approximate energy density of *Daphnia* sp. (Luecke and Brandt 1993, Tabor et al. 1996)
[5]Energy density of Chironomidae larvae (Myrvold and Kennedy 2015)
[6]Energy density of fathead minnow *Pimephales promelas* (Chipps et al. 2000, Schoenebeck et al. 2008)

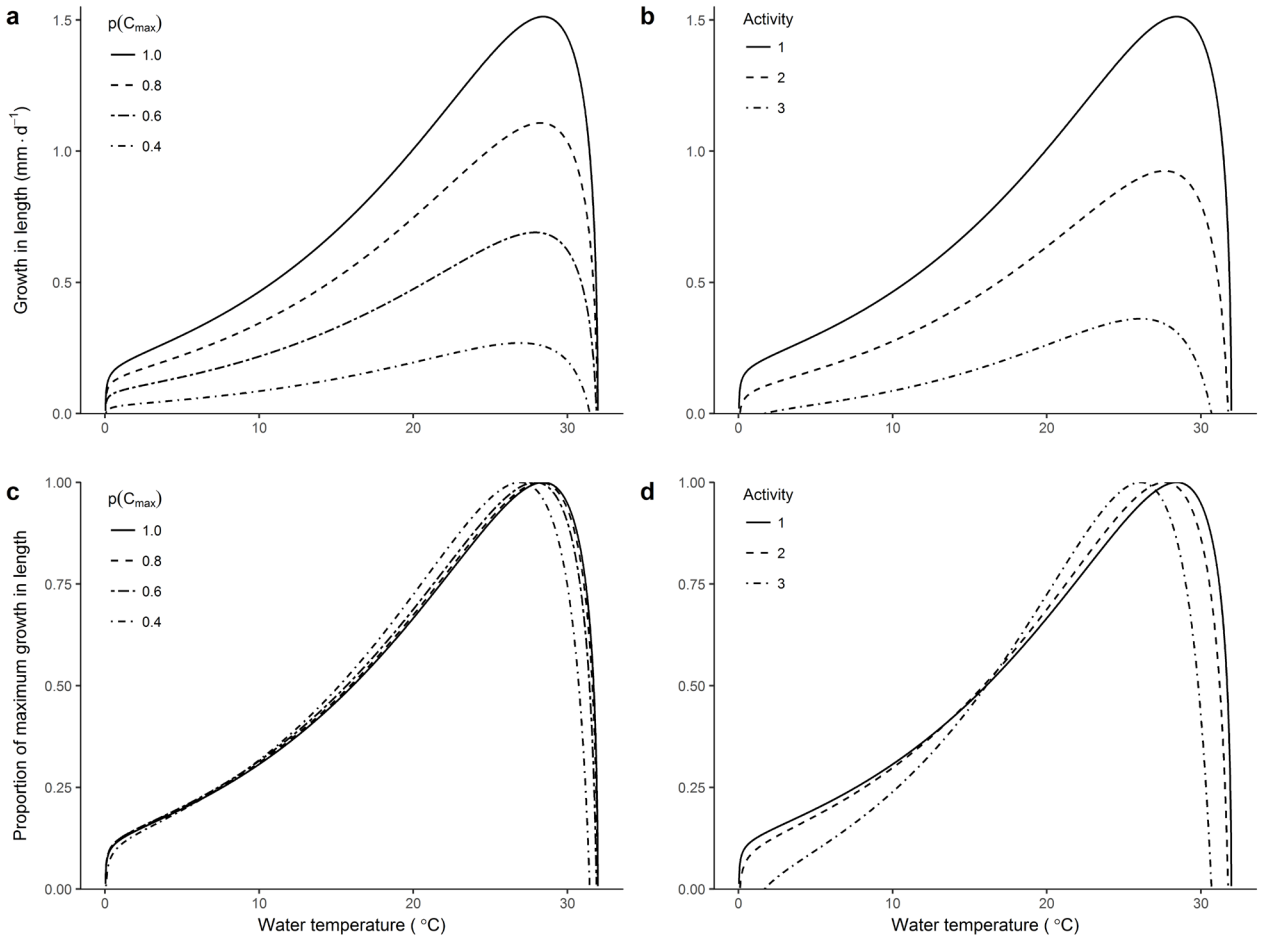

Figure 2.1 (a-b) The effect of temperature, activity level, and consumption (as a proportion of maximum consumption, $p(C_{max})$) on daily growth in length for yellow perch *Perca flavescens*, based on a bioenergetics model. (c-d) Relative yellow perch growth in length (i.e., growth as a proportion of maximum growth) across levels of temperature, activity, and consumption.

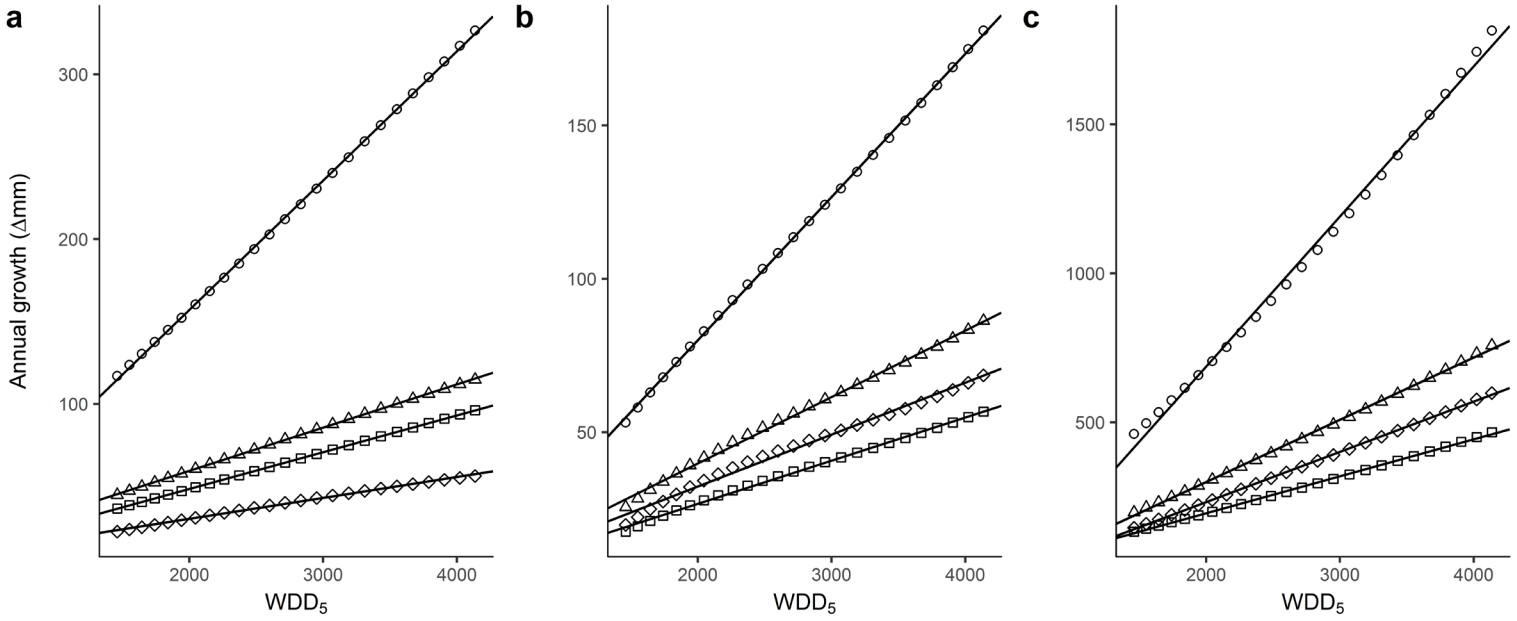

Figure 2.2 Simulated annual growth vs. degree-days above 5 °C derived from simulated water temperatures (WDD_5) across levels of activity and consumption for (a) yellow perch *Perca flavescens*, (b) brown bullhead *Ameiurus nebulosus*, and (c) tiger muskellunge *Esox lucius* X *Esox masquinongy*. Circles: satiation at resting metabolism; squares: satiation with activity multiplier = 3; triangles: 50% satiation with resting metabolism; diamonds: 85% satiation with activity multiplier = 2. Adjusted $R^2 \geq 0.99$ for all linear fits.

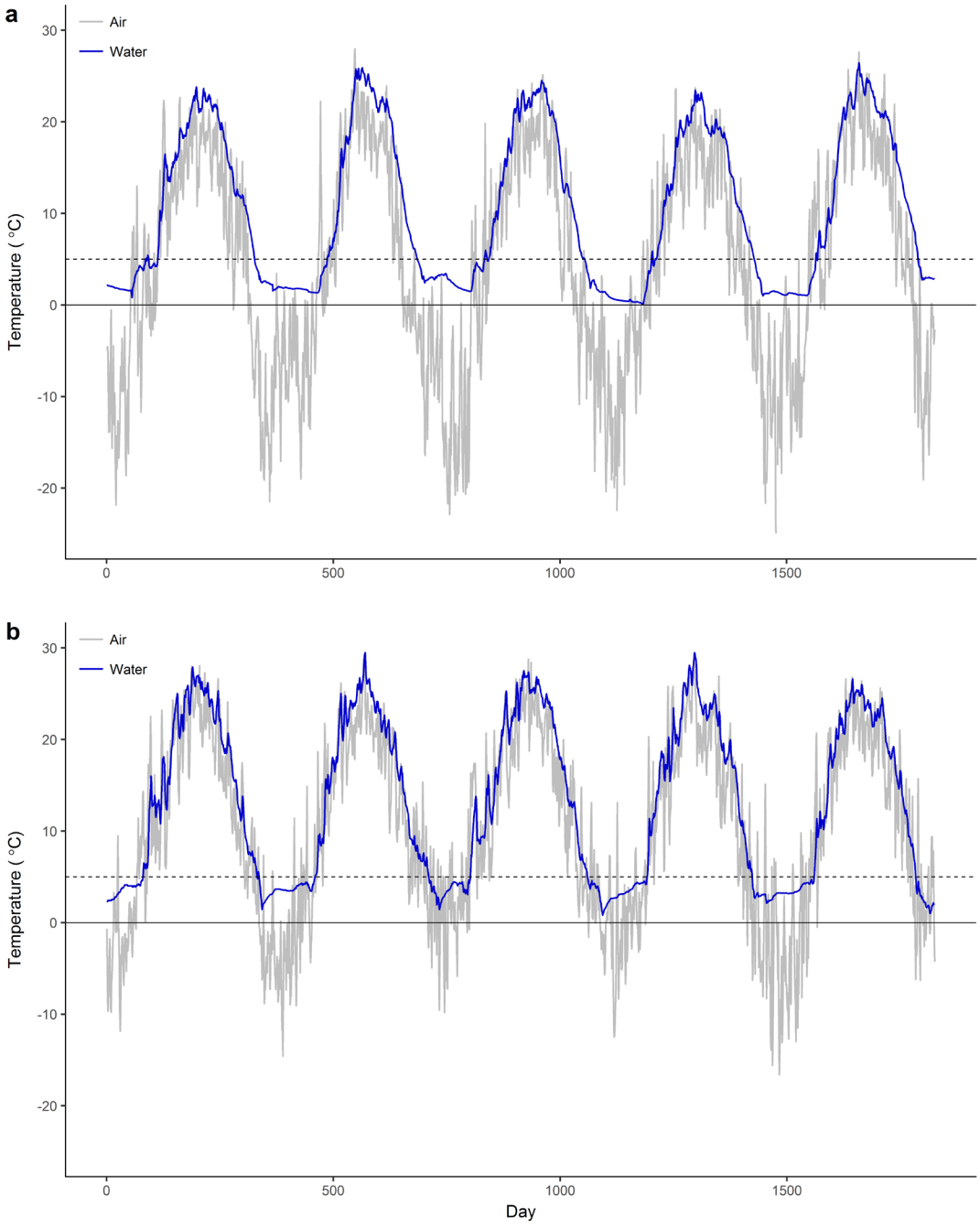

Figure 2.3 Daily mean surface water (1 m depth; blue line) and air (gray line) temperatures across five years in/near (a) Sparkling Lake, WI (2000, 2002-2005) and (b) Lake Lacawac, PA (2010-2014). Surface water and air temperatures were highly correlated in both cases ($\rho = 0.87$ and 0.91 for (a) and (b), respectively). The horizontal dashed line at 5 ºC indicates the base temperature for degree-day calculations used herein.

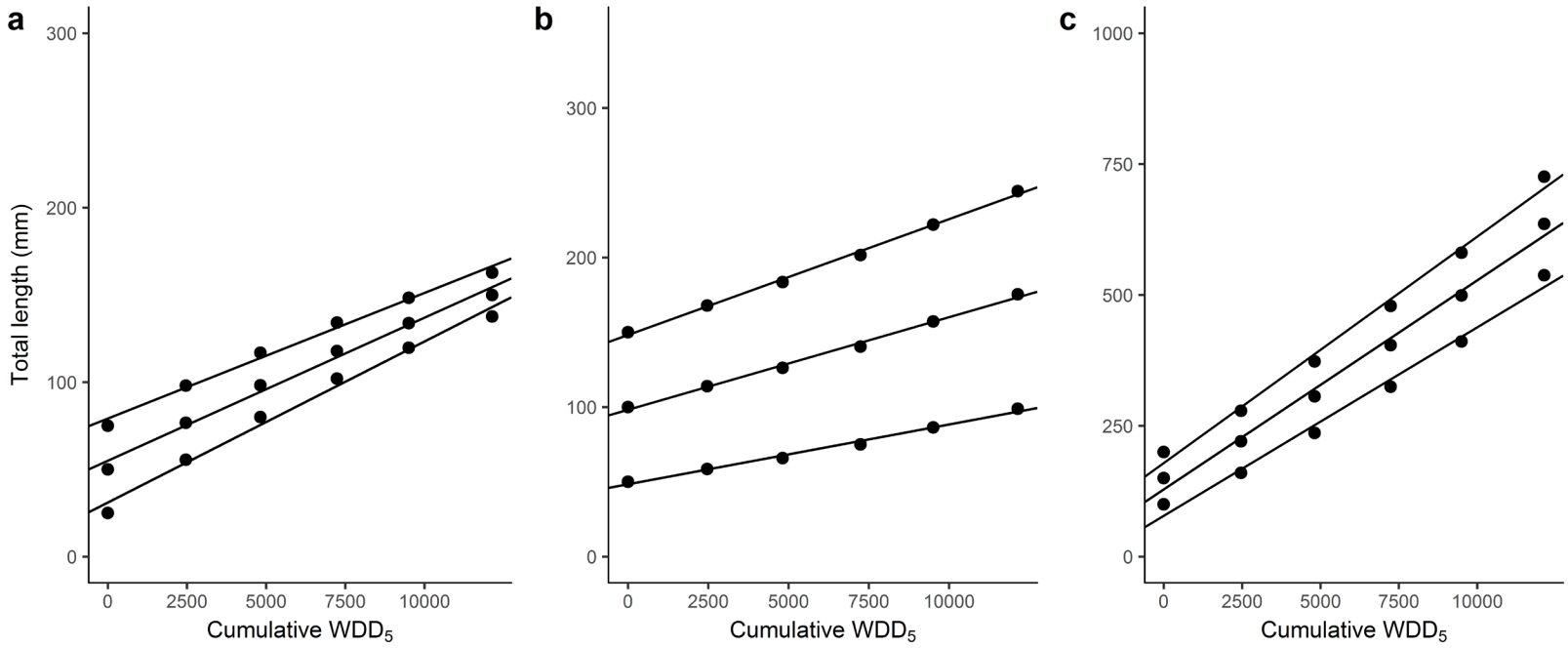

Figure 2.4 Example length-at-age vs cumulative water degree-days above 5 °C (WDD_5) trajectories for (a) yellow perch *Perca flavescens*, (b) brown bullhead *Ameiurus nebulosus*, and (c) tiger muskellunge *Esox lucius* X *Esox masquinongy*, based on bioenergetics models. In this example, consumption was set at 40% of satiation (p(Cmax) = 0.4), and the activity multiplier (ACT) was set to 1.2. Each panel shows growth trajectories across three initial sizes (25, 50 and 75 mm for yellow perch; 50, 100, and 150 mm for brown bullhead; 100, 150, and 200 mm for tiger muskellunge), with linear model fits to each trajectory. Adjusted R^2 values from fits such as these were used to evaluate the linearity of the length-at-age vs. degree-day relationship for a variety of bioenergetic scenarios.

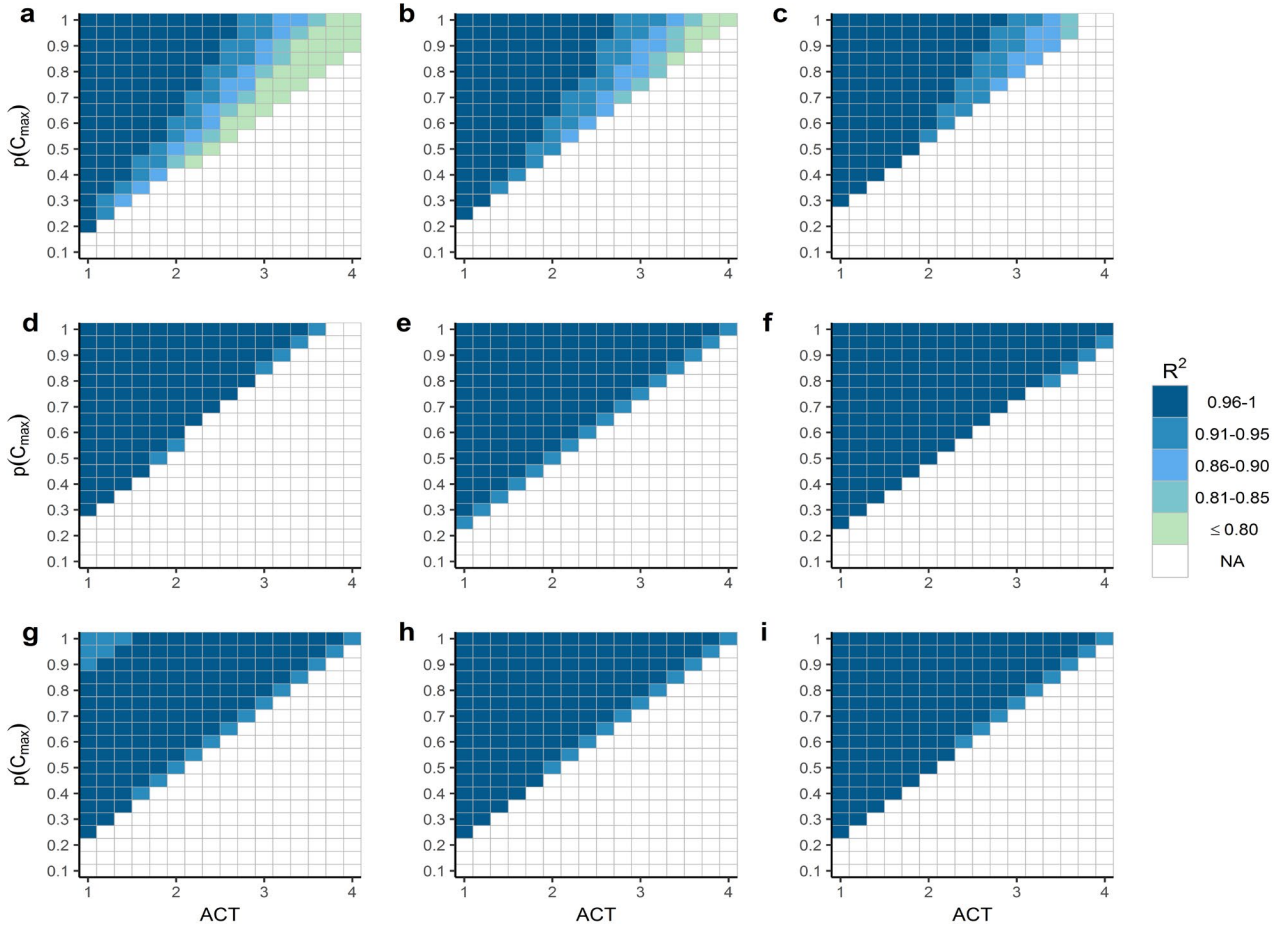

Figure 2.5 Coefficients of determination (adjusted R^2) from linear model fits to the length vs. water-based degree-day (WDD_5) relationship from five year growth simulations given various combinations of consumption (proportion of maximum consumption, $p(C_{max})$), activity (ACT), and initial size (columns). (a-c) Results from the yellow perch *Perca flavescens* bioenergetics model, with initial sizes of (a) 25 mm, (b) 50 mm, and (c) 75 mm. (d-f) Results from the brown bullhead *Ameiurus nebulosus* bioenergetics model, with initial sizes of (d) 50 mm, (e) 100 mm, and (f) 150 mm. (g-i) Results from the tiger muskellunge (northern pike *Esox lucius* X muskellunge *Esox masquinongy*) bioenergetics model, with initial sizes of (g) 100 mm, (h) 150 mm, and (i) 200 mm. Bioenergetics simulations incorporated empirical water temperature data (1 m depth) from Sparkling Lake, WI, USA. White cells ("NA") denote cases in which individuals did not grow across all five years.

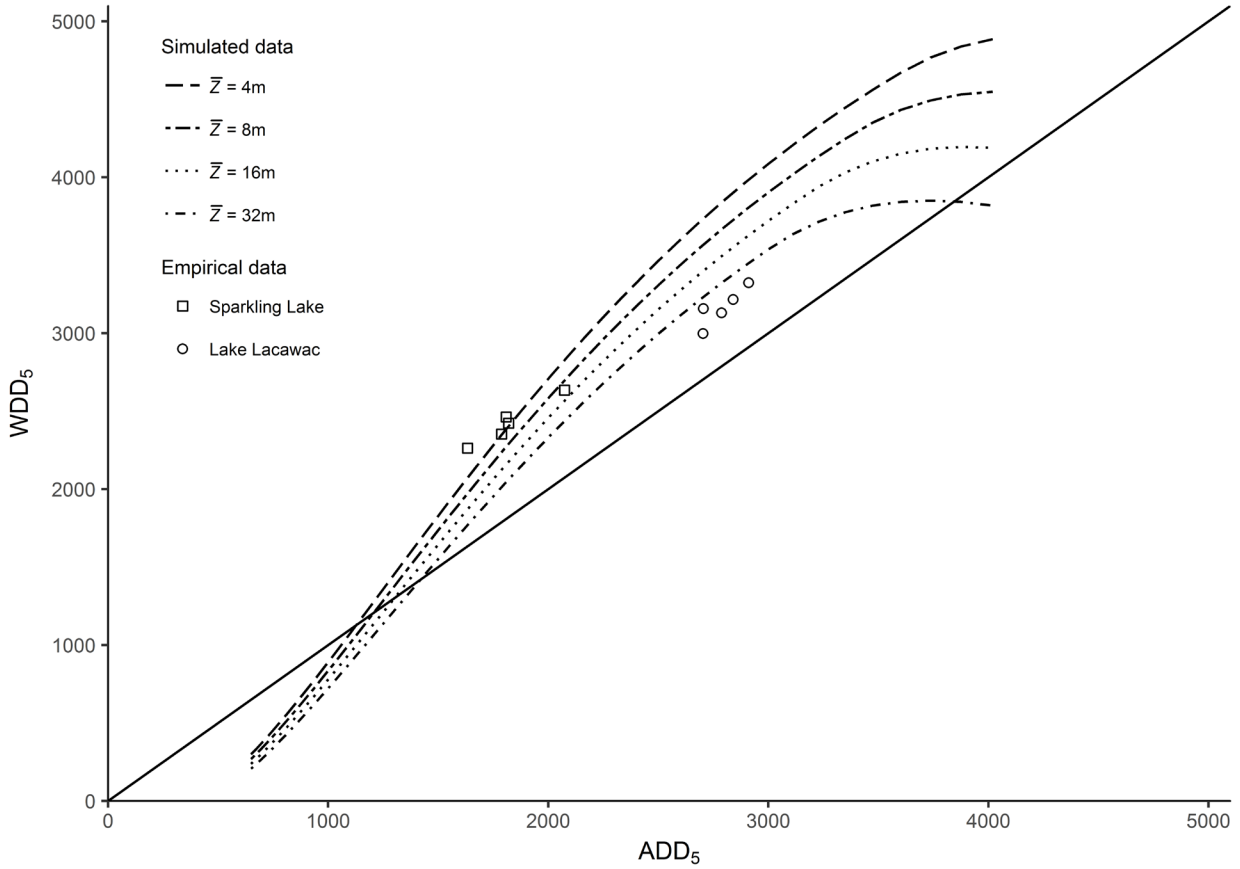

Figure 2.6 Relationships between annual degree-days above 5 °C derived from air (ADD_5) and water (WDD_5) temperatures. Points denote empirical datasets from Sparkling Lake, WI, USA and Lake Lacawac, PA, USA ($\rho = 0.97$ and 0.87, respectively). Dotted and dashed lines denote simulated data generated using the Shuter water temperature model and an empirically-derived relationship between mean annual air temperature and ADD_5 (see Section 2.3 for details). The solid line is a 1:1 line.

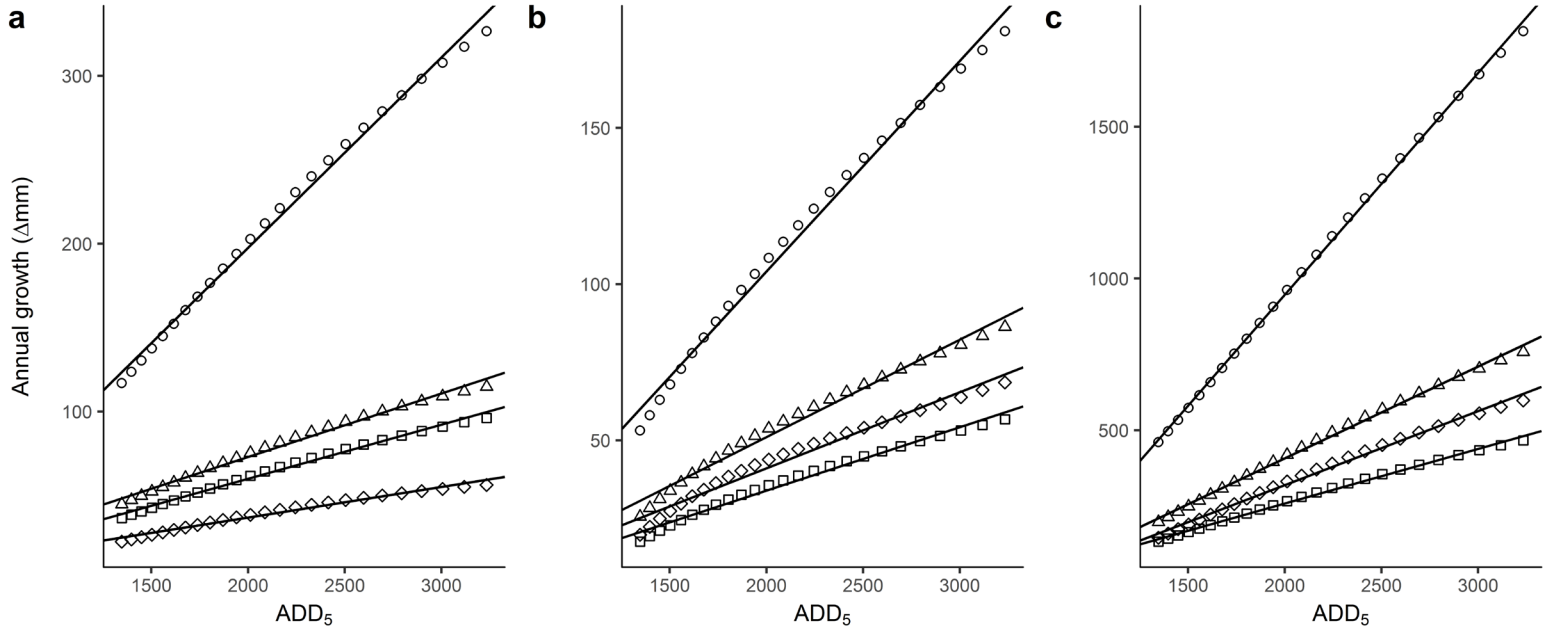

Figure 2.7 Simulated annual growth vs. air degree-days above 5 °C (ADD_5; derived from an empirical relationship between ADD_5 and mean annual air temperature) across levels of activity and consumption for (a) yellow perch *Perca flavescens*, (b) brown bullhead *Ameiurus nebulosus*, and (c) tiger muskellunge *Esox lucius* X *Esox masquinongy*. Circles: satiation at resting metabolism; squares: satiation with activity multiplier = 3; triangles: 50% satiation with resting metabolism; diamonds: 85% satiation with activity multiplier = 2. Adjusted $R^2 \geq 0.98$ for all linear fits.

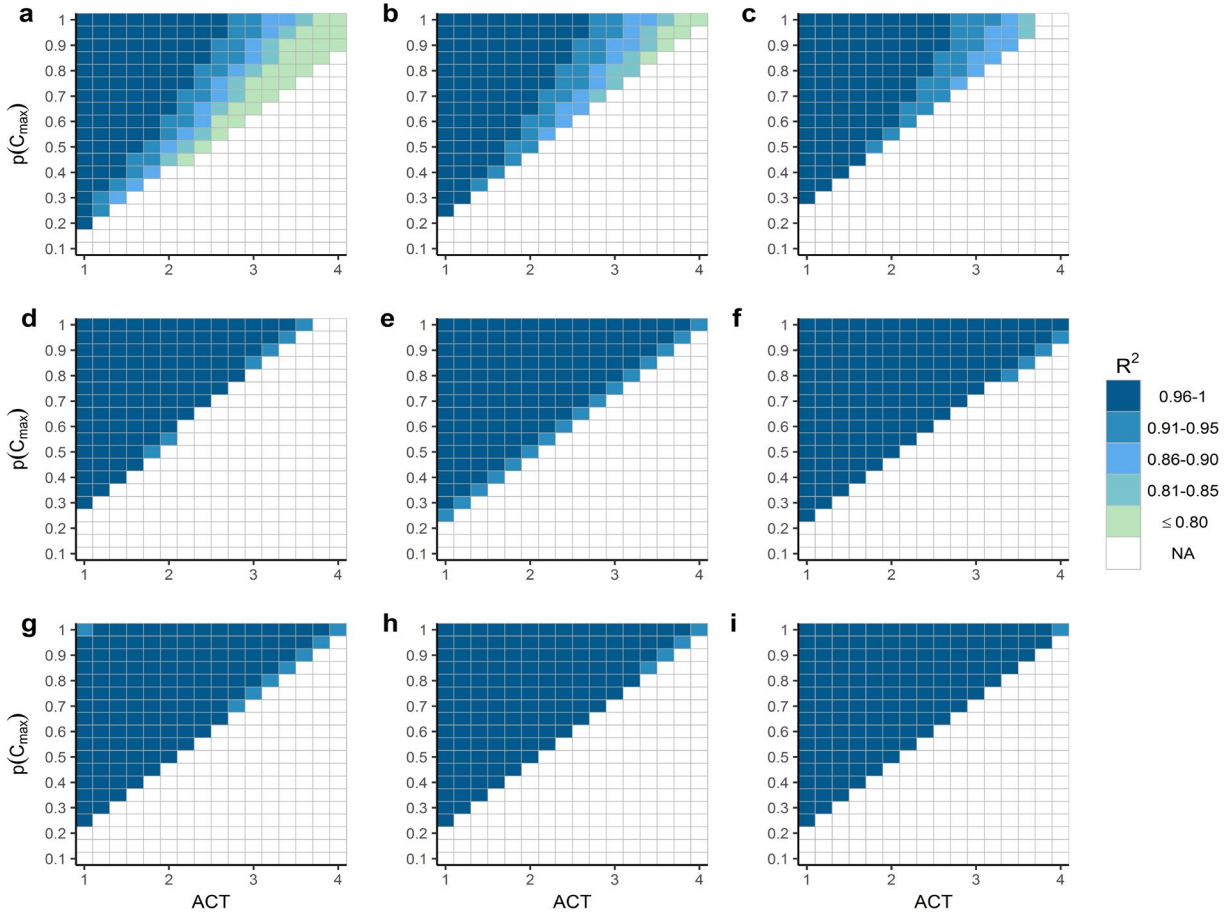

Figure 2.8 Coefficients of determination (adjusted R^2) from linear model fits to the length vs. air-based degree-day (ADD_5) relationship from five year growth simulations given various combinations of consumption (proportion of maximum consumption, $p(C_{max})$), activity (ACT), and initial size (columns). (a-c) Results from the yellow perch *Perca flavescens* bioenergetics model, with initial sizes of (a) 25 mm, (b) 50 mm, and (c) 75 mm. (d-f) Results from the brown bullhead *Ameiurus nebulosus* bioenergetics model, with initial sizes of (d) 50 mm, (e) 100 mm, and (f) 150 mm. (g-i) Results from the tiger muskellunge (northern pike *Esox lucius* X muskellunge *Esox masquinongy*) bioenergetics model, with initial sizes of (g) 100 mm, (h) 150 mm, and (i) 200 mm. Bioenergetics simulations incorporated empirical water temperature data (1 m depth) from Sparkling Lake, WI, USA. White cells ("NA") denote cases in which individuals did not grow across all five years.

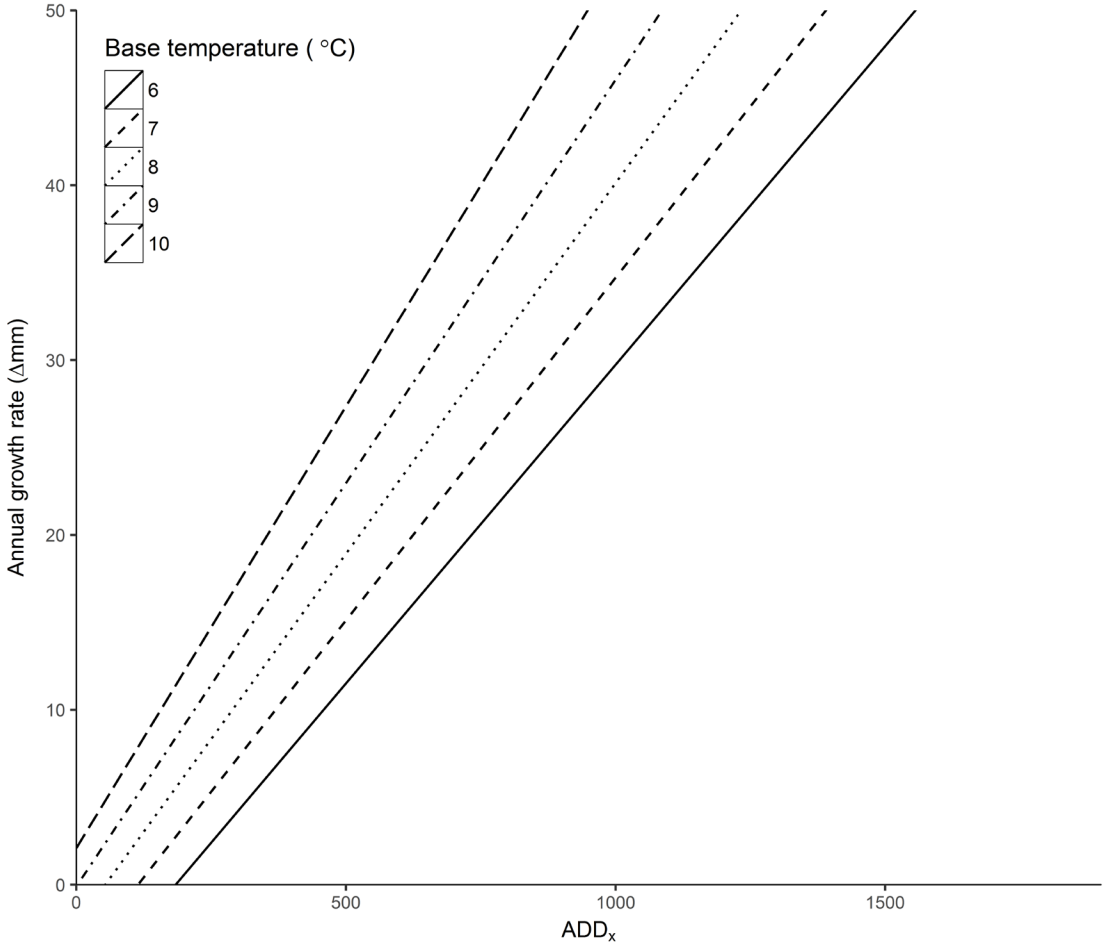

Figure 2.9 Air-based degree-days calculated using various base temperatures for growth (ADD_x; base temperatures from 6-10 ºC) vs. annual growth (Δmm) from a yellow perch *Perca flavescens* bioenergetics model. The growth vs. degree-day relationship is roughly proportional when the base temperature is 9 ºC, suggesting that this base temperature is most appropriate for among-population studies of yellow perch growth.

Chapter 3

Advice for selecting base temperatures when using degree-days to describe fish growth

Synopsis

Degree-days (DD) are becoming increasingly popular as a metric for describing fish growth and other physiological processes. However, there is a lack of advice regarding how to calculate DD for different fish species. In particular, appropriate values for the base temperature for growth (T_0) are unknown for most fish species. Previous work showed that error in the value of T_0 can bias growth rate estimates and lead to erroneous conclusions when comparing growth among populations. It is therefore critical to use appropriate and biologically-valid T_0 values when calculating DD. We used two approaches that leverage empirical growth data and bioenergetics models to estimate T_0 for 82 fish species. We found that T_0 varied among fish species and across thermal guilds, with coldwater species having relatively low T_0 values and warmwater species having higher T_0 values. In addition, we found that T_0 varied across life stages and depending on whether one uses air or water temperature data to calculate DD. Our results provide guidance for calculating DD in fish science for many species and scenarios.

3.1 Introduction

Ambient temperature drives ectotherm growth and other physiological processes (Hazel and Prosser 1974, Atkinson 1994, Diana 2003). More specifically, ectotherm metabolic processes and phenologies are tightly linked to the amount of thermal energy accrued over a given time period, i.e., the thermal integral (Charnov and Gillooly 2003, Neuheimer and Taggart 2007). Recent studies have found strong relationships between thermal integrals and fish growth and physiology (Honsey et al. in press, Venturelli et al. 2010a, Chezik et al. 2014b, 2014a). As such, the application of thermal integrals in the aquatic sciences is becoming increasingly common (e.g., Kumar et al. 2009, Hansen et al. 2017, Rypel and David 2017, Ward et al. 2017).

The degree-day (DD) is perhaps the most commonly-used and well-supported thermal integral metric. DD are calculated as

$$DD = \sum_{t=1}^{N} T_t - T_0\,, \qquad T_t > T_0$$

where N is the number of days, T_t is the mean temperature on day t, and T_0 is the base temperature below which thermal energy is assumed to be irrelevant to the physiological process in question (e.g., growth, maturity). DD can provide an accurate description of the thermal energy available for fish growth and are an increasingly popular metric in fish science (Neuheimer and Taggart 2007, Righton et al. 2010, Venturelli et al. 2010, Chezik et al. 2014a, 2014b, Lester et al. 2014).

Although DD are a useful metric and are becoming more popular, there are few guidelines in fish science for how to apply DD or interpret results. For example, there are

competing approaches to determining the base temperature for growth (T_0) and a relatively poor understanding of the effect that the choice of T_0 has on our ability to describe growth. As a result, fish scientists have used a variety of base temperatures to calculate DD, often with little or no justification (Chezik et al. 2014a). Chezik et al. (2014b) combined theory, simulations, and empirical data to show that error in the value of T_0 can complicate inference and lead to erroneous conclusions when comparing growth rates among populations (e.g., the apparent evolution of countergradient growth; Levins 1969, Conover and Present 1990). These results highlight the need for objective, biologically-sound estimates of T_0 among fishes.

Our goal was to provide guidance for calculating DD in fish science by estimating T_0 for as many fish species as possible. We used two approaches to do this. Our first approach used empirical fish growth data and model-estimated air temperatures to provide T_0 estimates that are most appropriate for calculating DD using air temperature data (ADD). Our second approach used fish bioenergetics models and hypothetical water temperatures to generate T_0 estimates that are most appropriate for calculating DD using water temperature data (WDD). Our results provide advice for calculating DD across a broad range of scenarios and should help to facilitate the interpretation and comparability of analyses using DD in fish science.

3.2 Methods

i) *Empirical growth analysis*

Our first approach for estimating T_0 hinges on the notion that growth should respond similarly to accumulated thermal energy among populations of a given fish species, and that variation in growth rates (in terms of thermal time, e.g., mm·DD^{-1}) among populations should be largely due to local factors such as habitat quality and food availability (but see Conover and Present 1990 and discussion below). We can therefore estimate T_0 by finding the value for T_0 that minimizes variation in growth rates among populations (Chezik et al. 2014b). To do this, we compiled empirical mean length-at-age data for freshwater fish species across lentic systems in North America and Europe from the literature, agency sources, and personal communication (see Supplementary Data File 1 for more details). We excluded lotic, marine, estuarine, and very large lentic (i.e., the Laurentian Great Lakes, Great Bear Lake, Great Slave Lake, Lake Athabasca, Lake Winnipeg, Lake Winnipegosis, and Lake Manitoba) systems because (1) we used air temperatures to approximate the thermal energy available to individuals at each location (see below), and (2) air and surface water temperatures can become decoupled in these systems due to physical factors (e.g., flow, wind; Ward 1985, Rouse et al. 2005, Desai et al. 2009).

We indexed thermal energy using air temperatures because we were unable to find water temperature data for all locations in our dataset, and because air temperatures are often highly correlated with surface water temperatures in lacustrine systems (e.g., Macan and Maudsley 1966, Livingstone and Lotter 1998, Livingstone and Dokuli 2001). Moreover, ADD can serve as an accurate proxy for WDD (Honsey et al. in press). Estimates of T_0 generated using this approach are therefore most appropriate for

calculating ADD. Given that our samples covered a broad temporal range (see Section 3.3), our goal was to generate estimates of mean annual thermal energy over a relatively long period of time. To do this, we used the ClimateNA v5.21 (http://tinyurl.com/ClimateNA; Wang et al. 2016) and ClimateEU v4.63 (http://tinyurl.com/ClimateEU; based on the methodology described by Hamann et al. 2013; see also Hamann and Wang 2005, Wang et al. 2006, 2012, Mbogga et al. 2009) software tools to generate estimates of mean annual ADD for each location at integer T_0 values from 0-20 ºC, based on the 1970-2000 climate normal. We then converted fish calendar ages to thermal ages by multiplying calendar age by the mean annual ADD values for each location and T_0 value.

We used a linear model to regress the mean length data against thermal age (in ADD). This approach is appropriate because immature fish growth is approximately linear with ADD (Honsey et al. in press). However, this linear approximation may not hold for adults due to energetic investment in reproduction and other factors (Lester et al. 2004, Honsey et al. 2017). We therefore made an effort to exclude data describing adult growth. Unfortunately, doing so is not straightforward because age at maturity can vary among populations (e.g., due to varying annual DD, local biotic factors, etc.; Venturelli et al. 2010a, Lester et al. 2014, Feiner et al. 2015). In an effort to mitigate bias due to incidental inclusion of adult growth data, we fit linear models to 2-3 sets of ages per species and compared results. For example, walleye *Sander vitreus* mature at ages 3-6+ in most systems (Bozek et al. 2011, Honsey et al. 2017). In an attempt to exclude adult growth data for walleye, we fit linear models to mean lengths-at-ages ≤ 3, ≤ 4, and ≤ 5

(converted to ADD) and compared results. We provide a complete list of the age ranges used for each species in Table A2.1. We then calculated the coefficient of variation (CV) in growth rate estimates (i.e., slope estimates in mm·ADD^{-1}) across locations for each combination of species, age range, and T_0 value. We estimated T_0 by finding the T_0 value for which the CV in growth rate estimates was minimized. In addition, we used the modified signed likelihood ratio test for equality of CVs (Krishnamoorthy and Lee 2014) within the R package cvequality (Marwick and Krishnamoorthy 2018; see also Feltz and Miller 1996) to find the range of T_0 values for which the CV in growth rate estimates did not significantly differ from the minimum. We carried out these and all subsequent calculations in R version 3.4.1 (R Core Team 2017).

ii) *The 10 ^{o}C rule*

Chezik et al. (2014b) showed that T_0 can be estimated by subtracting 10 ^{o}C from the mean development temperature for a given species (i.e., the "10 ^{o}C rule"; Charnov and Gillooly 2003), and that the mean development temperature can be estimated using bioenergetics models. Bioenergetics models simulate fish growth using an energy balance approach in which the potential for growth is based on energetic gains (via consumption) minus metabolic costs and waste (Kitchell et al. 1977, Jobling 1995, Hanson et al. 1997). We can therefore use bioenergetics models to estimate the mean growth rate across a range of temperatures for various fish species, and we can use the temperature that corresponds with that mean growth rate (i.e., T_{mean}) as a proxy for the mean development temperature. To do this, we simulated fish growth using bioenergetics

models from the Fish Bioenergetics 4.0 software (Deslauriers et al. 2017) that conform to the Wisconsin bioenergetics framework (Kitchell et al. 1977, Hanson et al. 1997). For each of these models, we (1) simulated daily growth across hypothetical water temperatures (range = 0-40 ºC), (2) calculated the mean growth rate ($g \cdot d^{-1}$) between the low-temperature minimum and maximum growth rates (i.e., not including growth rates at temperatures higher than the optimum growth temperature), (3) identified T_{mean}, and (4) subtracted 10 ºC from T_{mean} to estimate T_0. We implemented these simulations in a proprietary framework in R (see Appendix 2, Section A2.1 for code). We set the proportion of maximum consumption ($p(C_{max})$) at 1 for all models for the sake of simplicity and because varying consumption levels had negligible effects on T_0 estimates (results not shown). When possible, we set predator energy densities and initial fish masses based on values from literature sources and FishBase (Froese and Pauly 2016). For cases in which we could not find estimates for these parameters, we used values that were reasonable and/or similar to those of closely-related species. We provide a complete description of model parameters and settings in Supplementary Data File 2. We set T_0 at 0 ºC for cases in which this process resulted in T_0 estimates < 0 ºC. Because these simulations used hypothetical water temperatures, T_0 estimates generated using this approach are most appropriate for calculating WDD.

iii) *Comparison to thermal guilds*

We assigned each species to a thermal guild using Coker et al.'s (2001) classification based on summer preferred temperatures. We classified species as cold (< 19 ºC), cool

(19 to 25 ºC) or warm (> 25 ºC). We assigned a species to an intermediate class (e.g., cold/cool) when its preferred temperature range overlapped the ranges of adjacent categories (Coker et al. 2001, Hasnain et al. 2013). We used temperature preference range data from FishBase (Froese and Pauly 2016), Coker et al. (2001), and other literature sources (see Table 3.1). Finally, we calculated mean T_0 values for each guild. For species with multiple T_0 estimates across life stages, we included the T_0 for the most advanced life stage available in our guild-level mean calculations.

3.3 Results

i) *Empirical growth analysis*

Our dataset included length-at-age data for 978 populations of 28 freshwater fish species across nine families, with Centrarchidae (11 species), Ictaluridae (6 species) and Salmonidae (4 species) having the highest representation (Fig. 3.1; Table 3.1). We compiled data for an average of 35 populations per species (range = 4-132 populations per species; see Table 3.1). Our dataset spanned almost 90 years (1928-2017), although the sampling dates were unknown for many samples (see Supplementary Data File 1).

Our estimate of the appropriate value for T_0 was 0 ºC for 19 (68%) species (Table 3.1). In addition, the CV in growth rate estimates at T_0 = 0 ºC did not significantly differ from the minimum CV for all cases. Our T_0 estimates agreed well across the age ranges that we included in the regressions for each species, suggesting that our results were likely not biased due to incidental inclusion of adult growth data (see Table A2.1). We

provide examples of the relationships between T_0 and the CV in growth rate estimates for four example species in Figure 3.2.

ii) *The 10 ^oC rule*

We estimated T_0 using the 10 ºC rule for 84 bioenergetics models describing 61 species (multiple life stages for some species; Table 3.1). Our estimates of T_0 fell below 10 ºC for all but three species (red river shiner *Notropis bairdi*, plains killifish *Fundulus zebrinus*, and Indo-pacific lionfish *Pterois* spp.). Our T_0 estimates from this approach were often similar for closely-related species (e.g., $\widehat{T_0}$ = 0 ºC for all salmonids, gadids, and osmerids) and varied predictably across thermal guilds (see below). We provide examples of bioenergetics-based growth curves, along with estimates of T_{mean} and T_0, for four example species in Figure 3.3.

iii) *Comparison to thermal guilds*

We were unable to find thermal preference data for two species: humpback chub *Gila cypha* and northern pikeminnow *Ptychocheilus oregonensis*. In addition, we did not classify *Tilapia* spp. in a single thermal guild because the genus is highly diverse (~100 species).

Our T_0 estimates from the empirical growth analysis were similar across thermal guilds (cold, $\overline{T_0}$ = 0 ºC (n = 4); cold/cool, $\overline{T_0}$ = 0 ºC (n = 1); cool, $\overline{T_0}$ = 2.17 ºC (n = 6); and warm, $\overline{T_0}$ = 3.06 ºC (n = 17; Fig. 3.4a)), although variability in $\widehat{T_0}$ was higher in the cool and warm guilds compared to the cold and cold/cool guilds. There were no T_0

estimates from the empirical growth analysis for species in the cool/warm guild. In contrast, our T_0 estimates from the 10 ºC rule approach varied predictably with thermal guild (i.e., $\widehat{T_0}$ consistently increased from the cold through warm guilds; cold, $\overline{T_0}$ = 0.23 ºC (n = 21); cold/cool, $\overline{T_0}$ = 1.33 ºC (n=3); cool, $\overline{T_0}$ = 3.12 ºC (n = 13); cool/warm, $\overline{T_0}$ = 5.81 ºC (n = 7); and warm, $\overline{T_0}$ = 8.66 ºC (n = 14; Fig. 3.4b)).

3.4 Discussion

We provide biologically-based estimates of T_0 for 82 fish species. Our empirical growth analysis provided T_0 estimates appropriate for calculating ADD for 28 freshwater species, and our 10 ºC rule approach yielded T_0 estimates appropriate for calculating WDD for 61 freshwater and marine species. We provide T_0 estimates from both approaches for seven species. In general, our results suggest that relatively low T_0 values are often most appropriate (e.g., $T_0 \leq$ 10 ºC), particularly when calculating ADD. Moreover, we found that T_0 estimates were often similar for closely-related species and within thermal guilds. Below, we provide advice for selecting T_0 in various scenarios, discuss caveats to our analyses, and suggest additional approaches for estimating T_0.

Low T_0 values appear to be most appropriate for calculating ADD. The results from our empirical growth analysis suggest that T_0 should be set to 0 ºC for the majority of the freshwater species in our dataset. Moreover, the coefficient of variation in growth rate estimates at T_0 = 0 ºC was not significantly different from the minimum for all species. As such, T_0 = 0 ºC might be a reasonable choice for calculating ADD in nearly all situations. Our results also show that selecting relatively high T_0 values (e.g., $T_0 \geq$ 15

ºC) can lead to increased variation in temperature-corrected growth rate estimates among populations. Our advice therefore echoes that of Chezik et al. (2014b), who recommend erring low when selecting T_0. Our T_0 estimate for yellow perch *Perca flavescens* from the empirical growth analysis (T_0 = 5 ºC) is slightly lower than that of Chezik et al. (2014b; $T_0 \approx 9$ ºC). However, whereas we used juvenile growth data, Chezik et al. (2014b) used young-of-the-year growth data, and thermal optima are generally expected to be higher for early life stages than for later life stages (e.g., Edsall and Colby 1970, Karas and Thoresson 1992; see Table 3.1). In addition, our T_0 estimates from this approach are similar to those of Rypel and David (2017) for some species (e.g., yellow perch, cisco *Coregonus artedi*), but differ for many species (e.g., largemouth bass *Micropterus salmoides*, smallmouth bass *Micropterus dolomieui*, common carp *Cyprinus carpio*, bluegill *Lepomis macrochirus*). These differences may result from the fact that Rypel and David (2017) used production rather than growth data to estimate T_0 (i.e., the "base temperature for production" may differ from the base temperature for growth).

Our T_0 estimates from the 10 ºC rule approach were slightly more variable than those from the empirical growth analysis. However, almost all of our T_0 estimates fell below 10 ºC. Our results from the 10 ºC rule approach therefore echo those from the empirical growth analysis in suggesting that low T_0 values are generally more appropriate than high T_0 values. In addition, we found that T_0 estimates based on the 10 ºC rule were often similar for closely-related species. For example, $\widehat{T_0}$ = 0 ºC for all gadids, salmonids, clupeids, and osmerids. These results highlight the potential for using phylogeny to estimate T_0 among closely-related species (see below). In addition, these results align

well with those of Hasnain et al. (2013), who found that evolutionary history plays an important role in determining thermal traits across species.

We found that T_0 estimates from the 10 ºC rule approach were tightly linked to thermal guilds, with estimates consistently increasing from cold to warm guilds (Fig. 3.4b). This is unsurprising given that the 10 ºC rule approach relies on bioenergetics models, and that bioenergetics models leverage a deep understanding of thermal tolerances and optima across species (e.g., Kitchell et al. 1977, Hanson et al. 1997). Indeed, thermal guilds are often defined using data from the same experiments that are used to estimate parameters for bioenergetics models (e.g., Coker et al. 2001). These results echo those of Hasnain et al. (2010), who found that many temperature-related traits (e.g., optimum growth temperature, upper incipient lethal temperature, critical thermal maximum) vary predictably across thermal guilds. Additionally, these results highlight the potential for predicting T_0 based on thermal guild and/or using information on other traits (see below). In contrast, T_0 estimates from the empirical growth analysis were similar across thermal guilds, although estimates for some species were higher in the cool and warm guilds compared to the cold and cold/cool guilds (Fig. 3.4a). The lack of a tight relationship between these T_0 estimates and thermal guild may result from, for example, the disconnect between air and water temperatures (although ADD can serve as a good proxy for WDD; see Honsey et al. in press). Alternatively, it may simply result from the fact that mean air temperatures are generally lower than mean water temperatures, and that relatively low base temperatures are therefore appropriate for most species and scenarios when calculating ADD.

Our empirical growth analysis involved finding the T_0 value for which growth rate variation among populations was minimized, and it operated under the assumption that growth should respond similarly to thermal energy among populations (within species). This assumption may have been violated in some cases due to countergradient growth (CGG), whereby individuals living in colder environments grow faster per unit thermal energy (e.g., per DD) than conspecifics in warmer environments (Conover and Present 1990, Chavarie et al. 2010, Rypel 2012b). Given that our empirical growth data spanned a broad latitudinal gradient for many species (Supplementary Data File 1), it is possible that our dataset included some populations that exhibit CGG. However, even the minimum coefficients of variation in growth rates were relatively high across species (CV ≈ 0.2-0.5 or higher; Table A2.1). This variation is likely due to myriad local factors (e.g., per capita prey availability, predation, water clarity, differences in the relationship between ADD and WDD among lakes), perhaps including CGG in some cases. Moreover, even if populations exhibiting CGG were present, they may not have affected T_0 estimates; faster growth per unit thermal energy does not necessarily coincide with differing T_0. Finally, large sample sizes (mean = 35 and maximum = 135 populations per species) likely mitigated any effects of CGG on T_0 estimates. We therefore argue that it is unlikely that CGG significantly biased our results, although we encourage future research to explore the effects of CGG on T_0 and T_0 estimation.

Bioenergetics model parameters and settings were seldom fully reported in the Fish Bioenergetics 4.0 software. For instance, predator energy densities (i.e., the energy density of the modeled species) were not reported in many cases, and settings such as

prey energy density and initial fish mass were almost always omitted because users typically adjust them to match the systems that they are modeling. Importantly, we found that varying prey energy densities had minimal impacts on T_0 estimates (results not shown). As such, we initially set prey energy density to a middling value (3500 $J \cdot g^{-1}$) for all models; however, we found that some models required higher prey energy density values to produce realistic results (i.e., positive growth), possibly due to a lack of proper accounting for the energy density of oxygen during model parameterization (B. Shuter, University of Toronto, personal communication; see Supplementary Data File 2). As noted in Section 3.2ii, we set predator energy densities and initial fish masses based on literature sources and/or values for closely-related species. Our T_0 estimates from the 10 ^{o}C rule approach would likely benefit from a better understanding of these parameters and settings across species.

Honsey et al. (in press) suggested another approach for estimating T_0 that involves simulating annual fish growth. This approach hinges on the idea that, if DD are an accurate representation of the thermal scope for growth, then growth should be proportional to DD when DD are calculated using the proper T_0 value. One can therefore estimate T_0 by finding the T_0 value that forces the growth versus DD relationship through the origin (i.e., when growth is proportional to DD). We tried this approach using the Shuter et al. (1983) water temperature model and the bioenergetics models mentioned above. We found that T_0 estimates varied dramatically with changes in model settings. For example, changing the proportion of maximum consumption parameter from 1 to 0.5 led to a shift in $\widehat{T_0}$ from roughly 0 ^{o}C to 8 ^{o}C for the generalized coregonid bioenergetics

model (Rudstam et al. 1994; Table A2.2). We also found that T_0 estimates were highly sensitive to the range of temperatures used to drive the bioenergetics models. Unfortunately, selecting appropriate values for these and other model settings across species is highly subjective, particularly given that they may vary among systems. As such, we chose not to include T_0 estimates from this approach (but see Appendix 2, Section A2.2 for more details and example results).

Future work should aim to provide T_0 estimates for additional species using multiple approaches. Extending our empirical approach will require the compilation of growth data for additional species. In addition, the 10 ºC rule approach can be used to estimate T_0 for more species as new bioenergetics models become available. Finally, we recommend estimating T_0 using two additional approaches and existing T_0 estimates. The first approach is based on the fact that life history traits are often correlated (e.g., Roff 1984, Hasnain et al. 2010, 2013). Because T_0 is effectively a life history trait, it may be possible to predict T_0 using regressions of existing T_0 estimates versus other life history traits. This approach may be particularly effective given information on other thermal traits (e.g., estimating T_0 from optimum growth temperature or final temperature preferendum; Hasnain et al. 2010). Moreover, this approach may be more useful for estimating T_0 values for calculating WDD compared to ADD given that many of our T_0 estimates for calculating ADD were 0 ºC. The second approach is based on the idea that T_0 may be similar for closely-related species, a notion which is generally supported by our results (see also Hasnain et al. 2013). It may therefore be possible to predict T_0 using phylogeny. Specifically, for clusters of taxa with known T_0 values, one can withhold each

T_0 value in turn and determine how well it is predicted by phylogeny. If these predictions are accurate, then one can estimate T_0 for a given species using existing T_0 estimates for closely-related taxa.

Table 3.1 Estimates of the base temperature for growth (T_0; ºC) for calculating degree-days for 82 fish species, based on empirical growth data ("Growth analysis" column) and bioenergetics models ("10 ºC Rule" column). The "Growth analysis" column contains the T_0 value for which the coefficient of variation in growth rate estimates was minimized, followed by the (1) range of T_0 values with coefficients of variation that did not significantly differ from the minimum and (2) sample size (i.e., number of populations) in parentheses. There are multiple T_0 estimates for species that have bioenergetics models parameterized for multiple life stages and/or scenarios. Thermal classifications ("Classification" column) were determined using FishBase (Froese and Pauly 2016), Coker et al. (2001), and the sources listed in the footnotes. See Supplementary Data Files 1 and 2 for additional information.

						T_0 estimate (ºC)	
Order	**Family**	**Scientific name**	**Common name**	**Life stage**	**Classification**	**Growth analysis**	**10 ºC Rule**
Acipenseriformes	Acipenseridae	*Acipenser fulvescens*	Lake sturgeon	Juvenile	Cold/cool	0 (0-20; n = 4)	
Acipenseriformes	Acipenseridae	*Scaphirhynchus albus*	Pallid sturgeon	Larvae	Cool/warm[1]		5.67
Acipenseriformes	Acipenseridae	*Scaphirhynchus albus*	Pallid sturgeon	Juvenile	Cool/warm[1]		6.76
Beloniformes	Scomberesocidae	*Cololabis saira*	Pacific saury	Juvenile	Cold[2]		0.52
Beloniformes	Scomberesocidae	*Cololabis saira*	Pacific saury	Adult	Cold[2]		0
Charcharhiniformes	Carcharhinidae	*Prionace glauca*	Blue shark		Cold/cool		2.76
Clupeiformes	Clupeidae	*Alosa pseudoharengus*	Alewife	Juvenile	Cold		0
Clupeiformes	Clupeidae	*Alosa pseudoharengus*	Alewife	Adult	Cold		0
Clupeiformes	Clupeidae	*Clupea harengus*	Herring	Young-of-year	Cold		0
Clupeiformes	Clupeidae	*Clupea harengus*	Herring	Adult	Cold		0
Clupeiformes	Clupeidae	*Clupea harengus*	Herring	Juvenile	Cold		0
Clupeiformes	Clupeidae	*Dorosoma cepedianum*	Gizzard shad		Cool		3.86
Cypriniformes	Catostomidae	*Catostomus commersoni*	White sucker	Juvenile	Cool	0 (0-15; n = 15)	
Cypriniformes	Cyprinidae	*Cyprinus carpio*	Common carp	Juvenile	Warm	0 (0-13; n = 30)	
Cypriniformes	Cyprinidae	*Gila cypha*	Humpback chub	Juvenile, sub-adult			7.84
Cypriniformes	Cyprinidae	*Hypophthalmichthys molitrix*	Silver carp		Cool/warm		7.96
Cypriniformes	Cyprinidae	*Hypophthalmichthys nobilis*	Bighead carp		Cool/warm		5.37
Cypriniformes	Cyprinidae	*Notropis bairdi*	Red River shiner		Warm		17.79
Cypriniformes	Cyprinidae	*Phoxinus* spp.	Dace	Juvenile and adult	Cool		5.5
Cypriniformes	Cyprinidae	*Pimephales promelas*	Fathead minnow		Cool/warm[3]		3.28
Cypriniformes	Cyprinidae	*Ptychocheilus oregonensis*	Northern pikeminnow				3.23
Clupeiformes	Engraulidae	*Anchoa mitchilli*	Bay anchovy	Juvenile and adult	Cool/warm[4]		5.22
Cyprinodontiformes	Fundulidae	*Fundulus parvipinnis*	California killifish	Juvenile and adult	Cool/warm		5.93

Table 3.1 contd.

Cyprinodontiformes	Fundulidae	*Fundulus zebrinus*	Plains killifish		Warm		16.1
Cyprinodontiformes	Poeciliidae	*Gambusia affinis*	Western mosquitofish	Juvenile and adult	Warm[4]		7.54
Esociformes	Esocidae	*Esox lucius*	Northern pike	Juvenile	Cool	0 (0-6; n = 84)	
Esociformes	Esocidae	*Esox lucius*	Northern pike	Adult	Cool		4.35
Esociformes	Esocidae	*Esox masquinongy*	Muskellunge	Adult	Warm		6.27
Esociformes	Esocidae	*E. masquinongy* X *E. lucius*	Tiger muskellunge	Juvenile	Cool/warm		6.17
Gadiformes	Gadidae	*Gadus morhua*	Atlantic cod	Juvenile and adult	Cold		0
Gadiformes	Gadidae	*Gadus morhua*	North Sea cod		Cold		0
Gadiformes	Gadidae	*Theragra chalcogramma*	Walleye pollock	Adult	Cold		0
Gadiformes	Gadidae	*Theragra chalcogramma*	Walleye pollock	Juvenile	Cold		0
Gadiformes	Lotidae	*Lota lota*	Burbot	Juvenile and adult	Cold/cool		1.22
Gasterosteiformes	Gasterosteidae	*Gasterosteus aculeatus*	Threespine stickleback		Cold		4.27
Osmeriformes	Osmeridae	*Osmerus mordax*	Rainbow smelt	Adult	Cold		0
Osmeriformes	Osmeridae	*Osmerus mordax*	Rainbow smelt	Juvenile	Cold		0
Osmeriformes	Osmeridae	*Osmerus mordax*	Rainbow smelt	Young-of-year	Cold		0
Perciformes	Centrarchidae	*Ambloplites rupestris*	Rock bass	Juvenile	Cool	7 (0-17; n = 13)	
Perciformes	Centrarchidae	*Archoplites interruptus*	Sacramento perch		Cool[5]		0.82
Perciformes	Centrarchidae	*Centrarchus macropterus*	Flier	Juvenile	Warm	4 (0-20; n = 7)	
Perciformes	Centrarchidae	*Lepomis auritus*	Redbreast sunfish	Juvenile	Warm	6 (0-13; n = 10)	
Perciformes	Centrarchidae	*Lepomis cyanellus*	Green sunfish	Juvenile	Warm	4 (0-20; n = 6)	
Perciformes	Centrarchidae	*Lepomis gulosus*	Warmouth	Juvenile	Warm	0 (0-13; n = 28)	
Perciformes	Centrarchidae	*Lepomis macrochirus*	Bluegill sunfish	Adult	Warm		4.64
Perciformes	Centrarchidae	*Lepomis macrochirus*	Bluegill sunfish	Juvenile	Warm	0 (0-12; n = 68)	8.63
Perciformes	Centrarchidae	*Lepomis megalotus*	Longear sunfish	Juvenile	Warm	10 (0-20; n = 11)	
Perciformes	Centrarchidae	*Lepomis microlophus*	Redear sunfish	Juvenile	Warm	0 (0-19; n = 15)	
Perciformes	Centrarchidae	*Micropterus dolomieui*	Smallmouth bass	Young-of-year*	Warm		11.61
Perciformes	Centrarchidae	*Micropterus dolomieui*	Smallmouth bass	Sub-adult, adult*	Warm		5.78
Perciformes	Centrarchidae	*Micropterus dolomieui*	Smallmouth bass	Juvenile	Warm	0 (0-10; n = 29)	
Perciformes	Centrarchidae	*Micropterus salmoides*	Largemouth bass	Juvenile	Warm	0 (0-9; n = 132)	
Perciformes	Centrarchidae	*Micropterus salmoides*	Largemouth bass	Adult	Warm		7.36
Perciformes	Centrarchidae	*Pomoxis annularis*	White crappie	Adult	Cool		6.2
Perciformes	Centrarchidae	*Pomoxis nigromaculatus*	Black crappie	Juvenile	Cool	1 (0-14; n = 20)	
Perciformes	Cichlidae	*Tilapia* spp.	Tilapia	Adult			8.51
Perciformes	Gobiidae	*Neogobius melanostomus*	Round goby		Cool		2.17
Perciformes	Latidae	*Lates niloticus*	Nile perch		Warm[6]		7.17

Table 3.1 contd.

Perciformes	Moronidae	*Morone chrysops*	White bass	Larvae	Warm		9.35
Perciformes	Moronidae	*Morone chrysops*	White bass	Juvenile	Warm	0 (0-18; n = 40)	
Perciformes	Moronidae	*Morone saxatilis*	Striped bass	Larvae	Cool		9.35
Perciformes	Moronidae	*Morone saxatilis*	Striped bass	Young-of-year	Cool		0.63
Perciformes	Moronidae	*Morone saxatilis*	Striped bass	Age-1	Cool		0
Perciformes	Moronidae	*Morone saxatilis*	Striped bass	Age-2	Cool		0
Perciformes	Moronidae	*Morone saxatilis*	Striped bass	Adult	Cool		0
Perciformes	Percidae	*Gymnocephalus cernuus*	Ruffe		Cool		1.28
Perciformes	Percidae	*Perca flavescens*	Yellow perch	Larvae*	Cool		8.18
Perciformes	Percidae	*Perca flavescens*	Yellow perch	Juvenile	Cool	5 (0-14; n = 110)	6.28
Perciformes	Percidae	*Perca flavescens*	Yellow perch	Adult	Cool		0.9
Perciformes	Percidae	*Perca fluviatilus*	Eurasian perch	1 g	Cool		8.47
Perciformes	Percidae	*Perca fluviatilus*	Eurasian perch	100 g	Cool		5.5
Perciformes	Percidae	*Sander vitreus*	Walleye	Larvae, juvenile	Cool		4.26
Perciformes	Percidae	*Sander vitreus*	Walleye	Juvenile	Cool	0 (0-7; n = 57)	
Perciformes	Percidae	*Sander vitreus*	Walleye	Adult	Cool		0
Perciformes	Percidae	*S. vitreus* X *S. canadensis*	Saugeye		Cool		6.54
Perciformes	Percidae	*Sander lucioperca*	Zander	Adult	Cool		3.38
Perciformes	Pomatomidae	*Pomatomus saltatrix*	Bluefish	Age 0-2	Warm[7]		4.59
Perciformes	Sciaenidae	*Cynoscion regalis*	Weakfish	Young-of-year	Warm[7]		9.43
Perciformes	Sciaenidae	*Cynoscion regalis*	Weakfish	Juvenile and adult	Warm[7]		8.07
Petromyzontiformes	Petromyzontidae	*Petromyzon marinus*	Sea lamprey		Cold		0
Plueronectiformes	Achiropsettidae	*Paralichthys lethostigma*	Southern flounder		Warm		8.3
Salmoniformes	Salmonidae	*Brachymystax lenok*	Lenok		Cold		0
Salmoniformes	Salmonidae	*Coregonus artedi*	Cisco	Juvenile	Cold	0 (0-11; n = 35)	
Salmoniformes	Salmonidae	*Coregonus clupeaformis*	Lake whitefish	Juvenile	Cold	0 (0-7; n = 66)	
Salmoniformes	Salmonidae	*Coregonus clupeaformis*	Lake whitefish	Adult	Cold		0
Salmoniformes	Salmonidae	*Coregonus hoyi*	Bloater chub	Adult	Cold		0
Salmoniformes	Salmonidae	*Coregonus* spp.	Generalized coregonid		Cold		0
Salmoniformes	Salmonidae	*Oncorhynchus gorbuscha*	Pink salmon	Adult	Cold		0
Salmoniformes	Salmonidae	*Oncorhynchus kisutch*	Coho salmon	Adult	Cold		0
Salmoniformes	Salmonidae	*Oncorhynchus mykiss*	Steelhead	Adult	Cold		0
Salmoniformes	Salmonidae	*Oncorhynchus mykiss*	Rainbow trout	Juvenile	Cold	0 (0-16; n = 11)	0
Salmoniformes	Salmonidae	*Oncorhynchus nerka*	Sockeye salmon	Adult	Cold		0
Salmoniformes	Salmonidae	*Oncorhynchus tshawytscha*	Chinook salmon	Adult	Cold		0

Table 3.1 contd.

Salmoniformes	Salmonidae	*Salmo trutta*	Brown trout		Cold/cool		0
Salmoniformes	Salmonidae	*Salvelinus confluentus*	Bull trout	Adult	Cold		0
Salmoniformes	Salmonidae	*Salvelinus fontinalis*	Brook trout	Juvenile and adult	Cold		0
Salmoniformes	Salmonidae	*Salvelinus namaycush*	Lake trout	Juvenile	Cold	0 (0-7; n = 31)	
Salmoniformes	Salmonidae	*Thymallus arcticus baicalensis*	Baikal grayling		Cold		0
Scorpaeniformes	Cottidae	*Cottus asper*	Prickly sculpin	Adult	Cold		0.48
Scorpaeniformes	Scorpaenidae	*Pterois* spp.	Indo-Pacific lionfish	Juvenile and adult	Warm		13.11
Siluriformes	Ictaluridae	*Ameiurus melas*	Black bullhead	Juvenile	Warm	0 (0-12; n = 80)	
Siluriformes	Ictaluridae	*Ameiurus natalis*	Yellow bullhead	Juvenile	Warm	10 (0-20; n = 5)	
Siluriformes	Ictaluridae	*Ameiurus nebulosus*	Brown bullhead		Warm		5.19
Siluriformes	Ictaluridae	*Ameiurus nebulosus*	Brown bullhead	Juvenile	Warm	0 (0-14; n = 8)	
Siluriformes	Ictaluridae	*Ictalurus furcatus*	Blue catfish	Juvenile	Warm	0 (0-20; n = 25)	
Siluriformes	Ictaluridae	*Ictalurus punctatus*	Channel catfish	Juvenile	Warm	18 (0-20; n = 27)	
Siluriformes	Ictaluridae	*Pylodictus olivaris*	Flathead catfish	Juvenile	Warm	0 (0-20; n = 11)	

*Bioenergetics models that required modifications to parameters and settings in order to produce realistic results (see Supplementary Data File 2)
[1]Blevins (2011); [2]Tseng et al. (2011); [3]Cherry et al. (1977); [4]Coutant (1977); [5]Moyle and Knight (1984); [6]Nyboer and Chapman (2017); [7]Wyllie et al. (1976)

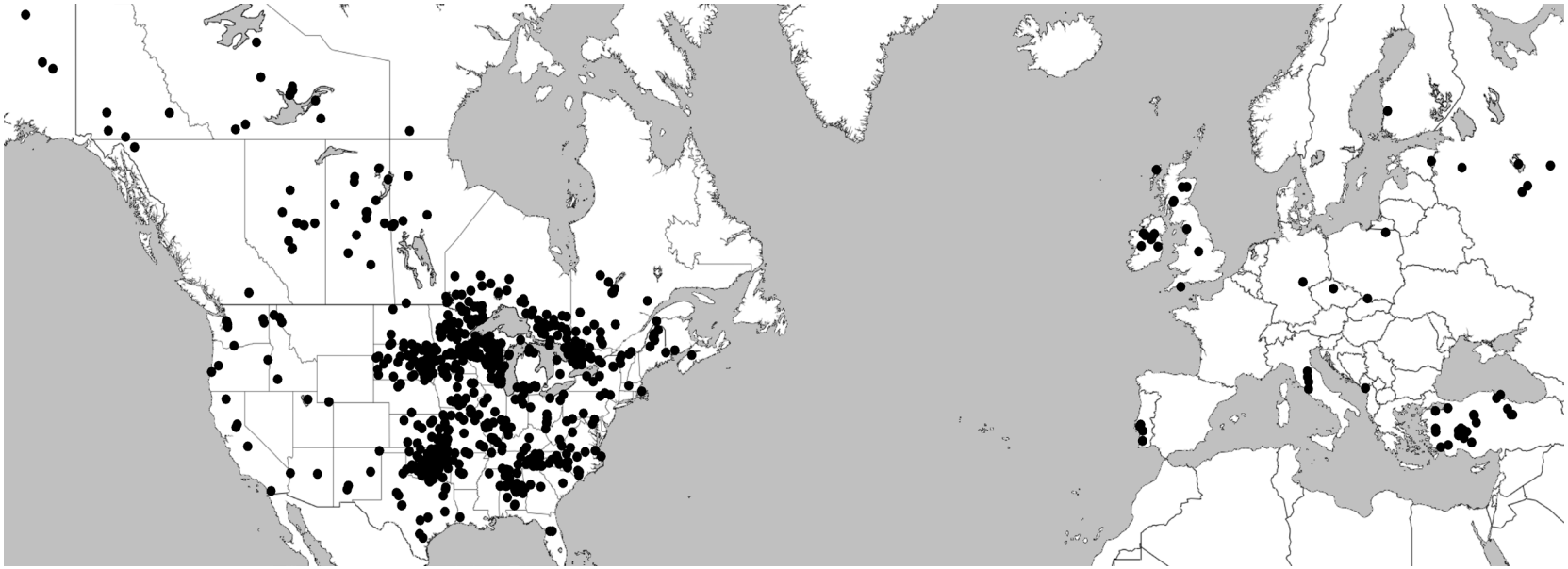

Figure 3.1 Locations of the 978 populations from which mean fish length-at-age data were compiled for estimating the base temperature for growth (T_0) via the empirical growth analysis. See Supplementary Data File 1 for a complete description of the data.

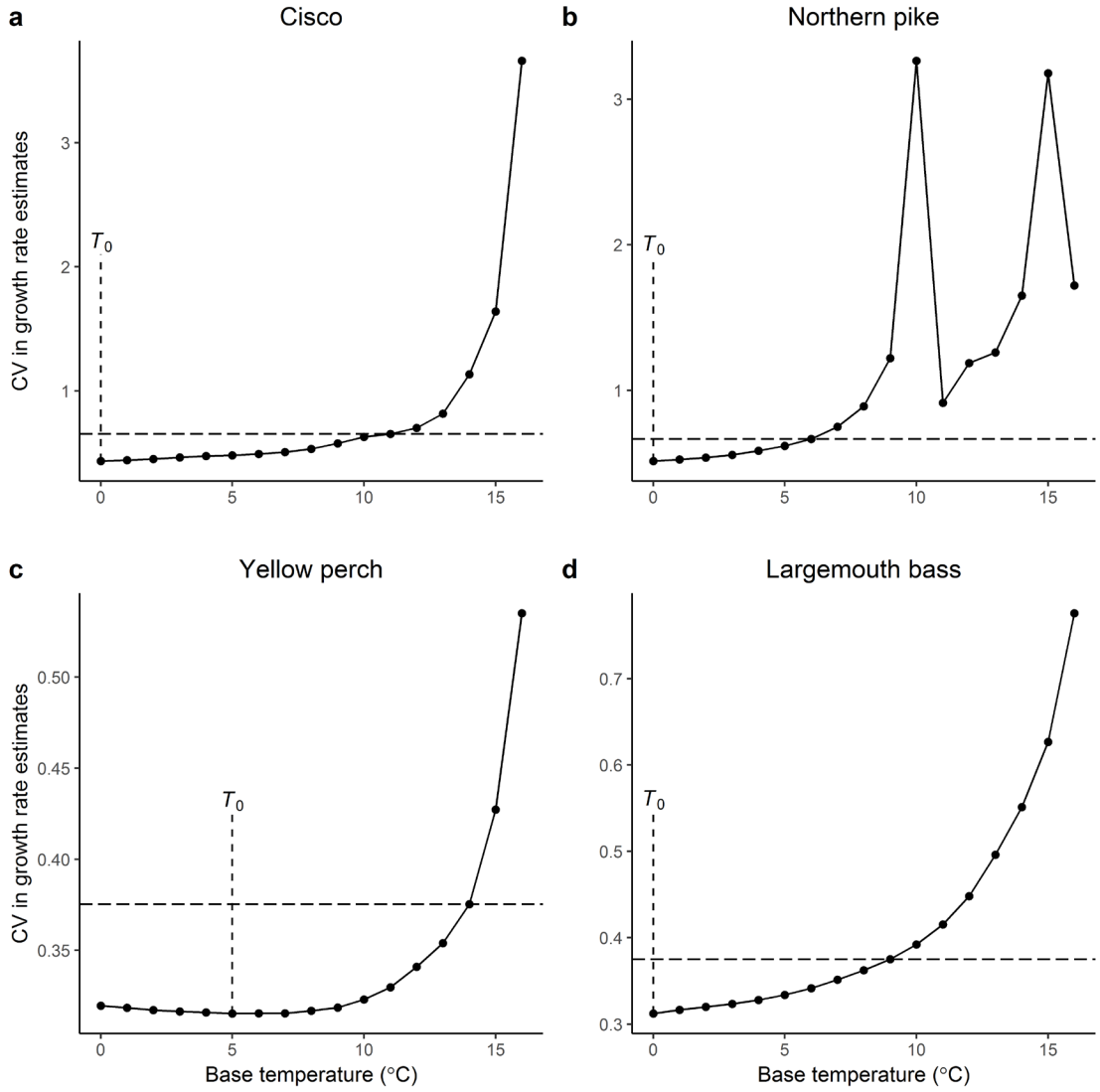

Figure 3.2 Example relationships between the coefficient of variation (CV) in temperature-corrected growth rate estimates among populations and the base temperature used to calculate degree-days for (a) *Coregonus artedi* (n = 35 populations), (b) *Esox lucius* (n = 84 populations), (c) *Perca flavescens* (n = 110 populations), and (d) *Micropterus salmoides* (n = 132 populations). We considered the base temperature at which the CV in growth rate estimates was minimized as the best estimate for the base temperature for growth (T_0; vertical dashed lines). The horizontal dashed line indicates the cutoff above which CVs in growth rate estimates were significantly different from the minimum. In some cases, such as in (b), CVs shifted dramatically at relatively high base temperatures due to changes in sample size (i.e., 0 degree-days at high base temperatures for some high-latitude populations). Although we conducted analyses at base temperatures ranging from 0-20 ºC, we show results for 0-16 ºC to facilitate the visualization of trends at low base temperatures.

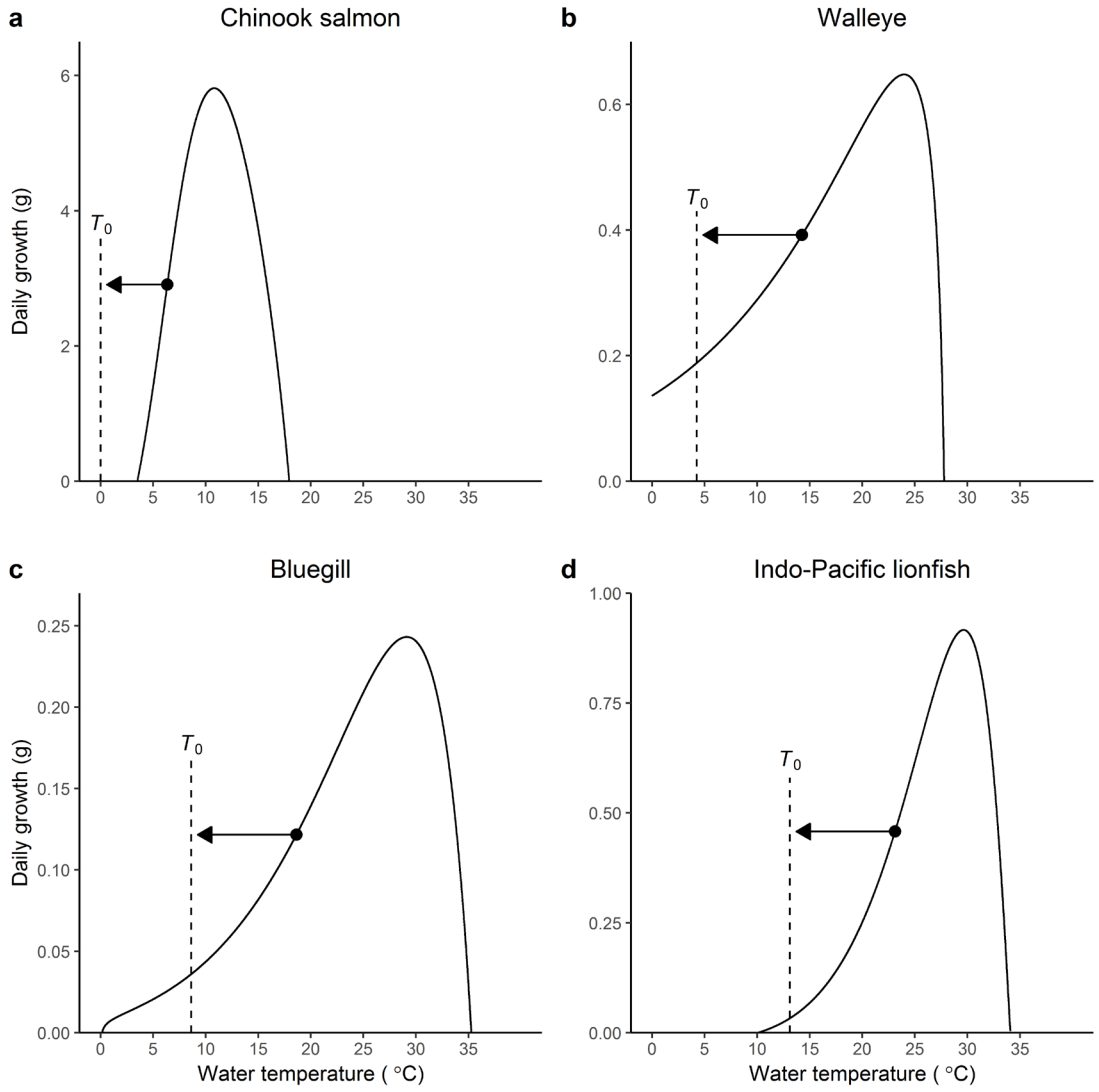

Figure 3.3 Example bioenergetics model-derived relationships between daily growth (g) and water temperature (ºC) for (a) adult *Oncorhynchus tshawytscha*, (b) larval and juvenile *Sander vitreus*, (c) juvenile *Lepomis macrochirus*, and (d) juvenile and adult *Pterois* spp. We estimated base temperatures for growth (T_0; vertical dashed lines) by subtracting 10 ºC (arrows) from the temperature at the mean growth rate (defined as the mean between the low-temperature minimum and maximum growth rates; points). We set T_0 to 0 ºC for cases in which this process resulted in a negative estimate for T_0, as in (a).

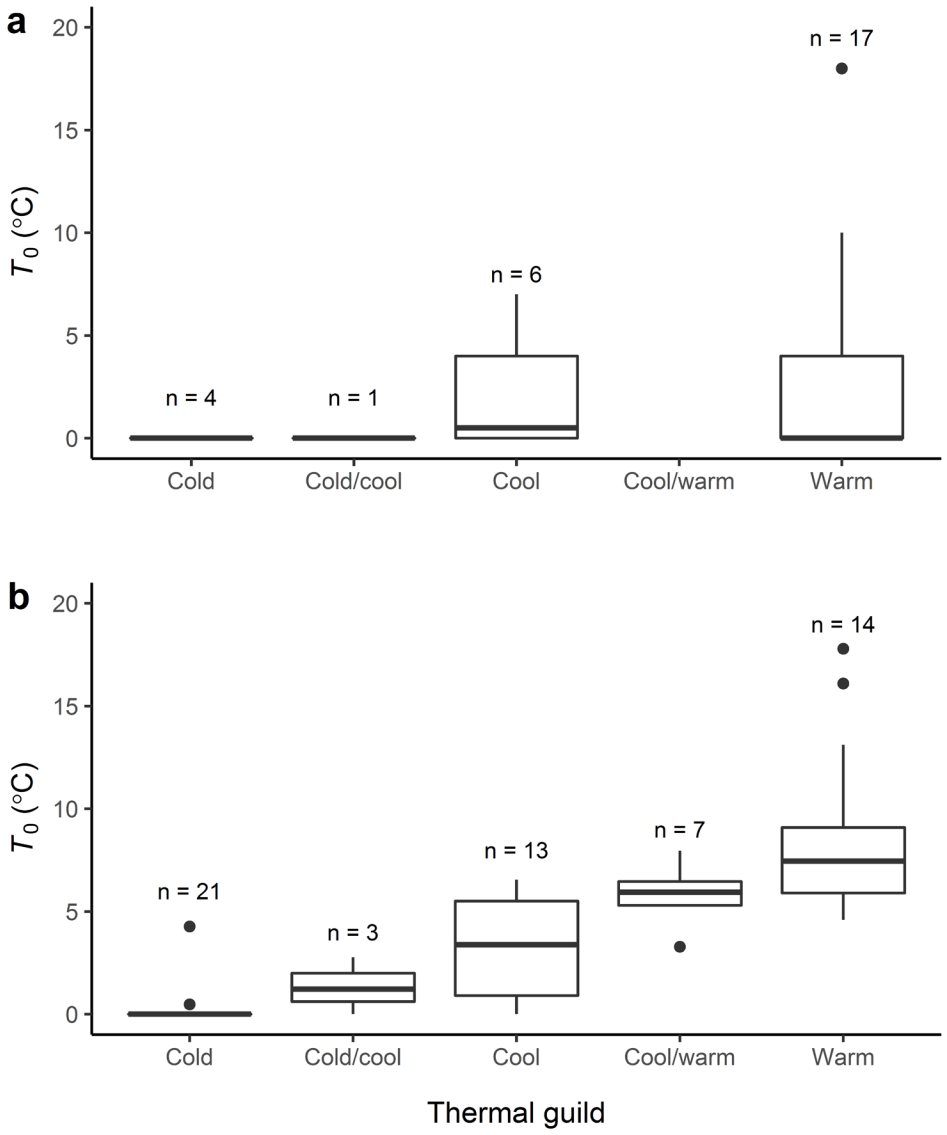

Figure 3.4 Estimates of the base temperature for growth (T_0; ºC) for species across thermal guilds from (a) the empirical growth analysis and (b) the 10 ºC rule approach.

Chapter 4

Accurate estimates of age at maturity from the growth trajectories of fishes and other ectotherms

Synopsis

Age-at-maturity (AAM) is a key life history trait that provides insight into ecology, evolution, and population dynamics. However, maturity data can be costly to collect or may not be available. Life history theory suggests that growth is biphasic for many organisms, with a change-point in growth occurring at maturity. If so, then it should be possible to use a biphasic growth model to estimate AAM from growth data. To test this prediction, we used the Lester biphasic growth model in a likelihood profiling framework to estimate AAM from length-at-age data. We fit our model to simulated growth trajectories to determine minimum data requirements (in terms of sample size, precision in length-at-age, and the cost to somatic growth of maturity) for accurate AAM estimates. We then applied our method to a large walleye *Sander vitreus* data set and show that our AAM estimates are in close agreement with conventional estimates when our model fits well. Finally, we highlight the potential of our method by applying it to length-at-age data for a variety of ectotherms. Our method shows promise as a tool for estimating AAM and other life history traits from contemporary and historical samples.

4.1 Introduction

Age-at-maturity (AAM) is an important life history trait in ecology and evolution that affects lifetime reproductive success and other fitness components (Stearns and Koella 1986, Roff 1992, Stearns 1992, Bernardo 1993, Berrigan and Charnov 1994, Engelhard et al. 2003, Stearns and Hoekstra 2005, Brunel et al. 2013). Estimates of AAM can be used to address questions related to life history plasticity (e.g., Reznick 1990, Augert and Joly 1993, Ebert 1994, Kuwamara et al. 1996, Lester et al. 2014) and evolution (e.g., Charnov and Berrigan 1990, Heino et al. 2002, Kuparinen and Merilä 2007), as indicators of stress (Trippel 1995), and for management purposes (e.g., fisheries stock assessment; Hilborn and Walters 1992). Conventional methods for estimating AAM at the population level include logistic regression (Chen and Paloheimo 1994), probit analysis (Hubert 1984), probabilistic methods (DeMaster 1978), visual inspection, and others (Trippel and Harvey 1991). All of these methods require individual maturity data, which can be costly to collect and may be absent for historical samples.

Life history theory suggests that resource allocation and therefore growth change throughout ontogeny (Roff 1992, Stearns 1992, Kozlowski 1996). In many organisms, a shift in resource allocation occurs at maturity, when individuals begin to invest energy in reproduction (Kozlowski 1996, Quince et al. 2008a, Mollet et al. 2010). For indeterminate growers, this shift in resource allocation leads to slower growth in adults (Day and Taylor 1997, Lester et al. 2004, Quince et al. 2008a, Lester et al. 2014, Minte-Vera et al. 2016). Unfortunately, conventional growth models (e.g., the von Bertalanffy growth model; VBGM; von Bertalanffy 1938, Beverton and Holt 1957) are single curves

that do not explicitly account for this shift (Day and Taylor 1997). To address this issue, a number of biphasic growth models have been proposed that include a change-point in growth that occurs at maturity (Lester et al. 2004, Quince et al. 2008a, Mollet et al. 2010, Boukal et al. 2014, Minte-Vera et al. 2016). For example, the basic form of the Lester model (LM) assumes that immature growth is linear because surplus energy is invested solely in somatic growth, while mature growth is asymptotic because energy is invested in both somatic growth and reproduction (Lester et al. 2004). Because it is grounded in life history theory, the LM is suitable for addressing life history questions (Boukal et al. 2014) and allows for the estimation of numerous life history traits (e.g., juvenile growth rate, length-at-maturity, asymptotic length, the cost to somatic growth of maturity, natural mortality rate; Lester et al. 2004).

The LM was designed for datasets that include estimates of AAM. However, if immature and mature growth rates differ, then it should be possible to use the LM to not only describe lifetime growth, but also estimate AAM. If the LM can be fit to length-at-age data without estimates of AAM, then it could be a powerful tool for estimating life history traits from contemporary and historical samples. Previous attempts to estimate AAM from growth data using breakpoint linear regressions (Rijnsdorp and Storbeck 1995, Baulier and Heino 2008, Scott and Heikkonen 2012), modified forms of the VBGM (Ohnishi et al. 2012), biphasic growth models (Mollet et al. 2010, Brunel et al. 2013, Uusi-Heikkilä et al. 2015, Chavarie et al. 2016, Minte-Vera et al. 2016), and discriminant and neural network analyses (Engelhard et al. 2003) have produced varying results (reviewed in Section 4.4iii). Two recent studies have used the LM to estimate

AAM from length-at-age data (Uusi-Heikkilä et al. 2015, Chavarie et al. 2016), but their methods have not been validated and rely on indirect assessments for inference on parameter values. Thus, the potential and limitations of the LM as a tool for estimating AAM and other life history parameters remain largely unexplored.

Herein, we (1) describe a likelihood-based method for estimating AAM from length-at-age data using the LM, (2) conduct a simulation study to outline data quality requirements and provide application guidelines, and (3) use empirical data to assess the performance of the method. Our method provides direct inference on parameter values, allows for simple assessments of fit quality, and, given sufficient data quality, accurately estimates AAM for fishes and other ectotherms.

4.2 Methods

i) *Overview*

We used the "fixed g" formulation of the LM (Lester et al. 2004, Quince et al. 2008a, Lester et al. 2014) to test the prediction that AAM can be accurately estimated from length-at-age data. This formulation assumes that metabolism scales with body size in a 2/3 power relationship and that the cost to somatic growth of maturity (typically assumed to be dominated by investment in reproduction; Roff 1983, Kozlowski 1996) is constant for adults. For length at time t (i.e., l_t), the growth trajectory is given by

(1) $$l_t = l_0 + ht, \ t \leq T \text{ for juveniles,}$$

(2) $$l_t = l_\infty\left(1 - e^{-k(t-t_0)}\right), \ t > T \text{ for adults,}$$

with

$$t_1 = -\frac{l_0}{h}$$

$$l_\infty = \frac{3h}{g}$$

$$k = \ln(1 + \frac{g}{3})$$

$$t_0 = T + \ln\left(1 - \frac{g(T - t_1)}{3}\right) / \ln\left(1 + \frac{g}{3}\right)$$

(see Table 4.1 for parameter descriptions). The deterministic model can be defined as a function of four parameters: l_0, h, T, and g. To fit the LM to length-at-age data, we assumed a normal distribution for length given age, the mean of which is given by equation 1 for immature individuals and equation 2 for mature individuals. The result is a joint likelihood function comprised of 5 unknown parameters, $Lik(l_0, h, T, g, \sigma^2)$. To improve model performance, we included information on l_0 and h in the form of normal marginal likelihoods (which account for uncertainty in l_0 and h estimates), and used the resulting estimated likelihood for inference (Pawitan 2013); i.e., $Lik(l_0, h, T, g, \sigma^2) = Lik(l_0)*Lik(h)*Lik(T, g, \sigma^2 | l_0, h)$. We used a two-step process to specify the marginal likelihoods and fit the full model from a single dataset. Note that if separate data are available for $Lik(l_0)$ and $Lik(h)$, then this becomes a combined likelihood that, like a Bayesian posterior, incorporates prior information (Pawitan 2013).

We used a likelihood-based evidentialist approach (Royall 1997, 2004, Sober 2008) to infer AAM and other life history parameters from length-at-age data. According to the law of likelihood (Hacking 1965), the ratio of the likelihood for different parameter values gives a direct measure of evidential support in the data for a given parameter value

relative to another value, allowing for the construction of likelihood ratio intervals that represent the range of parameter values that are supported by the data. We used profile likelihoods to generate likelihood intervals (Kalbfleisch and Sprott 1970, Taper and Lele 2011) for evaluating parameter estimability in application (Raue et al. 2009). To generate likelihood intervals for T (the Lester model parameter for AAM), we constructed vectors of $T_i = [T_1, T_2, \ldots, T_m]$ and maximized the likelihood over $[l_0, h, g, \sigma^2]$ for each T_i. The likelihood interval for T included all T_i such that $Lik(T_{MLE})/Lik(T_i) < \varkappa$. Royall (1997) recommends a value of $\varkappa = 8$ for strong evidence, meaning that every value outside of the interval is < 1/8 as likely as the maximum likelihood estimate. Although the likelihood method does not assume a distribution for the likelihood ratio, the intervals are similar in form to a frequentist confidence interval that is based on a chi-squared approximation of the likelihood ratio distribution. For comparison purposes, $\varkappa = 8$ in a likelihood interval corresponds to a ~96% confidence interval.

ii) *Simulation study*

We conducted a simulation study to determine the data requirements and estimate reliability of our Lester model likelihood profiling (LMLP) method. Specifically, we focused on the accuracy of the LMLP estimator for T across variation in three important factors: sample size, precision in length-at-age, and the maturity cost parameter g. We defined precision as the inverse of the coefficient of variation in length-at-age (i.e., as precision increases, variability in length-at-age decreases). We simulated individuals that grew according to the LM with growth parameters that were loosely based on walleye

Sander vitreus, a well-studied, predatory game fish that is common throughout northern North America (T = 5 yrs, l_0 = 100 mm, h = 50 mm·yr^{-1}, maximum age = 25 yrs; Bozek et al. 2011). Each population initially consisted of 1000 individuals from which we drew random samples of varying sizes. To replicate common sampling methods, we adjusted sample sizes-at-age for gear selectivity and natural mortality (see Appendix 3, Section A3.1, Table A3.1). We chose ten levels for each of the three sampling factors (ranges: sample size=50-1000 individuals; precision=4-30; g=0.05-0.3; Table A3.2). A new population of individuals was generated for each of 100 iterations of all possible three-way factor level combinations (100,000 simulations). We performed all simulations and subsequent calculations in R version 3.2.0 (R Core Team 2015) with the additional packages car (Fox and Weisberg 2011) and boot (Davison and Hinkley 1997, Canty and Ripley 2015).

We applied LMLP separately for each iteration and constructed profile likelihoods for T. The vector of T values ranged from 1-16 yrs in increments of 0.025 yrs (i.e., 601 values of T). We defined the marginal likelihoods for l_0 and h as normal distributions with standard deviations of 25 mm and 5 mm·yr^{-1}, respectively, with means equal to the slope (h) and intercept (l_0) estimates from a linear model fit to the first four ages in the simulated sample (actual ages varied due to random sampling). To maximize the likelihood for each T_i, we used the optim function with the following starting values: l_0=linear model intercept estimate, h=linear model slope estimate, g=0.15, σ=25. The likelihood intervals included all T_i such that $Lik(T_{MLE})/Lik(T_i) < 8$.

To quantify accuracy in T_{MLE} across factor levels, we calculated the mean percent error in T_{MLE} for each factor combination. We used an error contour plot (smoothed using LOESS with degree = 2 and α = 0.75) to determine the sample size and precision required for T_{MLE} to fall within +/- 0.5 yrs of the true value across levels of g. Because sample size is known and precision can be calculated *a priori*, the contour plot allows for visual estimation of the minimum value of g needed for accurate estimates of AAM.

iii) *Empirical assessment*

We compared the LMLP AAM estimator to a conventional approach (age-at-50% maturity; A_{50}) using age, length, sex, and maturity data from walleye that were collected in Ontario and Quebec, Canada during fall gill net surveys (1993-2008; Morgan 2002), and Minnesota, USA during trap-netting, trawling, seining, angling, gillnetting, electrofishing, and trot-lining surveys (March-December, 2001-2011; Chezik et al. 2014a). To prepare these data for analysis and minimize the incidence of erroneous ages, we removed (1) samples from the period December-July, (2) fish above age-0 that were aged in the field, (3) fish above age-5 that were aged using scales, and (4) males. We focused on females because (1) they are often the focus of life history studies in fisheries due to their importance with regard to evolution and stock productivity (e.g., Herczeg et al. 2012, Hixon et al. 2014), and (2) maturity status based on visual inspection of gonads may be more reliable for females than males due to the more obvious appearance of ovaries with eggs. The resulting dataset contained a large number of unsexed fish. Given that immature walleye grow at similar rates regardless of sex (Venturelli et al. 2010) and

in order to preserve realistic sample sizes-at-age, we assumed a 1:1 sex ratio for immature fish and randomly removed half of the unsexed fish that were smaller than the smallest mature male (143 mm total length). That is, we retained half of the unsexed fish that were very likely to be immature. We then removed all unsexed fish above this size to avoid including mature males, which could skew our estimates of female AAM and other parameters due to sexually dimorphic maturity (Venturelli et al. 2010).

We first applied LMLP to data from individual lakes in a single year (lake-year). We selected one lake-year from each lake in an effort to span as much of the sample size and precision parameter space as possible. To increase sample size, we then combined data from up to three consecutive lake-years and analyzed them as a single lake-year (multi-lake-year). We used the same LM fitting procedure for these data as for our simulation study. Because we had no prior knowledge of T for these datasets, and because other estimates of AAM can be inaccurate (Trippel and Harvey 1991), we identified a good fit as having one likelihood peak and a likelihood interval ≤ 2 yrs. We estimated precision in length-at-age for these datasets by averaging the inverse of the coefficient of variation in length at each age across all ages, weighted by sample size-at-age. As such, our estimate of precision in length-at-age included all potential sources of variation, including individual variation in growth, sampling bias, and processing error.

To compare LMLP to conventional estimators, we compared T_{MLE} from good fits to $\widehat{A_{50}}$ from logistic regression using a standard major axis regression, which assumes error in both variables. Given that female walleye gonadal investment during the preceding growing season is likely visible during August-November, T_{MLE} (the age at

which the average individual begins to invest in reproduction) and A_{50} (the age at which half of the individuals that were collected in fall had developed gonads) should be similar.

To explore LMLP performance in estimating AAM for a broad variety of taxa, we also applied LMLP to empirical length-at-age data describing another freshwater fish (lake whitefish *Coregonus clupeaformis*), a marine fish (haddock *Melanogrammus aeglefinus*), an elasmobranch (Alaska skate *Bathyraja parmifera*; Matta and Gunderson 2007), and an amphibian (the seal salamander *Desmognathus monticola*; Castanet et al. 1996; see Appendix 3, Section A3.2 for data descriptions). Because our goal was to demonstrate that LMLP can work for many species, we selected data for which LMLP fits were good. Due to the low sample size (n = 4), we compared T_{MLE} from these fits to $\widehat{A_{50}}$ by calculating the confidence interval for the difference between the two parameters (Daniel and Cross 2013). If this interval contained zero, the parameters were considered not significantly different from one another (see Appendix 3, Section A3.2 and Table A3.3).

4.3 Results

i) *Simulation study*

Simulation results suggest that LMLP performance is positively related to each data quality factor (i.e., sample size, precision, and g), and that a low value of one factor will result in poor LMLP performance unless the remaining factors are high enough to compensate. The sample size and precision required for T_{MLE} to fall within +/- 0.5 yrs of

T across values of g are shown in Fig. 4.1 (gray lines; see Fig. A3.1 for an error contour plot without empirical data points). In general, LMLP performed poorly for sample sizes < 100-150 individuals, precision in length-at-age < 6, and g < 0.1. Across all simulations, T_{MLE} was biased above the simulated value of 5 yrs (mean = 5.39 yrs, sd = 1.85 yrs); however, nearly all of this bias occurred when the likelihood interval was > 2 yrs wide (n = 47,419; mean = 5.74 yrs; sd = 2.46 yrs). Both bias and variability in T_{MLE} were smaller when LMLP likelihood intervals were ≤ 2 yrs (n = 52,581; mean = 5.07 yrs, sd = 0.92 yrs). Most of the remaining bias resulted from cases in which likelihood intervals were ≤ 2 yrs but T_{MLE} was very high (≥ 13 yrs; n=338), all of which occurred when sample size was < 150 individuals, precision was < 6, and/or g was < 0.1 (without these cases, mean = 5.01 yrs, sd = 0.37 yrs; see Appendix 3, Section A3.3 and Figs. A3.2-A3.11 for additional diagnostics). Results were similar for the remaining parameters in that estimates were biased when likelihood intervals were wide, but virtually unbiased when they were narrow.

ii) *Empirical assessment*

Our empirical analysis included 46 lake-years and 11 multi-lake-years (Table A3.4). LMLP fits were good for 40 of these datasets and poor for the remaining 17 (see Fig. 4.2 for examples of good and poor fits). When compared to our simulation results, 51 (89%) of the datasets were above their respective error contours (i.e., should be accurate within +/- 0.5 yrs) for the nearest (lower) value of g, based on $\hat{g}$ from a LMLP fit (Fig. 4.1; Table A3.4). LMLP fit poorly to twelve (21%) of these datasets. For seven of these poor

fits, T_{MLE} estimates were between 2-4 yrs, which might suggest a need for higher data quality when $T < 5$. Of the six (11%) datasets that were below their respective error contours, only one was a good fit (Lac Regnault in 1998; n=150, precision=14.30, $\hat{g}$=0.12).

The standard major axis regression indicated that T_{MLE} was not significantly different from $\widehat{A_{50}}$ when LMLP fits were good (Fig. 4.3). We excluded two lake-years (Lac Regnault in 1998 and Lake St. Joseph in 1999) from the regression due to a high likelihood of erroneous ageing and/or maturity classification (see Section 4.4). The fit to T_{MLE} and $\widehat{A_{50}}$ from the remaining datasets did not significantly differ from a 1:1 line (intercept = -0.01, 95% CI = (-0.83, 0.68); slope = 0.99, 95% CI = (0.84, 1.18)), and the mean difference between T_{MLE} and $\widehat{A_{50}}$ was 0.50 yrs (sd = 0.41 yrs, range 0-2 yrs).

The confidence intervals for the differences between T_{MLE} and $\widehat{A_{50}}$ contained zero for all four LMLP fits to data describing additional species (lake whitefish: (-0.81, 1.21); haddock: (-0.72, 0.44); Alaska skate: (-0.03, 1.45); seal salamander: (-0.65, 0.56)), suggesting that LMLP can accurately estimate AAM for a variety of ectotherms (Fig. 4.4; see Table A3.3 for additional details).

4.4 Discussion

i) *Simulation study*

We designed our simulation study to determine the conditions required for LMLP estimates of AAM (i.e., T_{MLE}) to fall within +/- 0.5 yrs of the true value given the "ideal" case in which individuals grow according to the LM. We found that T_{MLE} was biased

high for poor LMLP fits, likely because low information on AAM led to relatively high likelihood values (which are maximized over all other parameters) for a larger range of T values. It is not unexpected that mean T_{MLE} would fall above the true value given that (1) the simulations covered many sampling factor combinations for which the model fit poorly, and (2) our vector of possible T values included more values above the true value of 5 yrs (n = 440) than below it (n = 160). Importantly, bias in T_{MLE} was much smaller when the likelihood interval was ≤ 2 yrs wide.

The error contour plot (gray lines in Fig. 4.1; Fig. A3.1) shows the values of sample size, precision, and g required for average T_{MLE} to fall within +/- 0.5 yrs of the true value. This plot can be used to assess the likelihood of an accurate LMLP fit. For example, if sample size = 300 individuals and precision = 20, then it is likely that T_{MLE} will be accurate because (300, 20) falls above a large number of error contours across values of g. However, if sample size = 50 individuals and precision = 4, an accurate fit is unlikely because (50, 4) falls beneath all error contours for g values examined herein. Such assessments can be augmented by additional information about the species or population (e.g., if g is typically ≥ 0.2 for a given species or population). For instance, for cases in which AAM is known *a priori*, one could fit a Lester model in conjunction with the maturity information (e.g., with T fixed at AAM or with likelihoods of maturity-at-age from a logistic-type model) to estimate the remaining model parameters, thereby providing insight regarding reasonable values of g for a given species or population prior to using LMLP. Moreover, one can use the error contour plot together with (1) the sample size and precision of the dataset and (2) the LMLP $\hat{g}$ to evaluate whether T_{MLE}

should be an accurate estimate of AAM. If a dataset falls above the nearest contour for g (based on $\hat{g}$ from a LMLP fit) for a given combination of sample size and precision, then T_{MLE} should be accurate within +/- 0.5 yrs, particularly if $T_{MLE} \geq 5$. For example, if a dataset falls above the error contour for $g = 0.1$, then T_{MLE} should be accurate if $\hat{g} \geq 0.1$. To be conservative, we recommend referring to the nearest lower contour for g when using the contour plot to assess T_{MLE} accuracy (as we have done for our empirical assessment). That is, if $\hat{g}$ from a LMLP fit is 0.115, then we recommend referring to the contour for $g = 0.1$ as opposed to the contour for $g = 0.125$. This means of evaluating accuracy in parameter estimation can supplement assessments of fit quality from the likelihood profile, especially when one has reason to doubt the accuracy of the model (e.g., if a likelihood profile has a single peak and a narrow confidence interval but sample size is very low).

ii) *Empirical assessment*

When applied to empirical female walleye data, LMLP fits were generally good (based on likelihood profile assessments and likelihood interval width) when simulation results suggested that they should be accurate (i.e., when datasets were above their respective error contours), and vice versa. However, there were more poor LMLP fits when datasets fell above their respective error contours (n = 12; 23.5%) than good fits when datasets fell below their respective contours (n = 1; 16.7%). This discrepancy could be due to variation in AAM among the empirical datasets. For example, if AAM is < 5 yrs, then there are fewer age classes (i.e., less information) to describe immature growth, which

likely reduces LMLP fit quality. Consistent with this hypothesis, results from two additional sets of simulations in which we varied the LM parameter for age-at-maturity (i.e., T; one with T = 3 yrs and another with T = 7 yrs) suggest that LMLP requires higher data quality when T = 3 yrs but not when T = 7 yrs (Appendix 3, Section A3.4 and Figs. A3.12-A3.14). Furthermore, variation in AAM across cohorts or lake-years (e.g., due to plastic or evolutionary changes in growth and maturation; see Enberg et al. 2012) may reduce confidence in T_{MLE} and alter LMLP data requirements. The sensitivity of LMLP to AAM could explain some of our results. For instance, T_{MLE} was 11.05 yrs for the only lake-year that fell below its error contour but had a good fit (Lac Regnault in 1998), and was between 2-4 yrs for seven of the 12 lake-years that were above the error contours but had poor LMLP fits.

In addition to variation in AAM, LMLP may also be sensitive to data distribution, data coverage, and violations of the LM. Our simulations were based on sample distributions that were comparable to fisheries data (see Appendix 3, Section A3.1 and Table A3.1), but these distributions are not always realized. For example, LMLP fit poorly to a large dataset (Upper Red Lake in 2003, n = 465) because 91% of the fish in the sample were age 2 or 4 as a result of stocking (Logsdon 2006), thus providing little information on lifetime growth. Similarly, if AAM is 6 yrs but the dataset only contains ages 6-12, then LMLP will likely fail to detect AAM. Finally, LMLP may perform poorly because the LM is inappropriate. For example, growth leading up to maturity may be non-linear. Fortunately, the LM can be relaxed to allow for non-linear immature growth (Quince et al. 2008, Boukal et al. 2014; not explored here). Additionally, lifetime growth

may span major changes in per-capita food availability, leading to additional change-points in growth that could reduce LMLP accuracy (Lorenzen and Enberg 2002). However, such changes may only have a significant impact when analyzing longitudinal data.

The standard major axis regression indicated that T_{MLE} and $\widehat{A_{50}}$ do not significantly differ when LMLP fits well. We excluded two lake-years with questionable maturity data: Lac Regnault (1998) and Lake St. Joseph (1999; Fig. 4.3, Table A3.4). For Lac Regnault (n = 150), $\widehat{A_{50}}$ = 13.67 yrs but T_{MLE} = 11.05 yrs. This discrepancy stems from three fish aged 26, 16, and 15 that were recorded as immature, likely as a result of ageing error, observational error, or cryptic maturity such as skipped spawning (Rideout et al. 2005). These probable errors had high leverage on the logistic regression; $\widehat{A_{50}}$ decreased to 12.59 yrs after removing the oldest immature fish and to 11.82 yrs after removing all three probable errors. Data from Lake St. Joseph (n = 563) appeared to contain similar errors; although T_{MLE} = 3.5 yrs, the data included multiple immature fish aged 10-16 yrs. We considered these probable errors as sufficient justification for excluding these lake-years from the analysis. Because such errors have high leverage on A_{50}, LMLP (when it fits well) may be a more reliable method for estimating AAM. Both methods assume that ageing is accurate, but LMLP assumes that length is measured accurately whereas A_{50} assumes that maturity is classified correctly. Although further work is needed, we posit that length errors are usually small and therefore unlikely to have a large impact on LMLP estimates. In contrast, maturity classification errors can lead to large errors in $\widehat{A_{50}}$. However, A_{50} may be more reliable in certain cases; for

example, changes in per-capita food availability can lead to multiple change-points in growth that would impact LMLP but not A_{50}.

iii) *Comparison to Other Methods for Estimating AAM from Growth Data*

We are not the first to attempt to estimate AAM from growth data. Rijnsdorp and Storbeck (1995) estimated AAM using a segmented linear regression of annual body mass increments against body mass derived from female plaice *Pleuronectes platessa* otoliths. The method was somewhat inaccurate when compared to independent estimates and, like LMLP, was less accurate for early AAM. Baulier and Heino (2008) applied the method and found 47.6% agreement with AAM estimated from scales for Norwegian spring-spawning herring *Clupea harengus*. Scott and Heikkonen (2012) applied a conceptually similar approach in which a segmented linear regression was fit to plaice mean length-at-age data. Their model was sometimes inaccurate compared to estimates derived from a maturation reaction norm approach, especially for males, and was also inaccurate for early AAM. Unlike LMLP, these methods do not allow for estimation of life history parameters other than AAM (e.g., the cost to somatic growth of maturity, asymptotic length, natural mortality rate).

Engelhard et al. (2003) used discriminant analysis and artificial neural networks to predict AAM from individual scale measurements for Norwegian spring-spawning herring. This method correctly classified AAM in 66-68% of cases, although the margin of error was seldom > 1 yr (2.9-5.2% of cases). Importantly, the models were highly accurate for low AAM (unlike LMLP and the other methods discussed here). As with the

segmented linear methods, these methods did not allow for estimation of additional life history parameters, but they show significant potential for estimating AAM.

Mollet et al. (2010) proposed a biphasic approach to estimate AAM and other life history parameters from individual lifetime weight-at-age data. The Mollet model is conceptually similar to LMLP, but is founded on the metabolic theory of ecology (West et al. 1997, 1999), which assumes that metabolism scales with body size according to a 3/4 power law. The model showed confounding between variables when estimating four parameters (AAM, energy acquisition, maintenance, and reproductive investment). To avoid this issue, the authors proposed a three parameter model (by assuming constant maintenance) that increased the robustness of results. After this adjustment, Mollet model estimates of AAM for female plaice were in general agreement with independent estimates. Brunel et al. (2013) reduced the confounding between parameters in the Mollet model by incorporating random effects (Laird and Ware 1982). However, this model was sensitive to starting values and struggled to converge, particularly when estimating more than four parameters. Moreover, the Brunel model was biased in some cases (up to ~45%, although some cases involved unrealistic parameter combinations) and was sometimes inaccurate in estimating AAM when compared to scale-based estimates for Norwegian spring-spawning herring (30-61% agreement, although differences in AAM estimates were < 1 yr for 97% of cases). As with LMLP, both the Mollet and Brunel models were less accurate for early AAM.

Ohnishi et al. (2012) proposed an extended VBGM that allows for estimation of AAM. Unfortunately, they did not evaluate the accuracy of their model in estimating

AAM, and they noted that practical applications of the model would necessitate additional parameters. Despite this potential disadvantage, Ohnishi et al. present an intriguing model that deserves further attention.

Minte-Vera et al. (2016) presented a review and assessment of models that incorporate the cost of reproduction, including the LM and related models (Quince-Boukal; Quince et al. 2008, Boukal et al. 2014). Although they used some of these models to estimate AAM from size and age data (including Quince-Boukal but not the LM), they focused on describing two new biphasic models and comparing their goodness-of-fit to existing models. As such, they did not rigorously assess the ability of the models to estimate AAM. In addition, they fit the models to only four empirical datasets (split by sex) describing lake trout *Salvelinus namaycush*. A more complete examination of the accuracy of the various models (particularly the two novel ones) in estimating AAM and other life history parameters is merited.

iv) *Advantages and Additional Applications of LMLP*

The LMLP method offers many advantages over other techniques for estimating AAM. It requires only length-at-age data, which are common across disciplines, and can provide accurate estimates of AAM in the absence of maturity data. In addition, LMLP provides estimates of other life history parameters, such as juvenile growth rate (h), the average cost to somatic growth of maturity (g), asymptotic length (l_∞), mean length-at-maturity, and the instantaneous rate of natural mortality (Lester et al. 2004). One could use LMLP to track changes in life history parameters over time (see Kuparinen and Merilä 2007),

compare life history parameters among populations (Chavarie et al. 2016), or estimate the vital rates of a Leslie projection matrix (Uusi-Heikkilä et al. 2015).

We used a simple version of the LM, but the LMLP approach can also be used to fit models that relax the assumptions of the "fixed g" LM that may be difficult to fit otherwise. For instance, parameters could be added to fit the "generic biphasic" model proposed by Quince et al. (2008; see also Boukal et al. 2014), which (1) allows g to vary with age, e.g., as a result of increasing investment in reproduction (Kozlowski 1996) or activity costs (Ware 1978, Andersen and Beyer 2015) and (2) relaxes the assumption that metabolism scales with body size according to a 2/3 power law, which may be inaccurate for many species (Glazier 2010).

The likelihood function is a common basis for both frequentist and Bayesian statistics, and likelihood intervals have a clear interpretation as model parameter values supported by the data. Like Bayesian methods, LMLP can incorporate information about parameters, although in both cases inference depends upon assumptions about those parameters (either a Bayesian prior or in the specification of a marginal likelihood). For applications in which data are not informative of parameters (e.g., low sample size), asymptotic results on unbiasedness for likelihood inference may not apply for profile likelihoods (Pawitan 2013). It is therefore important to verify estimator performance *via* simulation. For our analyses, we used the same two-step algorithm for all LMLP fits to simulated and empirical data for insight on sample conditions when the empirical fits may be unreliable. Likelihood profiles provide a useful means of assessing fit quality because they show the number of likely parameter values (likelihood peaks) and the

degree of confidence in those values (the width of each peak). We found that as data became less informative on AAM, likelihood intervals became wider and estimates could be biased. We also found that parameter estimates were robust to starting values (not shown). Nonetheless, fit quality and accuracy may be improved by adjusting starting values or other aspects of the algorithm, particularly when data quality is poor.

Our study focused on data describing an entire population at a particular time (i.e., cross-sectional data), but our approach can also be applied to longitudinal data that track individuals or cohorts through time. Fitting to longitudinal data may be more theoretically consistent than fitting to cross-sectional data (Mollet et al. 2010), particularly for studies of life history evolution. In addition, LMLP fits to longitudinal data may provide a more realistic understanding of life history variation (e.g., by allowing for the construction of probabilistic maturation reaction norms; Heino et al. 2002). Random effects should be included when fitting to individual lifetime growth data (Laird and Ware 1982, Brunel et al. 2013). Although LMLP can be adjusted to include random effects, incorporating these additional parameters may make the model difficult to fit; however, this impact may be minimized by including additional information on parameters.

Our LMLP algorithm has potentially broad applicability. It can work well not only for walleye, but also for any species that has a similar lifetime growth trajectory and an associated shift in growth that corresponds to maturity. Our fits to four additional species (including fishes, an elasmobranch, and an amphibian) display the potential utility of LMLP in accurately estimating AAM for a variety of taxa. The LMLP

algorithm may be particularly useful when only length-at-age data are available or attainable. However, because LMLP may not work well for some species (e.g., due to violations in the assumptions of the LM), more work is needed to determine the reliability and data quality requirements of LMLP across taxa.

v) *Conclusion*

Our LMLP algorithm demonstrates that the LM can be leveraged to estimate AAM and other life history parameters for a variety of taxa. In addition, we provide a realistic assessment of the data requirements of LMLP. In general, our method performed poorly for sample sizes < 100-150 individuals, precision in length-at-age < 6, and $g < 0.1$. The algorithm is also sensitive to low AAM, sample distribution across ages, data coverage, and violations of the LM. Future work should address these factors and also investigate the validity and accuracy of LMLP given different reproductive strategies (e.g., hermaphroditism) or when compared to other approaches for assessing maturity (e.g., histology). Despite these drawbacks, LMLP shows promise as a tool for research and management. Given adequate data quality, LMLP accurately estimates AAM (compared to A_{50}) and allows for the estimation of additional life history parameters. As such, we argue that LMLP represents a valuable addition to the growth modeling toolbox. Future research should also (1) assess the capacity for more complex modeling algorithms to broaden the applicability and utility of LMLP, (2) adjust LMLP to fit to longitudinal data, and (3) apply LMLP to historical datasets and/or ancient data (e.g., lifetime growth back-calculated from hard structures in sediment cores or middens) to address questions related

to life history variation and evolution. More broadly, we argue that this work makes an important contribution to the expanding body of literature centered on extracting life history information from growth data. Recent efforts have also met with conditional success (see Section 4.4iii), suggesting that these growth-related methods have great potential for improving our understanding of life history.

4.5 Data accessibility

Example R code and data describing haddock, Alaska skate, seal salamanders, and walleye from Minnesota lakes are available from the Dryad Digital Repository: http://dx.doi.org/10.5061/dryad.vb957. To request data collected by the Ontario Ministry of Natural Resources and Forestry and the Quebec Ministry of Natural Resources and Wildlife, please contact Dr. Sandra Orsatti (OMNRF; sandra.orsatti@ontario.ca) and Dr. Michel Legault (QMNRW; michel.legault@mnrf.gouv.qc.ca).

Table 4.1 Description of Lester model parameters.

Parameter	Description
l_0	Theoretical length at age 0 (mm)
h	Net rate of energy acquisition expressed as somatic growth rate (mm·yr^{-1})
T	Last immature age (yr; Lester model parameter for age-at-maturity)
l_∞	Asymptotic length (mm)
k	von Bertalanffy growth coefficient (yr^{-1})
t_0	von Bertalanffy (adult) hypothetical age at length 0 (yr)
t_1	Lester (immature) hypothetical age at length 0 (yr)
g	Cost to somatic growth of maturity (expressed in equivalent energetic units)

Figure 4.1 Empirical data describing female walleye *Sander vitreus* from individual lakes (n = 57) in relation to simulated error contours for T_{MLE} to fall within +/- 0.5 yrs of T when T = 5 yrs across levels of sample size, precision, and g (gray lines, labeled according to levels of g; Table A3.2). Symbols indicate LMLP fit quality (see Section 4.2) and the position of each point relative to the nearest (lower) contour for g, based on $\hat{g}$ from a LMLP fit. Error contours were smoothed using LOESS (degree = 2, α = 0.75). Datasets that are above the nearest contour for g in the sample size and precision parameter space (based on $\hat{g}$ from a LMLP fit) are likely to provide accurate estimates of T. The position of points depends only on sample size and precision, and not on $\hat{g}$. See Table A3.4 for a description (including sample size, precision, and $\hat{g}$) of each dataset.

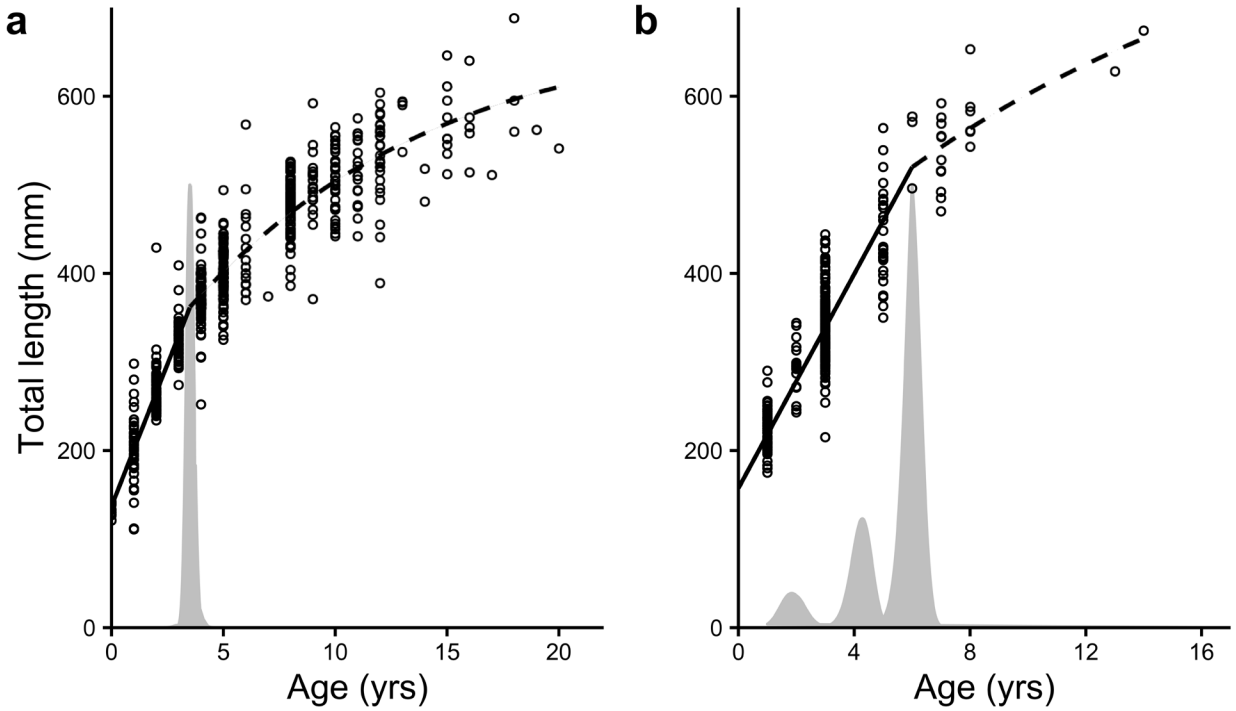

Figure 4.2 Examples of (a) good and (b) poor fits to empirical data describing female walleye *Sander vitreus*. A fit was considered good if it had a single likelihood peak and a likelihood interval of ≤ 2 years. Solid lines = immature growth, dashed lines = mature growth. Likelihood profiles are shown in light gray. (a) Data from Lake St. Joseph, ON, CA in 1999 (n = 563, precision = 12.52, $\hat{g}$ = 0.28). (b) Data from Lake of the Woods, ON, CA in 2004 (n = 322, precision = 9.82, $\hat{g}$ = 0.21).

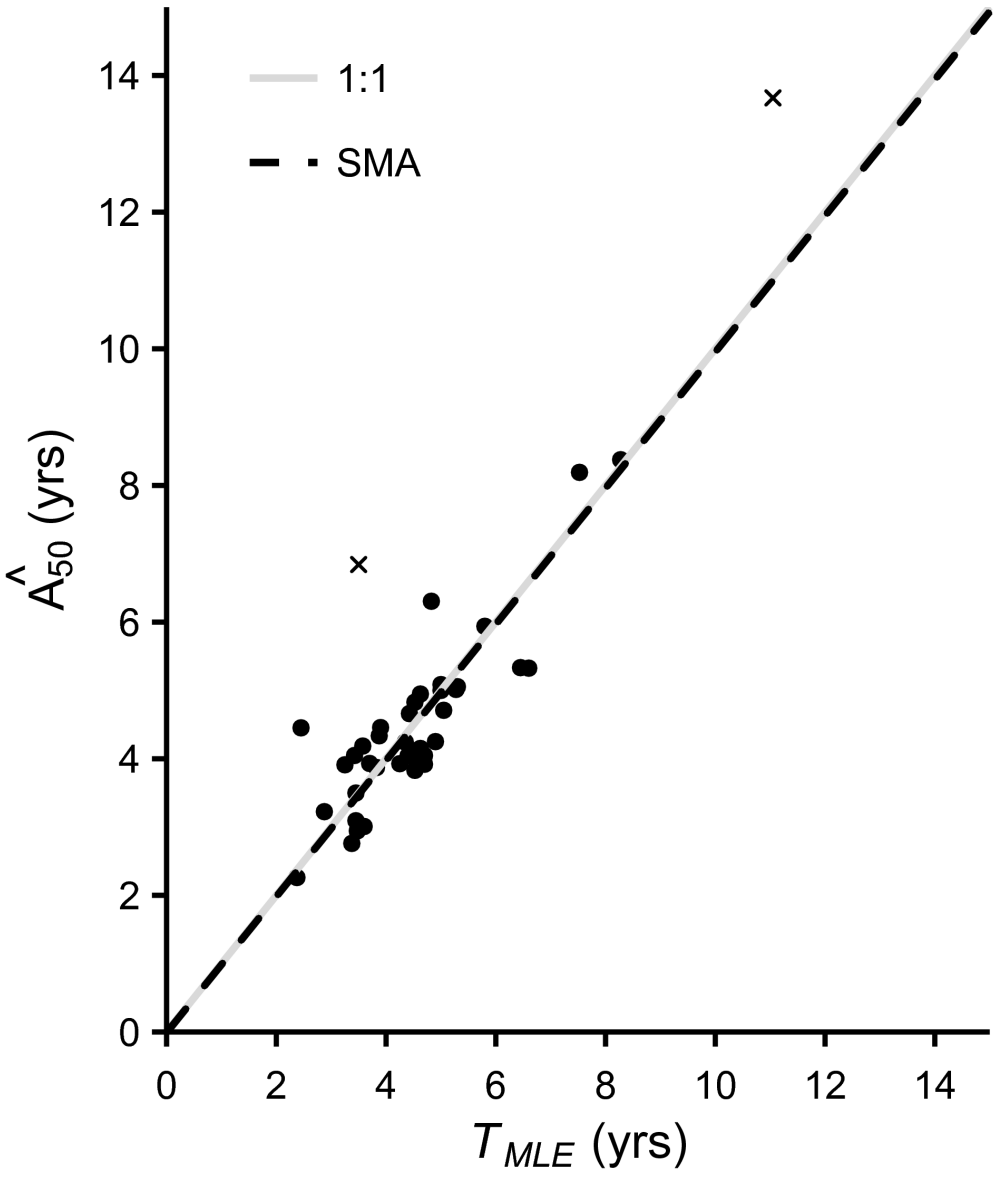

Figure 4.3 Standard major axis (SMA) regression comparing T_{MLE} from good fits to $\widehat{A_{50}}$ across datasets. Datasets marked with "x" were excluded from the regression due to probable errors in ageing and/or maturity assessment. The standard major axis regression line was not significantly different from a 1:1 line.

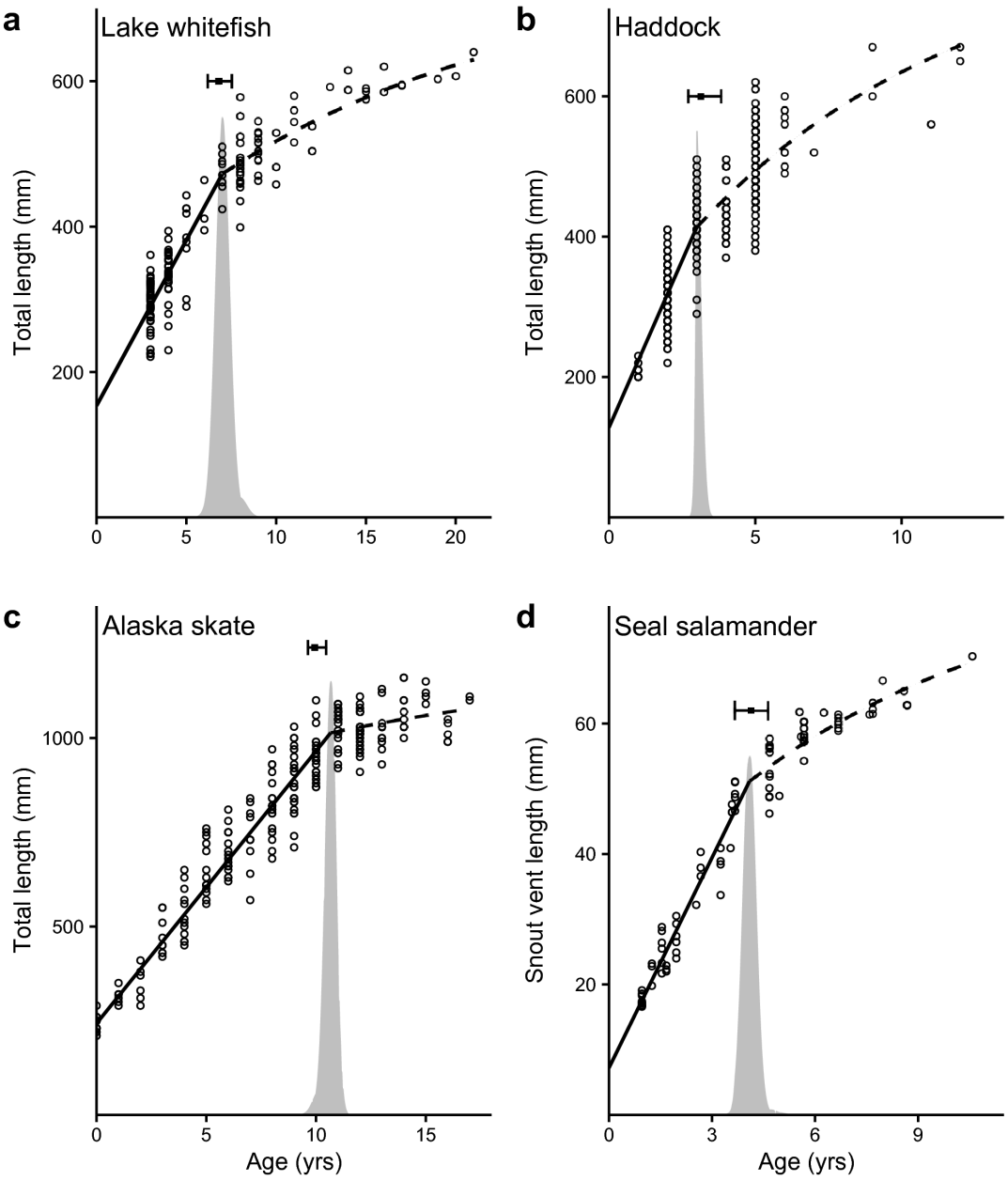

Figure 4.4 Examples of LMLP fits to data describing a variety of taxa, including (a) lake whitefish *Coregonus clupeaformis* (n=149, precision=24.26, $\hat{g}$=0.18), (b) haddock *Melanogrammus aeglefinus* (n=359, precision=10.12, $\hat{g}$=0.34), (c) Alaska skate *Bathyraja parmifera* (n=231, precision=15.87, $\hat{g}$=0.18), and (d) seal salamaders *Desmognathus monticola* (n=83, precision=50.79, $\hat{g}$=0.38). Solid lines = immature growth; dashed lines = mature growth; box and whiskers = $\widehat{A_{50}}$ and bootstrapped 95% confidence intervals, respectively. Likelihood profiles are shown in gray. For all four fits, T_{MLE} did not significantly differ from $\widehat{A_{50}}$ (see Appendix 3, Section A3.2 and Table A3.3 for details and data descriptions).

Chapter 5

A deep dive into the past: biphasic growth models reveal shifts in Gulf of Mexico red snapper *Lutjanus campechanus* life histories from 1941-2005

Synopsis

Fishing tends to select for faster fish life histories (e.g., faster growth, earlier maturity). In some cases, fisheries-induced shifts in life history can be hard to detect due to inadequate data. For example, maturity data are often insufficient or absent from historical samples, which can complicate the analysis of long-term trends in fish life histories. Recent work has shown that many life history traits, including maturity-based and reproductive traits, can be extracted from growth data using biphasic growth models. Herein, we use a biphasic growth model and length-at-age data back-calculated from otoliths to examine long-term trends in life history for an economically important and historically overexploited fish stock, Gulf of Mexico red snapper *Lutjanus campechanus*. We show that red snapper life histories were relatively slow in the 1940s-1960s, but shifted dramatically in the 1970s-1980s to a faster regime in the 1990s-2000s. These shifts do not appear to have been driven by temperature, but they coincide with increases in fishing pressure that occurred as the fishery developed after World War II. In addition, we found limited evidence for recovery of red snapper life histories through 2005 following the implementation of strict fishery regulations in 1991. We present otherwise unattainable

estimates of life history traits for Gulf of Mexico red snapper during the mid-20th century, thereby providing a more complete understanding of how red snapper life histories have shifted since the expansion of the fishery.

5.1 Introduction

Selectively harvesting fish can lead to plastic and/or evolutionary changes in fish life histories (Heino et al. 2015, Audzijonyte et al. 2016). For instance, increased mortality of older, larger fish due to harvest can select for faster life histories characterized by, e.g., faster juvenile growth, earlier maturation, and increased reproductive investment (e.g., Law 2000, Heino and Godo 2002, Kuparinen and Hutchings 2012). Fisheries-induced shifts in life history are likely widespread and can reduce both yield and economic benefit from global fisheries (Heino 1998, Zimmerman and Heino 2013). Unfortunately, these shifts can be difficult to detect. Experiments (e.g., Conover and Munch 2002) may not translate to real-world scenarios, many methods (e.g., Heino et al. 2002) require large amounts of data that can be hard to collect, and data describing fish population baselines (e.g., from pre-exploitation time periods or early in the development of a fishery) are often unavailable or inadequate.

Growth is the net result of myriad ecological and evolutionary factors and processes and is tightly linked to many life history traits (Roff 1983, Stearns 1992). Recent advances in growth modeling allow for the extraction of a wealth of life history information from growth data (e.g., Mollet et al. 2010, Boukal et al. 2014, Minte-Vera et al. 2016). For example, the Lester model (LM; Lester et al. 2004, 2014, Quince et al. 2008b) is rooted in life history theory and allows for the estimation of multiple life history traits from length-at-age data (e.g., age-at-maturity, juvenile growth rate, energetic investment in reproduction), many of which cannot be directly estimated using traditional growth models (e.g., the von Bertalanffy model; von Bertalanffy 1938, 1957,

Beverton and Holt 1957). The LM has been shown to provide accurate life history trait estimates for fishes and other ectotherms (Honsey et al. 2017; see also Wilson et al. 2018). As such, and given the relative abundance of fish length and age data compared to other types of data (e.g., maturity data), the LM is a potentially useful tool for detecting and monitoring shifts in fish life histories.

Red snapper *Lutjanus campechanus* is one of the top recreationally-landed species in the US (Figueira and Coleman 2010, Abbott et al. 2018) and is among the most ecologically and economically important fishes in the Gulf of Mexico (GOM; e.g., Bradley and Bryan 1975). Fishing effort for GOM red snapper increased dramatically following World War II due to advances in technology, fishery expansion to the northern Gulf shelf off of Louisiana and Texas, and increased recreational catches (Carpenter 1965, Porch et al. 2007, SEDAR 2018). Overfishing led to severe declines in GOM red snapper biomass during the 1940s-1990s, with commercial landings in 1991 comprising approximately 12-15% of those in 1965 (Wilson and Nieland 2001, SEDAR 2018). Since 1991, strict size limits and catch quotas have been enforced in an effort to reduce overfishing and promote stock recovery (Schirippa and Legault 1999). It is possible that these substantial shifts in fishing effort and biomass have driven fisheries-induced changes in GOM red snapper growth and life history. Unfortunately, estimating some life history traits (e.g., age-at-maturity) using traditional approaches can be challenging for red snapper (see Cook et al. 2009 and Section 5.4). Moreover, although some studies have focused on GOM red snapper growth (Bradley and Bryan 1975, Szedlmayer and Shipp 1994, Patterson III et al. 2001, Wilson and Nieland 2001), comparisons of growth

across time periods are limited to recent years and relatively narrow temporal ranges (e.g., 1998-2004, 2001-2012; Nieland et al. 2007, Patterson III et al. 2012, SEDAR 2013). As such, a comprehensive analysis of GOM red snapper life histories before, during, and after the period of high exploitation is lacking.

Our objectives were to (1) examine shifts in GOM red snapper life histories from the mid-20th century to recent decades, and (2) explore potential drivers of any observed shifts in red snapper life histories. To do this, we estimated life history traits for red snapper from cohorts stretching from 1941-2005 by fitting the LM to growth data back-calculated from otoliths. We then regressed our estimates against an important environmental factor (temperature) and examined the plausibility of that factor as a driver of the observed trends compared to other potential drivers (e.g., fishing pressure).

5.2 Methods

i) *Data*

We retrieved 166 GOM red snapper otoliths from archival collections located in the National Oceanic and Atmospheric Administration (NOAA) Panama City Laboratory (FL, USA). The otoliths were taken from individuals that were landed primarily in eastern GOM ports (NOAA Fisheries grids 1-12 in Appendix 4, Fig. A4.1) from 1980-2016**.** Individuals were landed via the commercial fishery (n = 105; 63%), recreational fisheries (n = 32; 19%), and fisheries-independent surveys (n = 29; 18%). We included otoliths from individuals that were estimated to be roughly 10 yr old or greater. Moreover, we selected otoliths in an effort to include a broad range of individual sizes-

and ages-at-capture within cohorts (or among a limited range of cohorts, e.g., 1991-1995) throughout the time series. That is, we tried to include otoliths from both older, larger individuals and younger, smaller individuals that hatched at roughly the same time. We did this in an effort to ensure that our dataset included the range of life history strategies present in the population for a given cohort or range of cohorts. Our dataset included individuals with ages-at-capture ranging from 7-59 yr from cohorts ranging from 1941-2005. In addition, we included only otoliths from known females when possible. We focused on females because of their importance with regard to evolution and stock productivity (i.e., females are often considered 'limiting'; Herczeg et al. 2012, Hixon et al. 2014). Unfortunately, many of the otoliths came from individuals that were captured via the commercial fishery, the data from which seldom included information on sex. The increased prevalence of data from recreational fisheries and fisheries-independent surveys (for which sex data were more common) in recent years allowed us to include only known females for recent cohorts. Of our 166 individuals, 58 (35%) were female, 2 (1%) were male, and 106 (64%) were of unknown sex. See Appendix 4, Table A4.1 for a description of each individual included in the analysis.

We thin-sectioned sagittal otoliths through the transverse plane with a high-speed saw to a thickness of 0.5 mm following Cowan et al. (1995). We assigned ages to sectioned otoliths based on the number of annuli (opaque zones). We analyzed growth increments along the dorsal side of the sulcal groove with a binocular dissecting microscope at 40x magnification under transmitted light. We photographed all samples with a digital camera and then measured growth increment widths using the program

ImagePro Plus v. 7.0 (Media Cybernetics, Silver Spring, Maryland). We measured growth increments (distances between opaque zones) continuously from the focus to the dorsal distal margin, including any partially formed translucent zone on the margin. We measured a total of two axes per otolith, always following the direction of growth (i.e. perpendicular to the growth increments). Allman et al. (2005) provides additional information on otolith reading protocols and practices.

ii) *Back-calculation of growth trajectories*

We back-calculated growth trajectories from otolith measurements in order to generate estimates of size-based life history traits (e.g., somatic growth rates, length-at-maturity, asymptotic size) which would be unattainable otherwise (although some life history traits such as age-at-maturity can be estimated directly from otolith measurements; see, e.g., Engelhard et al. 2003). We converted otolith measurements to body lengths-at-age via the 'age effect' model proposed by Morita and Matsuishi (2001), with a modification to include a biological intercept (an approximation of the length and otolith size of newly-hatched fish; Ashworth et al. 2017b). This method was found to be among the most accurate back-calculation approaches evaluated by Ashworth et al. (2017b). We used data describing age-0 red snapper from Allman et al. (2005) to estimate the biological intercept. We then fit a regression model to data describing otolith radius at capture, age at capture, and total length for all individuals included in the analysis (n = 166), as well as juveniles from Allman et al. (2005) (n=125; total n = 291). Our regression model took the form

$$R = R_{BI} + \beta(L - L_{BI}) + \gamma(t - t_{BI}),$$

where R is otolith radius at capture, R_{BI} is otolith radius at the biological intercept (set at 432.6 μm), L is total length at capture, L_{BI} is total length at the biological intercept (set at 50 mm), t is age at capture, t_{BI} is age at the biological intercept (set at 0.044 yr), and β and γ are estimated parameters (Ashworth et al. 2017b). We then estimated lengths-at-age for adult red snapper (n = 166) as:

$$\hat{L}_{j,i} = -\frac{R_{BI} - \beta L_{BI} - \gamma t_{BI}}{\beta} + \left(L_i + \frac{R_{BI} - \beta L_{BI} - \gamma t_{BI}}{\beta} + \left(\frac{\gamma}{\beta}\right) t_i\right)\left(\frac{R_{j,i}}{R_i}\right) - (\frac{\gamma}{\beta})t_j$$

(Ashworth et al. 2017b), where $\hat{L}_{j,i}$ is estimated length at age t_j for fish i, L_i is length at capture for fish i, t_i is age at capture for fish i, $R_{j,i}$ is otolith radius at age t_j for fish i, R_i is otolith radius at capture for fish i, and the remaining parameters are as described above.

iii) *Lester model fits to individual growth data*

We fit the "fixed g" formulation of the Lester model (LM; Lester et al. 2004, 2014, Quince et al. 2008b, 2008a, Honsey et al. 2017) to the back-calculated red snapper growth data. For length at time t (l_t), the growth trajectory is given by

$$l_t = l_0 + ht, \ t \leq T \text{ for juveniles,}$$

$$l_t = l_\infty\left(1 - e^{-k(t-t_0)}\right), \ t > T \text{ for adults,}$$

with

$$t_1 = -\frac{l_0}{h}$$

$$l_\infty = \frac{3h}{g}$$

$$k = \ln(1 + \frac{g}{3})$$

$$t_0 = T + \ln\left(1 - \frac{g(T - t_1)}{3}\right) / \ln\left(1 + \frac{g}{3}\right).$$

In these equations, l_0 is the theoretical length at age 0 (mm); h is the juvenile somatic growth rate (mm · yr^{-1}); T is the last immature age (LM parameter for age-at-maturity; yr); l_∞ is the asymptotic length (mm); k is the von Bertalanffy growth coefficient (yr^{-1}); t_0 is the von Bertalanffy theoretical age at length 0 (yr); t_1 is the Lester (immature) theoretical age at length 0 (yr); and g is the cost to somatic growth of maturity (expressed in equivalent energetic units), which is often assumed to be dominated by energetic investment in reproduction (Roff 1983, Kozlowski 1996, Honsey et al. 2017). We assumed that fish length at age t was normally distributed around the length predicted by the model for that age, $\hat{\mu}_t(\theta)$ (Quince et al. 2008b). In order to allow error to scale with fish size, we defined the standard deviation of this distribution, σ_t, as a power function of the predicted length: $\sigma_t = \phi \hat{\mu}_t{}^{\psi}$, where ϕ and ψ are estimated parameters (see Supplement in Quince et al. 2008a). As such, we estimated six parameters for each model fit: l_0, h, T, g, ϕ, and ψ.

We fit the LM in a Bayesian framework using Stan (Carpenter et al. 2017) via RStan (Stan Development Team 2018). We fit the model in a fixed-effects framework separately to data describing each individual. For each fit, we ran four Hamiltonian

Monte Carlo (HMC) chains for 10000 iterations each (3500 warmup, 6500 sampling). To improve model performance, we fit a linear model to the first 2-4 length-at-age data points for each individual and used the slope and intercept estimates to inform priors on h and l_0, respectively. This process promotes model convergence without leveraging information outside of the data and is similar to the approach used by Honsey et al. (2017). We used vague priors for the remaining parameters. We used the potential scale reduction factor ($\hat{R}$; Gelman and Rubin 1992) and visually examined HMC chain trace plots to assess convergence, and we inspected model fits to the data to assess fit quality. We provide code for this model in Appendix 4, Section A4.1.

The LM fits provided individual-level estimates of eight parameters (excluding variance parameters). Five of these parameters (h, T, g, k, and l_∞) can be considered estimates of life history traits. The remaining three parameters (l_0, t_0, and t_1) have limited biological interpretation (but see Lester et al. 2004). We used these parameter estimates to generate estimates of two additional life history traits**.** We estimated length-at-maturity (l_T; mm) by simply calculating the predicted length at age T:

$$l_T = l_0 + hT.$$

We then estimated the late-stage juvenile and adult instantaneous mortality rate (Z; yr^{-1}) using two empirically-derived relationships that leverage well-established tradeoffs between maturity, reproductive investment, and mortality (Lester et al. 2004, 2014):

(1) $$Z \approx -\ln\left(1 - \left(\frac{g}{1.18}\right)\right)$$

(2) $$Z \approx \ln\left(\left(\frac{1.95}{T - t_1}\right) + 1\right).$$

iv) *Cohort group-level mean life history traits*

We examined trends in mean life history trait values among red snapper individuals across the cohorts present in our dataset by first grouping individuals into one of nine cohort groups: 1941-1950, 1951-1960, 1961-1970, 1971-1980, 1981-1985, 1986-1990, 1991-1995, 1996-2000, and 2001-2005. We selected these groups in an effort to balance temporal resolution and sample size (e.g., low sample sizes precluded the use of five-year cohort groups for pre-1980 cohorts). We then extracted draws from the posterior probability distributions for each individual-level LM fit (random sample of 2500 draws per parameter per individual), and we compiled these subsampled draws across all individuals within a cohort group. We effectively treated these draws as data for estimating cohort group-level means in a hierarchical Bayesian framework, once again using Stan via RStan. The hierarchical framework was constructed with group-level parameters θ_g arising as $\theta_g \sim N(\theta_k, \sigma_\theta)$, where θ_k are individual-level parameter estimates (i.e., estimates for fish k) and σ_θ is the estimated standard deviation for a given group-level parameter estimate. In essence, the hierarchical model re-estimated individual-level means and standard deviations from the posterior draws, and then used this information to estimate group-level means. We used this approach to ensure that the uncertainty around individual-level parameter estimates was appropriately propagated when estimating group-level means. For each fit, we ran four HMC chains for 5000 iterations each (2000 warmup, 3000 sampling). We considered cases in which the 95% credible intervals did not overlap for a given pair of group-level parameter estimates to be significant differences. We provide code for this model in Appendix 4, Section A4.2.

Although most of the individuals included in our analysis were landed in the eastern Gulf, some were caught and/or landed in the western GOM (NOAA Fisheries grids 13-21 in Appendix 4, Fig. A4.1; see Table A4.1). There is evidence to suggest that red snapper life histories may differ across the Gulf, possibly due to historically different exploitation levels and/or other factors such as habitat quality (e.g., Fischer et al. 2004, Jackson et al. 2007). For this reason, we conducted an analysis to determine whether life histories differed among individuals in our dataset that were captured in the eastern versus western GOM. Specifically, we calculated group-level mean life history trait estimates separately for individuals captured in the eastern versus western GOM within each cohort group using the approach described above. We again considered cases in which the 95% credible intervals did not overlap to be significant differences. Additional details are provided in Appendix 4, Section A4.3.

v) *Life history trait estimates versus temperature*

Temperature is an important driver of fish growth, physiology, and life history (e.g., Hazel and Prosser 1974, Diana 2003). In general, higher temperatures tend to select for faster life histories (i.e., faster growth, earlier maturity, higher natural mortality rates, etc.; e.g., Pauly 1980, Berrigan and Charnov 1994, Thorson et al. 2017). To examine whether temperature is a plausible driver of shifts in red snapper life history, we obtained mean monthly sea surface temperature data from the Hadley HadISST 1.1 1 x 1 degree dataset (http://hadobs.metoffice.gov.uk/hadisst; Rayner et al. 2003, Dzaugis et al. 2017) for a location in the northeastern GOM (29.5ºN, 86.5ºW) and for all months from 1941-

2005. We used these data to calculate annual degree-days (DD), which are a useful metric for describing fish growth and life history (e.g., Neuheimer and Taggart 2007, Chezik et al. 2014a, Honsey et al. in press). We calculated DD as

$$DD = \sum_{m=1}^{12} (T_m - T_0) \cdot d_m, \qquad T_m > T_0,$$

where T_m is the mean sea surface temperature for month m, T_0 is the base temperature for growth (i.e., the temperature below which thermal energy is considered irrelevant to growth), and d_m is the number of days in month m. Previous work has shown that the selection of the base temperature (T_0) can influence growth rate estimates (Chezik et al. 2014b). In an effort to account for potential bias due to base temperature selection, we calculated DD above three base temperatures (0, 5, and 10 ºC) and compared results generated using the three metrics (i.e., DD_0, DD_5, and DD_{10}).

To provide an index of the average annual thermal energy available to red snapper individuals in early life, we calculated mean DD_0, DD_5, and DD_{10} across the years included in each cohort group (i.e., 1941-1950, 1951-1960, etc.) using a Bayesian model of the mean in Stan via RStan. We then regressed the group-level life history trait estimates against these metrics for each cohort group using a hierarchical modeling framework similar to the one described above. Specifically, we extracted draws from the posterior probability distributions for both the group-level life history trait estimates and the mean DD estimates (2500 random draws per trait/metric). We incorporated these draws in a hierarchical regression framework (again using Stan via RStan) in order to propagate error in both the life history trait estimates and the mean DD estimates. For

these fits, we again ran four HMC chains for 5000 iterations each (2000 warmup, 3000 sampling).

5.3 Results

i) *Lester model fits to individual growth data*

The LM generally provided good fits to the back-calculated length-at-age data despite a broad range of parameter estimates (i.e., dramatically different growth trajectories) among individuals and cohort groups. For instance, $\hat{T}$ ranged from 1.72-11.67 yr, and $\hat{h}$ ranged from 32.14-262.31 mm·yr^{-1} among individuals (Fig. 5.1). However, we considered LM fits for 19 individuals to be untrustworthy due to a lack of convergence and/or poor fits to the data (e.g., Fig. 5.1c,d). These poor model fits appear to have been caused by low sample size (i.e., fish that were relatively young at capture) and/or multiple plateaus in the growth trajectory (i.e., a 'stair-step-like' growth pattern), leading to multiple likelihood peaks for model parameters. We present results excluding parameter estimates from these unreliable fits (as well as for fits to males) throughout the remainder of the paper. Results including these fits were qualitatively almost identical; these results and additional details and are provided in Appendix 4 (Section A4.4, Figs. A4.9-4.15).

ii) *Cohort group-level mean life history traits*

Our results suggest that red snapper life histories were significantly faster in recent decades than they were in the mid-20th century (Figs. 5.2, 5.3). Mean age at maturity (T)

more than halved from 7.45 yr in 1941-1950 to 3.06 yr in 2001-2005 (Fig. 5.2), and mean juvenile growth rate (h) roughly doubled from 63.84 mm·yr^{-1} in 1941-1950 to 124.47 mm·yr^{-1} in 2001-2005 (Fig. 5.3a). Similarly, investment in reproduction (g; Fig. 5.3b), adult growth rate (k; Fig. 5.3c), and mortality rate (Z; Fig. 5.3d) all approximately doubled from 1941-1950 to 2001-2005. We did not find any significant trends in l_∞ (Fig. 5.3e) or l_T (Fig. 5.3f), although there is evidence for a non-significant decrease in both traits over time. Our estimates of Z from eq. 1 (Fig. 5.3d) were consistently higher than those from eq. 2 (see Appendix 4, Fig. A4.16), but the trends over time were similar for both approaches. In general, our results indicate that GOM red snapper life histories were relatively slow from 1941-1970, after which they transitioned during 1971-1990 to a faster life history regime in 1991-2005. We did not find any evidence for a significant recovery of life histories (i.e., to the slower life history regimes of the mid-20th century) by 2001-2005 (but see Section 5.4). Moreover, we did not detect any significant differences in life history traits within cohort groups among individuals captured in the eastern versus western GOM (see Appendix 4, Section A4.3 and Figs. A4.2-A4.8 for details).

iii) *Life history trait estimates versus temperature*

Our three thermal metrics (DD_0, DD_5, and DD_{10}) were highly correlated (Pearson's $r >$ 0.99 for all pairwise comparisons), and inference from the regression models was identical for each metric. We present results for DD_0 herein; results generated using the other two metrics are provided in Appendix 4, Table A4.2.

We found a marginally significant, positive relationship between DD_0 and T (slope = 0.016; 95% credible interval = (0.002, 0.031)), and marginally significant, negative relationships for regressions of DD_0 versus h (slope = -0.282; 95% credible interval = (-0.497, -0.066), and k (slope = $-2.81 \cdot 10^{-4}$; 95% credible interval = ($-5.55 \cdot 10^{-4}$, $-1.80 \cdot 10^{-6}$); Fig. 5.4). In contrast, we found non-significant relationships (i.e., the 95% credible intervals for slope estimates overlapped 0) for DD_0 versus g, Z, l_T, and l_∞.

5.4 Discussion

Our results suggest that Gulf red snapper life histories have become significantly faster since the mid-20th century. Specifically, we observed a roughly two-fold reduction in age-at-maturity, and a roughly two-fold increase in somatic growth rates, energetic investment in reproduction, and mortality rates from 1941-2005. In addition, we found weak but marginally significant relationships between temperature and three of our life history trait estimates: age-at-maturity, juvenile somatic growth rate, and adult somatic growth rate (i.e., the von Bertalanffy growth coefficient). However, the direction of these relationships was opposite to that predicted by life history theory. Increases in temperature generally lead to faster growth and earlier maturity (e.g., Pauly 1980, Berrigan and Charnov 1994, Venturelli et al. 2010). In contrast, we found that higher temperatures were correlated with slower growth and later maturity for the individuals in our dataset. These relationships appear to be driven by estimates from early portions of the time series in which temperatures were relatively warm and red snapper life histories were relatively slow. For instance, estimates of both DD_0 and T were highest for the

1941-1950 and 1951-1960 cohort groups (upper-rightmost points in Fig. 5.4a). Given our relatively low sample size (n = 9 cohort groups) and that the observed relationships contradict life history theory, we argue that these results are an example of correlation without causation, and we suggest that factors other than temperature likely drove the observed shifts in red snapper life histories.

Fishing pressure is perhaps the most plausible driver of the observed shifts in red snapper life histories. Fishing pressure for GOM red snapper increased dramatically following World War II (Fig. 5.5; SEDAR 2018), leading to substantial declines in biomass and the implementation of strict fishing regulations in 1991 (Schirippa and Legault 1999). It is plausible, and perhaps even likely, that the selective exploitation of GOM red snapper contributed to shifts in life history (see Nieland et al. 2007). We did not explicitly include an index of fishing pressure as a driver of life history shifts in our models because doing so was not as straightforward as for other factors that have more immediate effects (e.g., temperature), and may therefore have led to erroneous conclusions. For instance, we expect that there was a lag between fishing pressure and its effects on fish life histories, and the length of that lag was likely dynamic with shifts in life histories (e.g., changes in generation times). However, we note that GOM red snapper life histories appear to have shifted following the rapid increase in fishing pressure in the 1950s-1970s (Fig. 5.5), which is consistent with the hypothesis that fishing pressure is an important driver of the observed shifts.

We did not find evidence for significant recovery (i.e., ‘slowing down’) of life histories at the cohort group-level by 2001-2005 in response to the enforcement of strict

size limits and catch quotas since 1991 (Schirippa and Legault 1999). However, there is evidence to suggest that life histories for recent red snapper cohorts are indeed shifting toward historical regimes (Brown-Peterson et al. in press, SEDAR 2018)**.** Despite the fact that we did not see significant recovery at the cohort group level, our results at the individual level hint at potential recovery. For example, there were four individuals (16%) in the 2001-2005 cohort group with relatively slow life histories compared to the group-level mean (e.g., T estimates of 5.05, 5.11, 5.62, and 7.27 yr; group-level mean for 2001-2005 = 3.06 yr). Individuals with similar life histories were less common in the 1996-2000 (two individuals (10%) with T between 5 and 6 yr) and 1991-1995 (one individual (3%) with $T > 5$ yr) cohort groups. Future analyses using the LM or a similar approach may detect significant recovery at the group level by, for example, leveraging larger sample sizes and/or including older individuals from more recent cohorts, once they have aged sufficiently.

Our mortality rate estimates (Z) can be considered estimates of total mortality rate (i.e., fishing mortality rate + natural mortality rate) assuming an evolutionary equilibrium state. This assumption likely does not hold given the history of the Gulf red snapper fishery, which includes large shifts in fishing pressure, and therefore selective pressures, over time (Schirippa and Legault 1999; see Fig. 5.5). However, we argue that these estimates are still informative given that they provide insight regarding the mortality rates to which individuals are likely adapted, based on their growth and other life history traits. Moreover, our estimates appear to be reasonable given previous estimates of fishing and natural mortality rates. For example, fishing mortality rates for red snapper at artificial

reef sites have been estimated at roughly 0.27-0.44 yr^{-1} (Topping and Szedlmayer 2013, Williams-Grove and Szedlmayer 2016) for recent years, and natural mortality rate estimates for adults often fall near 0.1 yr^{-1} (Topping and Szedlmayer 2013, SEDAR 2018). An approximate range of plausible Z is therefore 0.37-0.54 yr^{-1}. The fact that our LM-based Z estimates for recent cohorts largely fall in this range (Z = 0.45-0.58 yr^{-1} for eq. 1 and 0.39-0.47 yr^{-1} for eq. 2 for 1986-2005) suggests that red snapper life histories may be well-adapted to current Z.

We were unable to make direct comparisons between our results and life history trait estimates generated from conventional approaches in most cases. For example, estimating age-at-maturity using traditional methods (e.g., age-at-50% maturity or A_{50}; Chen and Paloheimo 1994) requires maturity data, which were not available for most of the early portion of our time series. Moreover, estimating maturity-based traits can be challenging for red snapper even when maturity data are available. Specifically, young, small red snapper can be difficult to catch and are often rare in assessment datasets, which can lead to problems when calculating maturity metrics (e.g., unrealistic and/or highly uncertain estimates of A_{50}; Cook et al. 2009). For this reason, we did make any direct comparisons between T and A_{50}. In addition, many of our growth parameter estimates were not directly comparable to those from conventional models (e.g., von Bertalanffy growth models) due to differing functional forms and parameterizations among models. However, we did find that our estimates of asymptotic length (l_∞) align well with those generated from von Bertalanffy models in other studies ($l_\infty \approx$ 850-1025 mm; Szedlmayer and Shipp 1994, Patterson III et al. 2001, Wilson and Nieland 2001,

SEDAR 2013). Moreover, a recent meta-analysis found modest shifts toward slower life history strategies in female GOM red snapper reproductive parameters (e.g., increase in spawning interval, decrease in relative batch fecundity) from 1991-2017 (Brown-Peterson et al. in press). Our results show a somewhat similar trend: we observed a slight (non-significant) decrease in reproductive investment (g) from 1991-1995 to 1996-2000, although mean reproductive investment was similar for 1991-1995 and 2001-2005. Lester model-based analyses of more recent cohorts in future years may further elucidate trends in reproductive parameters since the implementation of strict fishing regulations in 1991.

Our methods did not allow us to explicitly disentangle plastic versus evolutionary change, a common difficulty with studies that leverage phenotypic data describing wild populations (Heino et al. 2015). With more data, it may be possible to pair our methods with a probabilistic reaction norm approach (e.g., Heino et al. 2002) to differentiate between plastic and evolutionary shifts in life history traits (although there is debate as to whether such approaches succeed in doing so; e.g., Law 2007, Uusi-Heikkilä et al. 2011, Salinas and Munch 2014). Importantly, we did not find evidence for significant decreases in asymptotic length or length-at-maturity over time (although there were non-significant decreases in both traits), both of which are often expected to occur as a result of fisheries-induced evolution (Heino 1998, Heino et al. 2015).

Although we attempted to include individuals spanning a broad range of ages- and sizes-at-capture within each cohort group, individuals from early cohorts were consistently older than individuals from more recent cohorts. This was largely unavoidable, given that, e.g., we did not have samples from before 1980, and therefore

we could not include younger individuals from these earlier cohorts. However, it is possible that there is (and has been) a broad range of life history strategies present in GOM red snapper populations, and that older individuals tend to display relatively slow life histories. Sampling may therefore have contributed to the observed shifts in life histories. For instance, individuals displaying slow life histories from recent cohorts may be present in the population, but may not have been sampled (and vice versa for earlier cohorts). As such, our results may be biased due to Lee's phenomenon (Lee 1920), whereby population-level estimates of life history traits can be skewed due to unrepresentative sampling. A more complete explanation of this potential bias would require sampling older fish from recent cohorts in the future (i.e., age 40-50+ individuals sampled 30-40 yr from now, if present), as well as younger fish from cohorts early in the time series (which may only be possible via the collection of otoliths from sediment cores; see below). That being said, we did observe traits suggestive of relatively slow life histories in some individuals from recent cohorts, despite the fact that they were captured at relatively young ages (see Appendix 4, Table A4.1). Moreover, we observed traits suggestive of slow life histories from individuals that were captured at relatively young ages earlier in the time series. For example, two individuals from the 1961-1970 cohort group that were captured at ages 11 and 15 yr displayed relatively slow growth rates (47.42 and 54.12 $mm \cdot yr^{-1}$, respectively) and late ages-at-maturity (5.97 and 5.73 yr, respectively). Two individuals from the same cohort group that were captured at older ages of 27 and 35 yr displayed faster life histories (growth rates = 97.74 and 106.98 $mm \cdot yr^{-1}$, respectively; ages-at-maturity = 4.80 and 3.85 yr, respectively). The fact that we

estimated relatively slow life histories for individuals that were captured at relatively young ages (and vice versa) suggests that our results are not solely a product of Lee's phenomenon.

Growth trajectories estimated via back-calculation from otoliths can be biased (e.g., Campana 1990). We used a method that was found to be among the most accurate back-calculation methods (Ashworth et al. 2017a, 2017b). We chose not use the method proposed by Ashworth et al. (2017a, 2017b), which was found to have similar accuracy to the approach used herein, because it requires applying the best-fitting growth curves to length-at-age and otolith size-at-age data. These growth curves may take various forms (e.g., von Bertalanffy, logistic, Pütter). Using growth curves that differ from the LM in form in the back-calculations could have complicated, and possibly confounded, the fitting of the LM to back-calculated length-at-age data. For example, using a von Bertalanffy or logistic model to inform back-calculations could influence the shape of the resultant growth trajectory (i.e., trajectory might be more von Bertalanffy-like or logistic in shape) and could therefore bias LM parameter estimates in nuanced and cryptic ways.

Our results may have been influenced by the incidental inclusion of males in our analyses. There is evidence to suggest that some male red snapper reproduce at younger ages and smaller sizes than females (Futch and Bruger 1976, White and Palmer 2004, Brown-Peterson et al. 2009). In contrast, Render (1995) reports similar lengths-at-50% maturity for male and female red snapper, with some females maturing at smaller sizes than males. In addition, Wilson and Nieland (2001) found that growth trajectories significantly differed between males and females, whereas Patterson III et al. (2001)

found a non-significant difference in growth between sexes. In an effort to mitigate this potential bias, we selected only otoliths from known females when possible, and we present results excluding known males. Unfortunately, most (64%) of the individuals in our dataset were of unknown sex. As such, the number of males in the dataset (and therefore the degree of potential bias in our results) is unclear. To examine the potential for bias driven by the inclusion of unknown sex individuals, we conducted an analysis to compare life history trait estimates for females versus unknown sex individuals within cohort groups. Importantly, we found that trait estimates did not significantly differ between females and unknown sex individuals for all but one case (l_∞ was slightly higher for females than for unknown sex individuals in 1981-1985), although we were only able to compare traits for two cohort groups due to sample size limitations (see Appendix 4, Section A4.5 and Table A4.3 for additional details and results).

Hierarchical frameworks offer some advantages over fixed-effects frameworks for fitting growth models, such as better partitioning of the variability in growth (Vigliola and Meekhan 2009, Ogle et al. 2018). However, hierarchical frameworks also have drawbacks; for example, the 'shrinkage effect', a phenomenon whereby individual-level parameter estimates are pulled toward the group mean (Helser and Lai 2004), can complicate inference from hierarchical models. This effect can be especially problematic for individuals with limited information (i.e., low sample size) and/or parameters that vary substantially from the mean. We attempted to fit the LM simultaneously to all individuals within a cohort group using a hierarchical framework, but the models often failed to converge and there appeared to be issues with shrinkage. For example, model

fits to data were often very poor for individuals with few data points and/or with growth trajectories that differed considerably from those of other individuals within a cohort group. Given these issues, we chose to use a fixed-effects framework for fits to individual growth data. This approach allowed us to make minor modifications (e.g., adjustments to priors for some parameters) to fits for each individual, thereby leading to better convergence and improved fits to the data. Although our LM fits at the individual level were coded in a fixed-effects framework, we used a hierarchical framework that incorporated error in the individual-level parameter estimates to generate cohort group-level mean parameter estimates, and we focused on these means for inference. Our hybrid approach leveraged advantages of both fixed-effects and hierarchical frameworks and allowed us to effectively propagate error without sacrificing fit quality at the individual level.

Our study provides a more thorough understanding of how red snapper life histories have changed since the expansion of the fishery following World War II, and we present otherwise unattainable estimates of life history traits for the early portion of that expansion. For example, using a growth-based approach allowed us to estimate age-at-maturity and other life history traits for red snapper cohorts stretching back into the 1940s despite insufficient maturity data. Furthermore, it may be possible to use the LM or a similar approach to estimate life history traits for red snapper even deeper into the past by back-calculating growth from otoliths collected in sediment cores. Leveraging growth data and theoretically-sound models to understand life history is a potentially fruitful and important direction for future life history studies.

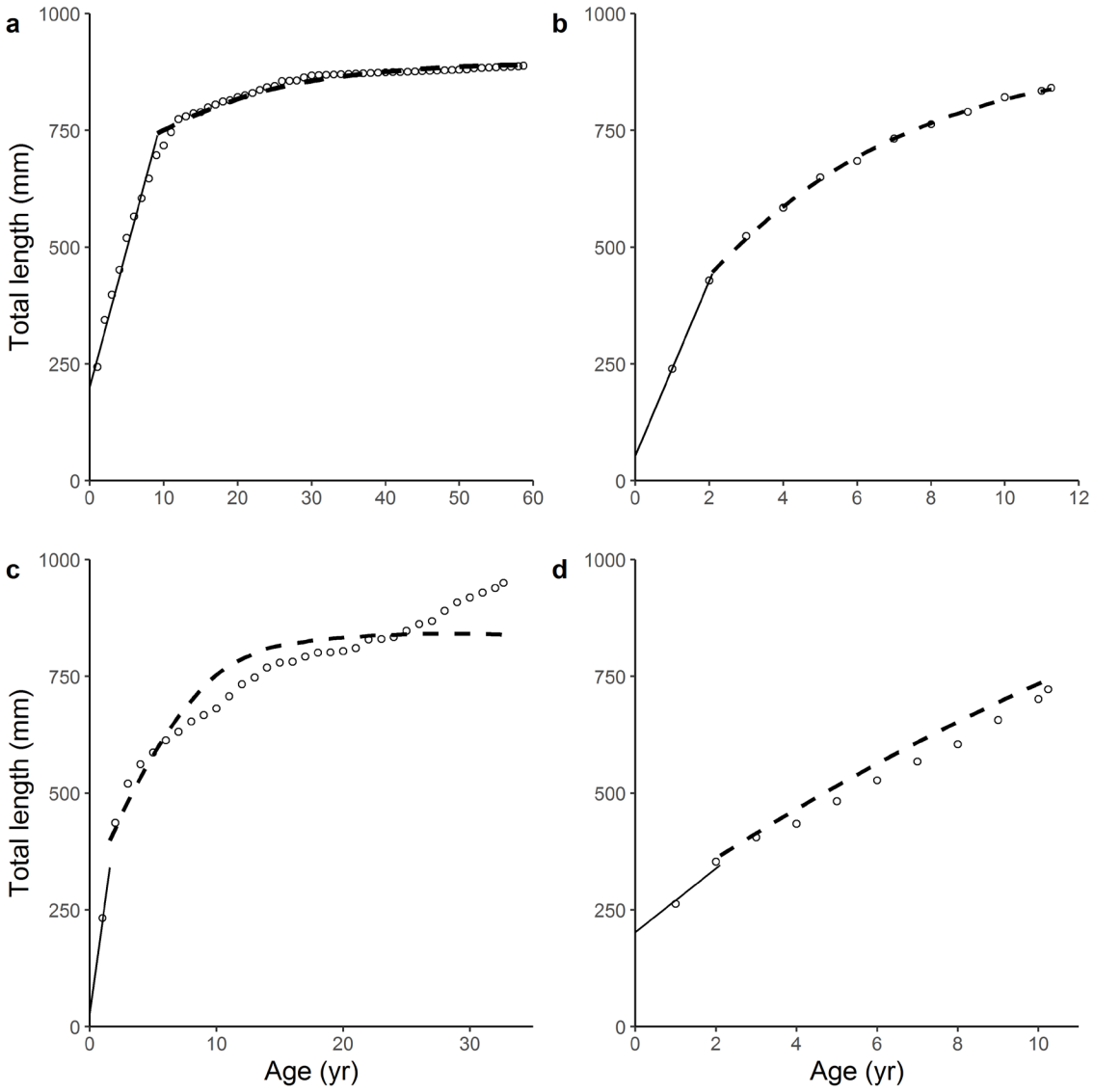

Figure 5.1 Example fits of the Lester biphasic growth model to back-calculated Gulf of Mexico red snapper *Lutjanus campechanus* length-at-age data. Panels depict model fits that were considered trustworthy (a,b) versus fits that were considered untrustworthy (c,d) for relatively old (a,c) and relatively young (b,d) individuals. The solid line denotes the juvenile growth phase, while the dashed line denotes the mature growth phase. The disconnect between the two growth phases in (c,d) is an indicator of poor model convergence. Note that x-axis ranges differ among panels.

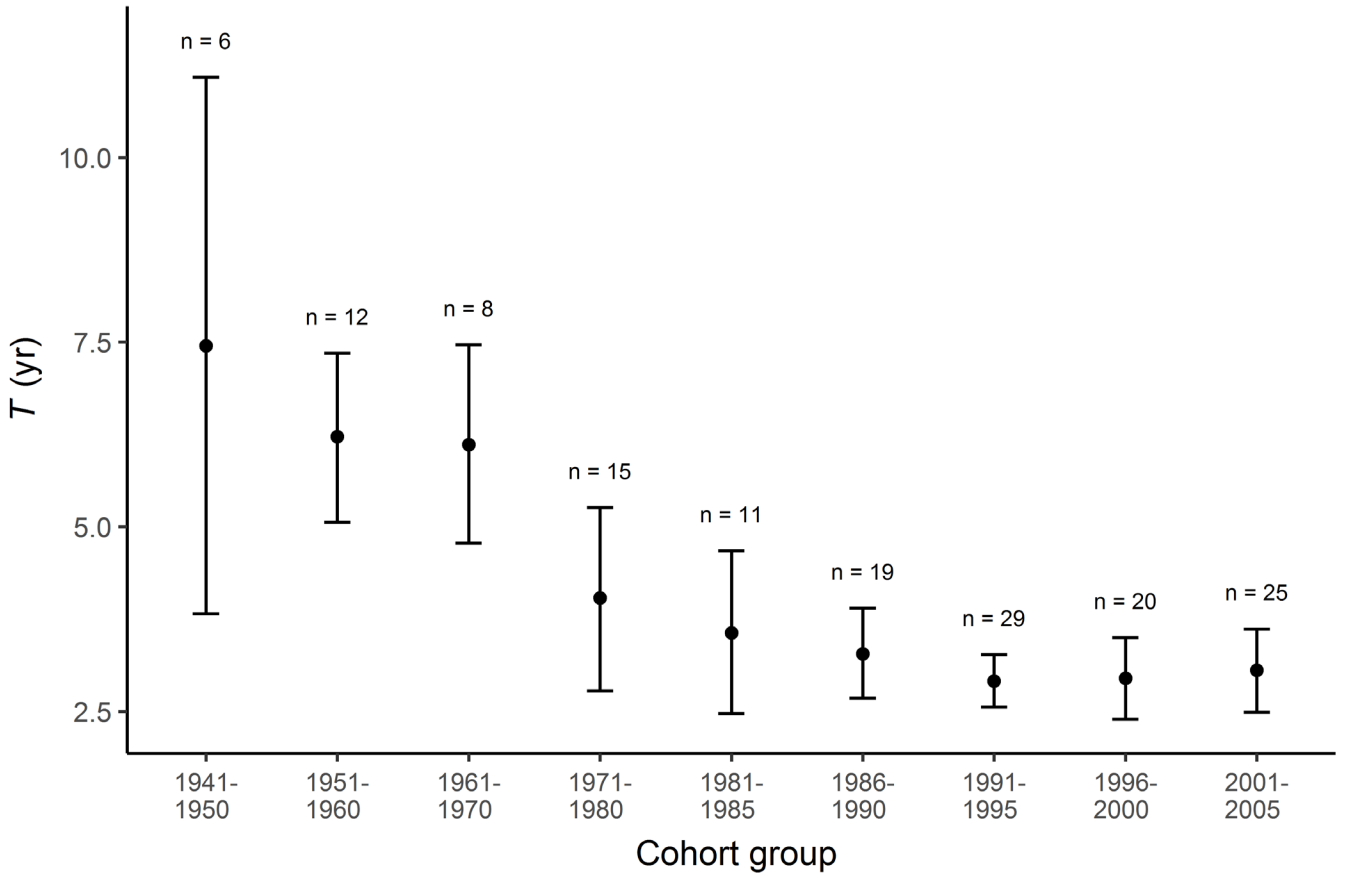

Figure 5.2 Mean cohort group-level estimates of age-at-maturity (*T*; yr) generated from Lester model fits to back-calculated Gulf of Mexico red snapper *Lutjanus campechanus* growth data for cohorts from 1941-2005. Points represent mean estimates of age-at-maturity for each cohort group, and error bars indicate 95% Bayesian credible intervals. Sample sizes (i.e., number of individuals) for each cohort group are displayed above the error bars.

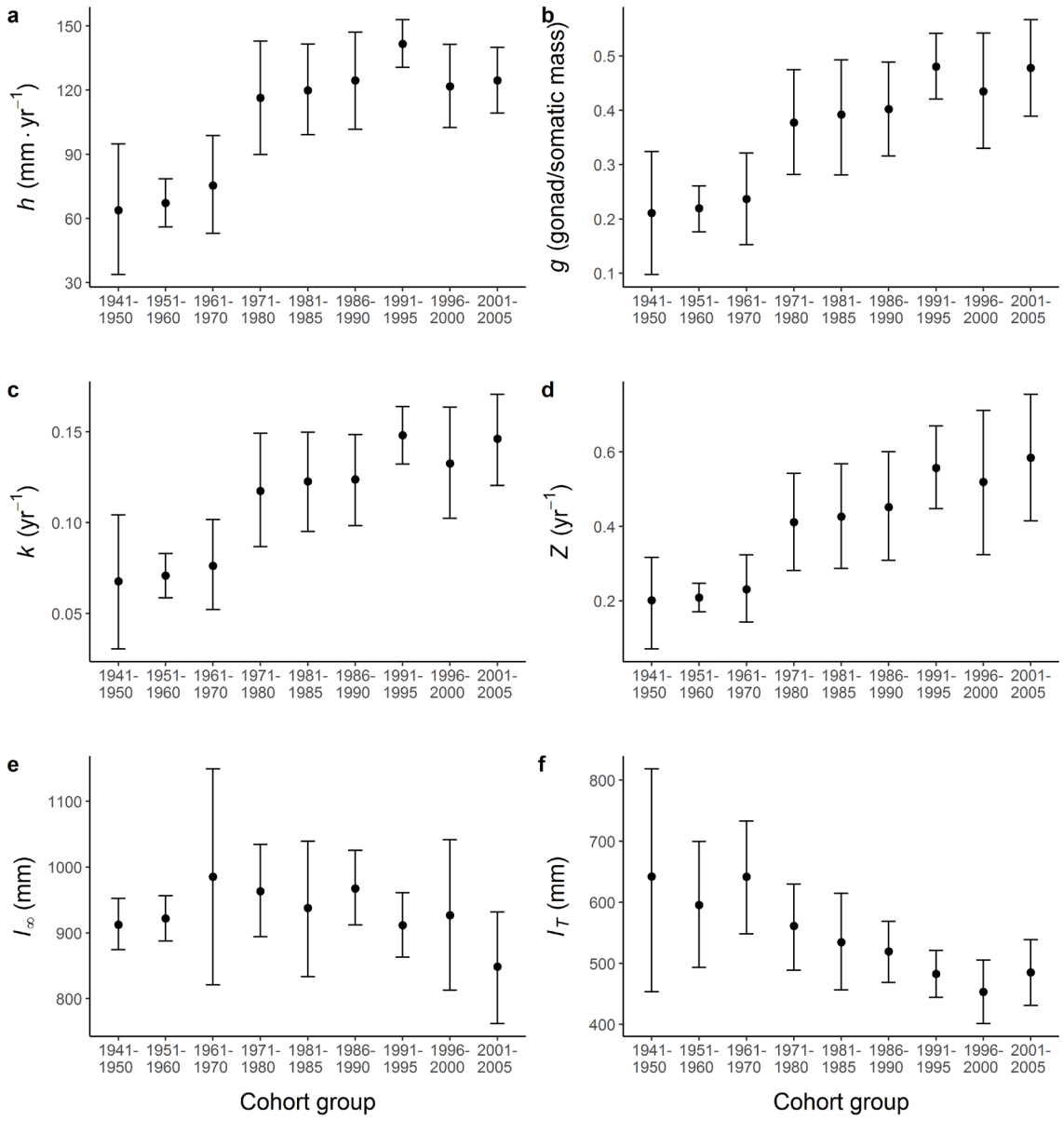

Figure 5.3 Mean cohort group-level life history trait estimates generated from Lester model fits to back-calculated Gulf of Mexico red snapper *Lutjanus campechanus* growth data for cohorts from 1941-2005. Parameters describe (a) juvenile growth rate h (mm·yr^{-1}), (b) the cost to somatic growth of maturity, typically assumed to be dominated by energetic investment in reproduction g (gonad mass/somatic mass), (c) adult growth rate k (the von Bertalanffy growth coefficient; yr^{-1}), (d) instantaneous total mortality rate Z (yr^{-1}), (e) asymptotic length l_∞ (mm), and (f) length-at-maturity l_T (mm). Points represent cohort group-level mean parameter estimates, and error bars indicate 95% Bayesian credible intervals. Sample sizes for each cohort group are identical to those displayed in Fig. 5.2.

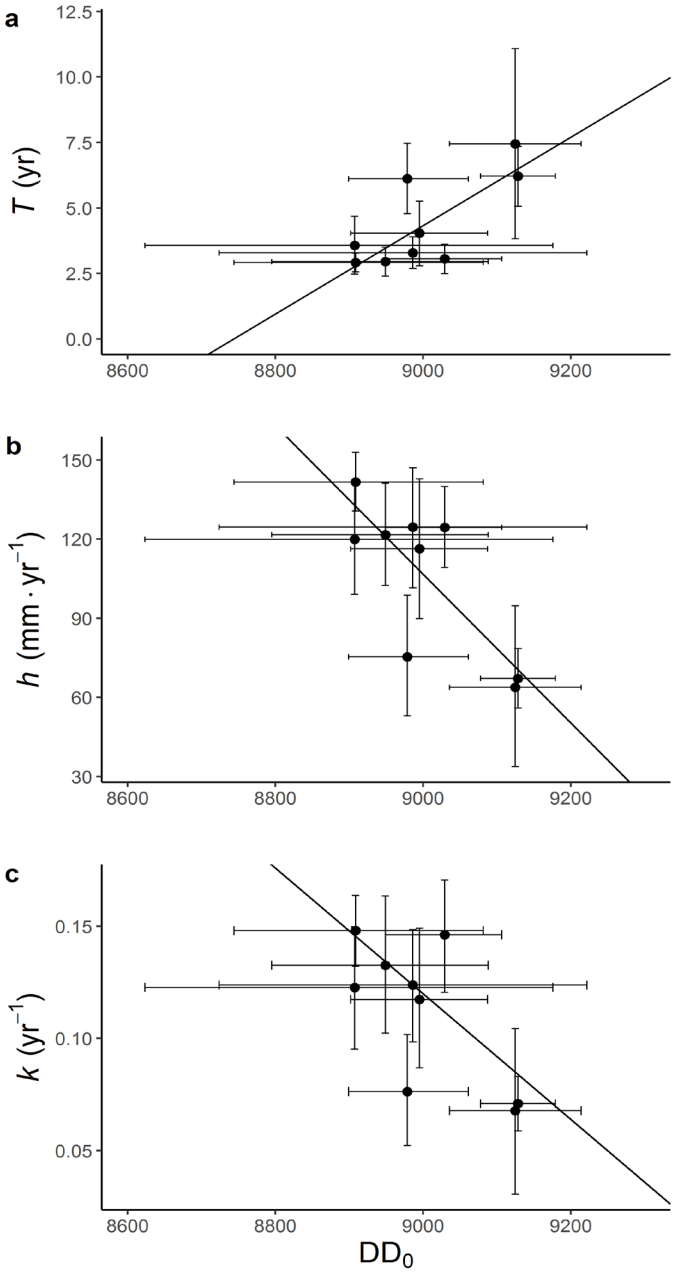

Figure 5.4 Statistically significant relationships of mean annual degree-days above 0 ºC (DD_0) vs. Lester model-based cohort group-level mean estimates of (a) age-at-maturity (T; yr), (b) juvenile somatic growth rate (h; mm·yr^{-1}), and adult growth rate (k, the von Bertalanffy growth coefficient; yr^{-1}) for Gulf of Mexico red snapper *Lutjanus campechanus* from 1941-2005. See Chapter 5 and Figs. 5.2-5.3 for a description of the cohorts included in each group. Annual DD_0 were averaged across the years included in each cohort group. Error bars indicate 95% Bayesian credible intervals. Relationships between DD_0 and the remaining Lester model-based life history trait estimates (g, Z, l_∞, l_T) were not significant.

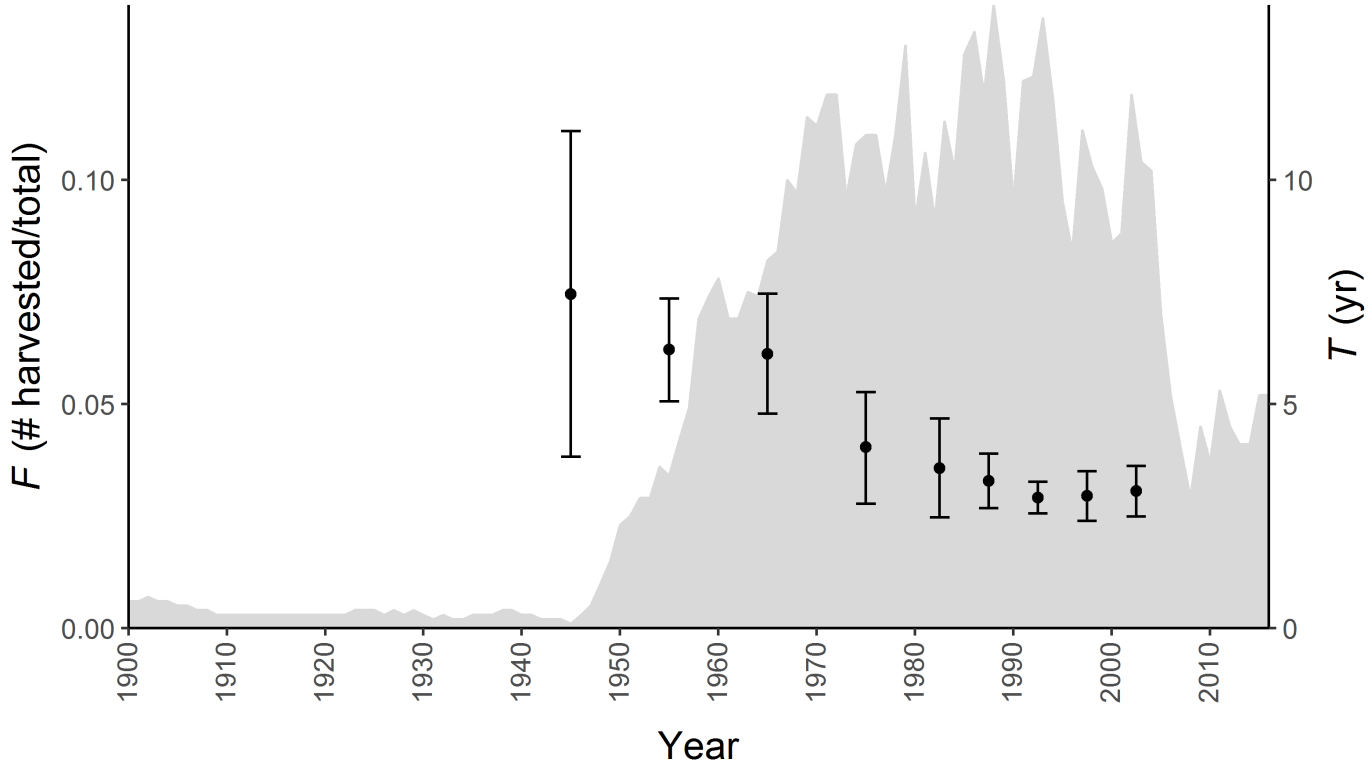

Figure 5.5 Fishing pressure (*F*; shaded region, maps to left axis) and estimated mean cohort group-level age-at-maturity (*T*; points and error bars, map to right axis) for Gulf of Mexico red snapper *Lutjanus campechanus* from 1900-2016. Fishing pressure was indexed as the number of individuals harvested divided by the estimated population size (model estimates; SEDAR 2018). Age-at-maturity estimates were generated using Lester model fits to back-calculated red snapper growth data and are centered on the years included in each cohort group (range = 1941-2005). Error bars indicate 95% Bayesian credible intervals. Sample sizes for each estimate are identical to those shown in Fig. 5.2.

Chapter 6

General discussion

6.1 Summary

Ectotherm growth is intricately linked to both temperature and other aspects of life history (e.g., Stearns 1992, Neuheimer and Taggart 2007, Lester et al. 2014). Understanding the way in which temperature influences growth, and using metrics that reflect that understanding to describe growth, is of paramount importance to ectotherm research and management. In Chapters 2 and 3, my coauthors and I combined theory, empirical data, and simulation modeling to provide (1) foundations for using degree-days (DD) derived from both air and water temperature data to describe fish growth, and (2) guidance for calculating DD for many fishes and scenarios. We showed that the linear relationship between DD and immature fish growth is rooted in fish bioenergetics, and that DD derived from air temperatures can serve as a good proxy for DD derived from water temperatures. We also provided estimates for the base temperature for growth, an important parameter for calculating DD, for many fishes and scenarios. In addition, recent advances in life history theory (e.g., West et al. 1999, Lester et al. 2004, Quince et al. 2008a) have led to the development of growth models that allow for the extraction of a wealth of life history information from growth data (e.g., Mollet et al. 2010, Boukal et al. 2014, Andersen and Beyer 2015). In Chapter 4, my coauthors and I developed a

statistical approach to use one such model, the Lester biphasic growth model (Lester et al. 2004), to estimate multiple life history traits from growth data. We showed that our approach can provide accurate estimates of age-at-maturity for fishes and other ectotherms, and we evaluated the performance of the method across various species and data quality scenarios. Finally, in Chapter 5, we applied the Lester model to investigate changes in life history traits for Gulf of Mexico red snapper *Lutjanus campechanus* from 1941-2005. We showed that red snapper life histories shifted toward a faster life history regime in the mid-20th century, likely in response to exploitation. Using this approach, we were able to paint a picture of red snapper life histories deeper into the past than would have been possible otherwise, thereby gaining a more complete understanding of how red snapper traits have changed in the face of fishing pressure and other stressors.

In essence, this work updates and expands the analytical toolkit used by fish scientists. As such, it has the potential to advance fish science and promote sustainable fisheries management. For example, justifying and providing guidance for the use of DD in fish science should improve estimates of sustainable exploitation rates (Lester et al. 2014), help to disentangle the effects of temperature and other factors (e.g., fishing) on growth and life history (Neuheimer and Grønkjær 2012), and provide insight into fundamental questions about the evolution of growth along a thermal gradient (Angilletta 2009). Inferring maturity and other life history information from growth data can be a powerful tool for adaptive management (Walters 1986) and for analyses of life history shifts in response to anthropogenic or other stressors (e.g., Audzijonyte et al. 2016), particularly when other methods cannot be used (e.g., for samples that lack life history

data). More broadly, this work may be applicable to many species (e.g., see Fig. 4.4) and could motivate similar research in other fields.

6.2 Future directions

Good scientific research raises more questions than it answers (Venturelli 2009). The work described in this volume is no exception. Below, I elaborate on the questions and suggested future directions for research highlighted in Chapters 2-5 that I would argue are most important for advancing fisheries research and management.

DD are particularly useful for comparing growth and physiological traits among populations because they account for differences in thermal energy experienced by individuals in those populations. That is, because DD integrate time and temperature, they allow for comparisons across thermal gradients that would be otherwise confounded by differences in temperature (e.g., Venturelli et al. 2010, Chezik et al. 2014b). The fact that air-based DD (ADD) can serve as an accurate proxy for water-based DD (WDD) is especially advantageous because air temperature data are much more common than water temperature data. However, as mentioned in Section 2.4, the relationship between ADD and WDD may vary among waterbodies. For example, although ADD and WDD may be highly correlated for many waterbodies, the nature (i.e., slope) of that correlation likely differs among waterbodies due to factors such as water clarity, waterbody morphometry, and flow. The two lakes used in Chapter 2 are a prime example of such a difference; although ADD and WDD were highly correlated for both Sparkling Lake and Lake Lacawac, the slopes of the correlations slightly differed. As such, 1 ADD for Sparkling

Lake is not equivalent to 1 ADD for Lake Lacawac from the perspective of an aquatic organism. For cases in which the slopes of ADD versus WDD relationships are substantially different among waterbodies, ADD may fail to accurately quantify differences in thermal environments among populations. It is therefore critical to examine the extent to which ADD versus WDD relationships vary among lakes and regions, and to account for any potential biases that those differences may introduce, when using ADD to describe growth and physiology among populations. Fortunately, given the ubiquity of air temperature data and the fact that there are well-studied and closely-monitored aquatic systems in many regions of the world (see, e.g., the Global Lake Ecological Observatory Network; http://gleon.org/), it should be rather straightforward to construct relationships between ADD and WDD among waterbodies with varying characteristics, and to develop quantitative tools to account for differences in those relationships (i.e., based on waterbody characteristics) that can inform studies that use ADD.

Section 2.4 also mentions the potential to improve DD calculations using upper threshold temperatures. Fish growth and physiological rates decrease dramatically as temperatures increase above optima and toward lethal temperatures (e.g., Kitchell et al. 1977, Jobling 1995). DD do not account for this decrease in physiological rates at high temperatures and may therefore provide an inadequate index of thermal habitat as it relates to fish growth and metabolism, particularly for cases in which individuals spend substantial portions of their time in superoptimal temperatures. Adding an upper threshold temperature, above which growth (or the physiological process in question) is assumed to be negligible, to the DD calculation can help to address this issue. This

practice is already common in plant science (e.g., Snyder et al. 1999). Determining upper threshold temperatures for fishes should be facilitated by the extensive knowledge of thermal traits for some species (e.g., upper incipient lethal temperatures, critical thermal maxima; Hasnain et al. 2010) and by the fish bioenergetics literature. Moreover, future research should explore imposing penalties (i.e., negative DD) when upper threshold temperatures are exceeded using appropriate functional forms; that is, the penalty to DD should increase nonlinearly as temperatures increase above the upper threshold, with higher temperatures leading to a greater penalty. The nature (and perhaps form) of this relationship will likely vary among species but should align with bioenergetics theory (e.g., Hanson et al. 1997).

In Chapters 4 and 5, my coauthors and I used the simplest form of the Lester biphasic growth model (the 'fixed *g*' formulation; Lester et al. 2004, Quince et al. 2008a) to estimate life history traits from length-at-age data. The model provided accurate estimates of age-at-maturity and generally fit well to the data. However, this simple model operates under a few key assumptions, one of which is that metabolism scales with body size to the 2/3 power. There is an extensive literature on metabolic scaling, with an entire body of theory resting on the assumption that metabolism scales with body size to the 3/4 power (i.e., the metabolic theory of ecology; see, e.g., West et al. 1997, 1999, 2001). Thorough reviews and empirical studies have found that this metabolic scaling exponent varies among taxa, typically falling between 2/3 and 1 (Glazier 2005, 2010, Killen et al. 2010). As such, assuming a value of 2/3 for the metabolic scaling exponent may be inaccurate for some species. Quince et al. (2008a) developed a generic

formulation of the biphasic model that relaxes this assumption and allows for the metabolic scaling exponent to be estimated during model fitting (see also Boukal et al. 2014). Using this model may therefore be more appropriate for many species and may help to inform our understanding of both life history and metabolic scaling among taxa. In addition, this generic model allows for the reproductive investment parameter to increase with individual size (i.e., hyperallometric scaling of reproductive investment), a phenomenon that recent work argues is common among fishes and has important implications for fisheries science and management (Marshall and White in press, Barneche et al. 2018). The downside to using the Quince et al. (2008a) model is that it requires the estimation of more parameters than the Lester et al. (2004) model, which will likely complicate model fitting. Future work should explore this more fully and evaluate the performance of the Quince et al. (2008a) model across species and data quality scenarios.

The analyses in Chapter 5 showed that it is possible to estimate life history traits by fitting biphasic growth models to length-at-age data that are back-calculated from hard structures such as otoliths. This approach provided estimates of red snapper life history traits from cohorts in the 1940s, a feat which would have been impossible using traditional approaches due to data limitations. It may be possible to use a similar approach to generate estimates of fish life history traits even further into the past using otoliths that have been preserved in lake or ocean sediments. Due to their aragonite structure, otoliths are readily preserved in sediments and are common teleost fossils (Smol et al. 2001). In addition, otolith morphology often varies among fish species (e.g.,

Reichenbacher et al. 2007, Zorica et al. 2010). Provided that sediment-preserved otoliths can be identified to species, and operating under some assumptions regarding the relationships between otolith size, fish body size, and fish age (which can be informed using present-day data), it may be possible to estimate life history traits for fishes far into the past using biphasic growth models and otoliths from sediment cores. As such, it may be possible to address questions related to fish life history evolution over millennia.

6.3 Conclusion

This work represents an important step forward in how we describe and model ectotherm growth that leverages mechanistic understandings of both the effects of temperature on growth and the inextricable links between growth and life history. Fish science lags behind other fields in the widespread adoption of DD. Chapters 2 and 3 provide justification and guidance for using DD and will help to encourage the application of this important metric in the aquatic sciences. In addition, growth data contain a wealth of information on life history. Chapters 4 and 5 show that we can use biphasic growth models to extract some of that information and use it to address ecological questions. Ultimately, this work introduces and promotes accurate and theoretically-sound methods for analyzing fisheries data. As such, it has the potential to stimulate a diversity of important basic and applied fisheries research, promote adaptive and sustainable fisheries management, and increase global food security.

References

Abbott, J. K., P. Lloyd-Smith, D. Willard, and W. Adamowicz. 2018. Status-quo management of marine recreational fisheries undermines angler welfare. Proceedings of the National Academy of Sciences 115(36):8948-8953.

Allen, J. C. 1976. A modified sine wave method for calculating degree days. Environmental Entomology 5:388–396.

Allman, R. J., G. R. Fitzhugh, K. J. Starzinger, and R. A. Farsky. 2005. Precision of age estimation in red snapper (*Lutjanus campechanus*). Fisheries Research 73:123–133.

Andersen, K. H., and J. E. Beyer. 2015. Size structure, not metabolic scaling rules, determines fisheries reference points. Fish and Fisheries 16:1–22.

Anderson, C. N. K., C. Hsieh, S. A. Sandin, R. Hewitt, A. Hollowed, J. Beddington, R. M. May, and G. Sugihara. 2008. Why fishing magnifies fluctuations in fish abundance. Nature 452:835–839.

Angilletta, M. J. 2009. Thermal adaptation: a theoretical and empirical synthesis. Oxford University Press, Oxford, England, UK.

Ashworth, E. C., N. G. Hall, S. A. Hesp, P. G. Coulson, and I. C. Potter. 2017a. Age and growth rate variation influence the functional relationship between somatic and otolith size. Canadian Journal of Fisheries and Aquatic Sciences 74:680–692.

Ashworth, E. C., S. A. Hesp, and N. G. Hall. 2017b. A new proportionality-based back-calculation approach, which employs traditional forms of growth equations, improves estimates of length at age. Canadian Journal of Fisheries and Aquatic Sciences 74:1088–1099.

Atkinson, D. 1994. Temperature and organism size - a biological law for ectotherms? Advances in Ecological Research 25:1–58.

Audzijonyte, A., E. Fulton, M. Haddon, F. Helidoniotis, A. J. Hobday, A. Kuparinen, J. Morrongiello, A. D. M. Smith, J. Upston, and R. S. Waples. 2016. Trends and management implications of human-influenced life-history changes in marine ectotherms. Fish and Fisheries 17:1005–1028.

Augert, D., and P. Joly. 1993. Plasticity of age at maturity between two neighbouring populations of the common frog (*Rana temporaria* L.). Canadian Journal of Zoology 71:26–33.

Bajer, P. G., R. S. Hayward, G. W. Whitledge, and R. D. Zweifel. 2004. Simultaneous identification and correction of systematic error in bioenergetics models: demonstration with a white crappie (*Pomoxis annularis*) model. Canadian Journal of Fisheries and Aquatic Sciences 61:2168–2182.

Barneche, D. R., D. R. Robertson, C. R. White, and D. J. Marshall. 2018. Fish reproductive-energy output increases disproportionately with body size. Science 360:642–645.

Baulier, L., and M. Heino. 2008. Norwegian spring-spawning herring as the test case of piecewise linear regression method for detecting maturation from growth patterns. Journal of Fish Biology 73:2452–2467.

Bernardo, J. 1993. Determinants of maturation in animals. Trends in Ecology and Evolution 8:166–173.

Berrigan, D., and E. L. Charnov. 1994. Reaction norms for age and size at maturity in

response to temperature: a puzzle for life historians. Oikos 70:474–478.

von Bertalanffy, L. 1938. A quantitative theory of organic growth (inquiries on growth laws II). Human Biology 10:181–213.

von Bertalanffy, L. 1957. Quantitative laws in metabolism and growth. The Quarterly Review of Biology 32:217–231.

Beverton, R. J. H., and S. J. Holt. 1957. On the dynamics of exploited fish populations. Fishery Investigations, Series II 19:1–533.

Blevins, D. W. 2011. Water-Quality Requirements, Tolerances, and Preferences of Pallid Sturgeon (*Scaphirhynchus albus*) in the Lower Missouri River. U.S. Geological Survey Scientific Investigations Report 2011-5186.

Boukal, D. S., U. Dieckmann, K. Enberg, M. Heino, and C. Jorgensen. 2014. Life-history implications of the allometric scaling of growth. Journal of Theoretical Biology 359:199–207.

Bozek, M. A., D. A. Baccante, and N. P. Lester. 2011. Walleye and sauger life history. Pages 233–301 *in* B. Barton, editor. Biology, management, and culture of walleye and sauger. American Fisheries Society, Bethesda, Maryland, USA.

Bradley, E., and C. E. Bryan. 1975. Life history and fisher of the red snapper, Lutjanus campechanus, in the Northwestern Gulf of Mexico: 1970-1974. Proceedings of the Gulf and Caribbean Fisheries Institute 27:77–106.

Brown-Peterson, N. J., K. M. Burns, and R. Overstreet. 2009. Regional Differences in Florida Red Snapper Regional Differences in Florida Red Snapper Reproduction. Proceedings of the Gulf and Caribbean Fisheries Institute 61:149–155.

Brown-Peterson, N. J., C. R. Peterson, and G. R. Fitzhugh. In press. Multi-decadal meta-analysis of female red snapper reproductive parameters in the northern Gulf of Mexico. Fishery Bulletin.

Brunel, T., B. Ernande, F. M. Mollet, and A. D. Rijnsdorp. 2013. Estimating age at maturation and energy-based life-history traits from individual growth trajectories with nonlinear mixed-effects models. Oecologia 172:631–643.

Campana, S. E. 1990. How reliable are growth back-calculations based on otoliths? Canadian Journal of Fisheries and Aquatic Sciences 47:2219–2227.

Canty, A., and B. Ripley. 2015. boot: Bootstrap R (S-plus) Functions. R package version 1.3-20.

Carpenter, B., A. Gelman, M. D. Hoffman, D. Lee, B. Goodrich, M. Betancourt, M. Brubaker, J. Guo, P. Li, and A. Riddell. 2017. Stan: a probabilistic programming language. Journal of Statistical Software 76:1–32.

Carpenter, J. S. 1965. A Review of the Gulf of Mexico Red Snapper Fishery. United States Fish and Wildlife Service Circular 208. Washington, D.C., USA.

Castanet, J., H. Francillon-vieillot, and R. C. Bruce. 1996. Age estimation in desmognathine salamanders assessed by skeletochronology. Herpetologica 52:160–171.

Charnov, E. L., and D. Berrigan. 1990. Dimensionless numbers and life history evolution: age of maturity versus the adult lifespan. Evolutionary Ecology 4:273–275.

Charnov, E. L., and J. F. Gillooly. 2003. Thermal time: body size, food quality and the 10

degrees C rule. Evolutionary Ecology Research 5:43–51.

Chavarie, L., J. B. Dempson, C. J. Schwarz, J. D. Reist, G. Power, and M. Power. 2010. Latitudinal variation in growth among Arctic charr in eastern North America: Evidence for countergradient variation? Hydrobiologia 650:161–177.

Chavarie, L., K. Howland, P. A. Venturelli, B. C. Kissinger, R. Tallman, and W. M. Tonn. 2016. Life-history variation among four shallow-water morphotypes of lake trout from Great Bear Lake, Canada. Journal of Great Lakes Research 42:193–203.

Chen, Y., and J. E. Paloheimo. 1994. Estimating fish length and age at 50% maturity using a logistic type model. Aquatic Sciences 56:206–219.

Cherry, D. S., K. L. Dickson, J. Cairns Jr., and J. R. Stauffer. 1977. Preferred, avoided, and lethal temperatures of fish during rising temperature conditions. Journal of the Fisheries Research Board of Canada 34:239–246.

Chezik, K. A. 2013. Fish growth and degree-days: advice for selecting base temperatures in both within- and among-lake studies. M.Sc. Thesis, University of Minnesota.

Chezik, K. A., N. P. Lester, and P. A. Venturelli. 2014a. Fish growth and degree-days I: selecting a base temperature for a within-population study. Canadian Journal of Fisheries and Aquatic Sciences 71:47–55.

Chezik, K. A., N. P. Lester, and P. A. Venturelli. 2014b. Fish growth and degree-days II: selecting a base temperature for an among-population study. Canadian Journal of Fisheries and Aquatic Sciences 71:1303–1311.

Chipps, S. R., L. M. Einfalt, and D. H. Wahl. 2000. Growth and food consumption by tiger muskellunge: effects of temperature and ration level on bioenergetic model

predictions. Transactions of the American Fisheries Society 129:186–193.

Coker, G. A., C. B. Portt, and C. K. Minns. 2001. Morphological and Ecological Characteristics of Canadian Freshwater Fishes. Canadian Manuscript Report of Fisheries and Aquatic Sciences 2554.

Colby, P. J., and S. J. Nepszy. 1981. Variation among stocks of walleye (*Stizostedion vitreum vitreum*): management implications. Canadian Journal of Fisheries and Aquatic Sciences 38:1814–1831.

Conover, D. O., and S. B. Munch. 2002. Sustaining fisheries yields over evolutionary time scales. Science 297:94–96.

Conover, D. O., and T. M. C. Present. 1990. Countergradient variation in growth rate: compensation for length of the growing season among Atlantic silversides from different latitudes. Oecologia 83:316–324.

Cook, M., B. K. Barnett, M. S. Duncan, R. J. Allman, C. E. Porch, and G. R. Fitzhugh. 2009. Characterization of red snapper (Lutjanus campechanus) size and age at sexual maturity for the 2009 Gulf of Mexico SEDAR update. Panama City Laboratory Contribution Series 09-16, Panama City, FL, USA.

Coutant, C. C. 1977. Compilation of Temperature Preference Data. Journal of the Fisheries Research Board of Canada 34:739–745.

Cowan, Jr., J. H., R. L. Shipp, H. K. Bailey, and D. W. Haywick. 1995. Procedure for rapid processing of large otoliths. Transactions of the American Fisheries Society 124:280–282.

Daniel, W. W., and C. L. Cross. 2013. Biostatistics: a foundation for analysis in the

health sciences. Tenth edition. John Wiley and Sons, New York, New York, USA.

Davison, A. C., and D. V. Hinkley. 1997. Bootstrap methods and their applications. Cambridge University Press, Cambridge, England, UK.

Day, T., and P. D. Taylor. 1997. von Bertalanffy's growth equation should not be used to model age and size at maturity. The American Naturalist 149:381–393.

DeMaster, D. P. 1978. Calculation of the average age of sexual maturity in marine mammals. Journal of the Fisheries Research Board of Canada 35:912–915.

Desai, A. R., J. a. Austin, V. Bennington, and G. a. McKinley. 2009. Stronger winds over a large lake in response to weakening air-to-lake temperature gradient. Nature Geoscience 2:855–858.

Deslauriers, D., S. R. Chipps, J. E. Breck, J. A. Rice, and C. P. Madenjian. 2017. Fish Bioenergetics 4.0: An R-Based Modeling Application. Fisheries 42:586–596.

Diana, J. S. 2003. Biology and ecology of fishes. Cooper Publishing Group, Traverse City, MI, USA.

Doubleday, Z. A., C. Izzo, J. A. Haddy, J. M. Lyle, Q. Ye, and B. M. Gillanders. 2015. Long-term patterns in estuarine fish growth across two climatically divergent regions. Oecologia 179:1079–1090.

Dumas, A., J. France, and D. Bureau. 2010. Modelling growth and body composition in fish nutrition: where have we been and where are we going? Aquaculture Research 41:161–181.

Dunlop, E. S., Z. S. Feiner, and T. O. Höök. 2018. Potential for fisheries-induced evolution in the Laurentian Great Lakes. Journal of Great Lakes Research 44:735–

747.

Dzaugis, M. P., R. J. Allman, and B. A. Black. 2017. Importance of the spring transition in the northern Gulf of Mexico as inferred from marine fish biochronologies. Marine Ecology Progress Series 565:149–162.

Ebert, D. 1994. A maturation size threshold and phenotypic plasticity of age and size at maturity in *Daphnia magna*. Oikos 69:309–317.

Edinger, J. E., D. W. Duttweiler, and J. C. Geyer. 1968. The response of water temperatures to meteorlogical conditions. Water Resources Research 4:1137–1143.

Edsall, T. A., and P. J. Colby. 1970. Temperature tolerance of young-of-the-year cisco, *Coregonus artedii*. Transactions of the American Fisheries Society 99:526–531.

Elliott, J. M., and W. Davison. 1975. Energy equivalents of oxygen consumption in animal energetics. Oecologia 19:195–201.

Enberg, K., C. Jørgensen, E. S. Dunlop, Ø. Varpe, D. S. Boukal, L. Baulier, S. Eliassen, and M. Heino. 2012. Fishing-induced evolution of growth: concepts, mechanisms and the empirical evidence. Marine Ecology 33:1–25.

Engelhard, G. H., U. Dieckmann, and O. R. Godø. 2003. Age at maturation predicted from routine scale measurements in Norwegian spring-spawning herring (*Clupea harengus*) using discriminant and neural network analyses. ICES Journal of Marine Science 60:304–313.

Erickson, T. R., and H. G. Stefan. 2000. Linear air/water temperature correlations for streams during open water periods. Journal of Hydrologic Engineering 5:317–321.

Feiner, Z. S., S. C. Chong, C. T. Knight, T. E. Lauer, M. V. Thomas, J. T. Tyson, and T.

O. Höök. 2015. Rapidly shifting maturation schedules following reduced commercial harvest in a freshwater fish. Evolutionary Applications 8:724–737.

Feltz, C. J., and G. E. Miller. 1996. An asymptotic test for the equality of coefficients of variation from k populations. Statistics in Medicine 15:647–658.

Figueira, W. F., and F. C. Coleman. 2010. Comparing landings of United States recreational fishery sectors. Bulletin of Marine Science 86:499–514.

Fischer, A. J., M. S. Baker Jr., and C. A. Wilson. 2004. Red snapper (*Lutjanus campechanus*) demographic structure in the northern Gulf of Mexico based on spatial patterns in growth rates and morphometrics. Fishery Bulletin 102:593–603.

Fox, J., and S. Weisberg. 2011. An R companion to applied regression, 2nd edition. Sage Publications, Thousand Oaks, California, USA.

Froese, R., and D. Pauly, editors. 2016. FishBase. World wide web electronic publication. www.fishbase.org.

Futch, R. B., and G. E. Bruger. 1976. Age, growth, and reproduction of red snapper in Florida waters. Pages 165–185 *in* H. R. Bullis and A. C. Jones, editors. Proceedings: Colloquium on snapper-grouper fishery resources for the western central Atlantic Ocean. Florida SeaGrant College Report 17.

García-Berthou, E., G. Carmona-Catot, R. Merciai, and D. H. Ogle. 2012. A technical note on seasonal growth models. Reviews in Fish Biology and Fisheries 22:635–640.

Gelman, A., and D. B. Rubin. 1992. Inference form iterative simulation using multiple sequences. Statistical Science 7:457–511.

Glazier, D. S. 2005. Beyond the “3/4-power law”: Variation in the intra- and interspecific scaling of metabolic rate in animals. Biological Reviews of the Cambridge Philosophical Society 80:611–662.

Glazier, D. S. 2010. A unifying explanation for diverse metabolic scaling in animals and plants. Biological Reviews 85:111–138.

Hacking, I. 1965. Logic of statistical inference. Cambridge University Press, Cambridge, England, UK.

Hamann, A., and T. L. Wang. 2005. Models of climatic normals for genecology and climate change studies in British Columbia. Agricultural and Forest Meteorology 128:211–221.

Hamann, A., T. Wang, D. L. Spittlehouse, and T. Q. Murdock. 2013. A comprehensive, high-resolution database of historical and projected climate surfaces for western North America. Bulletin of the American Meteorological Society 94:1307–1309.

Hansen, G. J. A., J. S. Read, J. F. Hansen, and L. A. Winslow. 2017. Projected shifts in fish species dominance in Wisconsin lakes under climate change. Global Change Biology 23:1463–1476.

Hanson, P. C., T. B. Johnson, D. E. Schindler, and J. F. Kitchell. 1997. Fish Bioenergetics 3.0 for Windows. University of Wisconsin Sea Grant Institute, Madison, WI.

Hartman, K. J. 2017. Bioenergetics of brown bullhead in a changing climate. Transactions of the American Fisheries Society 146:634–644.

Hartman, K. J., and M. K. Cox. 2008. Refinement and testing of a brook trout

bioenergetics model. Transactions of the American Fisheries Society 137:357–363.

Hartman, K. J., and F. J. Margraf. 1992. Effects of prey and predator abundances on prey consumption and growth of walleyes in western Lake Erie. Transactions of the American Fisheries Society 121:245–260.

Hasnain, S. S., C. K. Minns, and B. J. Shuter. 2010. Key ecological temperature metrics for Canadian freshwater fishes. Ontario Ministry of Natural Resources Climate Change Research Report CCRR-17.

Hasnain, S. S., B. J. Shuter, and C. K. Minns. 2013. Phylogeny influences the relationships linking key ecological thermal metrics for North American freshwater fish species. Canadian Journal of Fisheries and Aquatic Sciences 70:964–972.

van der Have, T. M., and G. de Jong. 1996. Adult size in ectotherms: temperature effects on growth and differentiation. Journal of Theoretical Biology 183:329–340.

Hazel, J. R., and C. L. Prosser. 1974. Molecular mechanisms of temperature compensation in poikilotherms. Physiological Reviews 54:620–677.

Heino, M. 1998. Management of evolving fish stocks. Canadian Journal of Fisheries and Aquatic Sciences1 55:1971–1982.

Heino, M., L. Baulier, D. S. Boukal, B. Ernande, F. D. Johnston, F. M. Mollet, H. Pardoe, N. O. Therkildsen, S. Uusi-Heikkilä, A. Vainikka, R. Arlinghaus, D. J. Dankel, E. S. Dunlop, A. M. Eikeset, K. Enberg, G. H. Engelhard, C. Jorgensen, A. T. Laugen, S. Matsumura, S. Nussle, D. Urbach, R. Whitlock, A. D. Rijnsdorp, and U. Dieckmann. 2013. Can fisheries-induced evolution shift reference points for fisheries management? ICES Journal of Marine Science 70:707–721.

Heino, M., B. Díaz Pauli, and U. Dieckmann. 2015. Fisheries-induced evolution. Annual Review of Ecology, Evolution, and Systematics 46:461–480.

Heino, M., U. Dieckmann, and O. R. Godø. 2002. Measuring probabilistic reaction norms for age and size at maturation. Evolution 56:669–678.

Heino, M., and O. R. Godo. 2002. Fisheries-induced selection pressures in the context of sustainable fisheries. Bulletin of Marine Science 70:639–656.

Helser, T. E., and H. L. Lai. 2004. A Bayesian hierarchical meta-analysis of fish growth: with an example for North American largemouth bass, *Micropterus salmoides*. Ecological Modelling 178:399–416.

Herczeg, G., A. Gonda, A. Kuparinen, and J. Merila. 2012. Contrasting growth strategies of pond versus marine populations of nine-spined stickleback (*Pungitius pungitius*): a combined effect of predation and competition? Evolutionary Ecology 26:109–122.

Hilborn, R., and C. J. Walters. 1992. Quantitative fisheries stock assessment: choice, dynamics, and uncertainty. Springer Science and Business Media, Dordrecht, The Netherlands.

Hixon, M. A., D. W. Johnson, and S. M. Sogard. 2014. BOFFFFs: on the importance of conserving old-growth age structure in fishery populations. ICES Journal of Marine Science 71:2171–2185.

Hondzo, M., and H. G. Stefan. 1993. Regional water temperature characteristics of lakes subjected to climate change. Climatic Change 24:187–211.

Honsey, A. E., D. B. Bunnell, C. D. Troy, D. G. Fielder, M. V. Thomas, C. T. Knight, S. C. Chong, and T. O. Höök. 2016. Recruitment synchrony of yellow perch (*Perca*

flavescens, Percidae) in the Great Lakes region, 1966 – 2008. Fisheries Research 181:214–221.

Honsey, A. E., D. F. Staples, and P. A. Venturelli. 2017. Accurate estimates of age-at-maturity from the growth trajectories of fishes and other ectotherms. Ecological Applications 27:182–192.

Honsey, A. E., P. A. Venturelli, and N. P. Lester. In press. Bioenergetic and limnological foundations for using air-based degree-days to describe fish growth. Canadian Journal of Fisheries and Aquatic Sciences.

Hubert, J. J. 1984. Bioassay, 2nd edition. Kendall/Hunt, Dubuque, Iowa, USA.

Hutchings, J. A., and D. J. Fraser. 2008. The nature of fisheries- and farming-induced evolution. Molecular Ecology 17:294–313.

IPCC. 2014. Climate change 2014: Impacts, adaptation, and vulnerability. Part A: Global and sectoral aspects. Contribution of Working Group II to the Fifth Assessment Report of the Intergovernmental Panel on Climate Change. Page (C. B. Field, V. R. Barros, D. J. Dokken, K. J. Mach, M. D. Mastrandrea, T. E. Bilir, M. Chatterjee, K. L. Ebi, Y. O. Estrada, R. C. Genova, B. Girma, E. S. Kissel, A. N. Levy, S. MacCracken, P. R. Mastrandrea, and L. L. White, Eds.). Cambridge University Press, Cambridge, England, UK and New York, NY, USA.

Jackson, M. W., J. H. Cowan, Jr., and D. L. Nieland. 2007. Demographic differences in northern Gulf of Mexico red snapper reproductive maturation: implications for the unit stock hypothesis. American Fisheries Society Symposium 60:217–227.

Jacobson, P. C., H. G. Stefan, and D. L. Pereira. 2010. Coldwater fish oxythermal habitat

in Minnesota lakes: influence of total phosphorus, July air temperature, and relative depth. Canadian Journal of Fisheries and Aquatic Sciences 67:2002–2013.

Jobling, M. 1995. Fish bioenergetics. Chapman and Hall, London, England, UK.

Kalbfleisch, J. D., and D. A. Sprott. 1970. Application of likelihood methods to models involving large numbers of parameters. Journal of the Royal Statistical Society, Series B 32:175–208.

Karas, P., and G. Thoresson. 1992. An application of a bioenergetics model to Eurasian perch (*Perca fluviatilis* L.). Journal of Fish Biology 41:217–230.

Killen, S. S., D. Atkinson, and D. S. Glazier. 2010. The intraspecific scaling of metabolic rate with body mass in fishes depends on lifestyle and temperature. Ecology Letters 13:184–193.

Kitchell, J. F., D. J. Stewart, and D. Weininger. 1977. Applications of a bioenergetics model to yellow perch (*Perca flavescens*) and walleye (*Stizostedion vitreum vitreum*). Journal of the Fisheries Research Board of Canada 34:1922–1935.

Kozlowski, J. 1996. Optimal allocation of resources explains interspecific life-history patterns in animals with indeterminate growth. Proceedings of the Royal Society of London B 263:559–566.

Kratz, T. 1983. Minocqua Dam Daily Meteorological Data at North Temperate Lakes LTER 1978 - current. Long Term Ecological Research Network. http://dx.doi.org/10.6073/pasta/f81f16c816e73c76705b1e9d9792b9b3.

Krishnamoorthy, K., and M. Lee. 2014. Improved tests for the equality of normal coefficients of variation. Computational Statistics 29:215–232.

Kumar, S., S. A. Spaulding, T. J. Stohlgren, K. A. Hermann, T. S. Schmidt, and L. L. Bahls. 2009. Potential habitat distribution for the freshwater diatom Didymosphenia geminata in the continental US. Frontiers in Ecology and the Environment 7:415–420.

Kuparinen, A., and J. A. Hutchings. 2012. Consequences of fisheries-induced evolution for population productivity and recovery potential. Proceedings of the Royal Society of London B 279:2571–2579.

Kuparinen, A., and J. Merilä. 2007. Detecting and managing fisheries-induced evolution. Trends in Ecology and Evolution 22:652–659.

Kuwamara, T., Y. Nakashima, and Y. Yogo. 1996. Plasticity in size and age at maturity in a monogamous fish: effect of host coral size and frequency dependence. Behavioral Ecology and Sociobiology 38:365–370.

Laird, N. M., and J. H. Ware. 1982. Random-effects models for longitudinal data. Biometrics 38:963–974.

Lantry, B. F., and D. J. Stewart. 1993. Ecological energetics of rainbow smelt in the Laurentian Great Lakes: an interlake comparison. Transactions of the American Fisheries Society 122:951–976.

Law, R. 2000. Fishing, selection, and phenotypic evolution. ICES Journal of Marine Science 57:659–668.

Law, R. 2007. Fisheries-induced evolution: present status and future directions. Marine Ecology-Progress Series 335:271–277.

Lee, R.M. 1920. A review of methods of age and growth determination in fishes by

means of scales. Fishery Investigations, Series II 4(2):1-32.

Lester, N. P., B. J. Shuter, and P. A. Abrams. 2004. Interpreting the von Bertalanffy model of somatic growth in fishes: the cost of reproduction. Proceedings of the Royal Society of London B 271:1625–1631.

Lester, N. P., B. J. Shuter, P. A. Venturelli, and D. Nadeau. 2014. Life-history plasticity and sustainable exploitation: a theory of growth compensation applied to walleye management. Ecological Applications 24:38–54.

Levins, R. 1969. Thermal acclimation and heat resistance in *Drosophila* species. The American Naturalist 103:483–499.

Livingstone, D. M., and M. T. Dokuli. 2001. Eighty years of spatially coherent Austrian lake surface temperatures and their relationship to regional air temperature and the North Atlantic Oscillation. Limnology and Oceanography 46:1220–1227.

Livingstone, D. M., and A. F. Lotter. 1998. The relationship between air and water temperatures in lakes of the Swiss Plateau: a case study with palaeolimnological implications. Journal of Paleolimnology 19:181–198.

Logsdon, D. E. 2006. Contribution of fry stocking to the recovery of the walleye population in the Red Lakes. Minnesota Department of Natural Resources, Section of Fisheries Investigational Report 535. St. Paul, MN, USA.

Lorenzen, K. 2016. Toward a new paradigm for growth modeling in fisheries stock assessments: Embracing plasticity and its consequences. Fisheries Research 180:4–22.

Lorenzen, K., and K. Enberg. 2002. Density-dependent growth as a key mechanism in the

regulation of fish populations: evidence from among-population comparisons. Proceedings of the Royal Society of London B 269:49–54.

Luecke, C., and D. Brandt. 1993. Estimating the energy density of daphnid prey for use with rainbow trout bioenergetics models. Transactions of the American Fisheries Society 122:386–389.

Macan, T. T., and R. Maudsley. 1966. The temperature of a moorland fishpond. Hydrobiologia 27:1–22.

Madon, S. P., G. D. Williams, J. M. West, and J. B. Zedler. 2001. The importance of marsh access to growth of the California killifish, *Fundulus parvipinnis*, evaluated through bioenergetics modeling. Ecological Modelling 136:149–165.

Malzahn, A. M., C. Clemmesen, and H. Rosenthal. 2003. Temperature effects on growth and nucleic acids in laboratory-reared larval coregonid fish. Marine Ecology Progress Series 259:285–293.

Marshall, D. J., and C. R. White. In press. Have we outgrown the existing models of growth? Trends in Ecology & Evolution.

Marwick, B., and K. Krishnamoorthy. 2018. cvequality: Tests for the equality of coefficients of variation from multiple groups. R software package version 0.1.3.

Matta, M. E., and D. R. Gunderson. 2007. Age, growth, maturity, and mortality of the Alaska skate, *Bathyraja parmifera*, in the eastern Bering Sea. Environmental Biology of Fishes 80:309–323.

Mbogga, M. S., A. Hamann, and T. Wang. 2009. Historical and projected climate data for natural resource management in western Canada. Agricultural and Forest

Meteorology 149:881–890.

Minte-Vera, C. V., M. N. Maunder, J. M. Casselman, and S. E. Campana. 2016. Growth functions that incorporate the cost of reproduction. Fisheries Research 180:31–44.

Mohseni, O., and H. G. Stefan. 1999. Stream temperature air temperature relationship: a physical interpretation. Journal of Hydrology 218:128–141.

Mollet, F. M., G. H. Engelhard, A. Vainikka, A. T. Laugen, A. D. Rijnsdorp, and B. Ernande. 2013. Spatial variation in growth, maturation schedules and reproductive investment of female sole *Solea solea* in the Northeast Atlantic. Journal of Sea Research 84:109–121.

Mollet, F. M., B. Ernande, T. Brunel, and A. D. Rijnsdorp. 2010. Multiple growth-correlated life history traits estimated simultaneously in individuals. Oikos 119:10–26.

Morgan, G. E. 2002. Manual of instructions -- fall walleye index netting (FWIN). Edited by Ontario Ministry of Natural Resources, Peterborough, Ontario, Canada.

Morita, K., and T. Matsuishi. 2001. A new model of growth back-calculation incorporating age effect based on otoliths. Canadian Journal of Fisheries and Aquatic Sciences 58:1805–1811.

Moyle, P. B., and N. K. Knight. 1984. Temperature requirements of Pacific coastal fishes. University of California, Davis Technical Completion Report UCAL-WRC-W-641.

Myrvold, K. M., and B. P. Kennedy. 2015. Interactions between body mass and water temperature cause energetic bottlenecks in juvenile steelhead. Ecology of

Freshwater Fish 24:373–383.

Neuheimer, A. B., and P. Grønkjær. 2012. Climate effects on size-at-age: growth in warming waters compensates for earlier maturity in an exploited marine fish. Global Change Biology 18:1812–1822.

Neuheimer, A. B., and C. T. Taggart. 2007. The growing degree-day and fish size-at-age: the overlooked metric. Canadian Journal of Fisheries and Aquatic Sciences 64:375–385.

Nieland, D. L., C. A. Wilson, III, and A. J. Fischer. 2007. Declining size at age among red snapper in the northern Gulf of Mexico off Louisiana, USA: recovery or collapse? American Fisheries Society Symposium 60:301–307.

NTL LTER. 1991a. North Temperate Lakes LTER: High Frequency Water Temperature Data - Sparkling Lake Raft 1989 - current. University of Wisconsin Center for Limnology, Long Term Ecological Research Network. https://portal.lternet.edu/nis/mapbrowse?packageid=knb-lter-ntl.5.

NTL LTER. 1991b. North Temperate Lakes LTER Meteorological Data - Woodruff Airport 1989 - current. University of Wisconsin Center for Limnology, Long Term Ecological Research Network. https://portal.lternet.edu/nis/mapbrowse?packageid=knb-lter-ntl.17.21.

Nyboer, E. A., and L. J. Chapman. 2017. Elevated temperature and acclimation time affect metabolic performance in the heavily exploited Nile perch of Lake Victoria. Journal of Experimental Biology:jeb.163022.

Ogle, D. H., T. O. Brenden, and J. L. McCormick. 2018. Growth estimation: growth

models and statistical inference. Pages 265–359 *in* M. Quist and D. Isermann, editors. Age and growth of fishes: principles and techniques. American Fisheries Society, Bethesda, Maryland, USA.

Ohnishi, S., T. Yamakawa, H. Okamura, and T. Akamine. 2012. A note on the von Bertalanffy growth function concerning the allocation of surplus energy to reproduction. Fishery Bulletin 110:223–229.

Pääkkönen, J. P. J., O. Tikkanen, and J. Karjalainen. 2003. Development and validation of a bioenergetics model for juvenile and adult burbot. Journal of Fish Biology 63:956–969.

Patterson III, W. F., J. H. Cowan, Jr., C. A. Wilson, and R. L. Shipp. 2001. Age and growth of red snapper, *Lutjanus campechanus*, from an artificial reef area off Alabama in the northern Gulf of Mexico. Fisheries Bulletin 99:617–627.

Patterson III, W. F., J. H. Tarnecki, and J. T. Neese. 2012. SEDAR31-RD27. Examination of red snaper fisheries ecology on the Northwest Florida Shelf (FWC-08304): Final report. Pensacola, Florida, USA.

Pauly, D. 1980. On the interrelationships between natural mortality, growth parameters, and mean environmental temparature in 175 fish stocks. Journal du Conseil International pour l'Exploration de la Mer 39:175–192.

Pawitan, Y. 2013. In all likelihood: statistical modelling and inference using likelihood. Oxford University Press, Oxford, England, UK.

Petersen, J. H., and C. P. Paukert. 2005. Development of a bioenergetics model for humpback chub and evaluation of water temperature changes in the Grand Canyon,

Colorado River. Transactions of the American Fisheries Society 134:960–974.

Piccolroaz, S., N. C. Healey, J. D. Lenters, S. G. Schladow, S. J. Hook, G. B. Sahoo, and M. Toffolon. 2017. On the predictability of lake surface temperature using air temperature in a changing climate: A case study for Lake Tahoe (U.S.A.). Limnology and Oceanography.

Pilgrim, J. M., X. Fang, and H. G. Stefan. 1998. Stream temperature correlations with air temperatures in Minnesota: implications for climate warming. Journal of the American Water Resources Association 34:1109–1121.

Pitcher, T. J., and P. D. M. Macdonald. 1973. Two models for seasonal growth in fishes. Journal of Applied Ecology 10:599–606.

Porch, C., C. E. Porch, S. C. Turner, and M. J. Schirripa. 2007. Reconstructing the commercial landings of red snapper in the Gulf of Mexico from 1872 to 1963. American Fisheries Society Symposium 60:337–353.

Power, M., and R. S. McKinley. 1997. Latitudinal variation in lake sturgeon size as related to the thermal opportunity for growth. Transactions of the American Fisheries Society 126:549–558.

Purchase, C. F., N. C. Collins, G. E. Morgan, and B. J. Shuter. 2005. Predicting life history traits of yellow perch from environmental characteristics of lakes. Transactions of the American Fisheries Society 134:1369–1381.

Quince, C., P. A. Abrams, B. J. Shuter, and N. P. Lester. 2008a. Biphasic growth in fish I: theoretical foundations. Journal of Theoretical Biology 254:197–206.

Quince, C., P. A. Abrams, B. J. Shuter, and N. P. Lester. 2008b. Biphasic growth in fish

II: empirical assessment. Journal of Theoretical Biology 254:207–214.

R Core Team. 2015. R: a language and environment for statistical computing. R Foundation for Statistical Computing, Vienna, Austria. https://www.R-project.org/.

R Core Team. 2017. R: a language and environment for statistical computing. R Foundation for Statistical Computing, Vienna, Austria. https://www.R-project.org/.

Rand, P. S., D. J. Stewart, P. W. Seelbach, M. L. Jones, and L. R. Wedge. 1993. Modeling steelhead population energetics in Lakes Michigan and Ontario. Transactions of the American Fisheries Society 122:977–1001.

Raue, A., C. Kreutz, T. Maiwald, J. Bachmann, M. Schilling, U. Klingmuller, and J. Timmer. 2009. Structural and practical identifiability analysis of partially observed dynamic models by exploiting the profile likelihoods. Bioinformatics 25:1923–1929.

Rayner, N. A., D. E. Parker, E. B. Horton, C. K. Folland, L. V. Alexander, D. P. Rowell, E. C. Kent, and A. Kaplan. 2003. Global analyses of sea surface temperature, sea ice, and night marine air temperature since the late nineteenth century. Journal of Geophysical Research 108:4407.

Read, J. S., L. A. Winslow, G. J. A. Hansen, J. Van Den Hoek, P. C. Hanson, L. C. Bruce, and C. D. Markfort. 2014. Simulating 2368 temperate lakes reveals weak coherence in stratification phenology. Ecological Modelling 291:142–150.

Réamur, R. A. 1735. Observations du thermomètre faites pendant l'annee MDCCXXXV comparées à celles qui ont été faites sous la ligne à l'Isle-de-France, à Alger et en quelques-unes de nos Isles de l'Amerique. Memoires de l'Academie Royal des Sciences:545–576.

Reichenbacher, B., U. Sienknecht, H. Kuchenhoff, and N. Fenske. 2007. Combined otolith morphology and morphometry for assessing taxonomy and diversity in fossil and extant killifish (*Aphianus*, *Prolebias*). Journal of Morphology 268:898–915.

Render, J. H. 1995. The life history (age, growth, and reproduction) of red snapper (*Lutjanus campechanus*) and its affinity for oil and gas platforms. Ph.D. Dissertation, Louisiana State University.

Rennie, M. D., C. F. Purchase, B. J. Shuter, N. C. Collins, P. A. Abrams, and G. E. Morgan. 2010. Prey life-history and bioenergetic responses across a predation gradient. Journal of Fish Biology 77:1230–1251.

Reznick, D. N. 1990. Plasticity in age and size at maturity in male guppies (*Poecilia reticulata*): an experimental evaluation of alternative models of development. Journal of Evolutionary Biology 3:185–203.

Rideout, R. M., G. A. Rose, and M. P. M. Burton. 2005. Skipped spawning in female iteroparous fishes. Fish and Fisheries 6:50–72.

Righton, D. A., K. H. Andersen, F. Neat, V. Thorsteinsson, P. Steingrund, H. Svedäng, K. Michalsen, H. H. Hinrichsen, V. Bendall, S. Neuenfeldt, P. Wright, P. Jonsson, G. Huse, J. Van Der Kooij, H. Mosegaard, K. Hüssy, and J. Metcalfe. 2010. Thermal niche of Atlantic cod Gadus morhua: limits, tolerance and optima. Marine Ecology Progress Series 420:1–13.

Rijnsdorp, A. D., and F. Storbeck. 1995. Determining the onset of sexual maturity from otoliths of individual female North Sea plaice, *Pleuronectes platessa* L. Pages 581–598 *in* D. Secor, J. Dean, and S. Campana, editors. Recent developments in fish

otholith research. University of South Carolina Press, Columbia, SC, USA.

Robertson, D. M., and R. A. Ragotzkie. 1990. Changes in the thermal structure of moderate to large sized lakes in response to changes in air temperature. Aquatic Sciences 52:360–380.

Roff, D. A. 1983. An allocation model of growth and reproduction in fish. Canadian Journal of Fisheries and Aquatic Sciences 40:1395–1404.

Roff, D. A. 1984. The evolution of life history parameters in teleosts. Canadian Journal of Fisheries and Aquatic Sciences 41:989–1000.

Roff, D. A. 1992. The evolution of life histories: theory and analysis. Chapman and Hall, New York, New York, USA.

Rose, K. C., L. A. Winslow, J. S. Read, and G. J. A. Hansen. 2016. Climate warming of lakes can be either amplified or suppressed by trends in water clarity. Limnology and Oceanography Letters 1:44–53.

Rouse, W. R., C. J. Oswald, J. Binyamin, C. Spence, W. M. Schertzer, P. D. Blanken, N. Bussieres, and C. R. Duguay. 2005. The role of northern lakes in a regional energy balance. Journal of Hydrometeorology 6:291–305.

Rowan, D. J., and J. B. Rasmussen. 1996. Measuring the bioenergetic cost of fish activity in situ using a globally dispersed radiotracer (137Cs). Canadian Journal of Fisheries and Aquatic Sciences 53:734–745.

Royall, R. M. 1997. Statistical evidence: a likelihood paradigm. Chapman and Hall/CRC, Boca Raton, Florida, USA.

Royall, R. M. 2004. The likelihood paradigm for statistical evidence. Pages 119–137 *in*

M. Taper and S. Lele, editors. The nature of scientific evidence: empirical, statistical, and philosophical considerations. University of Chicago Press, Chicago, Illinois, USA.

Rudstam, L. G., F. P. Binkowski, and M. A. Miller. 1994. A bioenergetics model for analysis of food consumption patterns of bloater in Lake Michigan. Transactions of the American Fisheries Society 123:344–357.

Rypel, A. L. 2012a. Meta-analysis of growth rates for a circumpolar fish, the northern pike (*Esox lucius*), with emphasis on effects of continent, climate and latitude. Ecology of Freshwater Fish 21:521–532.

Rypel, A. L. 2012b. Concordant estimates of countergradient growth variation in striped bass (*Morone saxatilis*) using comparative life-history data. Canadian Journal of Fisheries and Aquatic Sciences 69:1261–1265.

Rypel, A. L., and S. R. David. 2017. Pattern and scale in latitude-production relationships for freshwater fishes. Ecosphere 8:e01660.

Salinas, S., and S. B. Munch. 2014. Phenotypic complexity: Integrated responses of life-history characters to multiple environmental factors. Evolutionary Ecology Research 16:267–284.

Schaeffer, J. S., R. C. Haas, J. S. Diana, and J. E. Breck. 1999. Field test of two energetic models for yellow perch. Transactions of the American Fisheries Society 128:414–435.

Schirippa, M. J., and C. M. Legault. 1999. Status of the Red Snapper in U.S. Waters of the Gulf of Mexico: updated through 1998. National Marine Fisheries Service,

Southeast Fisheries Science Center Report SFD-99/00-75. 106 pp.

Schlesinger, D. A., and H. A. Regier. 1982. Climatic and morphoedaphic indices of fish yields from natural lakes. Transactions of the American Fisheries Society 111:141–150.

Schoenebeck, C. W., S. R. Chipps, and M. L. Brown. 2008. Improvement of an esocid bioenergetics model for juvenile fish. Transactions of the American Fisheries Society 137:1891–1897.

Scott, R. D., and J. Heikkonen. 2012. Estimating age at first maturity in fish from change-points in growth rate. Marine Ecology Progress Series 450:147–157.

Seamster, A. P. 1950. Developmental studies concerning the eggs of *Ascaris lumbricoides var. suum*. American Midland Naturalist 43:450–470.

SEDAR. 2013. SEDAR 31 - Gulf of Mexico Red Snapper stock assessment report. SEDAR (Southeast Data, Assessment, and Review), North Charleston SC. 1103 pp.

SEDAR. 2018. Stock assessment report of Gulf of Mexico Red Snapper 52. SEDAR (Southeast Data, Assessment, and Review), North Charleston, SC, USA. 435 p.

Sellers, T. J., B. R. Parker, D. W. Schindler, and W. M. Tonn. 1998. Pelagic distribution of lake trout (*Salvelinus namaycush*) in small Canadian Shield lakes with respect to temperature, dissolved oxygen, and light. Canadian Journal of Fisheries and Aquatic Sciences 55:170–179.

Shuter, B. J., D. A. Schlesinger, and A. P. Zimmerman. 1983. Empirical predictors of annual surface water temperature cycles in North American Lakes. Canadian Journal of Fisheries and Aquatic Sciences 40:1838–1845.

Smol, J. P., H. J. B. Birks, and W. M. Last, editors. 2001. Tracking environmental change using lake sediments volume 4: zoological indicators. Kluwer Academic, Dordrecht, The Netherlands.

Snover, M. L., M. J. Adams, D. T. Ashton, J. B. Bettaso, and H. H. Welsh. 2015. Evidence of counter-gradient growth in western pond turtles (*Actinemys marmorata*) across thermal gradients. Freshwater Biology 60:1944–1963.

Snyder, R. L., D. Spano, C. Cesaraccio, and P. Duce. 1999. Determining degree-day thresholds from field observations. International Journal of Biometeorology 42:177–182.

Sober, E. 2008. Evidence and evolution: the logic behind the science. Cambridge University Press, Cambridge, England, UK.

Soderberg, R. W. 1992. Linear fish growth models for intensive aquaculture. The Progressive Fish-Culturist 54:255–258.

Stan Development Team. 2018. RStan: the R interface to Stan. R package version 2.17.3. http://mc-stan.org.

Stearns, S. C. 1992. The evolution of life histories. Oxford University Press, Oxford, England, UK.

Stearns, S. C., and R. J. Hoekstra. 2005. Evolution, 2nd edition. Oxford University Press, Oxford, England, UK.

Stearns, S. C., and J. C. Koella. 1986. The evolution of phenotypic plasticity in life-history traits: predictions of reaction norms for age and size at maturity. Evolution 40:893–913.

Szedlmayer, S. T., and R. L. Shipp. 1994. Movement and growth of red snapper (*Lutjanus campechanus*) from an artificial reef area in the northeastern Gulf of Mexico. Bulletin of Marine Science 55:887–896.

Tabor, R., C. Luecke, and W. Wurtsbaugh. 1996. Effects of Daphnia availability on growth and food consumption of rainbow trout in two Utah reservoirs. North American Journal of Fisheries Management 16:591–599.

Taper, M. L., and S. R. Lele. 2011. Evidence, evidence functions, and error probabilites. Pages 513–534 *in* P. Bandyopadhyay and M. Forster, editors. Philosophy of Statistics. North Holland, Oxford, England, UK.

Thorson, J. T., S. B. Munch, J. M. Cope, and J. Gao. 2017. Predicting life history parameters for all fishes worldwide. Ecological Applications 27:2262–2276.

Topping, D. T., and S. T. Szedlmayer. 2013. Use of ultrasonic telemetry to estimate natural and fishing mortality of red snapper. Transactions of the American Fisheries Society 142:1090–1100.

Trippel, E. A. 1995. Age at maturity as a stress indicator in fisheries. BioScience 45:759–771.

Trippel, E. A., and H. H. Harvey. 1991. Comparison of methods used to estimate age and length of fishes at sexual maturity using populations of white sucker (*Catostomus commersoni*). Canadian Journal of Fisheries and Aquatic Sciences 48:1446–1459.

Tseng, C. Te, C. L. Sun, S. Z. Yeh, S. C. Chen, W. C. Su, and D. C. Liu. 2011. Influence of climate-driven sea surface temperature increase on potential habitats of the Pacific saury (*Cololabis saira*). ICES Journal of Marine Science 68:1105–1113.

Uusi-Heikkilä, S., A. Kuparinen, C. Wolter, T. Meinelt, A. C. O'Toole, and R. Arlinghaus. 2011. Experimental assessment of the probabilistic maturation reaction norm: condition matters. Proceedings of the Royal Society B: Biological Sciences 278:709–717.

Uusi-Heikkilä, S., A. R. Whiteley, A. Kuparinen, S. Matsumura, P. A. Venturelli, C. Wolter, J. Slate, C. R. Primmer, T. Meinelt, S. S. Killen, D. Bierbach, G. Polverino, A. Ludwig, and R. Arlinghaus. 2015. The evolutionary legacy of size-selective harvesting extends from genes to populations. Evolutionary Applications 8:597–620.

Venturelli, P. A. 2009. Life history, maternal quality and the dynamics of harvested fish stocks. Ph.D. Thesis, University of Toronto.

Venturelli, P. A., N. P. Lester, T. R. Marshall, and B. J. Shuter. 2010. Consistent patterns of maturity and density-dependent growth among populations of walleye (*Sander vitreus*): application of the growing degree-day metric. Canadian Journal of Fisheries and Aquatic Sciences 67:1057–1067.

Vigliola, L., and M. G. Meekhan. 2009. The back-calculation of fish growth from otoliths. Page *in* B. S. Green, B. D. Mapstone, G. Carlos, and G. A. Begg, editors. Tropical Fish Otoliths: Information for Assessment, Management, and Ecology. Springer Science and Business Media, Dordrecht, The Netherlands.

Walker, S., P. Addison, S. Sandstrom, and N. P. Lester. 2013. Contact retention selectivity of three types of gillnet gangs. Aquatic Research and Monitoring Section, Ontario Ministry of Natural Resources Aquatic Research Series 2013-07, 29 p.

Wallich, C. 1901. Method of recording egg development, for use of fish-culturists. Pages

185–195 in Report of Commissioner of Fish and Fisheries.

Walters, C. J. 1986. Adaptive management of renewable resources. MacMillan Publishing Company, New York, New York, USA.

Wang, T., A. Hamann, D. Spittlehouse, and C. Carroll. 2016. Locally downscaled and spatially customizable climate data for historical and future periods for North America. PLoS ONE 11:1–17.

Wang, T., A. Hamann, D. L. Spittlehouse, and S. N. Aitken. 2006. Development of scale-free climate data for western Canada for use in resource management. International Journal of Climatology 26:383–397.

Wang, T., A. Hamann, D. L. Spittlehouse, and T. Q. Murdock. 2012. ClimateWNA-high-resolution spatial climate data for western North America. Journal of Applied Meteorology and Climatology 51:16–29.

Ward, H. G. M., J. R. Post, N. P. Lester, P. J. Askey, and T. Godin. 2017. Empirical evidence of plasticity in life-history characteristics across climatic and fish density gradients. Canadian Journal of Fisheries and Aquatic Sciences 74:464–474.

Ward, J. V. 1985. Thermal characteristics of running waters. Hydrobiologia 125:31–46.

Ware, D. M. 1978. Bioenergetics of pelagic fish: theoretical change in swimming speed and ration with body size. Journal of the Fisheries Research Board of Canada Research Board of Canada 35:220–228.

West, G. B., J. H. Brown, and B. J. Enquist. 1997. General model for the origin of allometric scaling laws in biology. Science 276:122–126.

West, G. B., J. H. Brown, and B. J. Enquist. 1999. The fourth dimension of life: fractal

geometry and allometric scaling of organisms. Science 284:1677–1679.

West, G. B., J. H. Brown, and B. J. Enquist. 2001. A general model for ontogenetic growth. Nature 413:628–31.

Wetzel, R. G., and G. E. Likens. 2000. The heat budget of lakes. Pages 45–56 in Limnological Analyses. Springer-Verlag, New York, New York, USA.

White, D. B., and S. M. Palmer. 2004. Age, growth, and reproduction of the Red Snapper, *Lutjanus campechanus*, from the Atlantic waters of the southeastern US. Bulletin of Marine Science 75:335–360.

Williams-Grove, L. J., and S. T. Szedlmayer. 2016. Mortality estimates for red snapper based on ultrasonic telemetry in the Northern Gulf of Mexico. North American Journal of Fisheries Management 36:1036–1044.

Wilson, C. A., and D. L. Nieland. 2001. Age and growth of red snapper, *Lutjanus campechanus*, from the northern Gulf of Mexico off Louisiana. Fisheries Bulletin 99:653–664.

Wilson, K. L., A. E. Honsey, B. Moe, and P. Venturelli. 2018. Growing the biphasic framework: techniques and recommendations for fitting emerging growth models. Methods in Ecology and Evolution 9:822–833.

Wyllie, M. C., E. R. Holmstrom, and R. K. Wallace. 1976. Temperature preference, avoidance, shock, and swim speed studies with marine and estuarine organisms from New Jersey. Icthyological Associates, Inc. Bulletin No. 15, Brigantine, New Jersey, USA.

Zimmerman, F., and M. Heino. 2013. Is size-dependent pricing prevalent in fisheries?

The case of Norwegian demersal and pelagic fisheries. ICES Journal of Marine Science 70:1389–1395.

Zorica, B., G. Sinovcic, and V. Cikes Kec. 2010. Preliminary data on the study of otolith morphology of five pelagic fish species from the Adriatic Sea (Croatia). Acta Adriatica 51:85–92.

Appendix 1

Additional analyses and methodological details for Chapter 2

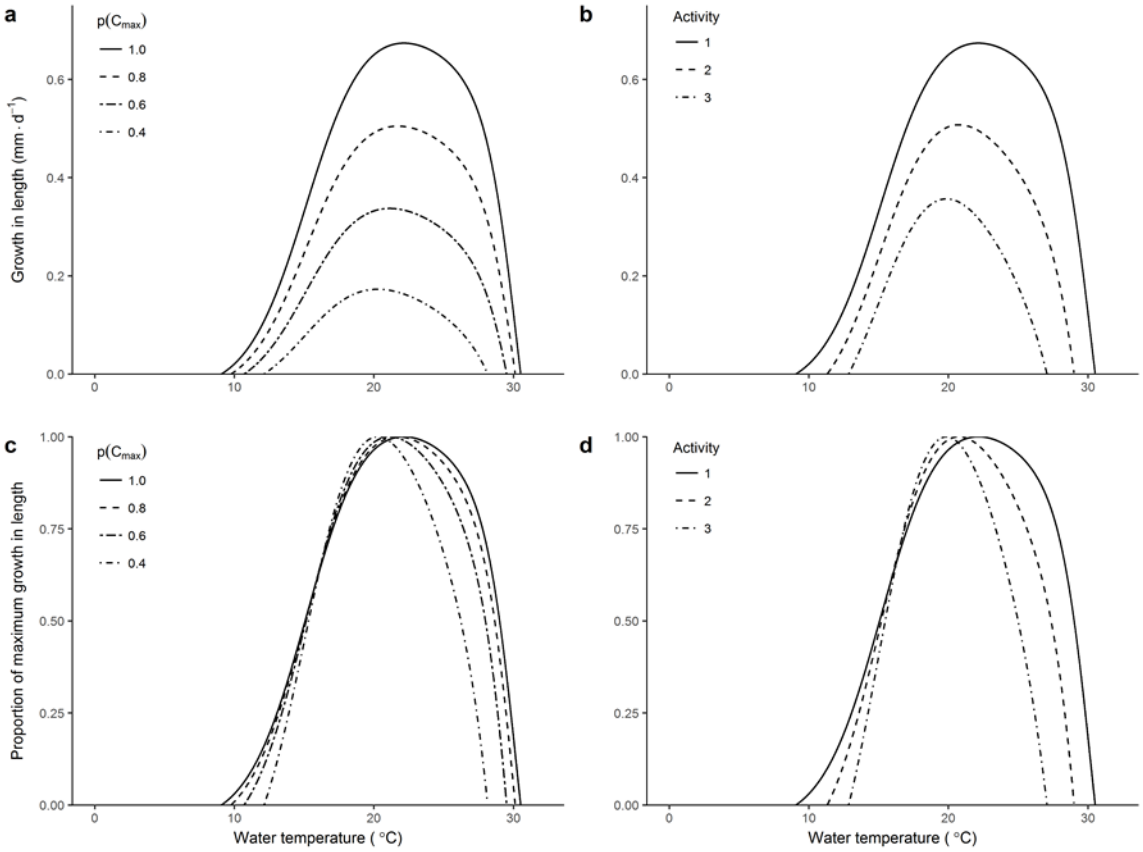

Figure A1.1 (a-b) The effect of temperature, activity level, and consumption (as a proportion of maximum consumption, p(Cmax)) on daily growth in length for brown bullhead *Ameiurus nebulosus*, based on a bioenergetics model. (c-d) Relative brown bullhead growth in length (i.e., growth as a proportion of maximum growth) across levels of temperature, activity, and consumption.

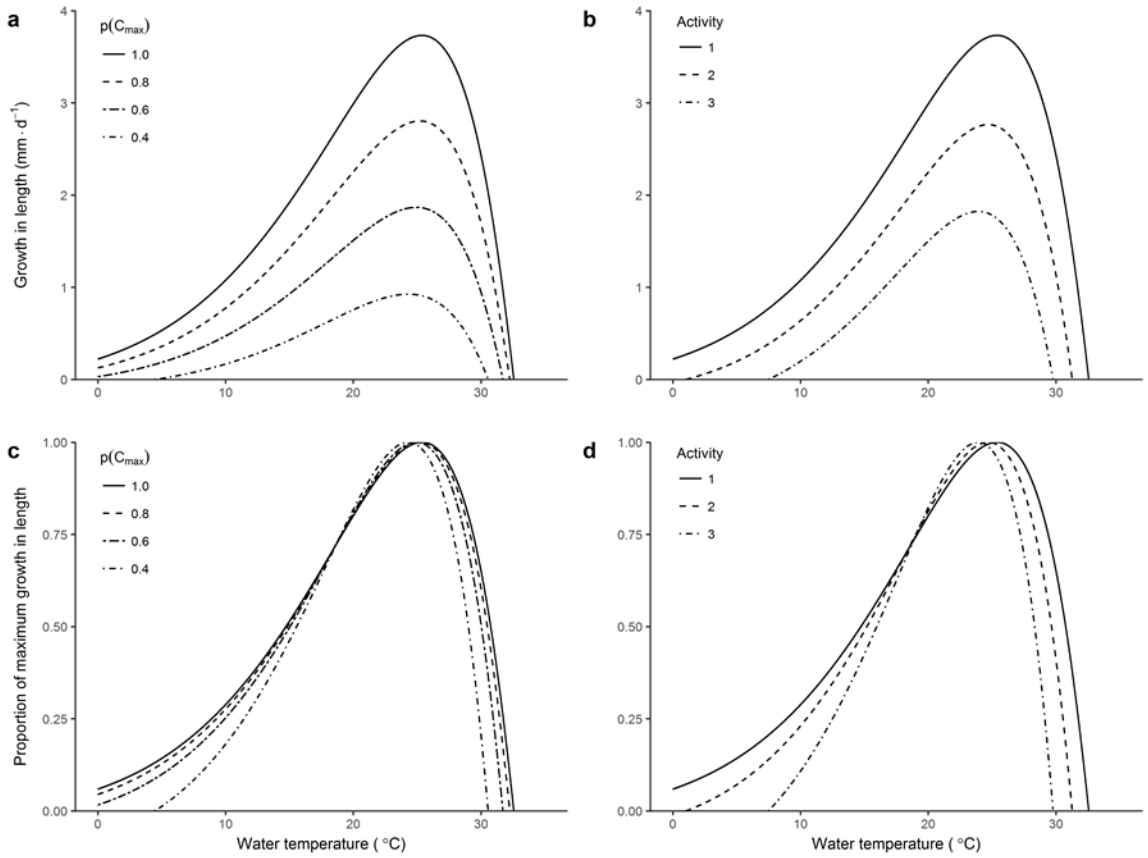

Figure A1.2 (a-b) The effect of temperature, activity level, and consumption (as a proportion of maximum consumption, p(Cmax)) on daily growth in length for tiger muskellunge (northern pike *Esox lucius* X muskellunge *Esox masquinongy*), based on a bioenergetics model. (c-d) Relative tiger muskellunge growth in length (i.e., growth as a proportion of maximum growth) across levels of temperature, activity, and consumption.

A1.1 Influence of mean annual air temperature and mean lake depth on the surface water temperature cycle

We used the Shuter et al. (1983) water temperature model (see Chapter 2 for details) to demonstrate the effect of varying mean annual air temperature ($\overline{AT}$) and mean lake/thermocline depth ($\bar{Z}$) on the surface water temperature cycle. We first simulated annual water temperature cycles with $\bar{Z}$ fixed at 8 m and $\overline{AT}$ at 2.5, 5, and 10 ºC. We then repeated the simulation with $\overline{AT}$ fixed at 5 ºC and $\bar{Z}$ at 4, 8, and 16 m. These values cover a range of scenarios that is realistic for many lakes in North America.

Our results suggest that variation in $\overline{AT}$ generally has a larger impact on the surface water temperature cycle than variation in $\bar{Z}$ across the range of values that we investigated (Fig. A1.3). In particular, variation in $\overline{AT}$ has a much larger impact on the duration of the ice-free season than variation in $\bar{Z}$.

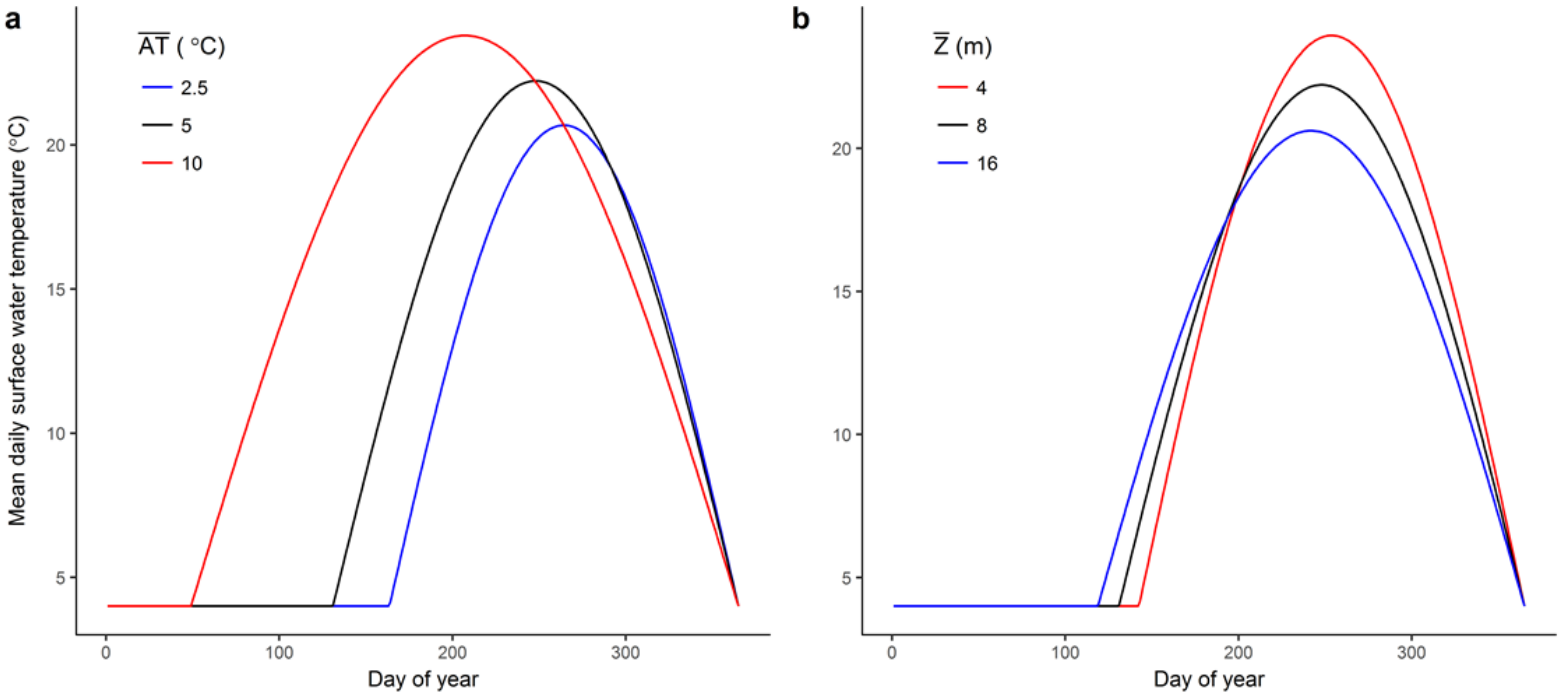

Figure A1.3 Effect of (a) mean annual air temperature ($\overline{AT}$) and (b) mean lake/thermocline depth ($\bar{Z}$) on the annual surface water temperature cycle, based on the Shuter et al. (1983) model. In these simulations, day 0 is the first day on which the surface of the simulated lake is frozen.

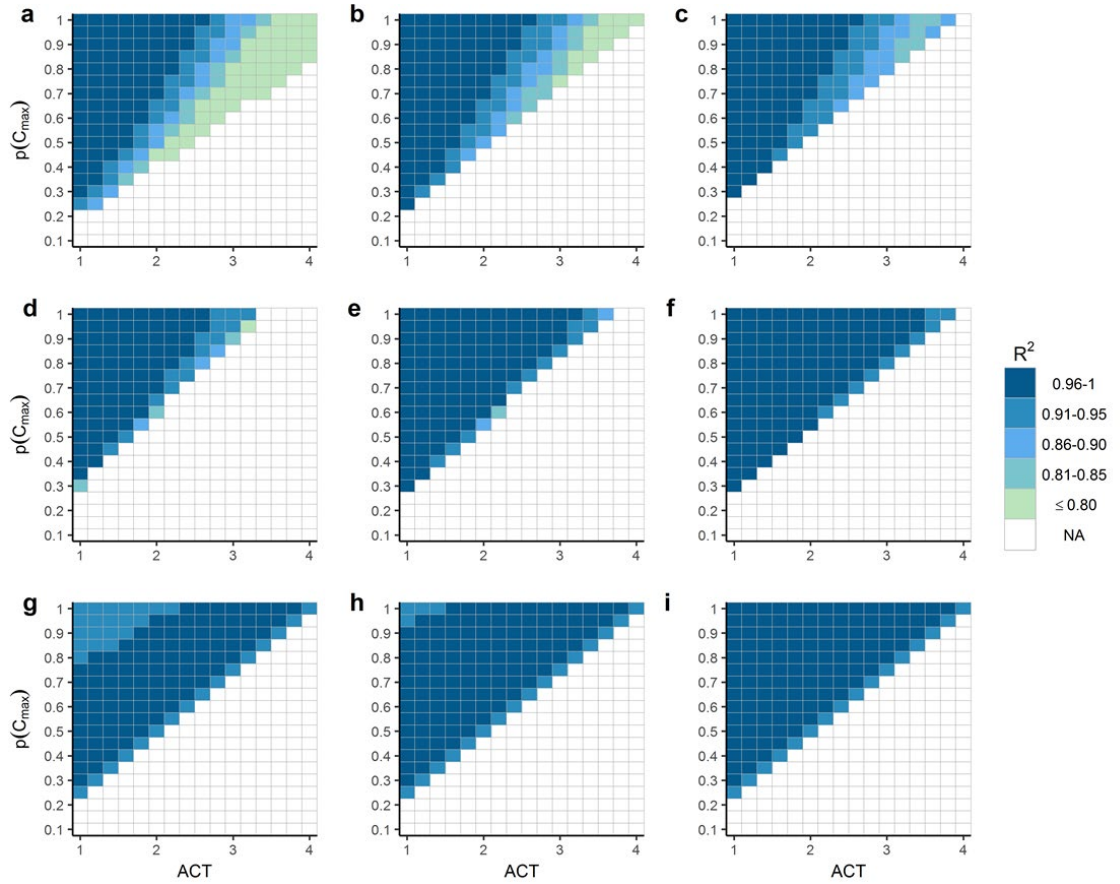

Figure A1.4 Coefficients of determination (adjusted R^2) from linear model fits to the length vs. water-based degree-day (WDD_5) relationship from five year growth simulations given various combinations of consumption (proportion of maximum consumption, $p(C_{max})$), activity (ACT), and initial size (columns). (a-c) Results from the yellow perch *Perca flavescens* bioenergetics model, with initial sizes of (a) 25 mm, (b) 50 mm, and (c) 75 mm. (d-f) Results from the brown bullhead *Ameiurus nebulosus* bioenergetics model, with initial sizes of (d) 50 mm, (e) 100 mm, and (f) 150 mm. (g-i) Results from the tiger muskellunge (northern pike *Esox lucius* X muskellunge *Esox masquinongy*) bioenergetics model, with initial sizes of (g) 100 mm, (h) 150 mm, and (i) 200 mm. Bioenergetics simulations incorporated empirical water temperature data (1 m depth) from Lake Lacawac, PA, USA. White cells ("NA") denote cases in which individuals did not grow across all five years.

A1.2 Empirical relationship for predicting air-based degree-days from mean annual air temperatures

To predict air-based degree-days above 5 °C (ADD_5) from mean annual air temperatures ($\overline{AT}$), we collected empirical air temperature data from 107 weather stations in the United States and Canada using the National Oceanic and Atmospheric Administration Climate Data Online tool (https://www.ncdc.noaa.gov/cdo-web/). The locations of these 107 weather stations are shown in Fig. A1.5. The data described mean daily air temperatures from 1 January through 31 December 2015, and all datasets were continuous. We used these data to calculate both $\overline{AT}$ and ADD_5, and we constructed a relationship to predict ADD_5 from $\overline{AT}$ (Fig. A1.6):

$$ADD_5 = 1346.8 \cdot e^{0.0729 \cdot \overline{AT}}.$$

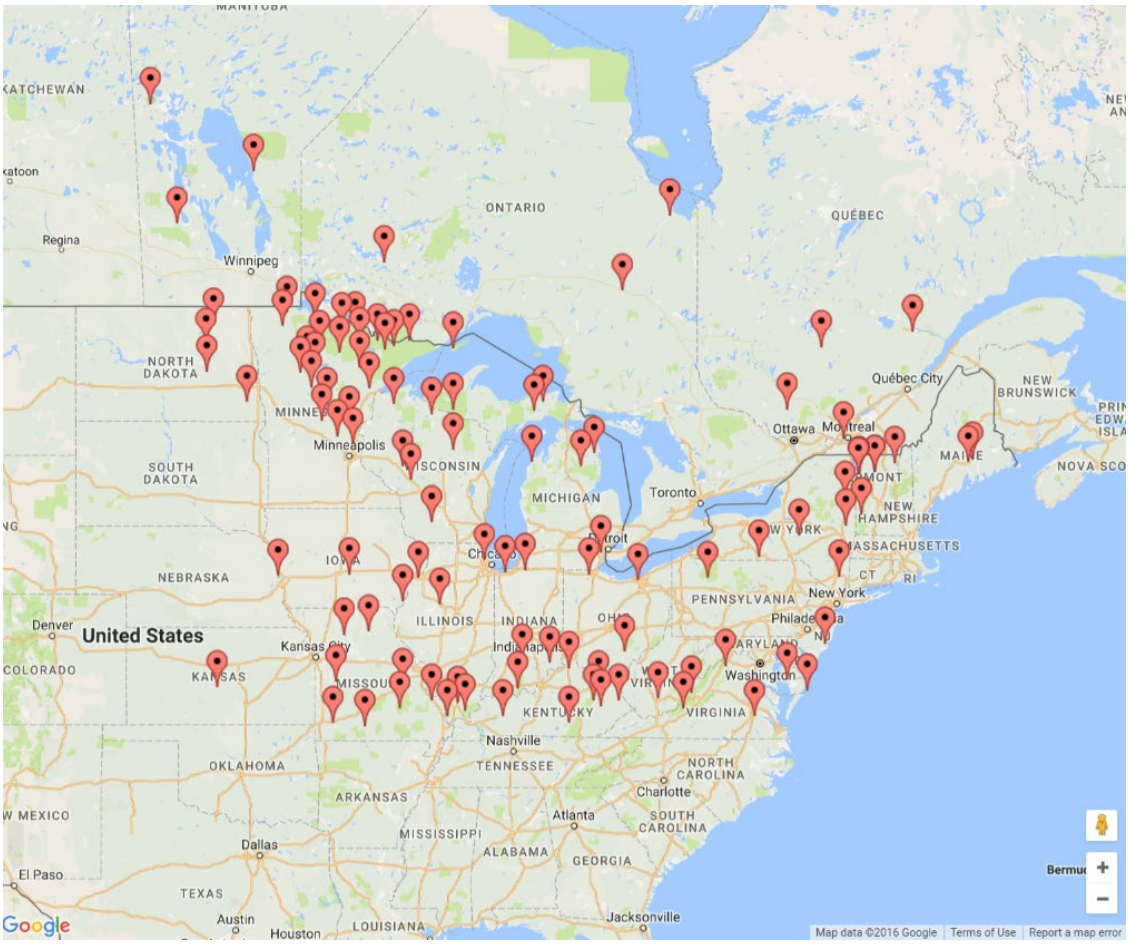

Figure A1.5 Locations of air temperature stations used to generate the empirical relationship for predicting air-based degree-days above 5 ºC from mean annual air temperatures. Image © 2016 Google.

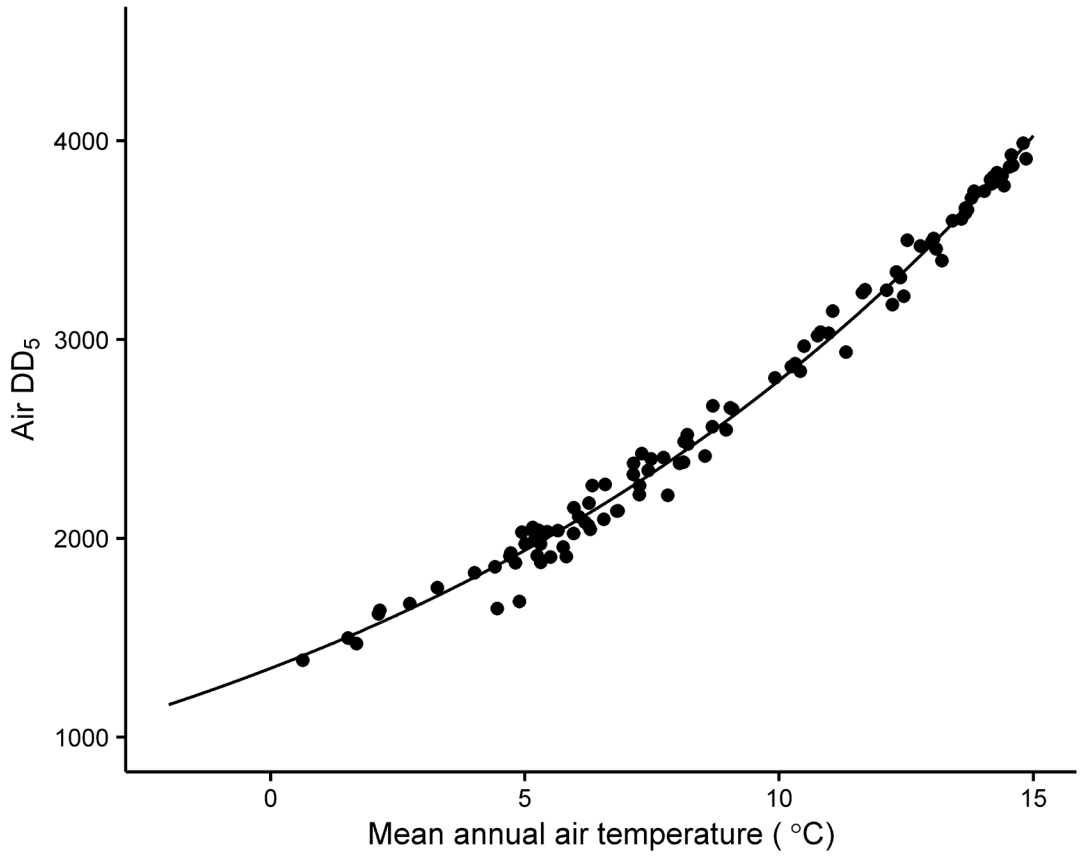

Figure A1.6 Empirical relationship between mean annual air temperature (ºC) and air-based degree-days above 5 ºC (Air DD_5) constructed using data from 107 weather stations in the United States and Canada.

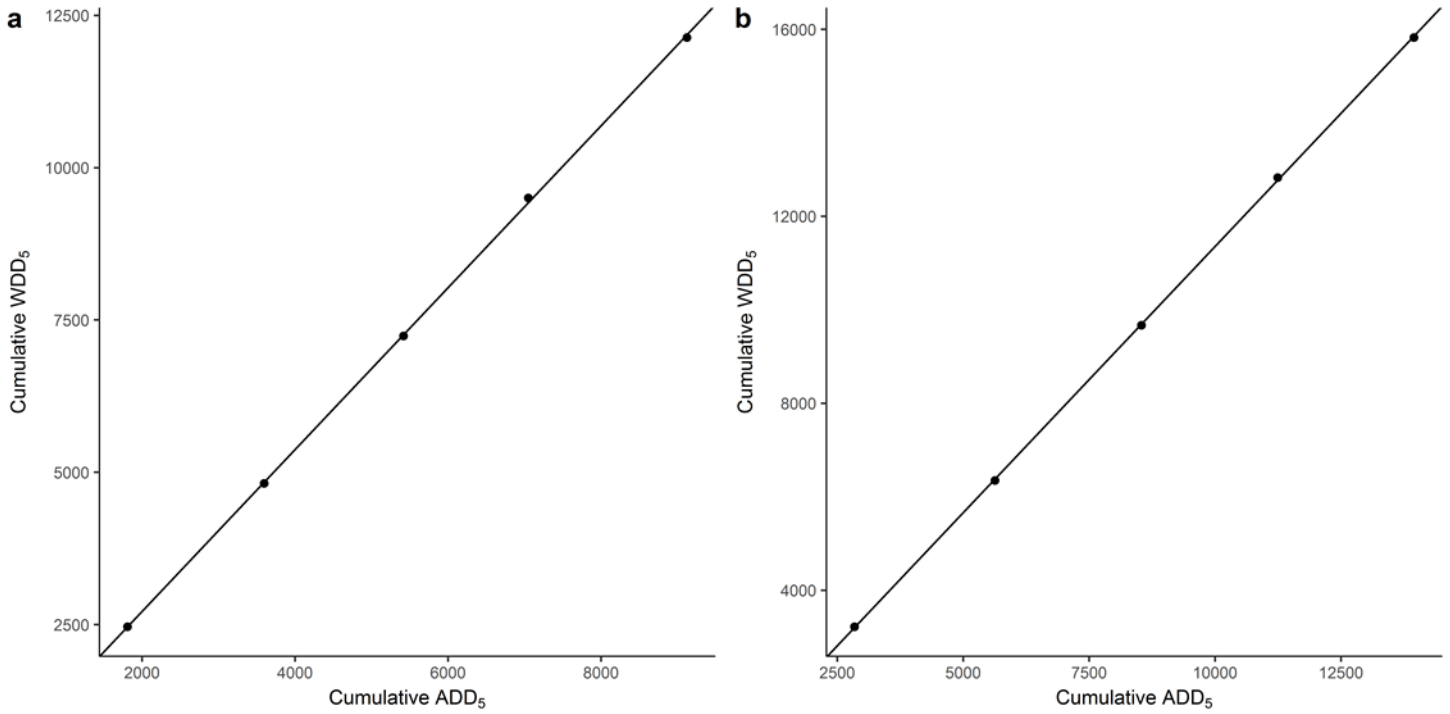

Figure A1.7 Cumulative air-based degree-days above 5 ºC (ADD_5) vs. cumulative water-based degree-days above 5 ºC (WDD_5) for (a) Sparkling Lake, WI, USA and (b) Lake Lacawac, PA, USA across five years. Empirical air and water temperature data sources used to calculate these metrics are described in Chapter 2. Pearson's $\rho > 0.99$ for both comparisons.

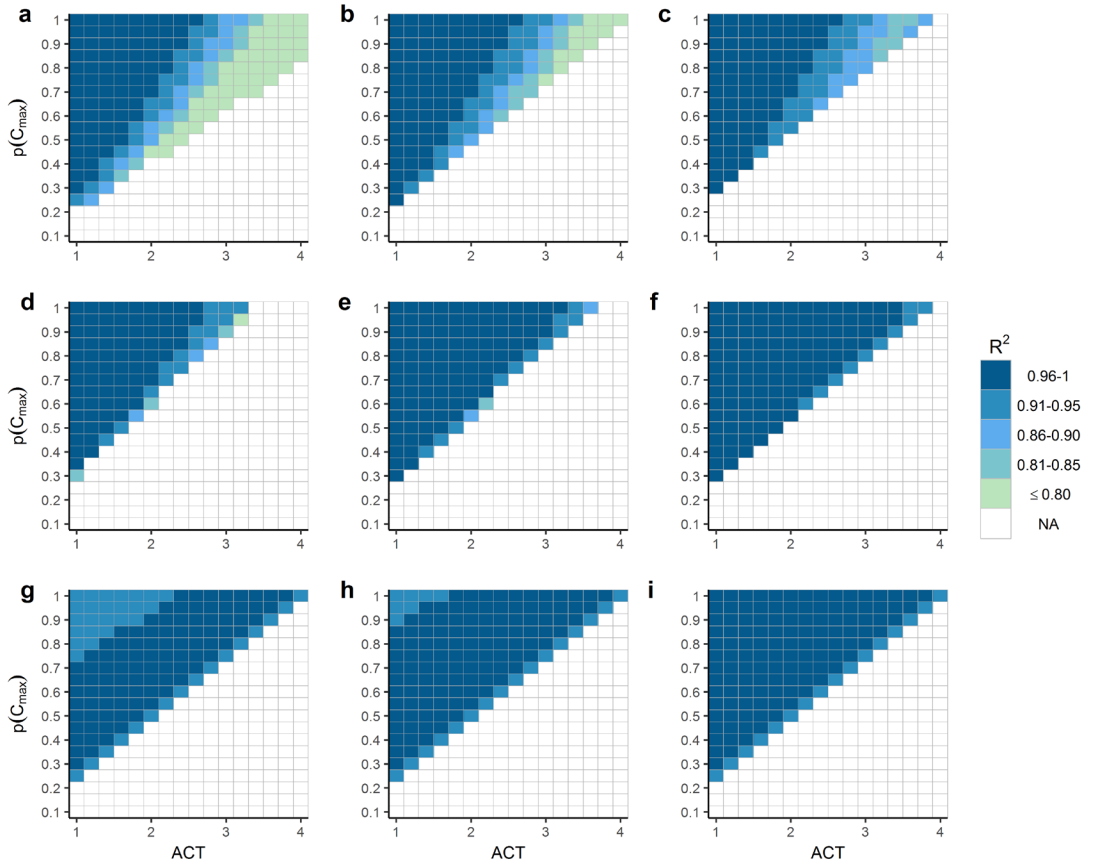

Figure A1.8 Coefficients of determination (adjusted R^2) from linear model fits to the length vs. air-based degree-day (ADD_5) relationship from five year growth simulations given various combinations of consumption (proportion of maximum consumption, $p(C_{max})$), activity (ACT), and initial size (columns). (a-c) Results from the yellow perch *Perca flavescens* bioenergetics model, with initial sizes of (a) 25 mm, (b) 50 mm, and (c) 75 mm. (d-f) Results from the brown bullhead *Ameiurus nebulosus* bioenergetics model, with initial sizes of (d) 50 mm, (e) 100 mm, and (f) 150 mm. (g-i) Results from the tiger muskellunge (northern pike *Esox lucius* X muskellunge *Esox masquinongy*) bioenergetics model, with initial sizes of (g) 100 mm, (h) 150 mm, and (i) 200 mm. Bioenergetics simulations incorporated empirical water temperature data (1 m depth) from Lake Lacawac, PA, USA. White cells ("NA") denote cases in which individuals did not grow across all five years.

A1.3 Daily growth across water temperatures for adult fishes

In Chapter 2, we focus on immature fish growth because the linear approximation of the length-at-age versus DD relationship is typically only valid for growth leading up to maturity (Lester *et al.* 2004; Andersen and Beyer 2015; Honsey *et al*. 2017). However, much like with immature growth, the response of adult growth to water temperature is often nearly linear over a midrange of temperatures. For this reason, some of our results (e.g., the linearity of annual growth versus DD) may also extend to adult growth.

To demonstrate the nearly linear response of adult growth in length to water temperature across middling water temperatures, we simulated daily fish growth using bioenergetics models that were parameterized for adults of three species: white crappie *Pomoxis annularis* (Bajer et al. 2004), steelhead *Oncorhynchus mykiss* (Rand et al. 1993), and rainbow smelt *Osmerus mordax* (Lantry and Stewart 1993). Parameters and equations for these models are given in Table A1.1. We assumed that individuals achieved satiation and set the activity multiplier to the suggested number (Table A1.1). We used geometric mean parameters for the length-weight relationship from FishBase (Froese and Pauly 2016) for length-weight conversions, and we set the energy density of oxygen at 13556 $J \cdot g^{-1}$ (Elliott and Davison 1975). We set initial fish sizes at 253 mm (250 g), 453 mm (1 kg), and 197 mm (60 g) for adult white crappie, steelhead, and rainbow smelt, respectively. Our results show that, although the shapes of the relationships differ, daily growth is nearly linear with water temperature across a midrange of temperatures for these adult fish models, much like it is for immature fishes (Fig. A1.9).

Table A1.1 Bioenergetics equations and parameters used for supplemental simulations. All models follow the Wisconsin bioenergetics framework; see Hanson *et al.* (1997) for equations and details. Sources are listed in footnotes.

Model component	Model species		
	White crappie[1]	Steelhead[2]	Rainbow smelt[3]
Consumption equation	2	3	3
CA	1.2589	0.628	0.18
CB	-0.661	-0.3	-0.275
CQ	2.945	5	3
CTO	24	20	10
CTM	32	20	12
CTL	-	24	18
CK1	-	0.33	0.4
CK4	-	0.2	0.01
Respiration equation	1	1	1
RA	0.02366	0.00264	0.0027
RB	-0.623	-0.217	-0.216
RQ	0.0237	0.06818	0.036
RTO	0	0.0234	0
RTM	0	0	0
RTL	0	25	0
RK1	1	1	0
RK4	0	0.13	0
ACT	1	9.7	1
BACT	0	0.0405	0
SDA	0.16	0.172	0.175
Egestion-excretion equation	1	3	1
FA	0.104	0.212	0.16
FB	0	-0.222	0
FG	0	0.631	0
UA	0.068	0.0314	0.1
UB	0	0.58	0
UG	0	-0.299	0
Energy density equation	1	2	1
Predator energy density ($J \cdot g^{-1}$)	4186	-	4814
$Alpha_1$	-	5764	-
$Beta_1$	-	0.9862	-
Cutoff (g)	-	4000	-
$Alpha_2$	-	7602	-
$Beta_2$	-	0.5266	-
Prey energy density ($J \cdot g^{-1}$)	3500	3500	3500

[1]Bajer et al. (2004), [2]Rand et al. (1993), [3]Lantry and Stewart (1993)

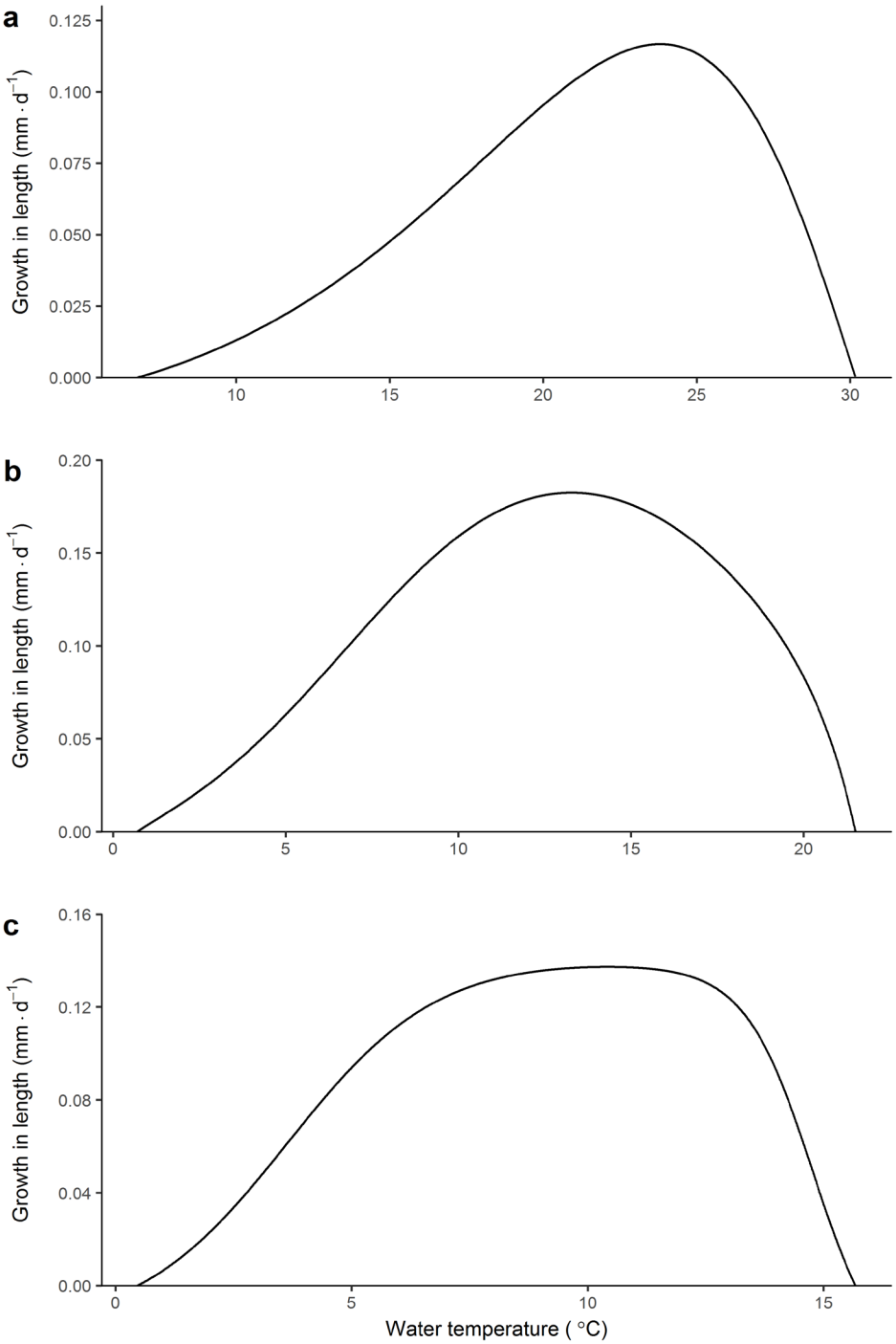

Figure A1.9 Daily growth in length (assuming satiation) across water temperatures for adult (a) white crappie *Pomoxis annularis*, (b) steelhead *Oncorhynchus mykiss*, and (c) rainbow smelt *Osmerus mordax*, based on bioenergetics models (Table A1.1).

A1.4 Estimating the base temperature for growth using annual growth simulations

If degree-days (DD) are an accurate index for the thermal scope for growth, then growth should be proportional to DD provided that DD are calculated using the correct base temperature for growth (T_0; the temperature below which growth is assumed to be negligible). Using this logic, one can estimate T_0 for a given species by finding the T_0 value for which the growth versus DD relationship is proportional (i.e., passes through the origin).

Here, we demonstrate this approach using the juvenile yellow perch bioenergetics model (Table 2.1) and the annual growth simulation framework described in Chapter 2 (see the two subsections entitled 'Annual growth'). We chose to estimate T_0 for air-based degree-days (ADD) in order to further promote their application. We used the approach and empirical data described in Section A1.2 to construct relationships between mean annual air temperatures and ADD at T_0 values ranging from 0-15 ºC. The parameters for these relationships are given in Table A1.2. We then used these relationships to estimate ADD from the hypothetical mean annual air temperatures used in the simulations, and we compared annual growth to ADD at various T_0 values. Our results suggest that the juvenile yellow perch annual growth versus ADD relationship passes through the origin when T_0 is roughly 9 ºC (Fig. 2.9).

Table A1.2 Parameters for relationships between mean annual air temperatures and air-based degree-days at various base temperature values (derived from empirical air temperature data; see Section A1.2). Equations take the following form: $ADD_{T_0} = \alpha e^{\beta \cdot \overline{AT}}$, where ADD_{T_0} is air-based degree-days at base temperature T_0, $\overline{AT}$ is mean annual air temperature, and α and β are parameters.

Base temperature (T_0; ºC)	**α**	**β**
0	2244.83	0.0613
1	2044.76	0.0635
2	1855.44	0.0657
3	1676.31	0.0680
4	1506.71	0.0704
5	1346.80	0.0729
6	1196.23	0.0757
7	1054.94	0.0786
8	922.88	0.0817
9	800.67	0.0851
10	687.39	0.0887
11	583.10	0.0927
12	486.54	0.0974
13	396.94	0.1032
14	315.02	0.1104
15	241.93	0.1193

Appendix 2

Additional details, results, and analyses for Chapter 3

Table A2.1 Estimates of the base temperature for growth (T_0; ºC) across species from the empirical growth analysis, including maximum ages included in regressions, minimum coefficients of variation (CV) in growth rate estimates among populations, and number of populations (N). Linear fits included ages up to and including the maximum age.

Scientific name	Common name	$\widehat{T_0}$	Maximum age	CV	N
Ameiurus melas	Black bullhead	0	2	0.362	78
Ameiurus melas	Black bullhead	0	3	0.349	80
Ameiurus melas	Black bullhead	0	4	0.302	81
Pomoxis nigromaculatus	Black crappie	1	2	0.222	20
Pomoxis nigromaculatus	Black crappie	1	3	0.238	20
Ictalurus furcatus	Blue catfish	0	3	0.510	24
Ictalurus furcatus	Blue catfish	0	4	0.457	25
Ictalurus furcatus	Blue catfish	0	5	0.487	25
Lepomis macrochirus	Bluegill	0	2	0.495	68
Lepomis macrochirus	Bluegill	0	3	0.451	68
Ameiurus nebulosus	Brown bullhead	0	2	0.553	5
Ameiurus nebulosus	Brown bullhead	0	3	0.378	8
Ameiurus nebulosus	Brown bullhead	0	4	0.313	8
Ictalurus punctatus	Channel catfish	11	2	0.656	7
Ictalurus punctatus	Channel catfish	18	3	0.749	19
Ictalurus punctatus	Channel catfish	18	4	0.934	27
Coregonus artedi	Cisco	0	3	0.479	32
Coregonus artedi	Cisco	0	4	0.435	35
Cyprinus carpio	Common carp	0	3	0.416	30
Cyprinus carpio	Common carp	0	4	0.352	30
Cyprinus carpio	Common carp	0	5	0.309	30
Pylodictus olivaris	Flathead catfish	0	3	0.317	10
Pylodictus olivaris	Flathead catfish	2	4	0.751	11
Pylodictus olivaris	Flathead catfish	0	5	0.471	11
Centrarchus macropterus	Flier	4	2	0.308	7
Centrarchus macropterus	Flier	4	3	0.249	7
Lepomis cyanellus	Green sunfish	4	2	0.324	6
Lepomis cyanellus	Green sunfish	4	3	0.311	6
Acipenser fulvescens	Lake sturgeon	0	6	0.280	4
Acipenser fulvescens	Lake sturgeon	0	7	0.277	4
Acipenser fulvescens	Lake sturgeon	0	8	0.305	4
Salvelinus namaycush	Lake trout	0	4	0.480	28
Salvelinus namaycush	Lake trout	0	5	0.395	31
Salvelinus namaycush	Lake trout	0	6	0.338	31
Coregonus clupeaformis	Lake whitefish	0	3	0.441	55
Coregonus clupeaformis	Lake whitefish	0	4	0.538	61
Coregonus clupeaformis	Lake whitefish	0	5	0.405	66
Micropterus salmoides	Largemouth bass	0	3	0.312	132
Micropterus salmoides	Largemouth bass	0	4	0.283	132
Lepomis megalotus	Longear sunfish	5	2	0.570	11

Table A2.1 contd.

Lepomis megalotus	Longear sunfish	10	3	0.523	11
Esox lucius	Northern pike	0	3	0.553	82
Esox lucius	Northern pike	0	4	0.515	84
Oncorhynchus mykiss	Rainbow trout	0	2	0.370	10
Oncorhynchus mykiss	Rainbow trout	0	3	0.398	11
Lepomis auritus	Redbreast sunfish	0	2	0.217	10
Lepomis auritus	Redbreast sunfish	6	3	0.191	10
Lepomis microlophus	Redear sunfish	0	2	0.395	15
Lepomis microlophus	Redear sunfish	0	3	0.414	15
Ambloplites rupestris	Rock bass	7	2	0.324	12
Ambloplites rupestris	Rock bass	7	3	0.334	13
Micropterus dolomieui	Smallmouth bass	0	3	0.249	29
Micropterus dolomieui	Smallmouth bass	0	4	0.239	29
Sander vitreus	Walleye	0	3	0.242	57
Sander vitreus	Walleye	0	4	0.245	57
Sander vitreus	Walleye	0	5	0.252	57
Lepomis gulosus	Warmouth	0	2	0.397	28
Lepomis gulosus	Warmouth	0	3	0.402	28
Morone chrysops	White bass	0	2	0.385	40
Morone chrysops	White bass	0	3	0.358	40
Morone chrysops	White bass	0	4	0.375	40
Catostomus commersoni	White sucker	0	3	0.328	12
Catostomus commersoni	White sucker	0	4	0.479	15
Catostomus commersoni	White sucker	0	5	0.377	15
Ameiurus natalis	Yellow bullhead	10	2	0.348	4
Ameiurus natalis	Yellow bullhead	10	3	0.441	5
Ameiurus natalis	Yellow bullhead	9	4	0.336	6
Perca flavescens	Yellow perch	9	2	0.330	82
Perca flavescens	Yellow perch	5	3	0.315	110
Perca flavescens	Yellow perch	4	4	0.287	110

A2.1 R code for estimating base temperatures for growth using bioenergetics models and the 10 ^{o}C rule

```
## Estimating base temperatures for growth using the 10 degree C rule
## Author: Andrew E. Honsey, University of Minnesota

## Read in the file of bioenergetics parameters (Supplementary Data File 2) and
## name it "params"
params<-read.csv("All_bioenergetics_parameters.csv")

## Add a column to store base temperature estimates
Base.estimate<-rep(NA,length(params$Order))
params<-cbind(params,Base.estimate)

## define energy density of oxygen
oxygen.energy.density<-13556

## loop through models
for (j in 1:length(params$Order)){

## Set other initial parameters
t=seq(from=0.01,to=40,by=0.01) # temperature range
```

```
w=params$initial.mass[j] # initial mass in g
p=1 # proportion of max consumption

## Create empty vecors to record consumption, respiration, egestion, excretion,
## total wastes (redundant with egestion + excretion),
## energy lost to specific dynamic action, specific growth in mass, absolute growth
## in mass
cons<-rep(NA,length(t))
resp<-rep(NA,length(t))
eges<-rep(NA,length(t))
excr<-rep(NA,length(t))
wastes<-rep(NA,length(t))
spec<-rep(NA,length(t))
energy.gain<-rep(NA,length(t))
energy.change<-rep(NA,length(t))
resp.energy.loss<-rep(NA,length(t))
growth.mass<-rep(NA,length(t))

## Loop through values of temperature, using
## correct equations for each model
for (i in 1:length(t)){
```

```
  ## Consumption equations
  if (params$CEQ[j] == 1){
    f.t=exp(params$CQ[j]*t[i])
    c.max=params$CA[j]*w^params$CB[j]
    cons[i]=c.max*p*f.t
  }
  else (
  if (params$CEQ[j] == 2){
  z=log(params$CQ[j])*(params$CTM[j]-params$CTO[j])
  y=log(params$CQ[j])*(params$CTM[j]-params$CTO[j]+2)
  v=(params$CTM[j]-t[i])/(params$CTM[j]-params$CTO[j])
  x=(z^2*(1+(1+(40/y))^0.5)^2)/400
  f.t=(v^x)*exp(x*(1-v))
  c.max=params$CA[j]*w^params$CB[j]
  cons[i]=c.max*p*f.t
  }
  else (
  if (params$CEQ[j] == 3){
    g1=(1/(params$CTO[j]-params$CQ[j]))*log((0.98*(1-
params$CK1[j]))/(params$CK1[j]*0.02))
    l1=exp(g1*(t[i]-params$CQ[j]))
```

```
    g2=(1/(params$CTL[j]-params$CTM[j]))*log((0.98*(1-
params$CK4[j]))/(params$CK4[j]*0.02))
    l2=exp(g2*(params$CTL[j]-t[i]))
    ka=(params$CK1[j]*l1)/(1+params$CK1[j]*(l1-1))
    kb=(params$CK4[j]*l2)/(1+params$CK4[j]*(l2-1))
    f.t=ka*kb
    c.max=params$CA[j]*w^params$CB[j]
    cons[i]=c.max*p*f.t
  }
  )
  )
  ## Respiration equations
  if (params$REQ[j] == 1) {
    if (t[i] > params$RTL[j]) vel<-params$RK1[j]*w^(params$RK4[j]) else vel <-
params$ACT[j]*w^(params$RK4[j])*exp(params$BACT[j]*t[i])
    activ<-exp(params$RTO[j]*vel)
    if (activ == 1) activity <- params$ACT[j] else activity <- activ
    f.t2=exp(params$RQ[j]*t[i])
    resp[i]=params$RA[j]*w^params$RB[j]*f.t2*activity
  }
  else(
```

```
if (params$REQ[j] == 2){
  z2=log(params$RQ[j])*(params$RTM[j]-params$RTO[j])
  y2=log(params$RQ[j])*(params$RTM[j]-params$RTO[j]+2)
  v2=(params$RTM[j]-t[i])/(params$RTM[j]-params$RTO[j])
  x2=(z2^2*(1+(1+40/y2)^0.5)^2)/400
  f.t2=(v2^x2)*exp(x2*(1-v2))
  resp[i]=params$RA[j]*w^params$RB[j]*f.t2*params$ACT[j]
}
)
## Egestion and excretion
if (params$EGEXEQ[j] == 1) {
  eges[i]<-params$FA[j]*cons[i]
  excr[i]<-params$UA[j]*(cons[i]-eges[i])
  wastes[i]<-eges[i]+excr[i]
}
else(
if (params$EGEXEQ[j] > 1){
  eges[i]<-params$FA[j]*(t[i]^params$FB[j])*(exp(params$FG[j]*p))*cons[i]
  excr[i]<-params$UA[j]*(t[i]^params$UB[j])*(exp(params$UG[j]*p))*(cons[i]-eges[i])
  wastes[i]<-eges[i]+excr[i]
}
)
```

```
  ## Energy lost to specific dynamic action
  spec[i]=params$SDA[j]*(cons[i]-eges[i])

 ### Predator energy density
  if (params$PREDEDEQ[j] == 1){
    pred.energy.density <- params$ED[j]
  }
  else(
    if (params$PREDEDEQ[j] == 2){
      if (w <= params$Cutoff[j]) pred.energy.density <- params$Alpha1[j] +
params$Beta1[j]*w else pred.energy.density <- params$Alpha2[j] + params$Beta2[j]*w
    }
  )

  #Growth in mass
  energy.gain[i]<-(cons[i]-wastes[i]-spec[i])*params$PREYED[j]*w
  resp.energy.loss[i]<-resp[i]*w*oxygen.energy.density
  energy.change[i]<-energy.gain[i]-resp.energy.loss[i]
  growth.mass[i]<-energy.change[i]/pred.energy.density
}

# Compile results; calculate and store base temp using 10 C rule
```

```
res<-as.data.frame(cbind(t,growth.mass))
res<-res[is.finite(res$growth.mass) == T,]
res<-res[res$growth.mass > 0,]

## optional -- plot growth vs temp relationships for each species
plot(res$t,res$growth.mass,main=params$Species[j],xlab="Water
temperature",ylab="Daily growth (g)")

## find optimum temperature for growth, remove results above this temperature
opt<-res[which(res$growth.mass == max(res$growth.mass)),]
res<-res[res$t <= opt$t,]

## Calculate mean development temperature
mndev<-(max(res$growth.mass)+min(res$growth.mass))/2
MNDEV<-res[which(abs(res$growth.mass-mndev)==min(abs(res$growth.mass-
mndev))),]
mndevtemp<-MNDEV$t

## Calculate and store base temperature for growth
base.est<-mndevtemp-10
params$Base.estimate[j]<-base.est
}
```

A2.2 Example results using annual growth simulations to estimate T_0

Honsey et al. (in press) suggested that the base temperature for growth (T_0) can be estimated across fish species using annual growth simulations. This approach is based on the idea that, if degree-days are an accurate index of the thermal scope for growth, then growth should be proportional to degree-days when they are calculated using the appropriate value for T_0. We used the Shuter et al. (1983) water temperature model to generate annual water temperature cycles across mean annual air temperature ($\overline{AT}$) values (see Honsey et al. in press). We used these water temperatures to drive bioenergetics simulations that lasted 365 days using the bioenergetics models described in Supplemental Data File 2. We determined annual growth by subtracting initial fish length from the length on day 365. We then calculated degree-days across T_0 ranging from 0 to 20 ºC for water temperatures using the equation Section 3.1, and we used empirical relationships to predict air-based degree-days from $\overline{AT}$ for T_0 ranging from 0 to 15 ºC (see Appendix 1, Table A1.2). Finally, we fit linear models to the annual growth versus water- and air-based degree-day relationships (i.e., separately for each species and T_0 value), and we determined the T_0 value for which the relationship was nearest to proportional by finding the y-intercept value that was closest to 0. In general, we found that T_0 estimates were highly sensitive to changes in model settings (e.g., consumption levels, the range of $\overline{AT}$ values used). Although the selection of these model settings can be somewhat intuitive (e.g., models for coldwater species should include lower $\overline{AT}$ ranges than models for warmwater species), we argue that choosing "appropriate" settings for each species is ultimately highly subjective. As such, we chose to exclude results from

this approach. We provide results from two example models and for various consumption and $\overline{AT}$ settings in Table A2.2.

Table A2.2 Examples of variation in estimates of the base temperature for growth for calculating degree-days from water ($T_{0,W}$) and air ($T_{0,A}$) temperatures across bioenergetics and limnological model settings for two bioenergetics models. p(Cmax) = proportion of maximum consumption, $\overline{AT}$ = mean annual air temperature.

Model species	p(Cmax)	$\overline{AT}$ range (ºC)	$T_{0,W}$ (ºC)	$T_{0,A}$ (ºC)
Bighead carp	1	0-12.5	9	10
Bighead carp	1	-10-12.5	7	14
Bighead carp	1	-15-0	4	14
Bighead carp	0.5	0-12.5	15	>15
Bighead carp	0.5	-10-12.5	9	>15
Bighead carp	0.5	-15-0	4	>15
Generalized coregonid	1	0-12.5	<0	<0
Generalized coregonid	1	-10-12.5	<0	<0
Generalized coregonid	1	-15-0	3	11
Generalized coregonid	0.5	0-12.5	8	10
Generalized coregonid	0.5	-10-12.5	5	13
Generalized coregonid	0.5	-15-0	4	>15

Appendix 3

Supplementary methods and results for Chapter 4

A3.1 Adjusting sample sizes-at-age for gear selectivity and natural mortality

For our simulation study, we adjusted sample sizes-at-age to approximate data scenarios that are common in fisheries science (and may be similar in other disciplines) to provide realistic estimates of the data quality required for LMLP to perform well. To do this, we emulated sample sizes-at-age for walleye *Sander vitreus* caught in gill nets from the expansive Fall Walleye Index Netting surveys conducted by the Ontario Ministry of Natural Resources and Forestry (Morgan 2002). Sample sizes-at-age for all simulations are shown in Table A3.1. See Section A3.4 below for more details on the $T = 3$ and $T = 7$ simulations.

We did not include size selectivity on early age-classes (i.e., gears catching the largest individuals in a given young age-class) in our simulations; however, the potential impacts of gill net size selectivity on model estimates are likely relatively small for organisms such as walleye across the ages included in the simulations (Walker et al. 2013). Nevertheless, size selectivity may affect LMLP fits for some datasets and should be considered on a case-by-case basis.

Table A3.1 Sample sizes-at-age for populations of 1000 individuals used in Lester model likelihood profiling simulations. Random samples of varying sizes (see Table A3.2) were drawn from these populations for each of 100,000 iterations.

	Sample Size		
Age	***T* = 3**	***T* = 5**	***T* = 7**
1	50	30	5
2	120	70	20
3	160	130	50
4	155	140	95
5	135	150	115
6	70	130	125
7	50	65	125
8	41	45	110
9	36	38	70
10	32	32	50
11	28	28	38
12	24	24	30
13	21	22	26
14	18	18	22
15	15	15	19
16	13	12	17
17	11	10	15
18	9	8	13
19	7	7	11
20	5	6	9
21	-	5	8
22	-	5	7
23	-	4	6
24	-	3	4
25	-	3	3
26	-	-	2
27	-	-	2
28	-	-	1
29	-	-	1
30	-	-	1

Table A3.2 Levels of sample size, precision (CV^{-1}) in length-at-age, and the annual cost to somatic growth of maturity g (expressed in equivalent energetic units) used to simulate length-at-age data. Simulations consisted of 100 iterations of each parameter combination (N = 100,000 iterations).

Sample Size	Precision	g
50	4	0.05
100	5	0.075
150	6	0.1
200	7	0.125
250	8	0.15
300	9	0.175
400	10	0.2
500	12	0.225
750	20	0.25
1000	30	0.3

A3.2 LMLP fits to data describing species other than walleye *Sander vitreus*

To show the potentially broad applicability of our algorithm, we applied LMLP to four additional datasets describing four different species: lake whitefish *Coregonus clupeaformis*, haddock *Melanogrammus aeglefinus*, Alaska skate *Bathyraja parmifera*, and the seal salamander *Desmognathus monticola*. The lake whitefish data describe females from Shoal Lake, ON in 2000-2001 (n=149, precision=24.26, $\hat{g}$=0.18) and were collected by the Ontario Ministry of Natural Resources and Forestry as part of their fall gill netting surveys (Morgan 2002). The haddock data describe females from the Gulf of Maine collected during spring 2015 (n=359, precision=10.12, $\hat{g}$=0.34) as part of the National Oceanic and Atmospheric Administration (NOAA) Northeast Fisheries Science Center's bottom trawl surveys (data provided by Mike Palmer, NOAA). The Alaska skate data describe females taken from the eastern Bering Sea from 2003-2005 (n=231, precision=15.87, $\hat{g}$=0.18) and were collected by NOAA Fisheries groundfish trawl surveys during the summers of 2003 and 2004, and throughout 2004 and 2005 by the North Pacific Groundfish Observer Program on flatfish trawlers and Pacific cod longline vessels (see Matta and Gunderson 2007; data provided by Beth Matta, NOAA). Finally, the salamander data describe individuals collected from Wolf Creek, North Carolina, USA during 1994-1995 (see Castanet et al. 1996; n=83, precision=50.79, $\hat{g}$=0.38; data provided by Richard Bruce, Professor Emeritus, Western Carolina University).

Due to the low sample size (n=4), we did not use a standard major axis regression to compare T_{MLE} to $\widehat{A_{50}}$ for these fits. Instead, we calculated confidence intervals for the difference between the two parameters assuming that the likelihood interval (LI;

approximate 96% chi-squared confidence interval) was similar to a 95% confidence interval (CI). That is, we assumed that the LI was approximated by $T_{MLE} \pm 1.96\times$SE, where SE is the standard error of the parameter estimate. We used this formula and the known LIs for T_{MLE} and bootstrapped CIs for $\widehat{A_{50}}$ to calculate SEs for each parameter. Because the intervals were not necessarily symmetrical, we took the mean of the two SE estimates (derived from the upper and lower interval bounds) as the SE estimate for each case. We then used the following formula to calculate the confidence interval for the difference between the two parameters (Daniel and Cross 2013):

$$\left| T_{MLE} - \widehat{A_{50}} \right| \pm 1.96 \times \sqrt{{SE_{T_{MLE}}}^2 + {SE_{\widehat{A_{50}}}}^2}$$

If this interval contained 0, the parameters were considered not significantly different from one another. Complete results for these comparisons, including parameter estimates, LIs, CIs, and difference intervals, are shown in Table A3.3.

Table A3.3 Age-at-maturity (AAM) estimates from LMLP (T_{MLE}) and logistic regression ($\widehat{A_{50}}$) for four datasets describing a variety of species (Fig. 4.4). Also included are sample size (n), precision in length-at-age, standard error estimates for each AAM parameter, estimates for three additional LMLP parameters (g = annual cost to somatic growth of maturity (gonad mass/somatic mass expressed in equivalent energetic units); l_0 = theoretical length at age 0 (mm); h = net rate of energy acquisition expressed as somatic growth rate (mm·yr^{-1})), and the difference interval for the two AAM parameters. None of the AAM estimates significantly differed at α = 0.05 (see Section A3.2 for dataset descriptions and difference interval calculation methods).

Species	n	Precision (CV^{-1})	$\widehat{A_{50}}$	$SE_{\widehat{A_{50}}}$	T_{MLE}	$SE_{T_{MLE}}$	$\hat{g}$	$\hat{l_0}$	$\hat{h}$	Difference Interval
Lake whitefish	149	24.26	6.80 (6.19, 7.53)	0.34	7 (6.27, 7.78)	0.39	0.18	153.70	45.52	(-0.81, 1.21)
Haddock	359	10.12	3.14 (2.71, 3.83)	0.29	3 (2.93, 3.23)	0.08	0.34	128.01	95.14	(-0.72, 0.44)
Alaska skate	231	15.87	9.94 (9.63, 10.46)	0.21	10.65 (9.875, 11.1)	0.31	0.18	242.76	72.27	(-0.03, 1.45)
Seal salamander	83	50.79	4.14 (3.66, 4.63)	0.25	4.1 (3.72, 4.45)	0.19	0.38	7.21	10.74	(-0.65, 0.56)

Table A3.4 Results of model fits to empirical walleye *Sander vitreus* datasets from various locations, including lake name, jurisdiction, years, sample size, precision (i.e., CV^{-1}), whether the likelihood profile contained a single peak (Y=yes, N=no), the maximum likelihood estimate for T (yrs, with likelihood intervals), the A_{50} estimate (yrs, with bootstrapped 95% confidence intervals), and estimates for the remaining model parameters: g = annual cost to somatic growth of maturity (expressed in equivalent energetic units); l_0 = theoretical length at age 0 (mm); h = net rate of energy acquisition expressed as somatic growth rate ($mm \cdot yr^{-1}$). Data were collected by the Minnesota Deparment of Natural Resources, the Ontario Ministry of Natural Resources and Forestry, and the Quebec Ministry of Natural Resources and Wildlife.

Name	Jurisdiction	Years	n	Precision (CV^{-1})	Single Peak	$\widehat{A_{50}}$	T_{MLE}	$\hat{g}$	$\hat{l_0}$	$\hat{h}$
Nipigon	ON	2001-3	749	12.97	Y	3.91 (3.67, 4.19)	3.25 (3.03, 3.43)	0.31	170.51	84.47
Mille Lacs	MN	2011	736	16.06	Y	3.93 (3.80, 4.08)	4.25 (4.15, 4.38)	0.34	144.14	81.77
Lake of the Woods	MN	2003-5	638	12.20	Y	5.33 (5.16, 5.51)	6.6 (6.3, 6.9)	0.19	163.20	55.70
Winnibigoshish	MN	2009-11	636	18.66	Y	4.05 (3.96, 4.17)	4.7 (4.5, 4.93)	0.21	178.48	62.47
Mille Lacs	MN	1993-5	628	17.91	Y	4.04 (3.95, 4.15)	4.4 (4.25, 4.55)	0.26	156.20	74.25
St. Joseph	ON	1999	563	12.52	Y	6.84 (6.51, 7.17)	3.5 (3.2, 3.83)	0.28	137.17	64.07
Ombabika Bay (L. Nipigon)	ON	2002	557	16.01	Y	4.46 (4.33, 4.63)	3.9 (3.8, 4.13)	0.38	137.12	89.67
Cass	MN	1997-9	494	14.76	Y	4.66 (4.37, 4.98)	4.43 (4.1, 4.73)	0.21	203.74	61.48
Upper Red	MN	2003	465	11.94	N	4.57 (4.33, 4.82)	2.6 (1, 7.53)	0.10	161.50	69.86
Vermilion	MN	2009-11	445	12.91	Y	5.09 (4.74, 5.39)	5 (4.45, 5.33)	0.15	184.68	53.73
Leech	MN	2001-3	343	12.26	Y	3.09 (2.96, 3.26)	3.45 (3.2, 3.73)	0.33	211.57	71.22
Leech	MN	2009	342	15.55	Y	3.93 (3.71, 4.12)	3.7 (3.58, 3.83)	0.39	131.83	95.81
Chibougamau	QC	1998-9	325	14.19	Y	8.19 (7.49, 9.50)	7.53 (7.08, 7.9)	0.22	136.71	57.50
Minnitaki	ON	2001	324	10.42	Y	5.94 (5.57, 6.62)	5.8 (5.35, 6.7)	0.23	128.36	62.60
Lake of the Woods	ON	2004	322	9.82	N	4.78 (4.59, 5.03)	6 (3.93, 6.58)	0.21	157.52	60.42
Ottawa R.	QC	1999	306	11.98	Y	4.24 (4.02, 4.57)	4.35 (3.65, 5.05)	0.16	202.13	53.46
Rainy	MN	2005-7	305	7.59	N	5.78 (5.34, 6.14)	3 (2.05, 3.68)	0.20	121.33	63.73
Weakwaten	QC	1996-8	283	12.30	N	12.47 (11.65, 13.27)	10.48 (6.5, 11.68)	0.12	160.50	28.01
Nipissing	ON	2001-2	278	12.84	Y	3.92 (3.74, 4.10)	4.7 (3.73, 5.53)	0.17	211.78	53.01
Rice	ON	1999	274	17.13	Y	3.83 (3.66, 4.07)	4.53 (3.6, 5.05)	0.19	247.32	60.13
des Mille Lacs	ON	1999	222	9.02	N	6.64 (6.16, 7.12)	5 (3.28, 6.63)	0.14	167.75	54.38
Preissac	QC	2002	221	12.94	Y	6.70 (6.02, 7.40)	4 (1.35, 4.98)	0.07	165.64	41.31
Yasinsky	QC	1997	219	20.06	Y	8.38 (7.43, 10.06)	8.28 (7.75, 8.75)	0.22	157.80	43.81
Otter Tail	MN	2010	215	11.68	Y	4.19 (3.90, 4.42)	3.58 (2.68, 4.4)	0.18	170.29	61.40
Cass	MN	2000	213	16.48	Y	4.34 (4.15, 4.60)	3.88 (3.5, 4.3)	0.22	184.52	71.86
Red	ON	2006	211	10.83	Y	5.33 (4.90, 5.85)	6.45 (5.68, 7.5)	0.23	167.51	55.38
Baskatong	QC	1989	209	14.63	Y	3.50 (3.21, 3.92)	3.45 (3.13, 3.78)	0.33	172.23	76.47
Kipawa	QC	1999	202	13.76	Y	4.83 (4.09, 5.25)	4.53 (3.48, 5.13)	0.19	182.80	67.01

Table A3.4 contd.

Lake of the Woods	MN	1997	201	12.63	Y	4.95 (4.57, 5.29)	4.63 (4.2, 5.05)	0.30	156.39	71.83
Nipigon	ON	1999	186	18.97	Y	3.87 (3.58, 4.38)	3.83 (3.5, 4.2)	0.37	182.80	78.58
Cabonga	QC	2000	174	12.88	Y	4.05 (3.76, 4.47)	3.43 (2.63, 4.18)	0.19	231.31	61.29
Smoothrock	ON	2001	171	11.73	Y	6.30 (5.84, 6.91)	4.83 (4.15, 5.6)	0.21	142.08	52.60
Onaman	ON	2003	159	24.43	Y	4.45 (3.50, 5.24)	2.45 (2.18, 2.7)	0.57	154.58	119.83
Winnibigoshish	MN	2007	158	16.11	Y	4.04 (3.71, 4.40)	4.5 (4, 4.98)	0.21	184.38	65.27
Allumette	ON	1999	154	9.93	N	4.42 (3.95, 4.92)	3.5 (2.9, 4.73)	0.26	182.65	65.67
Regnault	QC	1998	150	14.30	Y	13.67 (11.63, 17.73)	11.05 (10.1, 11.75)	0.12	155.77	29.61
Pekagoning	ON	1999	149	17.54	Y	4.03 (3.99, 4.09)	6.15 (4.5, 7.03)	0.19	210.47	58.41
Shoal	ON	2001	131	21.18	Y	2.76 (2.33, 3.06)	3.38 (3.13, 3.68)	0.42	175.96	110.92
Ivanhoe	ON	1999	130	13.21	N	6.12 (5.06, 6.99)	5.35 (4.23, 6.28)	0.17	158.21	61.00
Kebskwasheshi	ON	1999	125	11.28	N	3.97 (3.52, 4.20)	3.38 (2.45, 3.95)	0.30	168.37	72.83
Dog	ON	1999	121	14.88	Y	5 (4.70, 5.06)	5 (4.55, 5.53)	0.24	144.92	70.78
Kabetogama	MN	2006	117	19.55	Y	4.15 (3.81, 4.89)	4.63 (4.23, 5.15)	0.26	176.90	61.74
West Kabenung	ON	1999	111	15.17	N	4.68 (4.09, 5.10)	3.85 (3.15, 4.9)	0.17	208.19	51.73
Wakami	ON	2001	94	26.24	Y	2.94 (2.51, 3.01)	3.48 (3.2, 3.73)	0.42	138.93	102.59
Rainy	ON	2008	92	12.75	N	6.83 (6.23, 7.82)	2 (1, 3.45)	0.12	166.09	48.83
Big Stone	MN	2006	84	15.11	Y	2.26 (1.98, 2.49)	2.38 (2.15, 2.6)	0.48	128.10	152.48
Sand Point	MN	2007	79	12.17	Y	5.05 (4.19, 5.94)	5.3 (4.68, 5.98)	0.25	141.25	59.51
Shenango	ON	2001	78	23.60	N	2.45 (0.61, 2.99)	3.38 (2.63, 4.98)	0.23	205.72	76.37
Cut Foot Sioux	MN	2007	75	23.79	Y	4.25 (3.83, 4.77)	4.9 (4.1, 5.38)	0.17	198.41	56.91
Jutten	ON	2001	72	13.19	N	7.19 (6.52, 7.94)	4.53 (3.93, 5.33)	0.26	84.46	67.74
Stormy	ON	1999	66	17.98	N	3.92 (3.02, 4.01)	3 (2.23, 3.8)	0.24	207.09	71.69
Matagami	QC	1992	63	11.21	N	13.39 (10.49, 19.36)	9.55 (1.75, 12. 63)	0.01	134.27	24.15
Birch	MN	2010	61	23.52	Y	3.01 (2.95, 3.07)	3.6 (3.35, 3.83)	0.40	188.84	86.79
Flanders	ON	1999	53	19.28	Y	5.01 (4.94, 5.08)	5.23 (4.2, 6.15)	0.19	202.05	53.58
Rennie	ON	1999	52	19.02	N	3.97 (3.50, 5.01)	2.55 (1.1, 3.15)	0.36	175.96	96.88
Mercutio	ON	2000	50	14.53	Y	4.71 (4.13, 5.39)	5.05 (4.45, 5.88)	0.24	136.08	66.95
Michel	ON	1999	49	14.50	Y	3.22 (2.57, 4.10)	2.88 (1.78, 3.7)	0.34	155.68	89.14

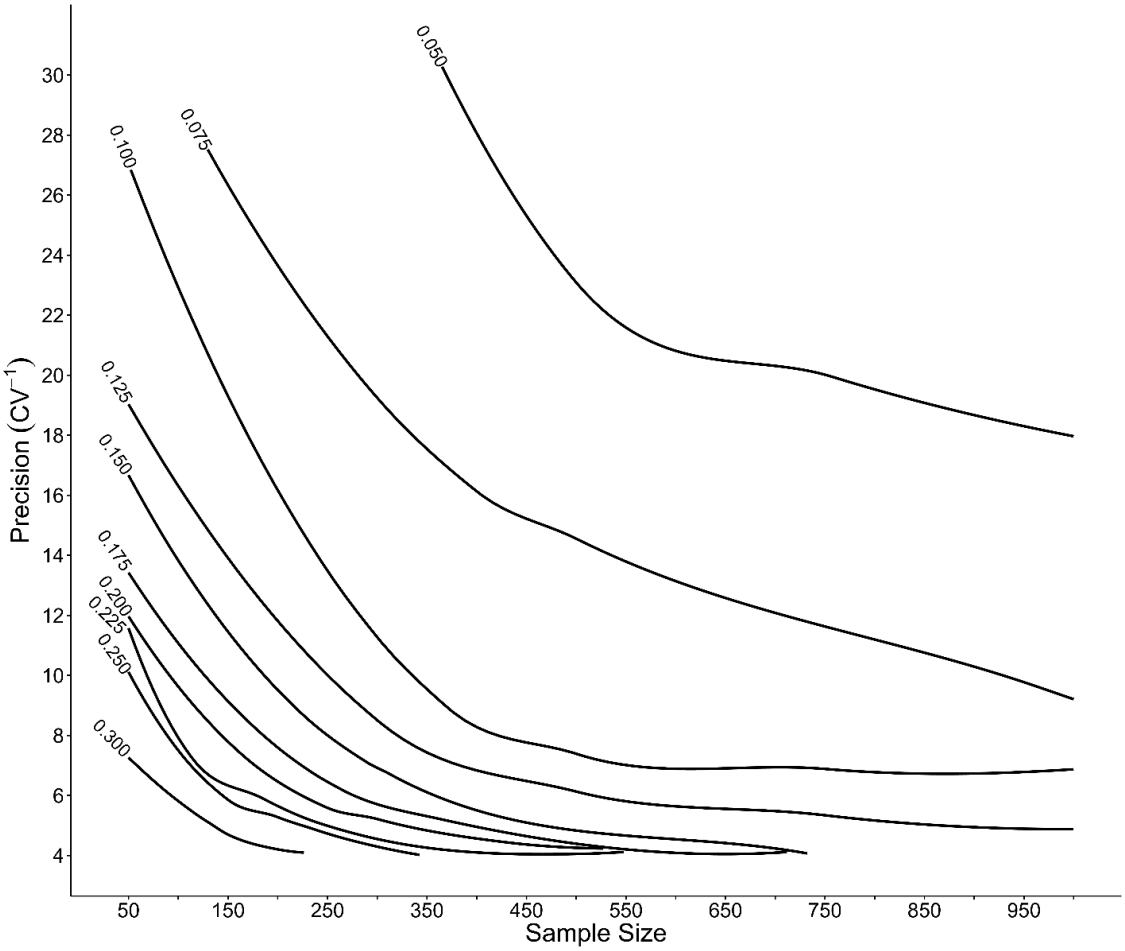

Figure A3.1 Simulated error contours for T_{MLE} to fall within +/- 0.5 yrs of T when T = 5 yrs across levels of sample size, precision, and g (labeled to the left of contours; Table A3.2), smoothed using LOESS (degree=2, α=0.75).

A3.3 Additional diagnostics

To provide a more complete picture of LMLP performance across the data quality scenarios investigated, we generated figures that show (1) the percent of cases in which the likelihood interval contained the true value for T and (2) the mean width of the likelihood intervals across levels of sample size, precision, and the maturity cost parameter g (Figs. A3.2-A3.11). Note that point size and colour scales vary among plots. Results for T = 3 and T = 7 simulations are available upon request.

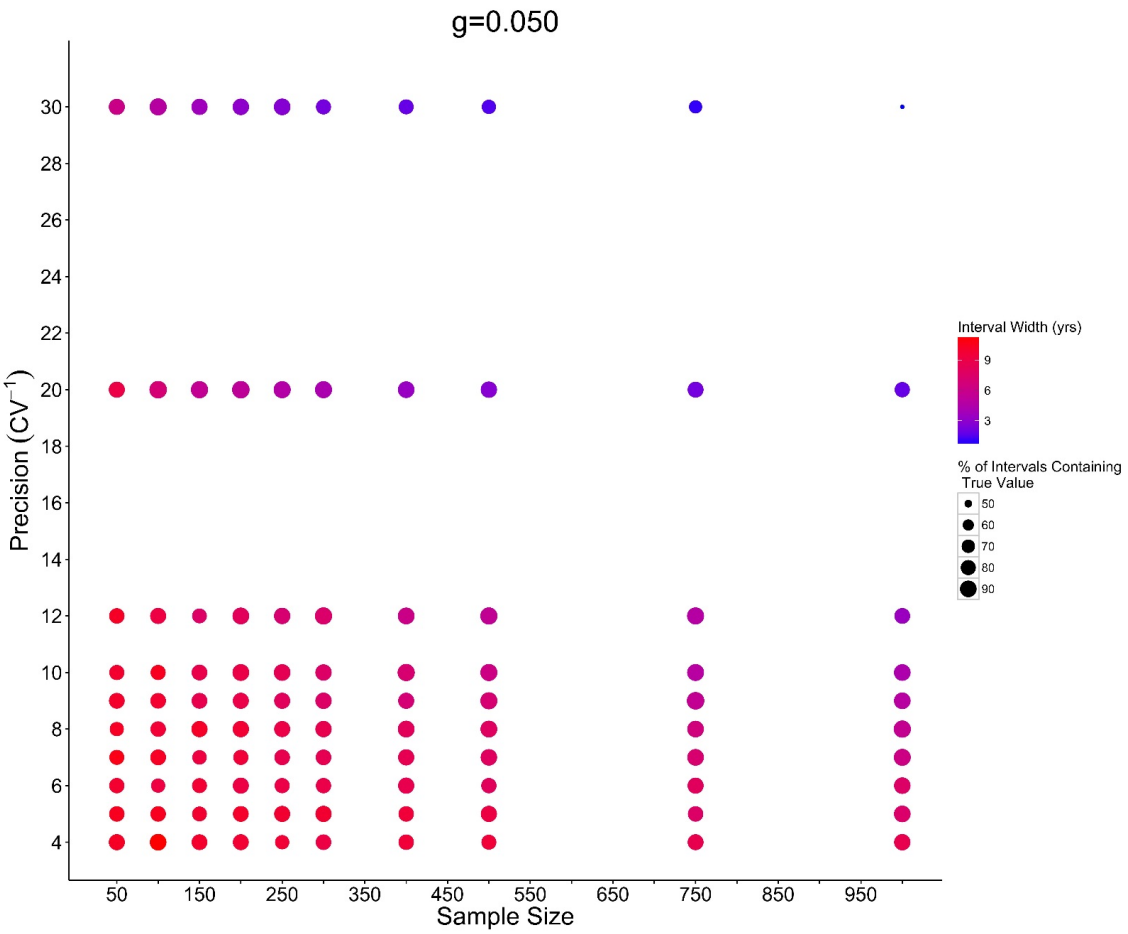

Figure A3.2 Mean likelihood interval width and the percent of likelihood intervals containing the true value for T across levels of sample size and precision (Table A3.2) when $T = 5$ and $g = 0.05$. Larger, bluer circles generally indicate better model performance.

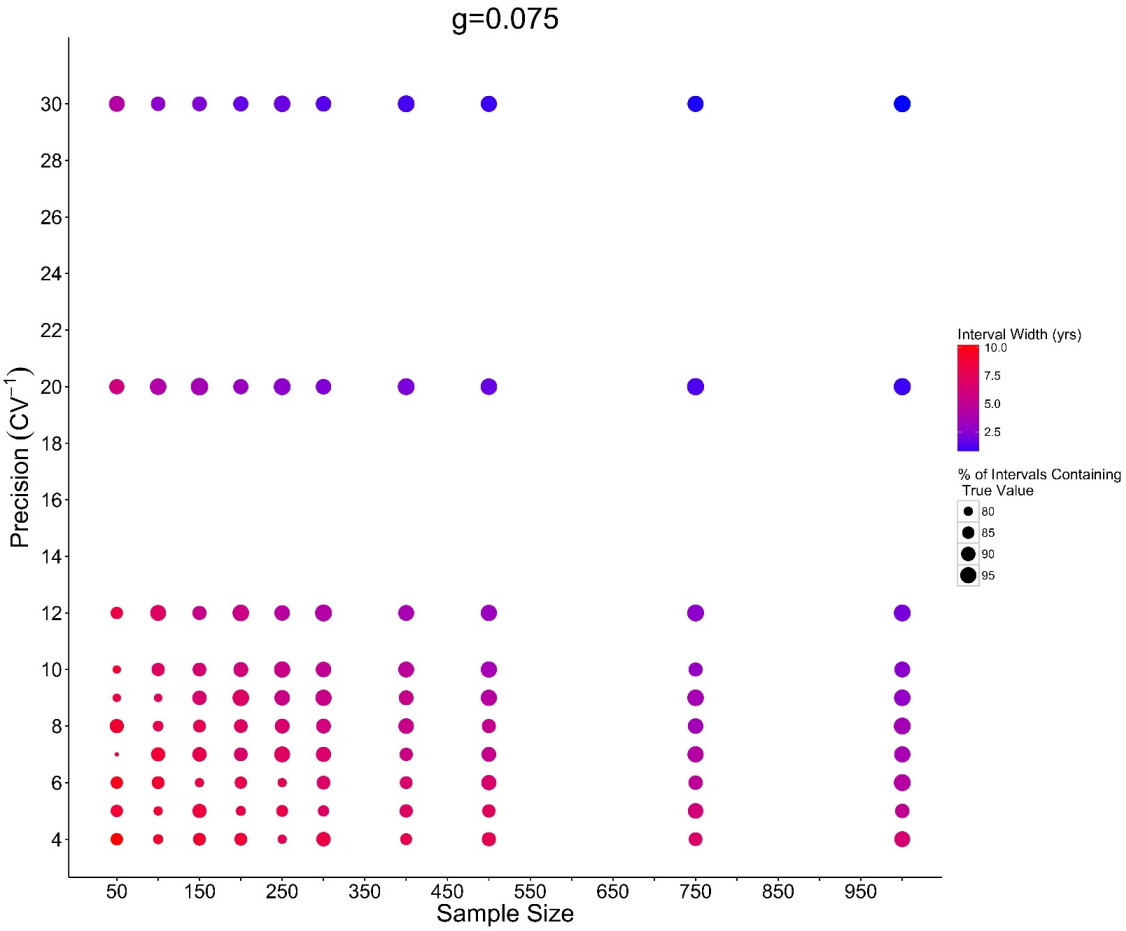

Figure A3.3 Mean likelihood interval width and the percent of likelihood intervals containing the true value for T across levels of sample size and precision (Table A3.2) when $T = 5$ and $g = 0.075$. Larger, bluer circles generally indicate better model performance.

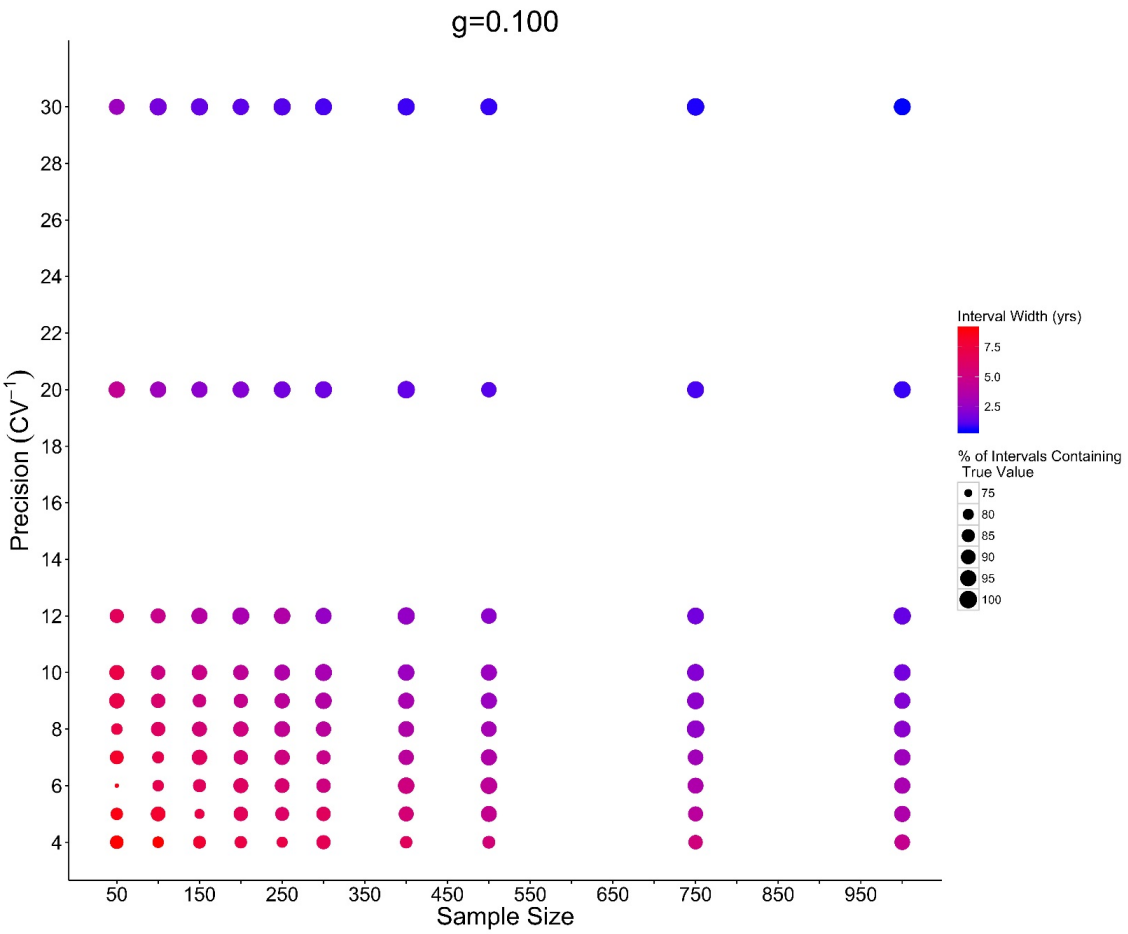

Figure A3.4 Mean likelihood interval width and the percent of likelihood intervals containing the true value for T across levels of sample size and precision (Table A3.2) when $T = 5$ and $g = 0.1$. Larger, bluer circles generally indicate better model performance.

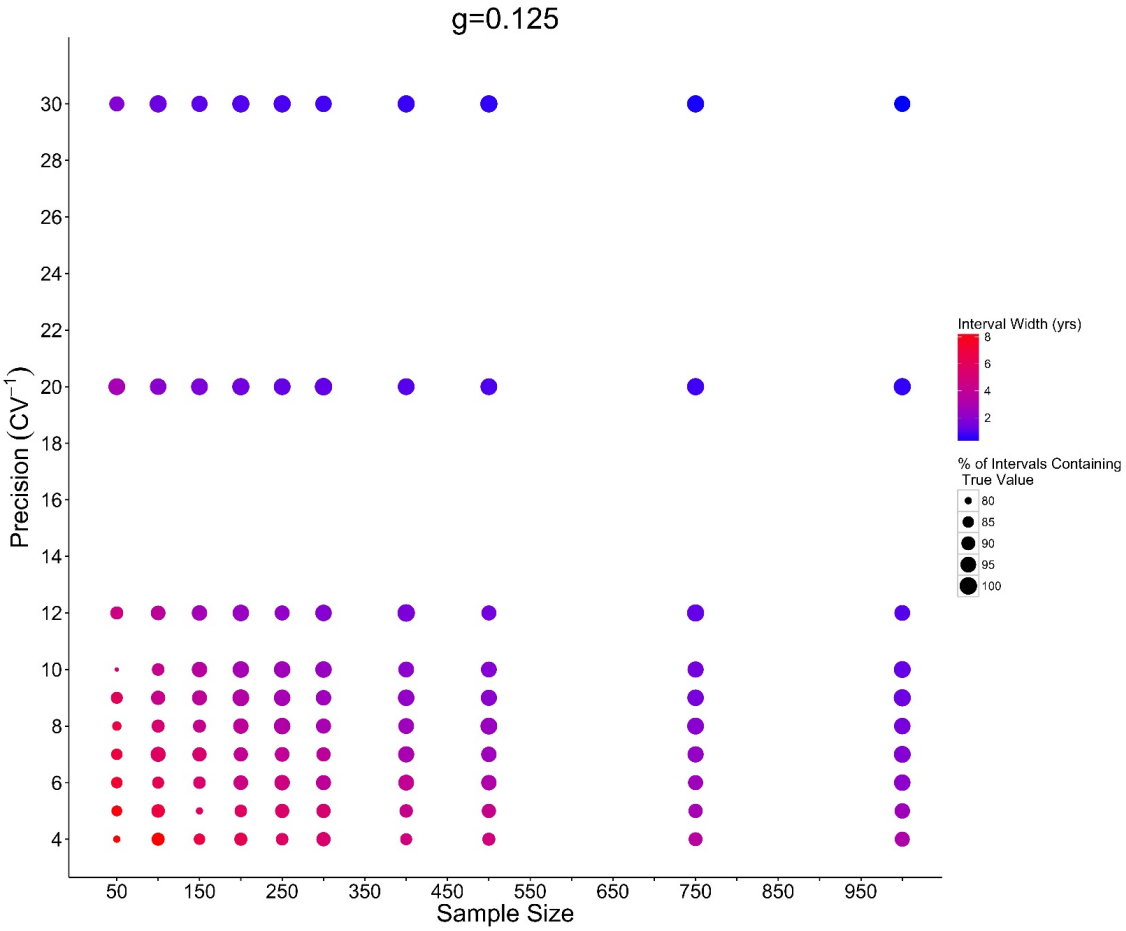

Figure A3.5 Mean likelihood interval width and the percent of likelihood intervals containing the true value for T across levels of sample size and precision (Table A3.2) when $T = 5$ and $g = 0.125$. Larger, bluer circles generally indicate better model performance.

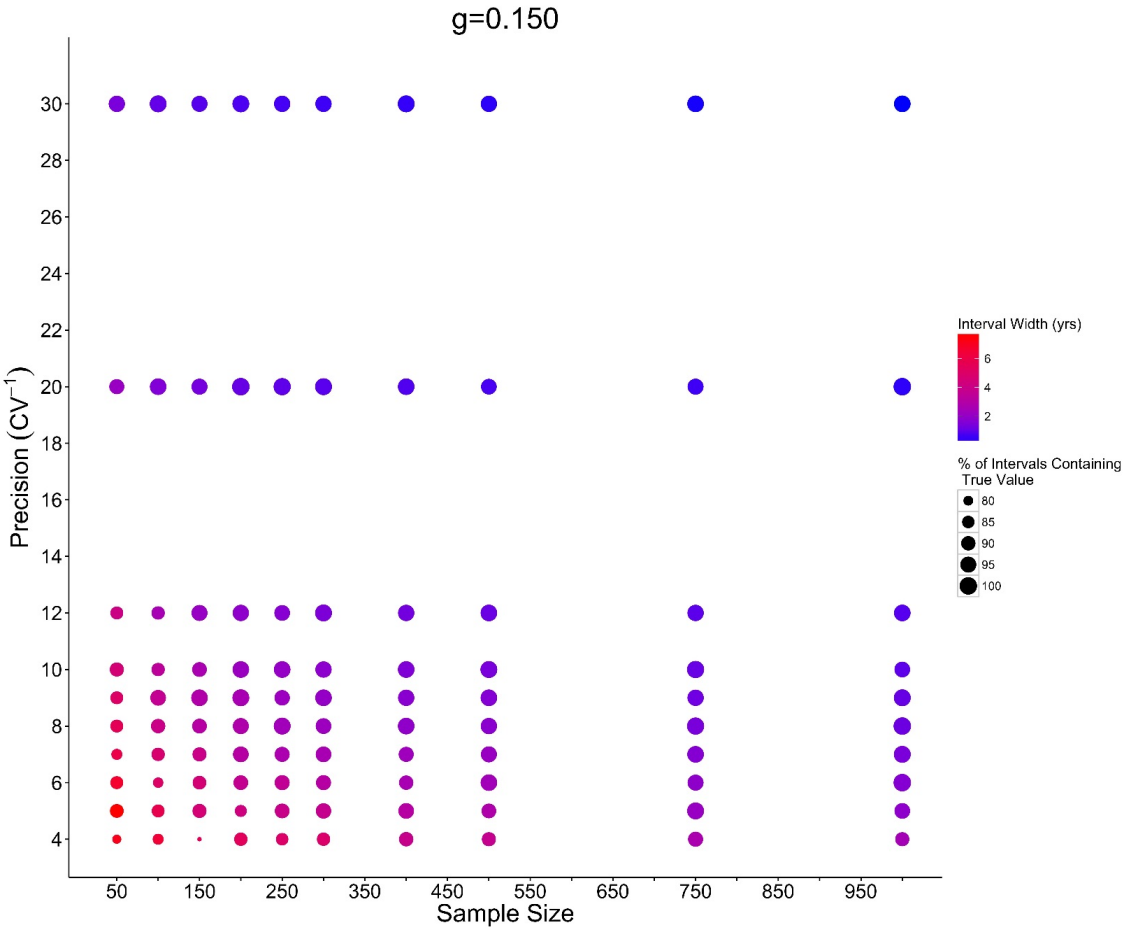

Figure A3.6 Mean likelihood interval width and the percent of likelihood intervals containing the true value for T across levels of sample size and precision (Table A3.2) when $T = 5$ and $g = 0.15$. Larger, bluer circles generally indicate better model performance.

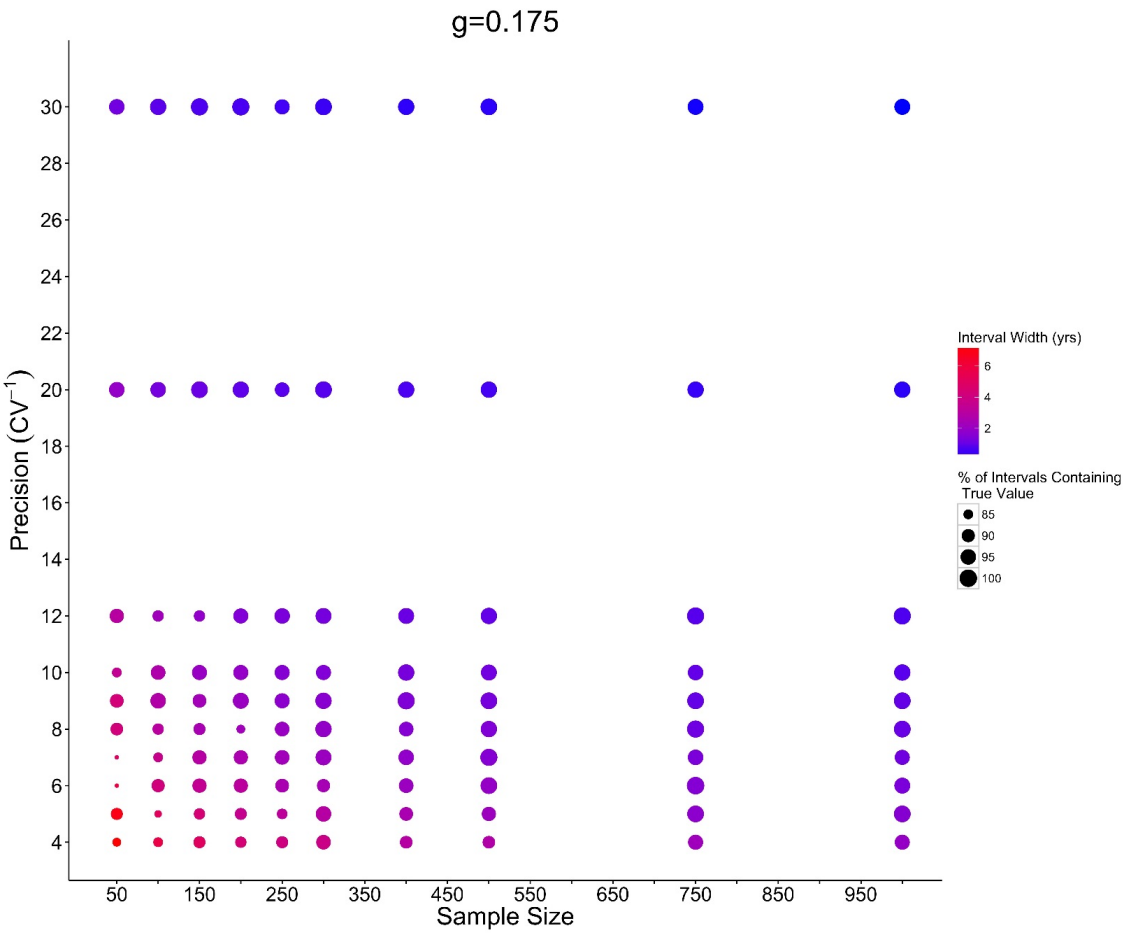

Figure A3.7 Mean likelihood interval width and the percent of likelihood intervals containing the true value for T across levels of sample size and precision (Table A3.2) when $T = 5$ and $g = 0.175$. Larger, bluer circles generally indicate better model performance.

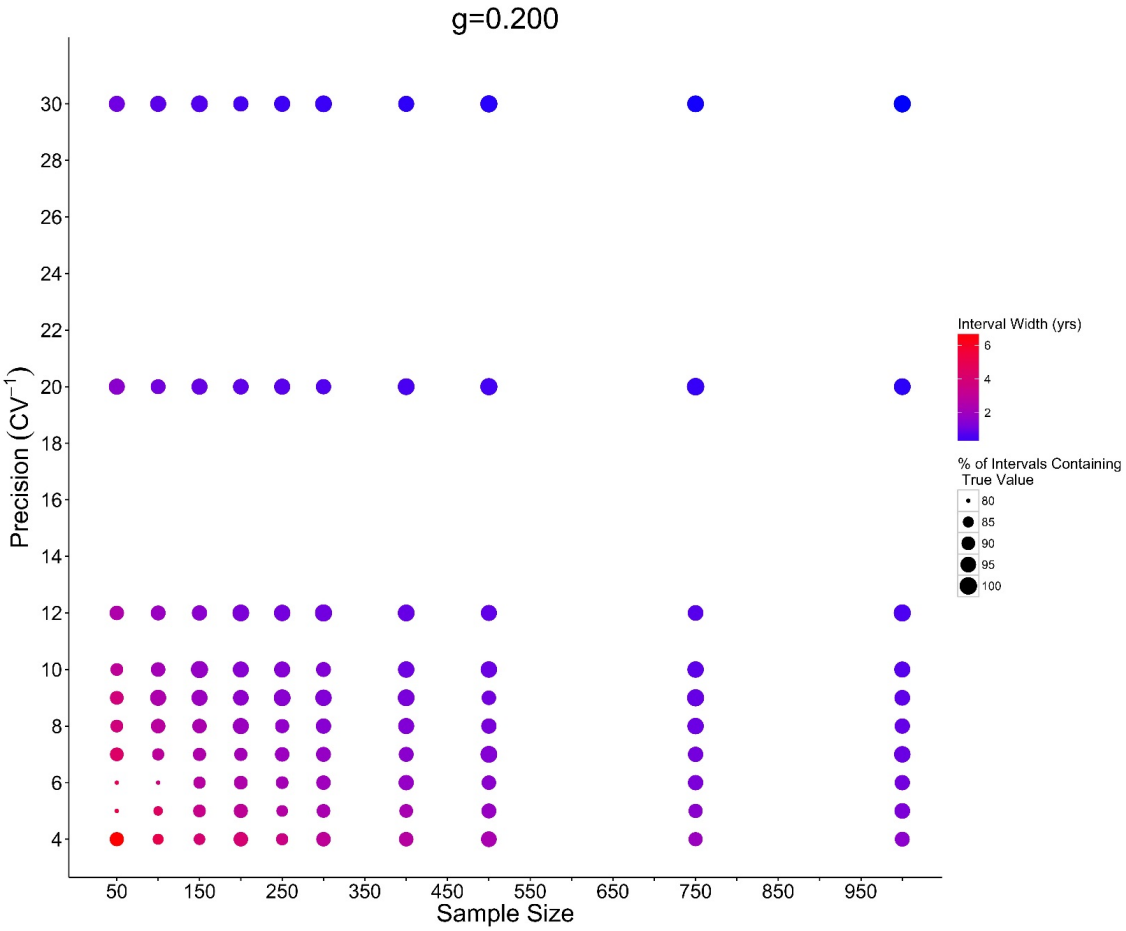

Figure A3.8 Mean likelihood interval width and the percent of likelihood intervals containing the true value for T across levels of sample size and precision (Table A3.2) when $T = 5$ and $g = 0.2$. Larger, bluer circles generally indicate better model performance.

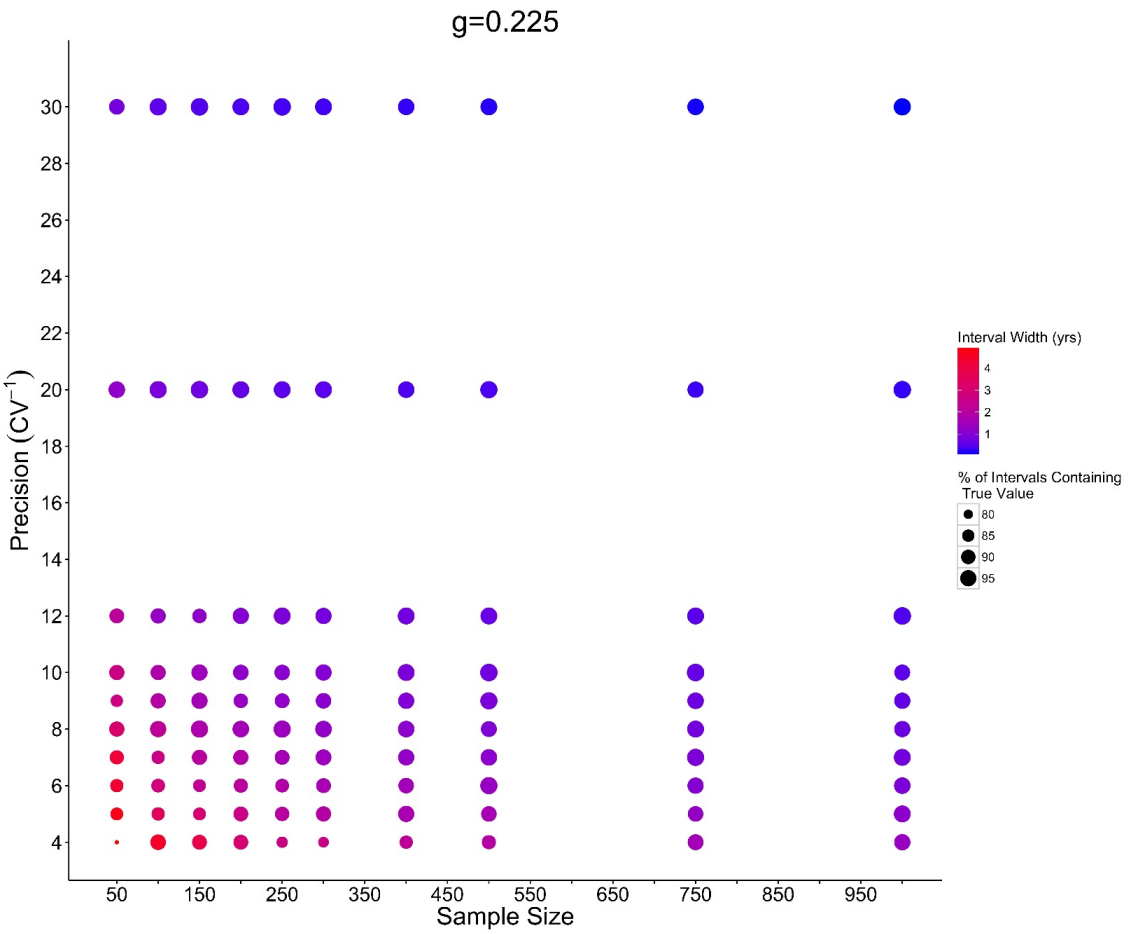

Figure A3.9 Mean likelihood interval width and the percent of likelihood intervals containing the true value for T across levels of sample size and precision (Table A3.2) when $T = 5$ and $g = 0.225$. Larger, bluer circles generally indicate better model performance.

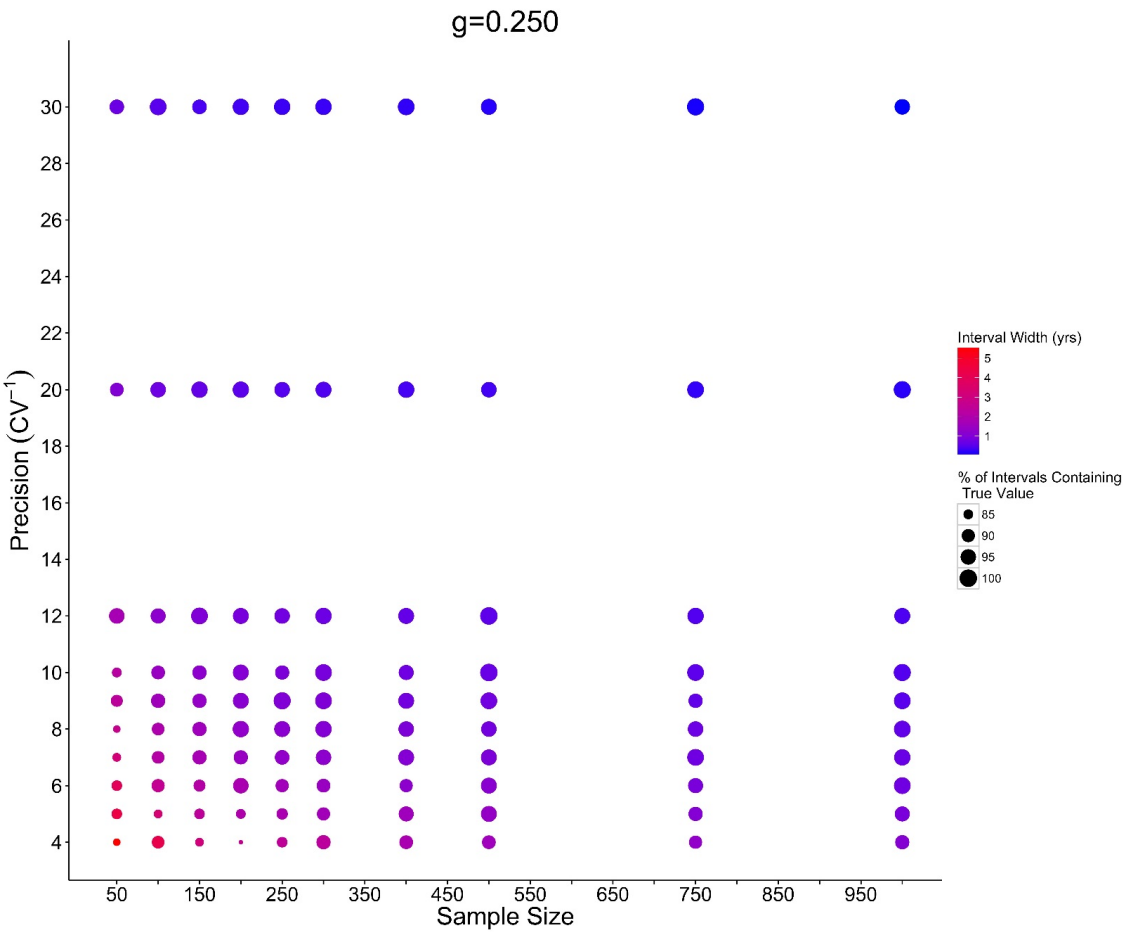

Figure A3.10 Mean likelihood interval width and the percent of likelihood intervals containing the true value for T across levels of sample size and precision (Table A3.2) when $T = 5$ and $g = 0.25$. Larger, bluer circles generally indicate better model performance.

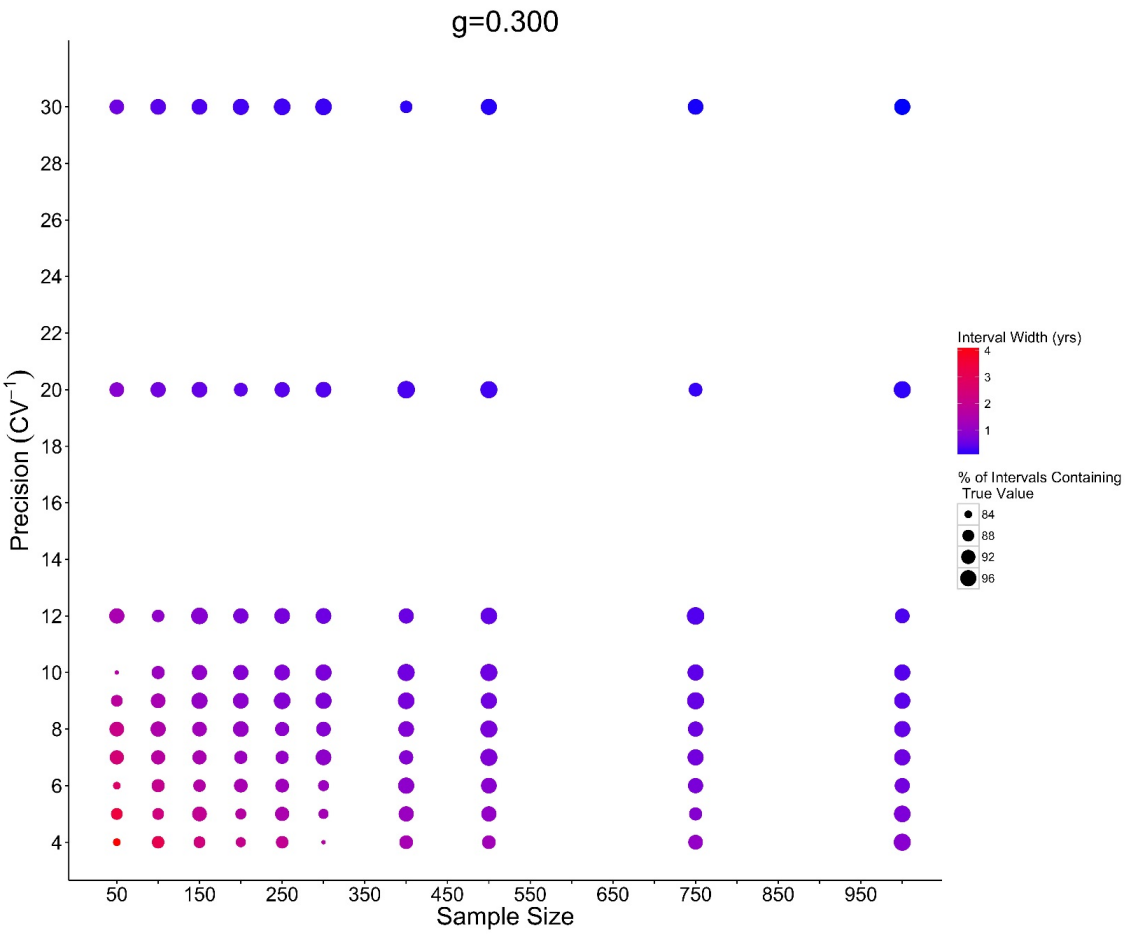

Figure A3.11 Mean likelihood interval width and the percent of likelihood intervals containing the true value for T across levels of sample size and precision (Table A3.2) when $T = 5$ and $g = 0.3$. Larger, bluer circles generally indicate better model performance.

A3.4 Additional simulations

We conducted two additional sets of simulations in which T = 3 and T = 7 to explore the sensitivity of our Lester model likelihood profiling (LMLP) method to varying age-at-maturity. Growth parameters for these simulations differed from T = 5 simulations and were also loosely based on walleye populations for which AAM was estimated at approximately 3 or 7. For T = 3 simulations, l_0 = 150 mm, h = 65 mm·yr^{-1}, and maximum age = 20 yrs (see Table 4.1 for parameter descriptions). For T = 7 simulations, l_0 = 80 mm, h = 40 mm·yr^{-1}, and maximum age = 30 yrs. Sample sizes-at-age also differed for these simulations (Table A3.1). Apart from these differences, T = 3 and T = 7 simulations were identical to T = 5 simulations (see Chapter 4). As with the T = 5 simulations, we used error contour plots (smoothed using LOESS with degree = 2 and α = 0.75) to determine the sample size and precision required for T_{MLE} to fall within +/- 0.5 yrs of the true value across levels of g. Results indicate that higher data quality (i.e., higher sample size, higher precision) is needed for T_{MLE} to fall within +/- 0.5 yrs of the true value for a given value of g when T = 3 (Fig. A3.12). Data quality requirements for T = 7 were similar to those for T = 5 (Figs. A3.13, A3.14). We expect that as $T \rightarrow 0$, data quality requirements become increasingly restrictive, likely in a nonlinear fashion. Thus, requirements for T = 5 seem to be appropriate for any scenario in which $T \geq 5$, and become increasingly conservative as T increases. Future work should more thoroughly address the data quality required for LMLP to provide accurate T_{MLE}, particularly when T < 5.

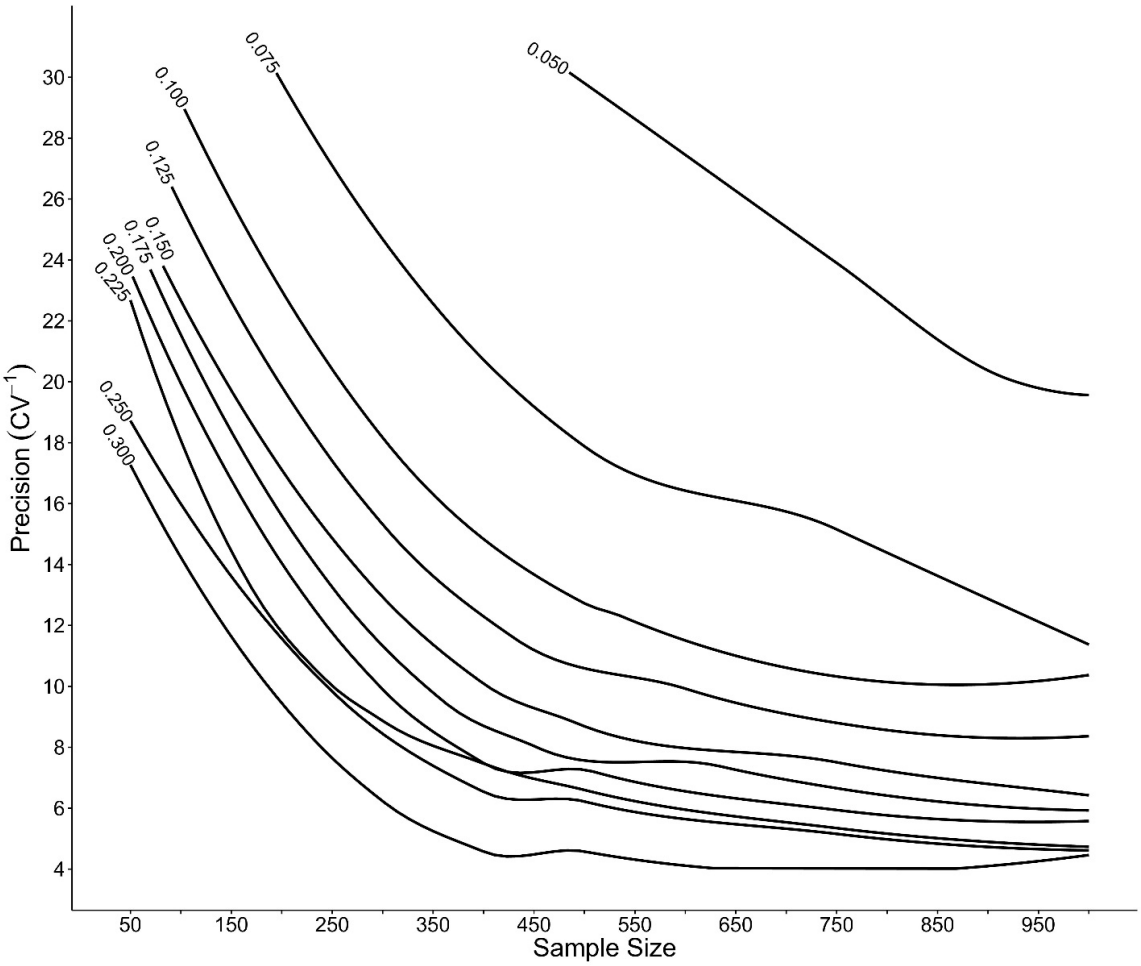

Figure A3.12 Simulated error contours for T_{MLE} to fall within +/- 0.5 yrs of T when T = 3 yrs across levels of sample size, precision, and g (labeled to the left of contours; Table A3.2), smoothed using LOESS (degree=2, α=0.75).

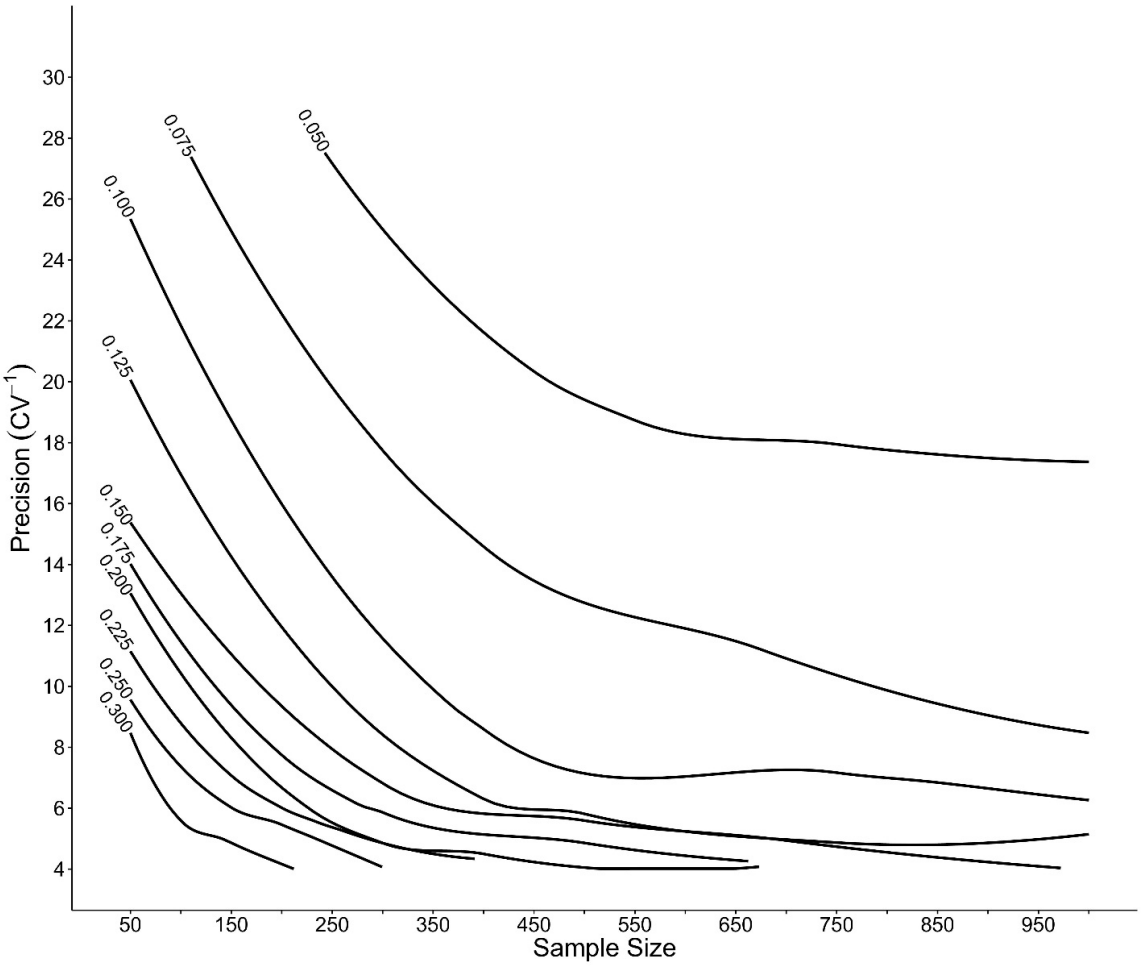

Figure A3.13 Simulated error contours for T_{MLE} to fall within +/- 0.5 yrs of T when T = 7 yrs across levels of sample size, precision, and g (labeled to the left of contours; Table A3.2), smoothed using LOESS (degree=2, α=0.75).

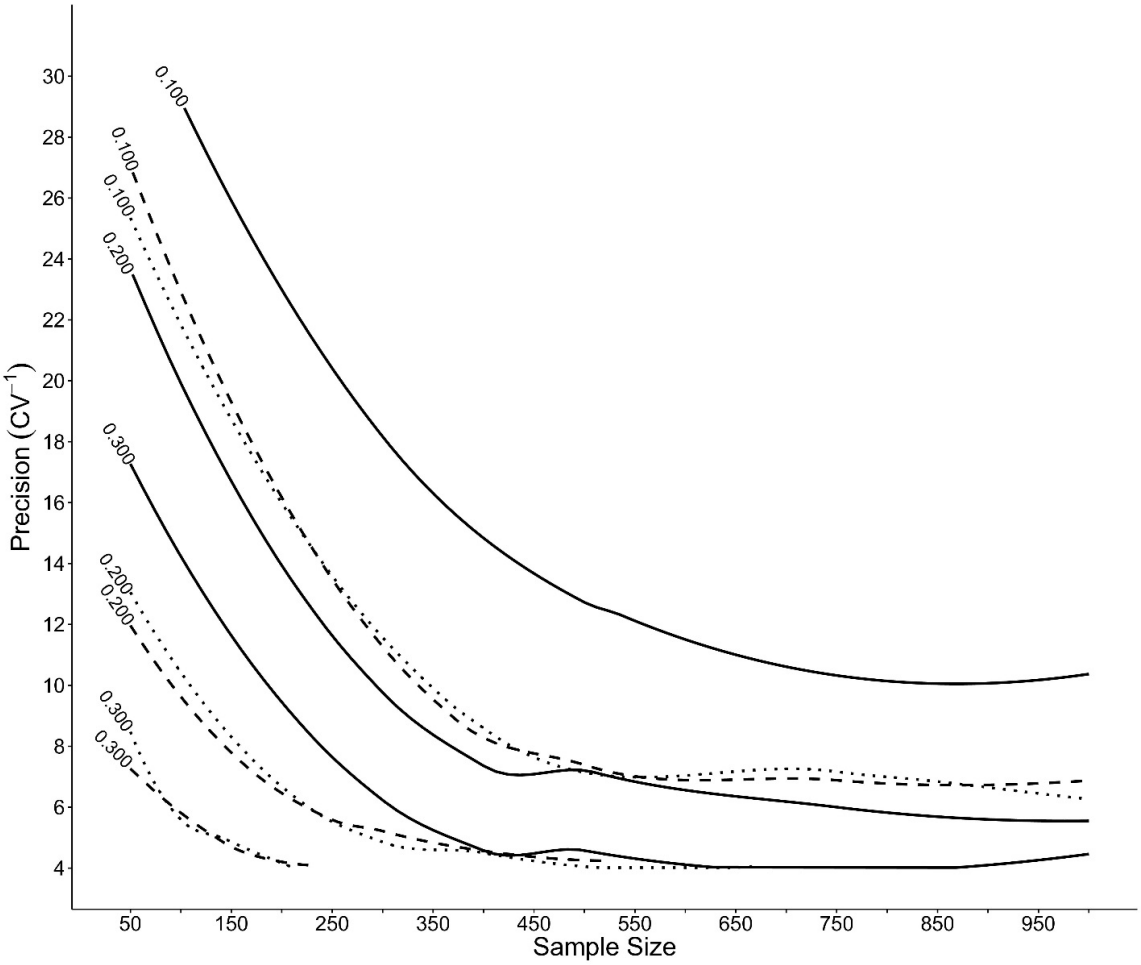

Figure A3.14 Simulated error contours for T_{MLE} to fall within +/- 0.5 yrs of T for all simulations across all levels of sample size and precision and three levels of g (labeled to the left of contours; Table A3.2), smoothed using LOESS (degree=2, α=0.75). Solid lines: T = 3 error contours; dashed lines: T = 5 error contours; dotted lines: T = 7 error contours.

Appendix 4

Additional details, methods, and results for Chapter 5

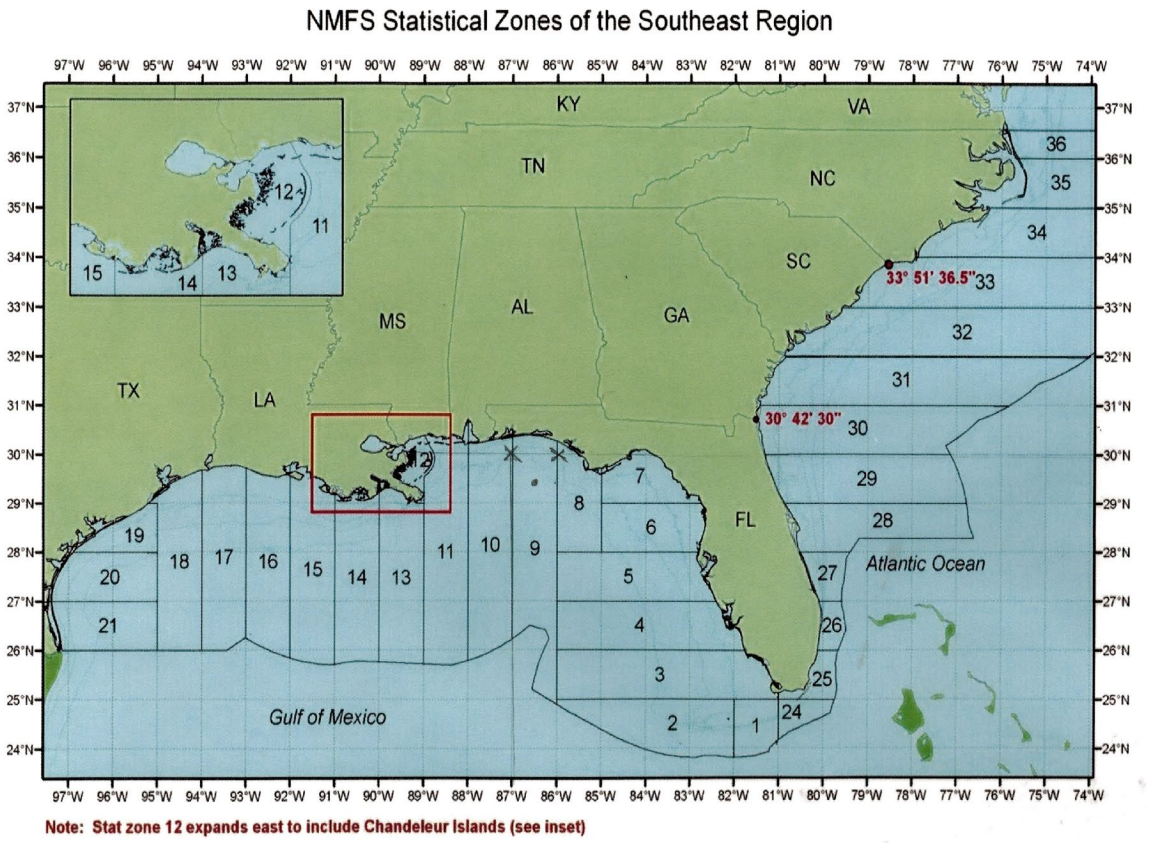

Figure A4.1 Map of the National Oceanic and Atmospheric Administration (NOAA) National Marine Fisheries Service (NMFS, now NOAA Fisheries) statistical zones in the Gulf of Mexico. Figure reproduced with the permission of Dr. Robert Allman, NOAA Southeast Fisheries Science Center, Panama City, FL, USA.

Table A4.1 Description of each Gulf of Mexico (GOM) red snapper *Lutjanus campechanus* individual included in analysis, including unique identifier (ID; corresponds with NOAA Fisheries SEDAR database), fishery type, year of capture, state landed, region in which the individual was caught (eastern GOM = grids 1-12 and western GOM = grids 13-21 in Figure A4.1), total length (TL; mm), age (yr), cohort, sex, Lester model fit quality (Fit), and mean Lester-model based estimates of age-at-maturity (T; yr), juvenile growth rate (h; mm·yr^{-1}), investment in reproduction (g; gonad mass/somatic mass), length-at-maturity (l_T; mm), asymptotic length (l_∞; mm), adult growth rate (k; yr^{-1}), and instantaneous total mortality rate (Z, calculated using eq. 1 in Chapter 5; yr^{-1}). COM = commercial fishery, FI = fisheries-independent survey, REC = recreational fishery, E = eastern GOM, W = western GOM, U = unknown, F = female, M = male, T = trustworthy, UT = untrustworthy.

ID	Fishery	Year	State	Region	TL	Age	Cohort	Sex	Fit	T	h	g	l_T	l_0	l_∞	k	Z
2000RS - 60 - 41	COM	2000	FL	W	888	59	1941	U	T	9.13	58.92	0.20	201.46	738.78	897.50	0.06	0.18
1993RS - 70 - 29	COM	1993	FL	E	890	46	1947	U	T	6.49	52.78	0.17	246.08	586.94	914.95	0.06	0.16
1993RS - 76 - 13	COM	1993	LA	W	906	46	1947	F	T	5.22	67.15	0.21	167.49	517.07	940.52	0.07	0.20
2000RS - 60 - 2	COM	2000	FL	W	889	53	1947	U	T	11.68	38.30	0.12	292.77	739.79	920.09	0.04	0.11
2000RS - 60 - 5	COM	2000	FL	W	859	52	1948	U	UT	12.52	35.58	0.12	316.54	761.44	909.98	0.04	0.10
2001RS - 19 - 9	COM	2001	LA	W	917	51	1950	U	T	8.57	55.00	0.18	345.97	816.73	938.80	0.06	0.16
2000RS - 60 - 7	COM	2000	FL	W	866	48	1950	U	T	3.41	110.37	0.38	90.29	466.18	860.61	0.12	0.39
2000RS - 60 - 35	COM	2000	FL	W	858	49	1951	U	T	4.79	63.78	0.22	171.71	474.18	864.81	0.07	0.21
2000RS - 60 - 6	COM	2000	FL	W	860	49	1951	U	T	3.93	71.75	0.25	84.46	365.95	873.54	0.08	0.23
2000RS - 263 - 3	FI	2000	TX	W	885	48	1952	F	T	6.45	75.95	0.25	227.34	716.81	915.86	0.08	0.24
2009RS - 490 - 1832	COM	2009	TX	W	898	56	1953	U	T	7.56	32.17	0.10	188.11	430.51	1002.09	0.03	0.09
2004RS - 98 - 1106	COM	2004	TX	W	863	50	1954	U	T	7.69	50.81	0.17	147.11	536.43	874.78	0.06	0.16
2000RS - 60 - 37	COM	2000	FL	W	885	46	1954	U	T	4.73	72.72	0.24	190.91	534.41	912.13	0.08	0.23
2004RS - 20 - 345	COM	2004	FL	E	853	49	1955	U	UT	3.62	79.52	0.27	149.49	435.78	883.63	0.09	0.26
2006RS - 408 - 684	COM	2006	TX	W	882	50	1956	U	T	6.88	75.51	0.26	184.99	703.30	882.62	0.08	0.25
1991RS - 74 - 22	COM	1991	LA	E	950	34	1957	U	T	8.01	71.82	0.22	274.79	849.43	984.63	0.07	0.21
2000RS - 60 - 36	COM	2000	FL	W	927	43	1957	U	T	6.35	64.96	0.21	239.22	649.48	938.28	0.07	0.19
1998RS - 1048 - 49	COM	1998	TX	W	864	40	1958	U	T	3.18	85.90	0.29	188.96	461.51	878.54	0.09	0.29
2000RS - 60 - 30	COM	2000	FL	W	896	41	1959	U	T	8.70	48.54	0.15	227.46	649.22	986.28	0.05	0.13
1991RS - 74 - 24	COM	1991	LA	E	910	31	1960	U	T	6.46	92.19	0.29	182.74	777.32	942.69	0.09	0.29
2004RS - 305 - 1	FI	2004	AL	E	898	40	1964	U	T	7.25	80.64	0.26	149.19	733.36	916.27	0.08	0.25
1980RS - 10 - 10	REC	1980	FL	E	808	15	1965	F	T	5.73	54.12	0.12	301.34	609.94	1347.73	0.04	0.11
1995RS - 119 - 9	REC	1995	AL	E	970	30	1965	F	T	7.24	56.35	0.15	206.43	613.42	1124.73	0.05	0.14
1993RS - 433 - 1	COM	1993	FL	E	883	27	1966	F	T	4.80	97.74	0.32	201.69	669.70	908.12	0.10	0.32

Table A4.1 contd.

2002RS - 308 - 173	FI	2002	AL	E	950	36	1966	F	T	6.64	87.65	0.28	207.77	790.00	952.58	0.09	0.27
2002RS - 312 - 136	FI	2002	AL	E	884	35	1967	M	T	3.85	106.98	0.35	194.19	605.03	910.55	0.11	0.36
2002RS - 308 - 185	FI	2002	AL	E	896	35	1967	U	T	7.73	59.08	0.19	195.77	651.31	926.53	0.06	0.18
1980RS - 23 - 5	REC	1980	FL	E	583	11	1969	F	T	5.97	47.42	0.18	181.85	463.62	779.71	0.06	0.17
2002RS - 312 - 143	FI	2002	AL	E	884	32	1970	M	T	4.77	97.07	0.32	209.98	671.54	908.47	0.10	0.32
2002RS - 318 - 201	FI	2002	AL	E	906	32	1970	F	T	3.56	117.56	0.38	190.43	607.60	925.57	0.12	0.39
2001RS - 162 - 5	COM	2001	FL	E	1057	30	1971	U	T	3.56	134.74	0.37	198.50	678.05	1085.32	0.12	0.38
1993RS - 455 - 57	REC	1993	AL	E	896	22	1971	F	T	6.45	62.75	0.18	260.20	664.73	1057.00	0.06	0.16
2000RS - 60 - 34	COM	2000	FL	W	842	28	1972	U	T	2.91	155.11	0.55	203.25	654.56	839.41	0.17	0.63
1995RS - 101 - 1	REC	1995	AL	E	939	23	1972	F	T	2.74	144.75	0.46	167.47	562.97	939.10	0.14	0.50
2000RS - 60 - 29	COM	2000	FL	W	836	27	1973	U	T	3.43	74.54	0.25	141.44	396.13	910.48	0.08	0.23
2000RS - 60 - 22	COM	2000	FL	W	891	27	1973	U	T	9.44	51.53	0.14	191.10	677.07	1089.64	0.05	0.13
2002RS - 114 - 17	COM	2002	FL	E	843	29	1973	U	T	4.30	56.02	0.17	132.54	372.23	1001.52	0.05	0.15
2002RS - 114 - 21	COM	2002	FL	E	805	27	1975	U	T	3.76	119.77	0.45	160.93	611.03	797.57	0.14	0.48
2008RS - 18 - 670	COM	2008	FL	W	950	33	1975	U	UT	1.52	201.00	0.72	28.56	333.83	841.36	0.21	0.94
2008RS - 18 - 674	COM	2008	FL	W	1003	33	1975	U	T	2.21	100.43	0.29	212.00	433.69	1027.20	0.09	0.29
2002RS - 312 - 147	FI	2002	AL	E	893	27	1975	U	UT	1.82	135.76	0.44	157.70	404.18	927.27	0.14	0.47
2000RS - 60 - 1	COM	2000	FL	W	842	24	1976	U	T	2.72	159.80	0.55	97.05	530.90	864.25	0.17	0.64
2001RS - 277 - 21	COM	2001	FL	E	926	24	1977	U	T	1.87	193.68	0.64	55.41	417.85	901.59	0.19	0.79
2008RS - 17 - 428	COM	2008	FL	E	834	30	1978	U	T	2.55	146.63	0.53	136.04	509.57	829.35	0.16	0.60
2000RS - 216 - 1	COM	2000	AL	E	882	21	1979	U	T	5.48	87.54	0.27	202.19	681.90	969.89	0.09	0.26
1991RS - 80 - 11	REC	1991	FL	E	810	12	1979	U	T	2.37	172.02	0.58	74.87	482.34	882.79	0.18	0.68
1993RS - 452 - 31	REC	1993	AL	E	954	14	1979	F	T	6.85	84.87	0.21	169.17	749.87	1244.10	0.07	0.19
2004RS - 199 - 2292	COM	2004	FL	W	837	24	1980	U	UT	3.01	116.40	0.41	198.88	548.83	860.49	0.13	0.42
2002RS - 313 - 164	FI	2002	AL	W	897	22	1980	F	UT	2.63	112.48	0.36	226.85	521.80	930.06	0.11	0.37
2000RS - 60 - 21	COM	2000	FL	W	798	19	1981	U	T	2.71	145.78	0.55	106.88	500.72	799.54	0.17	0.62
2000RS - 60 - 9	COM	2000	FL	W	739	19	1981	U	T	2.26	172.55	0.70	94.60	483.61	735.57	0.21	0.91
2004RS - 199 - 2291	COM	2004	FL	W	760	23	1981	U	T	2.81	90.71	0.34	129.72	383.18	808.74	0.11	0.34
1995RS - 16 - 19	COM	1995	FL	E	869	13	1982	F	T	3.13	120.17	0.35	175.40	551.14	1029.69	0.11	0.35
2000RS - 60 - 24	COM	2000	FL	W	830	17	1983	U	T	3.47	125.54	0.42	157.71	592.43	897.47	0.13	0.44
2008RS - 18 - 671	COM	2008	FL	W	874	25	1983	U	T	2.89	120.81	0.40	15.44	363.22	899.57	0.13	0.42
2002RS - 312 - 146	FI	2002	AL	E	912	19	1983	F	T	3.18	112.83	0.34	213.98	571.31	1001.26	0.11	0.34
2006RS - 41 - 545	COM	2006	FL	W	903	22	1984	U	T	7.93	63.82	0.18	228.39	733.80	1056.75	0.06	0.17
1995RS - 71 - 22	REC	1995	AL	E	884	11	1984	F	T	3.54	139.43	0.36	88.59	580.56	1165.38	0.11	0.36
2008RS - 4 - 135	COM	2008	FL	E	800	23	1985	U	T	3.06	92.06	0.34	178.85	459.66	812.23	0.11	0.34
1996RS - 47 - 28	REC	1996	FL	E	885	11	1985	F	T	4.21	135.04	0.36	93.09	660.32	1119.77	0.11	0.37

Table A4.1 contd.

2000RS - 60 - 31	COM	2000	FL	W	832	14	1986	U	T	1.91	117.46	0.44	128.55	351.82	797.61	0.14	0.47
2000RS - 60 - 33	COM	2000	FL	W	788	14	1986	U	T	4.75	101.00	0.33	159.21	637.71	905.85	0.11	0.33
2007RS - 50 - 344	COM	2007	FL	W	836	21	1986	U	UT	5.60	85.51	0.28	188.56	661.73	916.84	0.09	0.27
2009RS - 179 - 1463	COM	2009	FL	W	880	23	1986	U	T	2.75	144.56	0.49	165.59	562.93	893.95	0.15	0.53
2002RS - 313 - 163	FI	2002	AL	E	940	16	1986	F	UT	4.46	115.82	0.33	169.72	681.75	1067.86	0.10	0.32
2000RS - 60 - 13	COM	2000	FL	W	779	13	1987	U	T	2.84	118.58	0.39	180.57	514.33	903.02	0.12	0.41
2002RS - 114 - 9	COM	2002	FL	E	736	15	1987	U	T	2.14	103.43	0.29	119.20	339.48	1062.36	0.09	0.29
2006RS - 41 - 548	COM	2006	FL	W	893	19	1987	U	T	5.34	88.13	0.24	94.39	563.89	1111.61	0.08	0.23
2006RS - 41 - 546	COM	2006	FL	W	934	19	1987	U	T	5.23	79.70	0.22	247.09	663.16	1080.64	0.07	0.21
2008RS - 17 - 444	COM	2008	FL	E	844	21	1987	U	T	2.77	99.58	0.33	191.53	466.82	916.32	0.10	0.32
2009RS - 179 - 1461	COM	2009	FL	W	875	22	1987	U	T	2.10	262.40	0.90	42.21	593.55	876.81	0.26	1.43
2000RS - 60 - 10	COM	2000	FL	W	715	12	1988	U	T	2.42	138.88	0.52	132.47	467.80	797.99	0.16	0.59
2012RS - 356- 2327	COM	2012	FL	E	950	24	1988	U	T	3.50	81.96	0.23	261.35	542.54	1066.98	0.07	0.22
2003RS - 235 - 11	COM	2003	FL	E	838	14	1989	U	T	4.32	117.00	0.36	123.05	627.53	967.17	0.11	0.37
2006RS - 41 - 527	COM	2006	FL	W	874	17	1989	U	T	5.53	84.52	0.24	178.56	642.34	1068.31	0.08	0.23
2000RS - 60 - 14	COM	2000	FL	W	694	10	1990	U	T	2.47	167.25	0.67	79.79	492.17	749.84	0.20	0.84
2000RS - 60 - 26	COM	2000	FL	W	705	10	1990	U	T	1.88	127.34	0.42	98.65	337.70	921.22	0.13	0.44
2001RS - 184 - 7	COM	2001	FL	E	791	11	1990	U	T	3.66	94.55	0.26	184.87	530.56	1105.76	0.08	0.25
2001RS - 155 - 15	COM	2001	FL	E	861	11	1990	U	T	1.76	195.35	0.62	90.37	433.03	949.98	0.19	0.74
2002RS - 315 - 51	FI	2002	AL	E	886	12	1990	F	T	3.82	124.35	0.33	133.90	605.63	1115.42	0.11	0.33
2002RS - 566 - 8	FI	2002	FL	E	829	12	1990	F	T	3.12	118.56	0.33	130.32	498.29	1089.65	0.10	0.33
2001RS - 163 - 3	COM	2001	FL	E	768	10	1991	U	T	3.57	120.69	0.31	0.84	430.90	1165.18	0.10	0.31
2004RS - 224 - 3917	COM	2004	FL	E	715	13	1991	U	T	3.91	90.71	0.31	96.58	449.33	870.34	0.10	0.31
2005RS - 237 - 3702	COM	2005	FL	E	809	14	1991	U	T	3.69	127.65	0.42	2.53	473.01	903.18	0.13	0.45
2006RS - 41 - 529	COM	2006	FL	W	845	15	1991	U	T	2.41	142.29	0.47	185.25	527.15	904.52	0.15	0.51
2008RS - 17 - 446	COM	2008	FL	E	835	17	1991	U	UT	2.58	144.73	0.52	57.52	429.84	843.57	0.16	0.57
2008RS - 17 - 440	COM	2008	FL	E	817	17	1991	U	T	2.69	148.35	0.51	83.00	481.71	866.78	0.16	0.57
2000RS - 60 - 32	COM	2000	FL	W	704	8	1992	U	UT	4.20	73.68	0.12	226.39	528.98	2139.27	0.04	0.11
2003RS - 207 - 2	COM	2003	FL	E	865	11	1992	U	T	1.79	183.58	0.53	-58.51	268.38	1050.67	0.16	0.59
2006RS - 41 - 539	COM	2006	FL	W	825	14	1992	U	T	3.76	141.83	0.47	25.80	558.05	896.30	0.15	0.52
2006RS - 41 - 531	COM	2006	FL	W	800	14	1992	U	T	2.44	149.39	0.52	92.19	455.34	868.70	0.16	0.58
2008RS - 17 - 445	COM	2008	FL	E	863	16	1992	U	T	5.79	77.26	0.24	257.94	704.22	980.38	0.08	0.22
2009RS - 48 - 856	COM	2009	FL	W	849	17	1992	U	T	2.70	167.26	0.60	61.72	512.21	835.05	0.18	0.71
2015RS - 1381 - 76	FI	2015	FL	E	960	23	1992	F	T	2.04	125.00	0.37	145.05	399.79	1021.29	0.12	0.37
2004RS - 199 - 2293	COM	2004	FL	W	760	11	1993	U	T	3.41	161.73	0.58	-3.35	548.06	835.69	0.18	0.68
2006RS - 41 - 533	COM	2006	FL	W	796	13	1993	U	T	3.05	152.15	0.56	81.36	544.91	816.60	0.17	0.64

Table A4.1 contd.

2006RS - 41 - 526	COM	2006	FL	W	835	13	1993	U	T	2.55	187.76	0.63	10.09	488.33	898.41	0.19	0.76
2007RS - 50 - 337	COM	2007	FL	W	750	14	1993	U	T	2.73	129.75	0.48	143.89	496.41	807.32	0.15	0.53
2007RS - 48 - 501	COM	2007	FL	W	897	14	1993	U	T	1.98	157.65	0.48	170.77	482.32	977.73	0.15	0.53
2008RS - 18 - 672	COM	2008	FL	W	878	15	1993	U	T	2.26	166.47	0.54	67.73	443.92	930.19	0.16	0.61
2016RS - 441 - 1968	COM	2016	FL	E	874	23	1993	U	T	4.84	106.82	0.35	131.41	646.88	928.87	0.11	0.35
2002RS - 308 - 186	FI	2002	AL	E	806	9	1993	F	T	3.03	133.84	0.35	116.34	519.80	1146.09	0.11	0.36
2003RS - 235 - 8	COM	2003	FL	E	747	9	1994	U	T	2.05	154.52	0.51	111.80	427.69	913.12	0.16	0.56
2006RS - 41 - 543	COM	2006	FL	W	828	12	1994	U	T	3.98	129.19	0.42	129.48	643.42	930.15	0.13	0.44
2008RS - 116 - 1475	COM	2008	FL	E	935	14	1994	U	T	1.96	149.28	0.98	-66.41	226.02	454.89	0.28	1.80
2008RS - 17 - 435	COM	2008	FL	E	771	14	1994	U	T	2.81	164.40	0.59	55.25	515.16	837.29	0.18	0.69
2011RS - 1227 - 18	FI	2011	AL	E	911	17	1994	F	T	2.14	168.00	0.52	104.39	462.86	975.21	0.16	0.58
2006RS - 238 - 2557	COM	2006	FL	W	670	11	1995	U	T	2.45	97.58	0.37	180.29	417.86	800.08	0.12	0.37
2007RS - 50 - 334	COM	2007	FL	W	798	12	1995	U	T	2.91	124.83	0.39	142.67	504.80	963.06	0.12	0.40
2008RS - 17 - 427	COM	2008	FL	E	789	13	1995	U	T	2.03	206.09	0.72	-76.10	341.85	854.32	0.22	0.95
2008RS - 17 - 432	COM	2008	FL	E	868	13	1995	U	T	2.48	131.16	0.38	172.20	496.75	1025.24	0.12	0.39
2008RS - 17 - 438	COM	2008	FL	E	820	13	1995	U	T	3.04	107.57	0.33	208.09	534.33	980.51	0.10	0.33
2009RS - 43 - 620	COM	2009	FL	E	766	14	1995	U	UT	2.10	79.73	0.22	164.11	329.76	1090.28	0.07	0.21
2006RS - 41 - 535	COM	2006	FL	W	891	10	1996	U	T	2.27	111.85	0.24	246.92	498.79	1397.99	0.08	0.23
2006RS - 238 - 2572	COM	2006	FL	W	728	10	1996	U	T	1.91	153.77	0.55	67.51	359.98	839.44	0.17	0.63
2007RS - 49 - 356	COM	2007	FL	W	626	11	1996	U	T	3.08	120.63	0.51	114.34	484.18	713.80	0.16	0.56
2007RS - 50 - 329	COM	2007	FL	W	833	11	1996	U	T	2.41	211.01	0.72	60.83	569.59	879.53	0.22	0.94
2008RS - 4 - 129	COM	2008	FL	E	692	12	1996	U	T	5.19	83.67	0.32	141.42	574.98	793.86	0.10	0.31
2008RS - 180 - 1738	COM	2008	FL	E	659	12	1996	U	T	2.42	121.31	0.49	121.93	415.04	739.43	0.15	0.54
2008RS - 180 - 1764	COM	2008	FL	E	650	12	1996	U	T	3.27	92.46	0.37	164.94	466.39	758.72	0.12	0.37
2007RS - 56 - 423	COM	2007	FL	W	869	11	1996	U	T	1.73	146.58	0.40	123.02	375.61	1110.67	0.12	0.41
2006RS - 238 - 2578	COM	2006	FL	W	561	10	1996	U	T	1.89	161.70	0.81	-72.08	233.50	596.59	0.24	1.18
2010RS - 300 - 25	FI	2010	AL	E	874	14	1996	F	T	5.41	76.07	0.20	247.74	658.05	1171.08	0.06	0.18
2014RS - 1283 - 52	FI	2014	FL	E	912	18	1996	F	UT	1.30	218.46	0.77	17.40	301.39	853.56	0.23	1.06
2005RS - 8 - 920	COM	2005	FL	E	543	8	1997	U	T	4.48	66.04	0.23	155.78	451.10	891.75	0.07	0.21
2007RS - 406 - 3	REC	2007	FL	E	529	10	1997	F	T	2.09	175.70	0.98	-7.14	360.54	539.69	0.28	1.76
2013RS - 1023 - 18	REC	2013	FL	E	836	16	1997	F	UT	1.72	157.19	0.56	126.64	395.87	846.87	0.17	0.64
2008RS - 17 - 437	COM	2008	FL	E	835	10	1998	U	T	1.90	132.81	0.32	107.02	358.87	1266.12	0.10	0.31
2008RS - 117 - 1538	COM	2008	FL	W	724	10	1998	U	T	1.95	174.26	0.62	22.49	361.96	850.72	0.19	0.74
2009RS - 48 - 857	COM	2009	FL	W	642	11	1998	U	T	4.15	86.08	0.31	128.56	484.39	825.43	0.10	0.31
2009RS - 253 - 2270	COM	2009	FL	W	691	10	1999	U	T	2.13	162.72	0.59	28.09	373.70	821.72	0.18	0.70
2011RS - 1050 - 23	FI	2011	AL	E	791	12	1999	F	T	3.37	95.70	0.28	240.80	562.29	1033.52	0.09	0.27

Table A4.1 contd.

2014RS - 1118 - 4	REC	2014	AL	E	930	15	1999	F	T	3.80	92.94	0.21	196.47	546.37	1309.67	0.07	0.20
2007RS - 82 - 1879	COM	2007	FL	W	625	7	2000	U	UT	1.86	108.34	0.25	92.04	290.62	1356.58	0.08	0.23
2010RS - 130 - 968	COM	2010	FL	E	776	10	2000	U	T	3.41	87.08	0.23	271.22	566.79	1156.94	0.07	0.21
2013RS - 1248 - 6	REC	2013	AL	E	801	13	2000	F	UT	2.45	107.81	0.32	124.76	387.03	1024.56	0.10	0.31
2013RS - 1016 - 12	REC	2013	FL	E	681	13	2000	F	T	2.10	84.54	0.30	191.07	367.48	855.08	0.09	0.29
2016RS -482 - 5514	COM	2016	AL	E	761	15	2001	U	T	2.40	99.03	0.33	167.63	403.24	891.84	0.11	0.33
2011RS - 1040 - 17	FI	2011	FL	E	445	10	2001	F	T	2.34	136.53	0.90	54.21	373.97	455.26	0.26	1.44
2011RS - 1310 - 6	FI	2011	FL	E	617	10	2001	F	T	2.20	133.16	0.60	163.57	456.69	665.48	0.18	0.71
2012RS - 1017 - 1	FI	2012	FL	E	535	11	2001	F	UT	2.49	76.58	0.35	213.88	399.88	654.40	0.11	0.36
2014RS - 1285 - 96	FI	2014	AL	E	812	13	2001	F	UT	7.63	55.23	0.16	328.39	749.39	1011.61	0.05	0.15
2012RS - 1121 - 1	FI	2012	FL	E	722	10	2002	F	UT	2.12	68.32	0.13	202.71	344.70	1659.05	0.04	0.12
2013RS - 1257 - 43	REC	2013	FL	E	604	11	2002	F	T	1.80	108.59	0.48	125.59	320.61	679.63	0.15	0.52
2014RS - 1041 - 7	REC	2014	AL	E	757	12	2002	F	T	1.90	122.56	0.42	165.41	397.46	873.07	0.13	0.44
2014RS - 1045 - 58	REC	2014	AL	E	741	11	2002	F	T	2.03	169.44	0.65	39.22	381.96	778.59	0.20	0.81
2013RS - 1014 - 10	REC	2013	FL	E	870	12	2002	F	T	2.06	203.87	0.63	65.79	485.87	976.32	0.19	0.76
2014RS - 1123 - 25	REC	2014	FL	E	585	13	2002	F	T	2.77	108.61	0.49	48.15	347.70	667.17	0.15	0.54
2015RS - 1378 - 28	FI	2015	AL	E	852	12	2003	F	T	5.61	90.17	0.26	227.28	732.83	1028.31	0.08	0.25
2016RS - 4134 - 297	FI	2016	AL	E	821	13	2003	F	T	7.28	67.97	0.19	198.65	692.90	1100.34	0.06	0.17
2016RS - 4163 - 65	FI	2016	FL	E	900	13	2003	F	T	3.60	119.37	0.31	126.29	554.79	1167.59	0.10	0.30
2013RS - 1012 - 19	REC	2013	FL	E	589	10	2003	F	T	3.16	83.41	0.32	128.76	390.93	776.57	0.10	0.32
2014RS - 1127 - 31	REC	2014	FL	E	730	11	2003	F	T	2.06	157.33	0.59	105.19	428.37	796.97	0.18	0.70
2015RS - 1165 - 3	REC	2015	FL	E	658	12	2003	F	T	2.78	114.85	0.48	148.88	467.22	721.33	0.15	0.52
2015RS - 1006 - 3	REC	2015	FL	E	855	12	2003	F	UT	1.67	85.12	0.17	275.57	413.31	1526.01	0.06	0.16
2016RS - 1011 - 35	REC	2016	AL	E	847	13	2003	F	T	3.51	115.36	0.34	189.83	593.90	1004.81	0.11	0.35
2016RS - 1011 - 42	REC	2016	AL	E	890	13	2003	F	T	5.12	110.61	0.31	131.16	696.04	1078.63	0.10	0.30
2016RS - 4134 - 293	FI	2016	AL	E	806	12	2004	F	T	3.92	91.92	0.26	224.54	583.19	1047.87	0.08	0.25
2014RS - 1074 - 3	REC	2014	AL	E	844	10	2004	F	T	2.43	147.57	0.42	194.87	552.52	1055.11	0.13	0.44
2014RS - 1274 - 5	REC	2014	FL	E	596	10	2004	F	T	2.10	196.17	0.97	10.44	422.24	607.16	0.28	1.73
2015RS - 1142 - 8	REC	2015	AL	E	658	11	2004	F	T	2.37	123.98	0.50	123.75	416.90	749.67	0.15	0.55
2015RS - 1162 - 10	REC	2015	FL	E	610	11	2004	F	T	2.87	110.73	0.49	159.54	476.69	683.13	0.15	0.53
2016RS - 1030 - 13	REC	2016	FL	E	655	12	2004	F	T	2.79	77.69	0.26	198.60	413.47	898.05	0.08	0.25
2015RS - 1329 - 7	REC	2015	AL	E	885	11	2004	F	T	5.07	96.90	0.26	266.21	756.03	1108.86	0.08	0.25
2016RS - 4129 - 349	FI	2016	AL	E	841	11	2005	F	T	2.08	187.16	0.60	53.84	443.45	929.03	0.18	0.72
2015RS - 1261 - 636	REC	2015	FL	E	451	10	2005	F	T	2.10	139.09	0.88	45.74	337.88	474.40	0.26	1.38

A4.1 Stan model code for fitting the Lester biphasic growth model

```
// Stan model code for fitting the Lester biphasic growth model
// in a fixed-effects framework.
// Author: Andrew E. Honsey, University of Minnesota
// This code should be saved as a '.stan' file.
// See mc-stan.org for documentation.

// define data
data {
  int<lower=0> N; // number of data points
  int<lower=0> Nages; // number of unique ages
  vector<lower=0>[Nages] uniqueages; // vector of unique age values
  int<lower=0> ageindex[N]; // age index (first age, second age, etc.)
  vector<lower=0>[N] length; // length data
  real hest; // h estimate from a priori linear model fit to first few length-at-age data pts
  real l0est; // l0 estimate from a priori linear model fit to first few length-at-age data pts
}

// define parameters to be estimated
parameters{
  real<lower=0,upper=max(age)> Tmat; // age-at-maturity
  real<lower=0> h; // juvenile growth rate (slope of linear phase)
```

```
  real l0; // juvenile growth intercept
  real<lower=0,upper=1> g; // cost to somatic growth of maturity
  real<lower=0> phi; // "slope" of standard deviation (scaled with length)
  real<lower=0> psi; // power of standard deviation (scaled with length)
}

// define additional model parameters and relationships
transformed parameters {
  real t1; // juvenile age at length 0
  real<lower=0> Linf; // asymptotic length
  real k; // adult growth rate
  real t0; // adult age at length 0

  // relationships between parameters assumed by Lester model
  t1 = -l0/h;
  Linf = 3*h/g;
  k = log(1+g/3);
  t0 = Tmat + (log(1-(g*(Tmat-t1)/3)))/log(1+g/3);
}

model {
  // define vectors for loops below
```

```
  vector[Nages] juv;
  vector[Nages] adult;
  vector[Nages] pred;
  vector[Nages] sigma;

  // modify priors for some parameters
  g ~ uniform(0,(3/(Tmat-t1))); // analytical bounds for g
  h ~ normal(hest,7.5); // prior for h -- variance can be adjusted
  l0 ~ normal(l0est,15); // prior for l0 -- variance can be adjusted

  for (i in 1:Nages) {
  // growth functions
  juv[i] = l0 + h*uniqueages[i];
  adult[i] = Linf*(1-exp(-k*(uniqueages[i]-t0)));

  // if/then statement to estimate age-at-maturity
  pred[i] = uniqueages[i] <= Tmat? juv[i] : adult[i];

  // variance parameter (scales with age)
  sigma[i] = phi*pow(pred[i],psi);
}
```

```
  for (i in 1:N) {
  // assume that lengths are distributed normally around Lester model predictions
  length[i] ~ normal(pred[ageindex[i]],sigma[ageindex[i]]);
}
}
```

A4.2 Stan model code for fitting a hierarchical model of the mean

```
// Stan model code for fitting a hierarchical model of the mean.
// Author: Andrew E. Honsey, University of Minnesota.
// This code should be saved as a '.stan' file.
// See mc-stan.org for documentation.

// define data
data {
  int<lower=0> N; // number of data points
  int<lower=0> N_ind; // number of individuals
  int<lower=1, upper=N_ind> ID[N]; // individual ID
  vector[N] points; // data points
}

// define parameters
parameters {
  vector[N_ind] mu_ind; // individual-level means
  real<lower=0> mu_global; // group-level aka global mean
  real<lower=0> sigma_mu_global; // variance for global mean
  vector[N_ind] sigma_mu_ind; // variance for individual means
}
```

```
// model likelihoods
model {

  // individual means are assumed to be distributed normally around the global mean
  for (i in 1:N_ind){
    mu_ind[i] ~ normal(mu_global,sigma_mu_global);
}

  // data for each individual is assumed to be distributed normally around the individual
means
  for (i in 1:N){
    points[i] ~ normal(mu_ind[ID[i]],sigma_mu_ind[ID[i]]);
   }
}
```

A4.3 Comparing life history traits among red snapper *Lutjanus campechanus* individuals from the eastern versus western Gulf of Mexico

We conducted an analysis to determine whether our Lester model-based life history trait estimates significantly differed among red snapper *Lutjanus campechanus* individuals captured in the eastern (grids 1-12 in Figure A4.1) versus western (grids 13-21 in Figure A4.1) Gulf of Mexico. To do this, we used an approach similar to that used to estimate mean life history trait values at the cohort group-level (described in Chapter 5). Briefly, we extracted draws from the posterior probability distributions for each individual-level Lester model fit. We effectively treated these draws as data in hierarchical Bayesian models of the mean that were fit separately to individuals from each region (see Table A4.1) within each cohort group. For each fit, we ran four Hamiltonian Monte Carlo chains for 5000 iterations each (2000 warmup, 3000 sampling). We did not find evidence for any significant differences in life history traits among eastern versus western individuals across cohort groups; that is, the 95% credible intervals overlapped for all comparisons of life history traits among eastern versus western individuals within cohort groups (Fig. A4.2-A4.8).

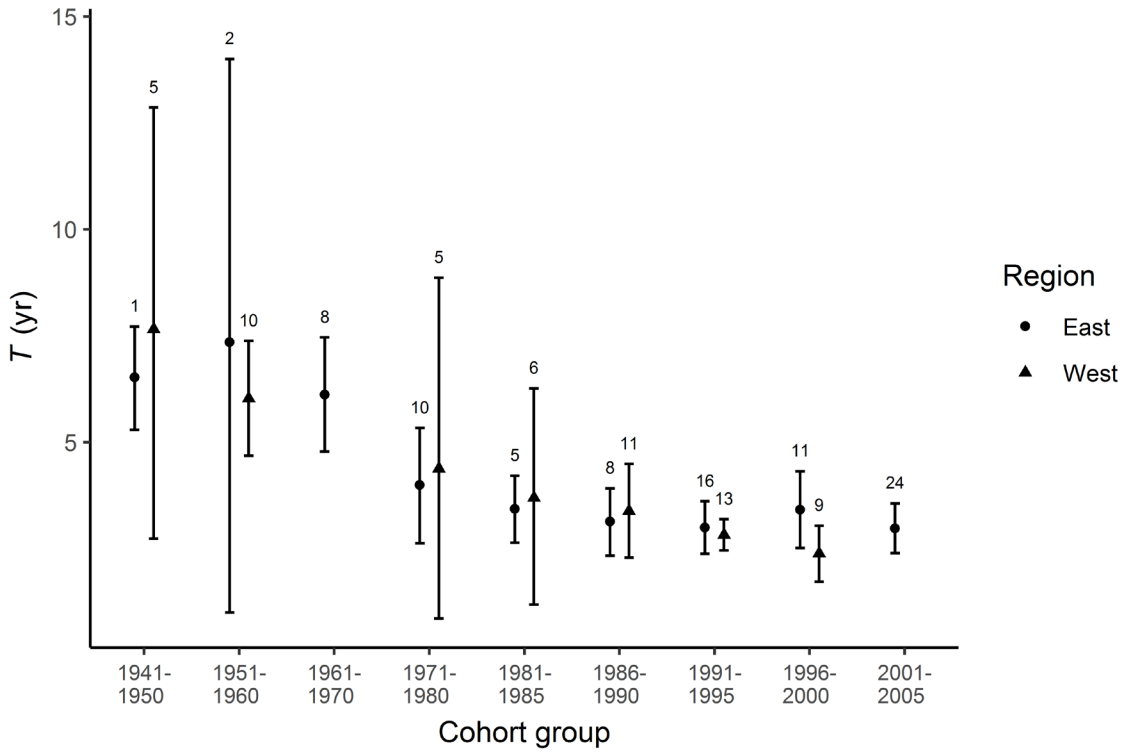

Figure A4.2 Mean cohort group-level estimates of age-at-maturity (*T*; yr) generated from Lester model fits to back-calculated red snapper *Lutjanus campechanus* growth data for individuals from the eastern (circles) versus western (triangles) Gulf of Mexico across cohorts from 1941-2005. Points represent mean estimates of age-at-maturity for each cohort group within each region, and error bars indicate 95% Bayesian credible intervals. Sample sizes for each group are displayed above the error bars. When sample size = 1, error bars represent 95% Bayesian credible intervals around the parameter estimate for that individual.

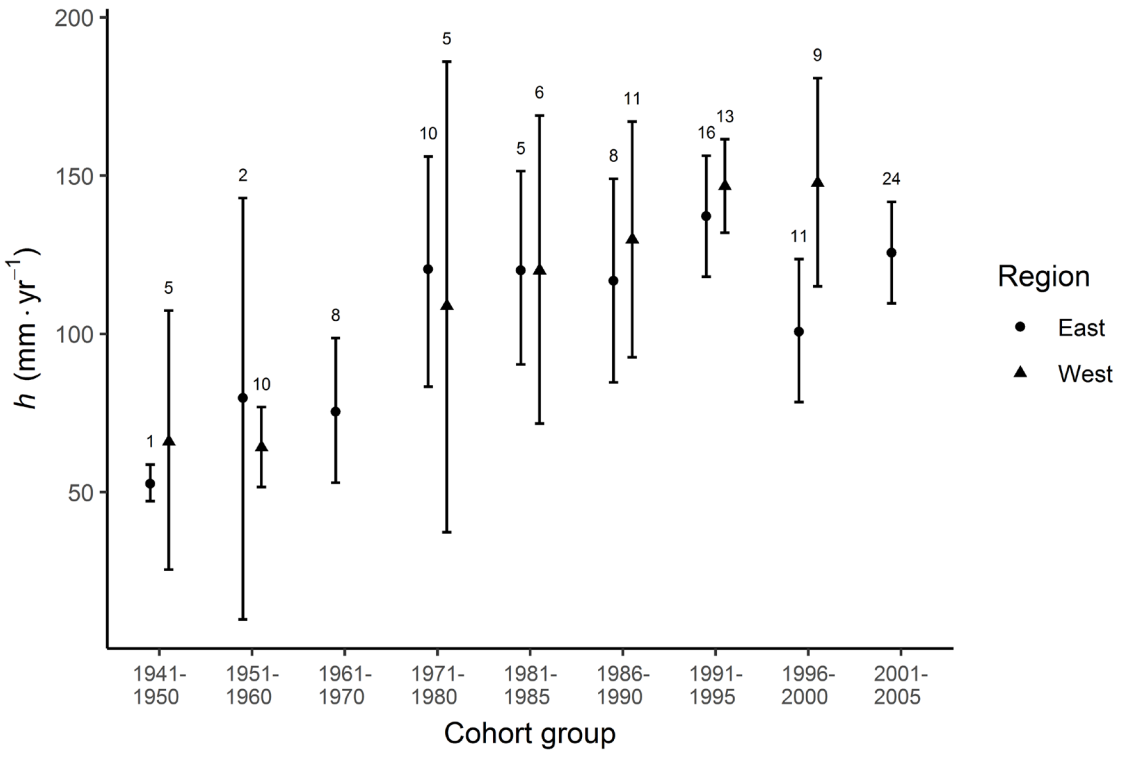

Figure A4.3 Mean cohort group-level estimates of juvenile growth rate (h; mm·yr^{-1}) generated from Lester model fits to back-calculated red snapper *Lutjanus campechanus* growth data for individuals from the eastern (circles) versus western (triangles) Gulf of Mexico across cohorts from 1941-2005. Points represent mean estimates of juvenile growth rate for each cohort group within each region, and error bars indicate 95% Bayesian credible intervals. Sample sizes for each group are displayed above the error bars. When sample size = 1, error bars represent 95% Bayesian credible intervals around the parameter estimate for that individual.

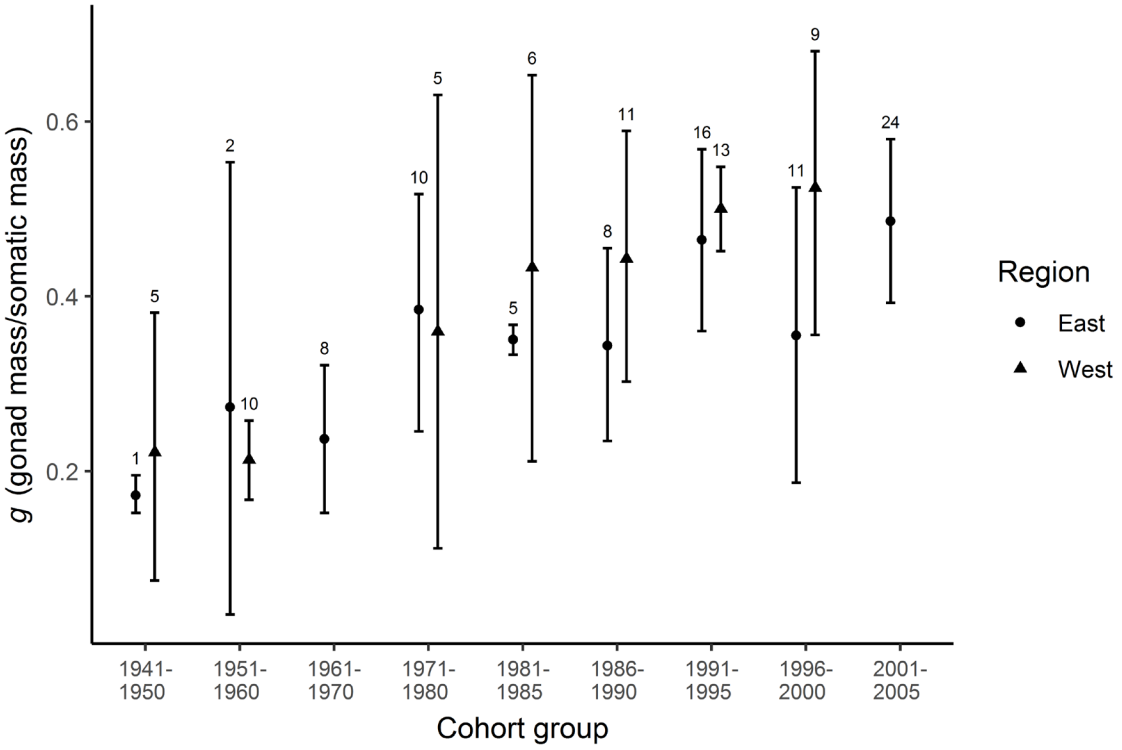

Figure A4.4 Mean cohort group-level estimates of the cost to somatic growth of maturity (*g*; gonad mass/somatic mass) generated from Lester model fits to back-calculated red snapper *Lutjanus campechanus* growth data for individuals from the eastern (circles) versus western (triangles) Gulf of Mexico across cohorts from 1941-2005. Points represent mean estimates of *g* for each cohort group within each region, and error bars indicate 95% Bayesian credible intervals. Sample sizes for each group are displayed above the error bars. When sample size = 1, error bars represent 95% Bayesian credible intervals around the parameter estimate for that individual.

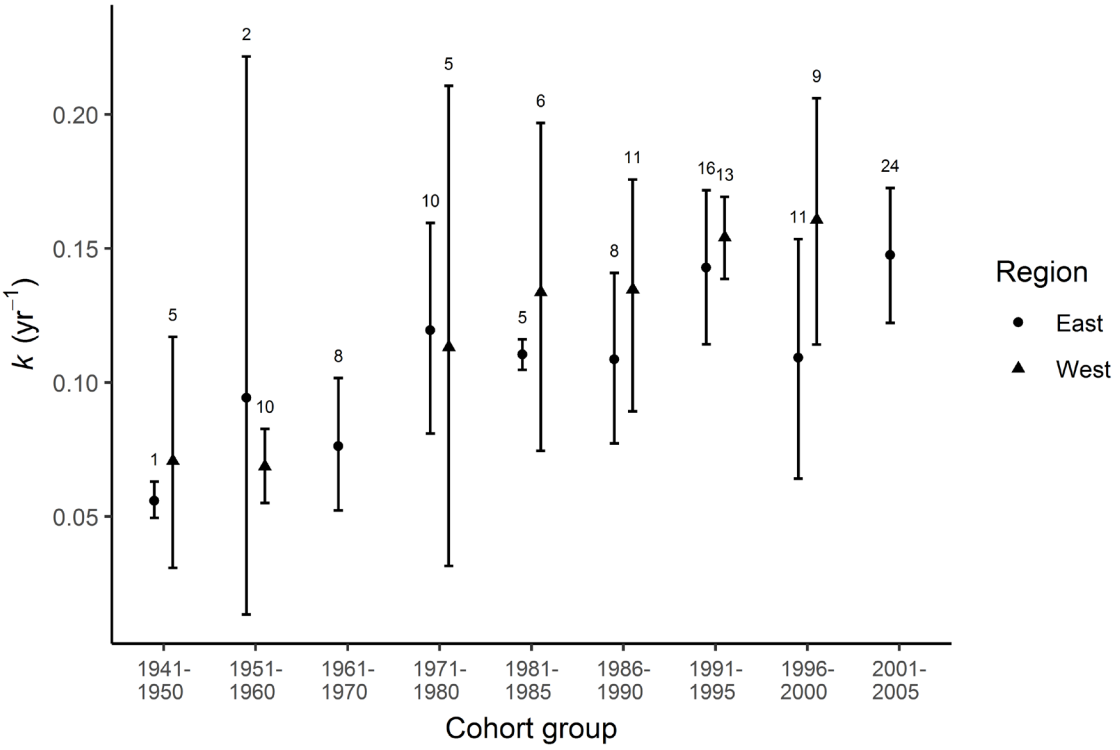

Figure A4.5 Mean cohort group-level estimates of adult growth rate (k; yr^{-1}) generated from Lester model fits to back-calculated red snapper *Lutjanus campechanus* growth data for individuals from the eastern (circles) versus western (triangles) Gulf of Mexico across cohorts from 1941-2005. Points represent mean estimates of k for each cohort group within each region, and error bars indicate 95% Bayesian credible intervals. Sample sizes for each group are displayed above the error bars. When sample size = 1, error bars represent 95% Bayesian credible intervals around the parameter estimate for that individual.

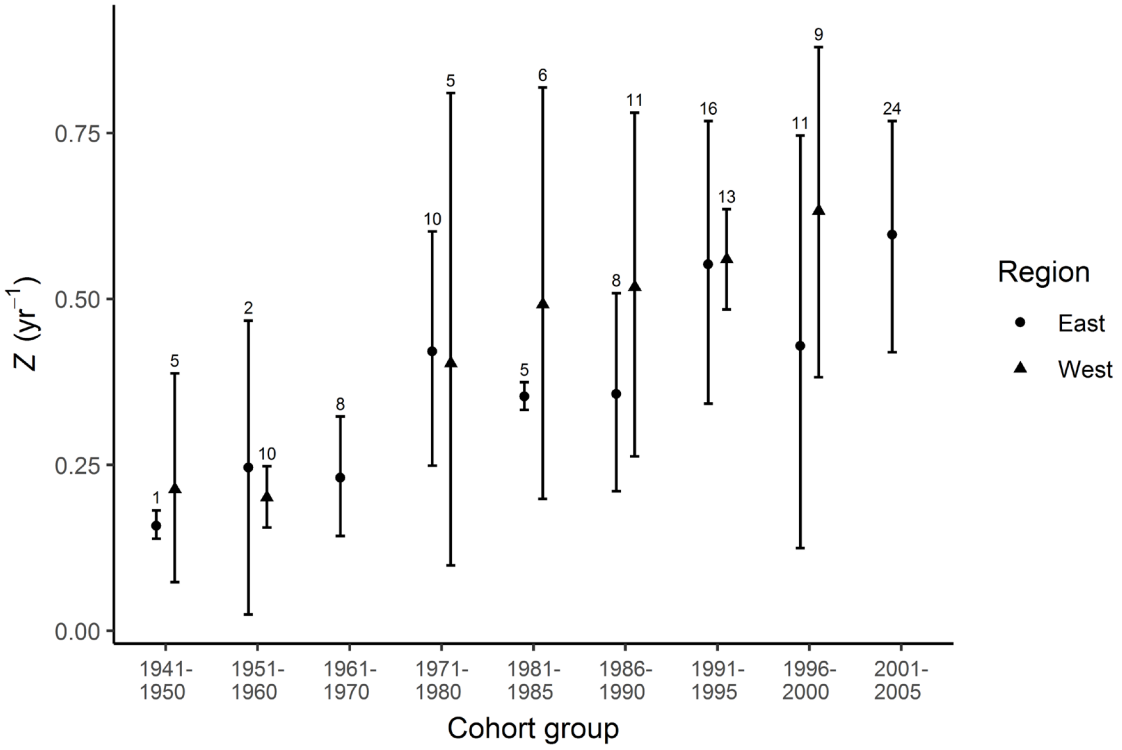

Figure A4.6 Mean cohort group-level estimates of mortality rate (Z, yr^{-1}; generated using eq. 1 in Chapter 5) from Lester model fits to back-calculated red snapper *Lutjanus campechanus* growth data for individuals from the eastern (circles) versus western (triangles) Gulf of Mexico across cohorts from 1941-2005. Points represent mean estimates of mortality rate for each cohort group within each region, and error bars indicate 95% Bayesian credible intervals. Sample sizes for each group are displayed above the error bars. When sample size = 1, error bars represent 95% Bayesian credible intervals around the parameter estimate for that individual.

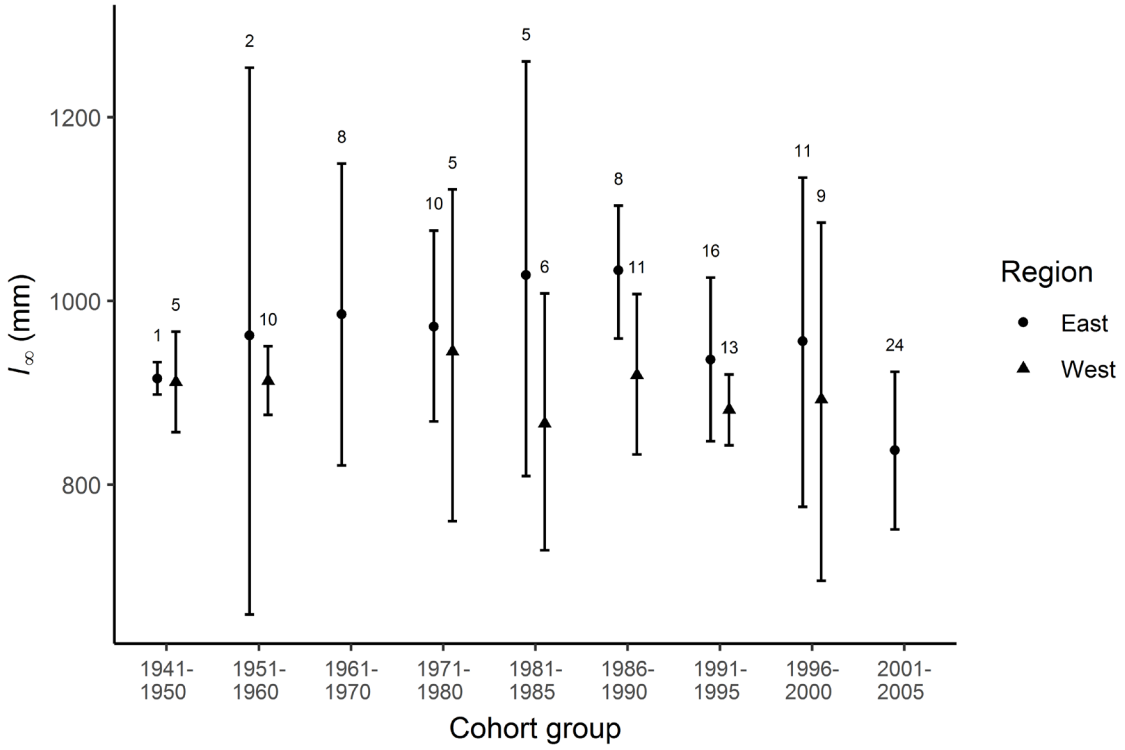

Figure A4.7 Mean cohort group-level estimates of asymptotic length (l_∞; mm) generated from Lester model fits to back-calculated red snapper *Lutjanus campechanus* growth data for individuals from the eastern (circles) versus western (triangles) Gulf of Mexico across cohorts from 1941-2005. Points represent mean estimates of asymptotic length for each cohort group within each region, and error bars indicate 95% Bayesian credible intervals. Sample sizes for each group are displayed above the error bars. When sample size = 1, error bars represent 95% Bayesian credible intervals around the parameter estimate for that individual.

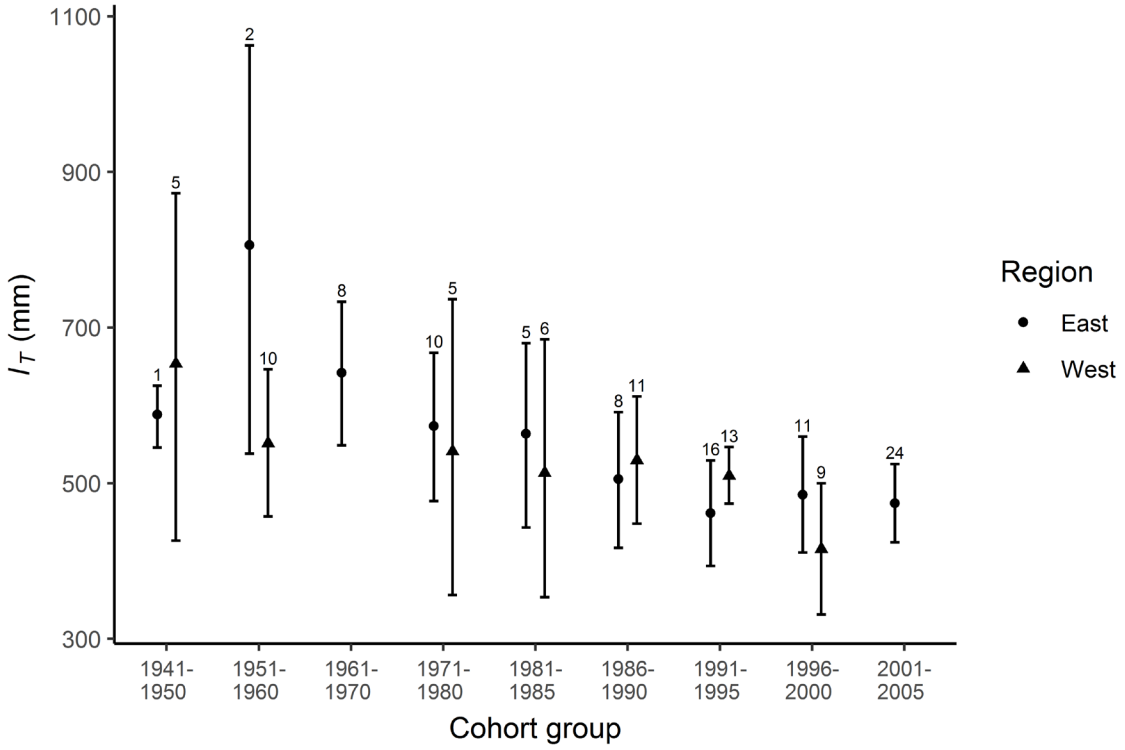

Figure A4.8 Mean cohort group-level estimates of length-at-maturity (l_T; mm) generated from Lester model fits to back-calculated red snapper *Lutjanus campechanus* growth data for individuals from the eastern (circles) versus western (triangles) Gulf of Mexico across cohorts from 1941-2005. Points represent mean estimates of length-at-maturity for each cohort group within each region, and error bars indicate 95% Bayesian credible intervals. Sample sizes for each group are displayed above the error bars. When sample size = 1, error bars represent 95% Bayesian credible intervals around the parameter estimate for that individual.

A4.4 Results of analyses including poor fits and males

For our analyses in Chapter 5, we excluded parameter estimates from Lester model fits to individual red snapper *Lutjanus campechanus* that we considered to be untrustworthy due to a lack of convergence and/or poor fits to the data (see Fig. 5.1c,d). These untrustworthy fits sometimes produced unrealistic parameter estimates (e.g., an asymptotic length of > 2000 mm for one individual, which is more than double the mean value; see Table A4.1) that could have skewed our results. However, results including these untrustworthy fits were qualitatively similar to those presented in Chapter 5 (Fig. A4.9-A4.15).

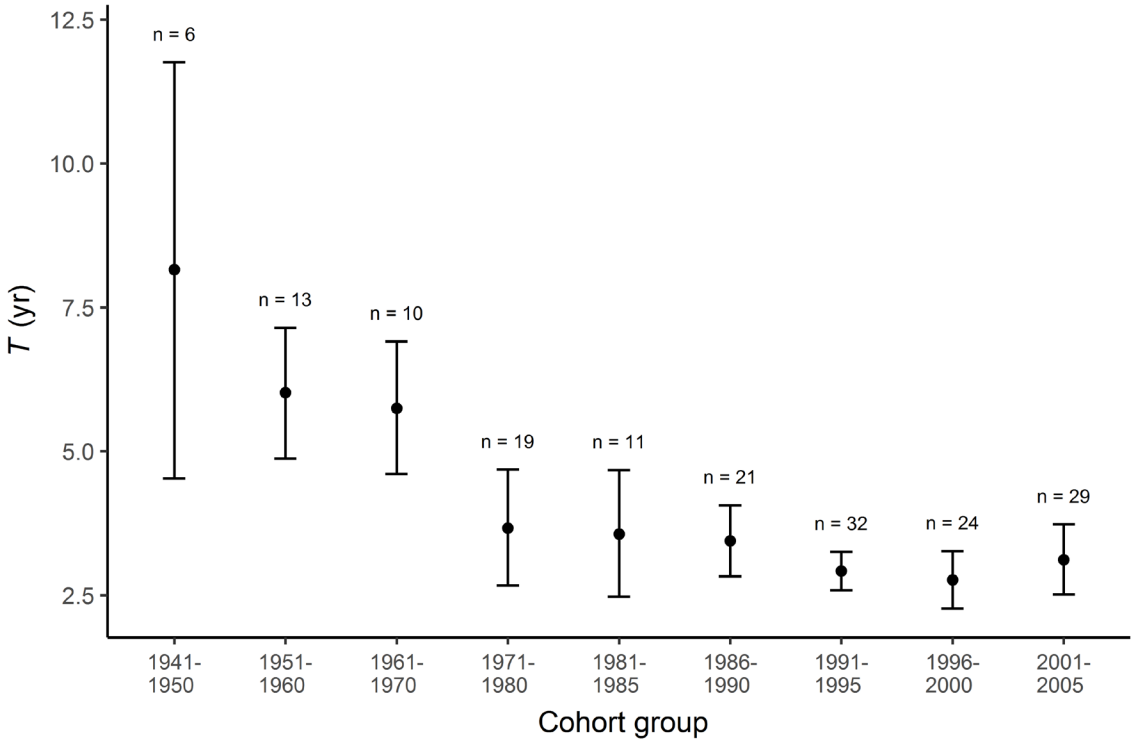

Figure A4.9 Mean cohort group-level estimates of age-at-maturity (*T*; yr) generated from both trustworthy and untrustworthy Lester model fits to back-calculated Gulf of Mexico red snapper *Lutjanus campechanus* growth data for cohorts from 1941-2005. Points represent mean estimates of age-at-maturity for each cohort group, and error bars indicate 95% Bayesian credible intervals. Sample sizes for each group are displayed above the error bars.

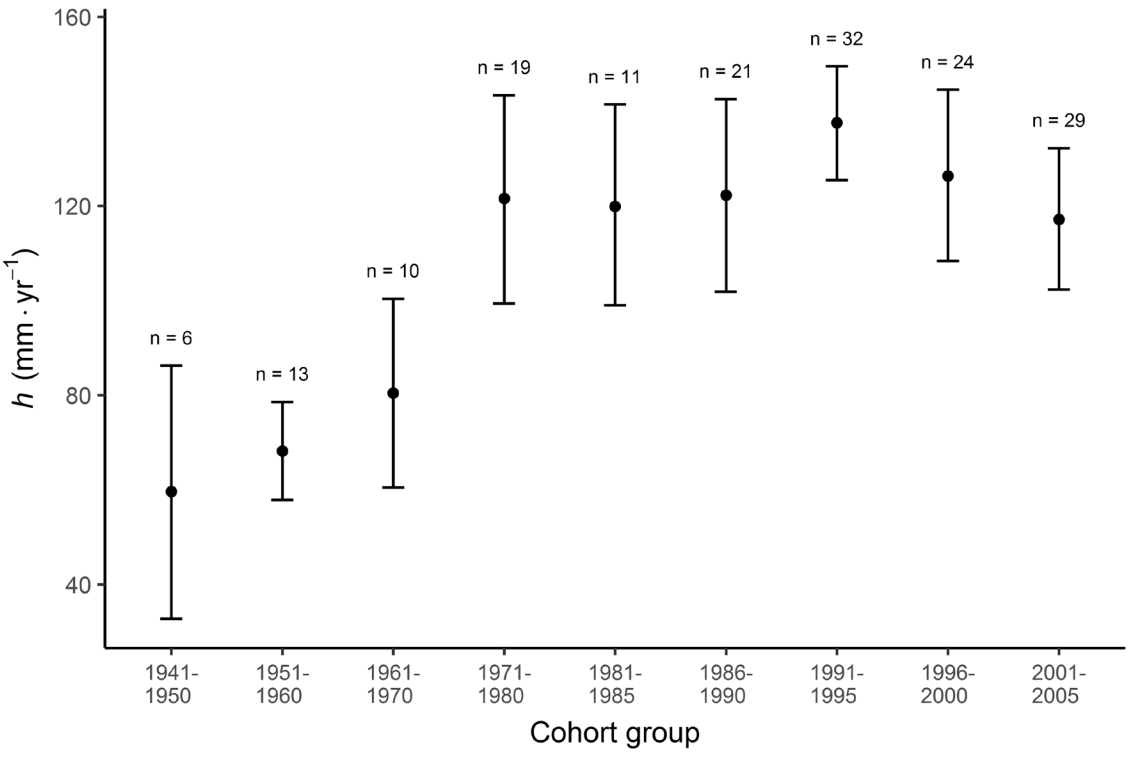

Figure A4.10 Mean cohort group-level estimates of juvenile growth rate (h; mm·yr^{-1}) generated from both trustworthy and untrustworthy Lester model fits to back-calculated Gulf of Mexico red snapper *Lutjanus campechanus* growth data for cohorts from 1941-2005. Points represent mean estimates of juvenile growth rate for each cohort group, and error bars indicate 95% Bayesian credible intervals. Sample sizes for each group are displayed above the error bars.

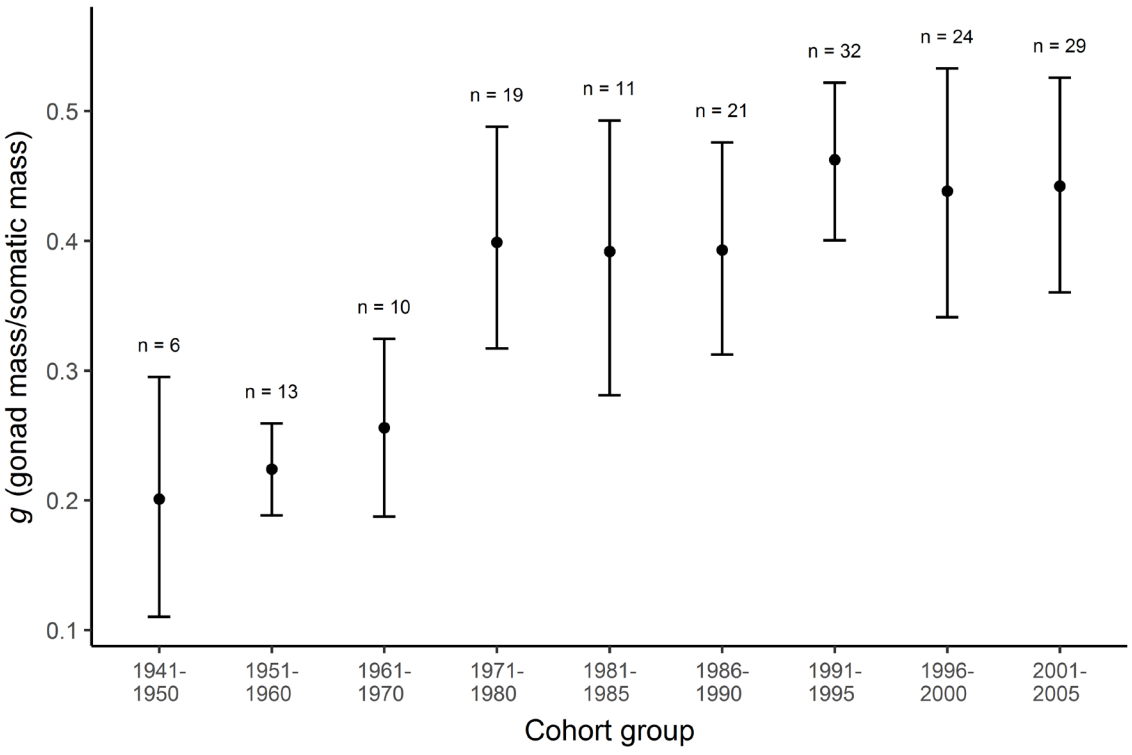

Figure A4.11 Mean cohort group-level estimates of the cost to somatic growth of maturity (g; gonad mass/somatic mass) generated from both trustworthy and untrustworthy Lester model fits to back-calculated Gulf of Mexico red snapper *Lutjanus campechanus* growth data for cohorts from 1941-2005. Points represent mean estimates of g for each cohort group, and error bars indicate 95% Bayesian credible intervals. Sample sizes for each group are displayed above the error bars.

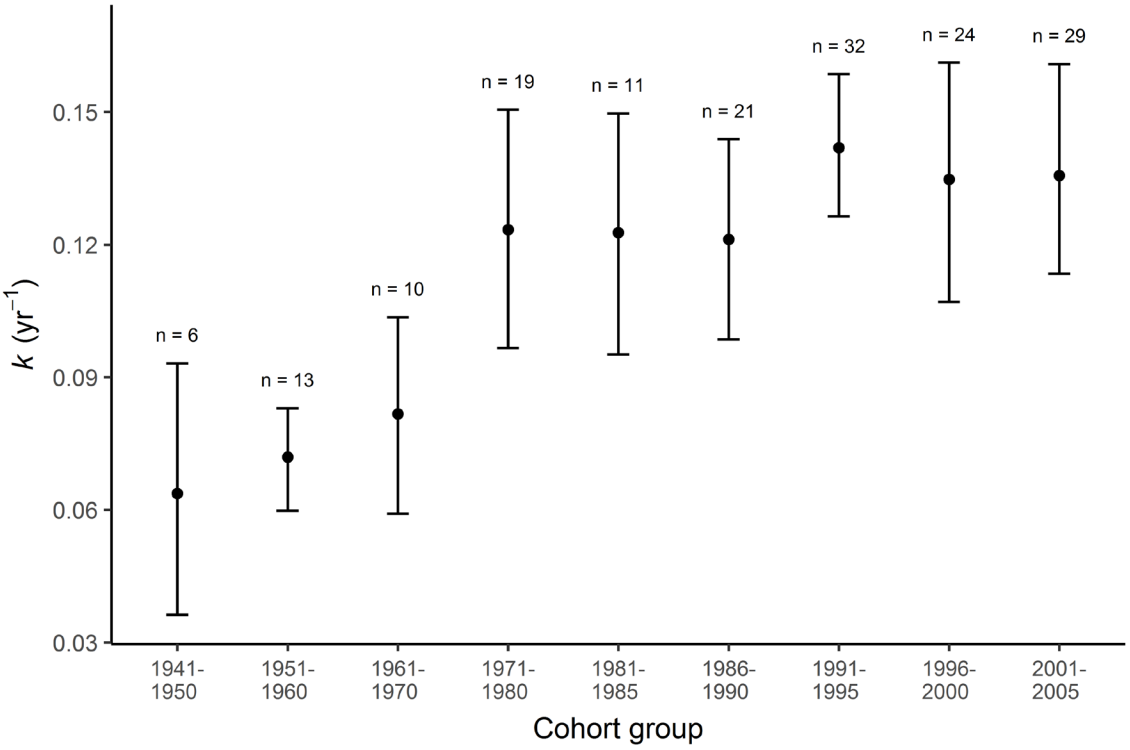

Figure A4.12 Mean cohort group-level estimates of adult growth rate (k; yr^{-1}) generated from both trustworthy and untrustworthy Lester model fits to back-calculated Gulf of Mexico red snapper *Lutjanus campechanus* growth data for cohorts from 1941-2005. Points represent mean estimates of k for each cohort group, and error bars indicate 95% Bayesian credible intervals. Sample sizes for each group are displayed above the error bars.

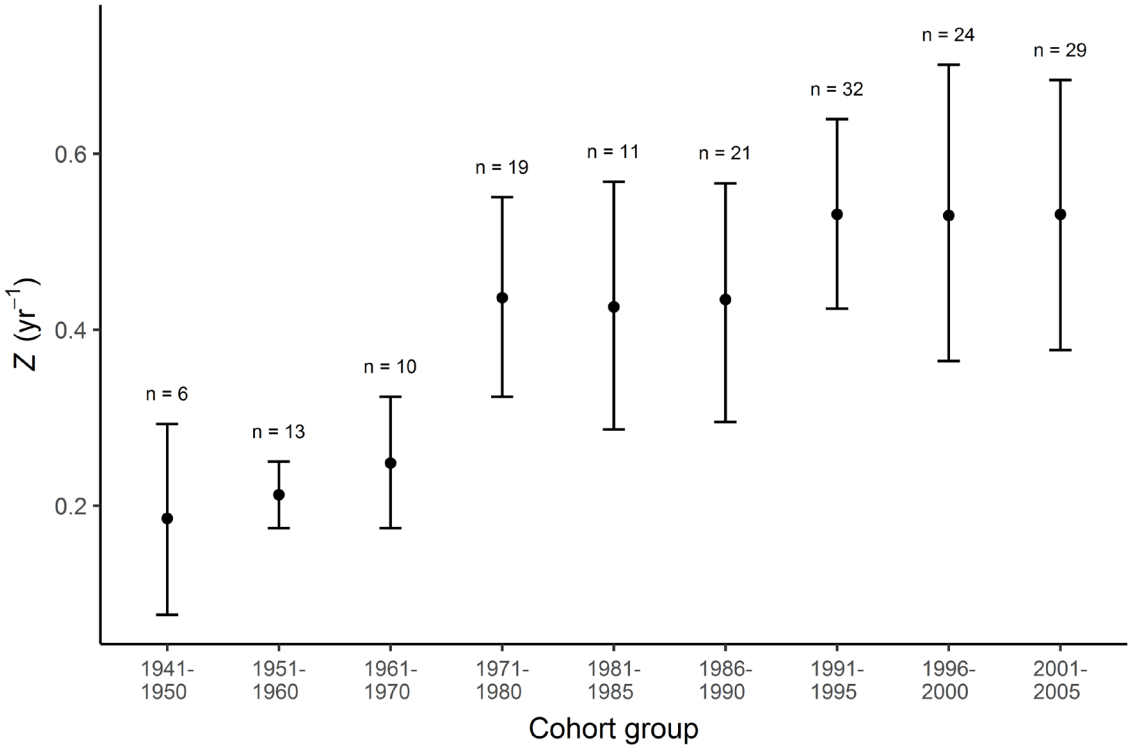

Figure A4.13 Mean cohort group-level estimates of mortality rate (Z, yr^{-1}; generated using eq. 1 in Chapter 5) generated from both trustworthy and untrustworthy Lester model fits to back-calculated Gulf of Mexico red snapper *Lutjanus campechanus* growth data for cohorts from 1941-2005. Points represent mean estimates of mortality rate for each cohort group, and error bars indicate 95% Bayesian credible intervals. Sample sizes for each group are displayed above the error bars.

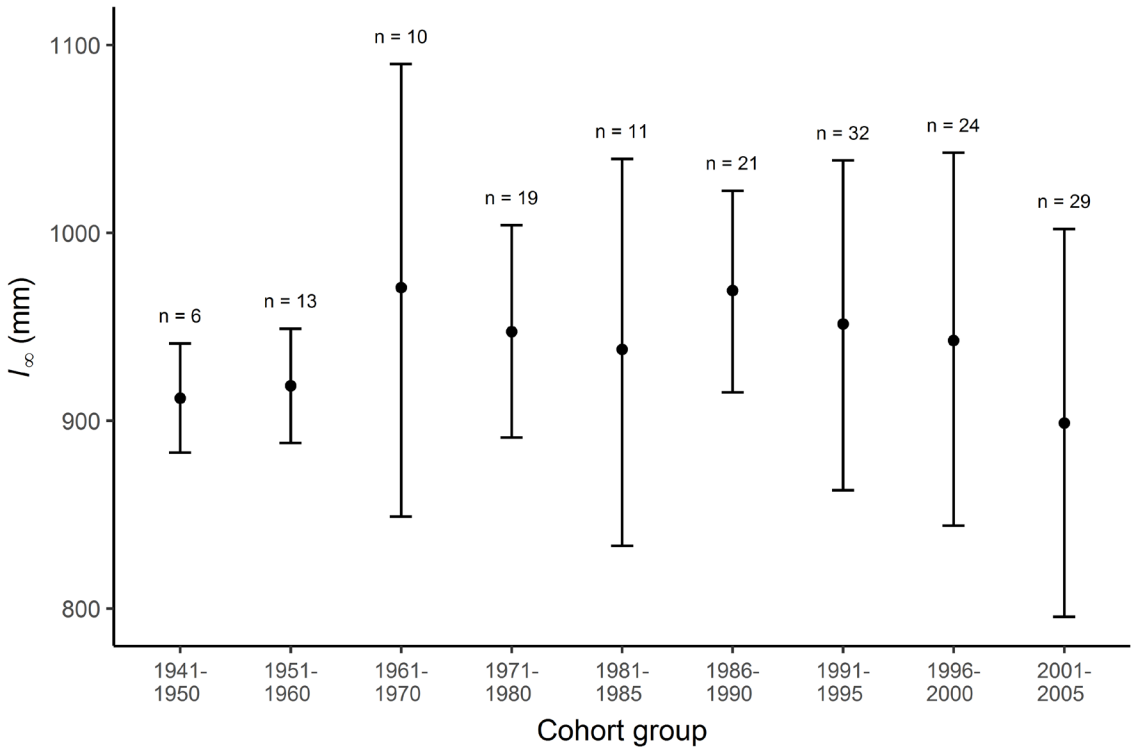

Figure A4.14 Mean cohort group-level estimates of asymptotic length (l_∞; mm) generated from both trustworthy and untrustworthy Lester model fits to back-calculated Gulf of Mexico red snapper *Lutjanus campechanus* growth data for cohorts from 1941-2005. Points represent mean estimates of asymptotic length for each cohort group, and error bars indicate 95% Bayesian credible intervals. Sample sizes for each group are displayed above the error bars.

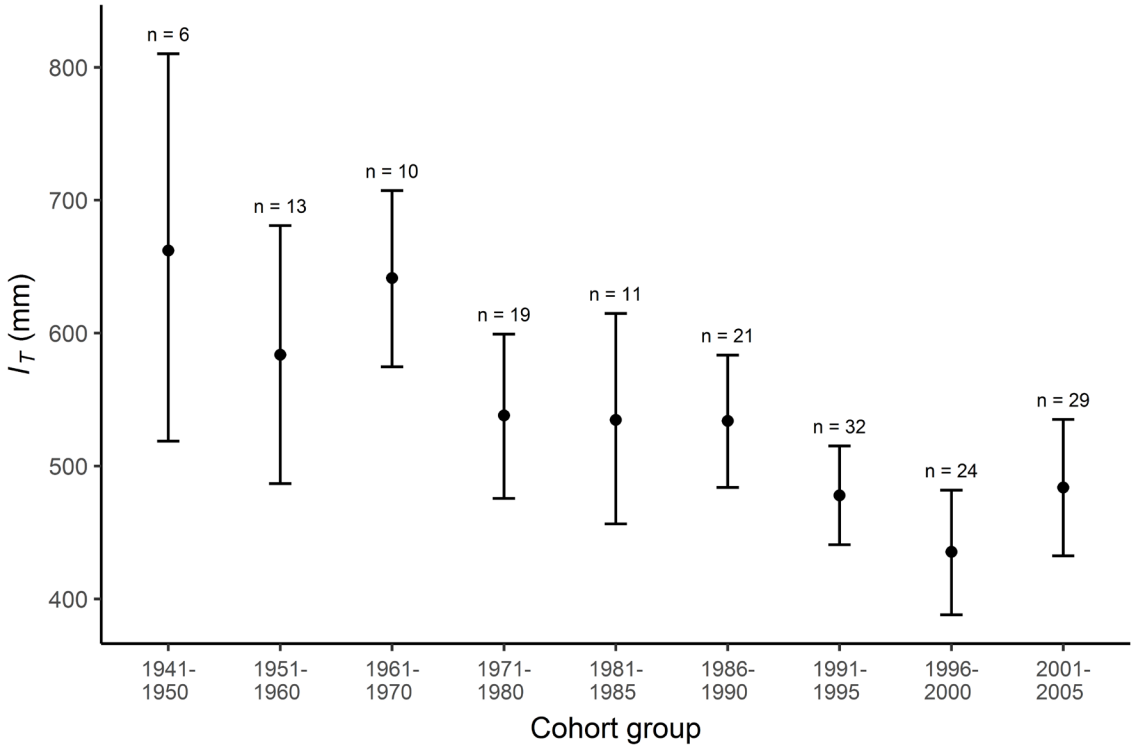

Figure A4.15 Mean cohort group-level estimates of length-at-maturity (l_T; mm) generated from both trustworthy and untrustworthy Lester model fits to back-calculated Gulf of Mexico red snapper *Lutjanus campechanus* growth data for cohorts from 1941-2005. Points represent mean estimates of length-at-maturity for each cohort group, and error bars indicate 95% Bayesian credible intervals. Sample sizes for each group are displayed above the error bars.

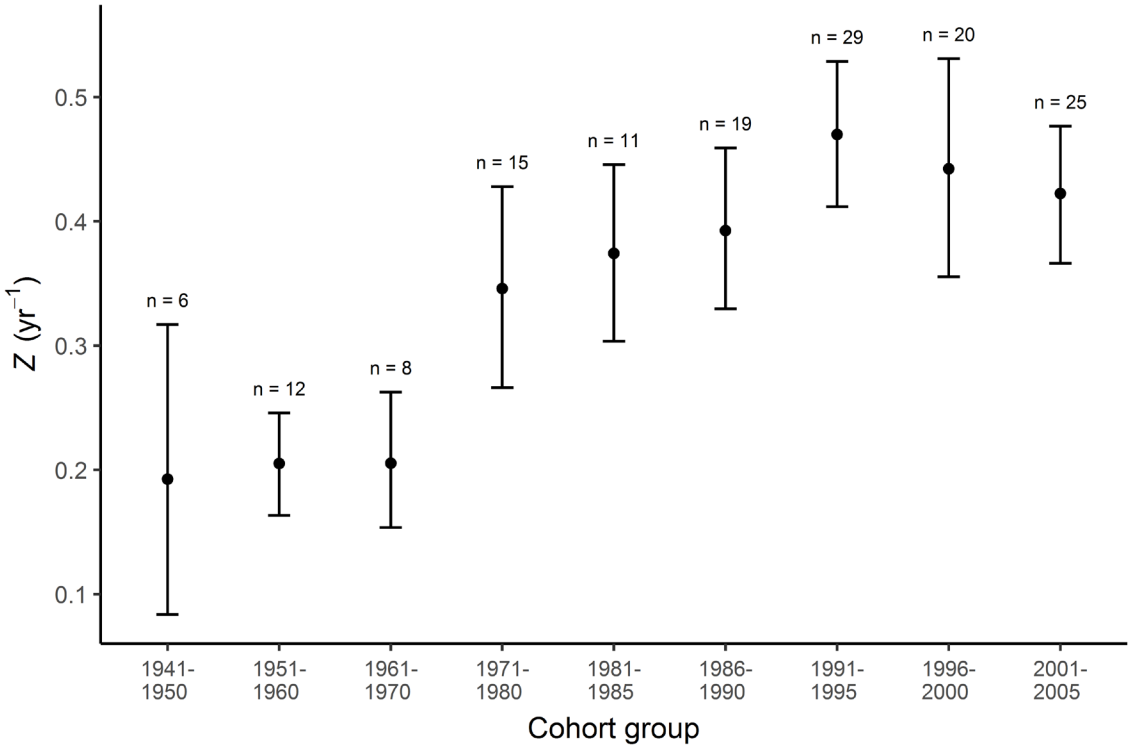

Figure A4.16 Mean cohort group-level estimates of instantaneous total mortality rate (*Z*, yr^{-1}; calculated using eq. 2 in Chapter 5) generated from Lester model fits to back-calculated Gulf of Mexico red snapper *Lutjanus campechanus* growth data for cohorts from 1941-2005. Points represent mean estimates of mortality rate for each cohort group, and error bars indicate 95% Bayesian credible intervals. Sample sizes (i.e., number of individuals) for each cohort group are displayed above the error bars.

Table A4.2 Parameter estimates from linear regressions of sea surface degree-days above 0, 5, and 10 °C (DD_0, DD_5, and DD_{10}, respectively) versus Lester model-based life history trait estimates. Bayesian 95% credible interval bounds are given in parentheses. Total mortality rate (Z) was estimated using equation 1 in Chapter 5.

Trait	Parameter	DD_0	DD_5	DD_{10}
Age-at-maturity (T)	slope	$1.61 \cdot 10^{-2}$ ($1.81 \cdot 10^{-3}$, $3.06 \cdot 10^{-2}$)	$1.63 \cdot 10^{-2}$ ($1.77 \cdot 10^{-3}$, $3.05 \cdot 10^{-2}$)	$1.58 \cdot 10^{-2}$ ($1.98 \cdot 10^{-3}$, $2.96 \cdot 10^{-2}$)
	intercept	-140.70 (-270.97, -12.03)	-112.43 (-214.85, -8.15)	-80.26 (-154.13, -6.06)
Juvenile growth rate (h)	slope	-0.28 (-0.50, -0.07)	-0.28 (-0.50, -0.05)	-0.28 (-0.50, -0.06)
	intercept	2643.79 (701.32, 4584.01)	2131.17 (486.26, 3752.15)	1588.33 (447.41, 2772.50)
Reproductive investment (g)	slope	$-9.34 \cdot 10^{-4}$ ($-1.94 \cdot 10^{-3}$, $6.62 \cdot 10^{-5}$)	$-9.20 \cdot 10^{-4}$ ($-1.92 \cdot 10^{-3}$, $1.24 \cdot 10^{-4}$)	$-9.29 \cdot 10^{-4}$ ($-1.90 \cdot 10^{-3}$, $2.70 \cdot 10^{-5}$)
	intercept	8.76 (-0.23, 17.81)	6.96 (-0.58, 14.14)	5.33 (0.22, 10.55)
Adult growth rate (k)	slope	$-2.81 \cdot 10^{-4}$ ($-5.55 \cdot 10^{-4}$, $-1.80 \cdot 10^{-6}$)	$-2.81 \cdot 10^{-4}$ ($-5.49 \cdot 10^{-4}$, $-1.00 \cdot 10^{-5}$)	$-2.79 \cdot 10^{-4}$ ($-5.56 \cdot 10^{-4}$, $-5.78 \cdot 10^{-6}$)
	intercept	2.64 (0.13, 5.11)	2.13 (0.19, 4.06)	1.60 (0.14, 3.09)
Mortality rate (Z)	slope	$-1.22 \cdot 10^{-3}$ ($-2.57 \cdot 10^{-3}$, $1.86 \cdot 10^{-4}$)	$-1.25 \cdot 10^{-3}$ ($-2.75 \cdot 10^{-3}$, $1.95 \cdot 10^{-4}$)	$-1.20 \cdot 10^{-3}$ ($-2.57 \cdot 10^{-3}$, $2.30 \cdot 10^{-4}$)
	intercept	11.34 (-1.30, 23.56)	9.35 (-1.01, 20.18)	6.81 (-0.83, 14.12)
Asymptotic length (l_∞)	slope	-0.12 (-0.61, 0.35)	-0.12 (-0.61, 0.37)	-0.11 (-0.57, 0.35)
	intercept	2052.89 (-2251.47, 6411.71)	1779.27 (-1730.21, 5285.60)	1516.89 (-970.21, 3963.78)
Length-at-maturity (l_T)	slope	0.50 (-0.20, 1.19)	0.51 (-0.17, 1.20)	0.48 (-0.21, 1.17)
	intercept	-3914.01 (-10175.30, 2335.29)	-3081.30 (-8084.25, 1780.15)	-2021.74 (-5688.91, 1680.50)

A4.5 Comparison of life history trait estimates between females and individuals of unknown sex

We were interested in examining whether life history trait estimates for known red snapper *Lutjanus campechanus* females differed from those for individuals of unknown sex. To do this, we calculated mean life history trait estimates separately for females and unknown sex individuals for the only two cohort groups that had > 3 individuals of each sex classification (1981-1985 and 1996-2000). We used a frequentist (i.e., conventional) approach to calculate means, and we calculated 95% confidence intervals as follows:

$$\mu \pm 1.96 \cdot SE,$$

where μ is the sex-specific group-level mean for a given life history parameter and SE is the standard error of the mean. Our results show that the 95% confidence intervals overlap for all comparisons of life history traits between females and unknowns, apart from one case: l_∞ was slightly higher, on average, for females than for unknowns in 1981-1985 (Table A4.3). This result was likely influenced by one individual in the unknown sex category with an abnormally low l_∞ value (735.57 mm). As a whole, these results suggest that life history trait estimates for females do not consistently significantly differ from those for unknown sex individuals; however, these conclusions are based on low sample sizes. Future work should explore the potential for differences in life history traits between females and individuals of unknown sex more fully, preferably with increased sample sizes.

Table A4.3 Mean (+/- 95% confidence intervals) estimates of Lester-model based life history traits for red snapper *Lutjanus campechanus* females versus individuals of unknown sex for the 1981-1985 and 1996-2000 cohort groups. See Chapter 5 and Appendix 4, Section A4.5 for details. The asterisk (*) indicates the comparison for which 95% confidence intervals did not overlap.

	1981-1985		1996-2000	
Trait	**Female (n = 4)**	**Unknown (n = 7)**	**Female (n = 5)**	**Unknown (n = 15)**
Age-at-maturity (T)	3.52 (3.03, 4.00)	3.59 (2.14, 5.03)	3.35 (2.15, 4.56)	2.81 (2.27, 3.35)
Juvenile growth rate (h)	126.87 (114.65, 139.09)	115.90 (88.62, 143.17)	104.99 (69.69, 140.28)	127.47 (106.84, 148.09)
Reproductive investment (g)	0.35 (0.34, 0.36)	0.42 (0.30, 0.54)	0.39 (0.10, 0.68)	0.45 (0.35, 0.54)
Adult growth rate (k)	0.11 (0.10, 0.12)	0.13 (0.09, 0.17)	0.12 (0.04, 0.20)	0.14 (0.11, 0.16)
Mortality rate (Z)	0.36 (0.34, 0.37)	0.46 (0.28, 0.64)	0.54 (-0.06, 1.14)	0.51 (0.37, 0.66)
Asymptotic length (l_∞)	1079.02 (1003.96, 1154.08)*	858.55 (781.02, 936.08)*	981.81 (719.75, 1243.86)	909.51 (796.91, 1022.11)
Length-at-maturity (l_T)	590.84 (543.87, 637.80)	502.37 (407.98, 596.77)	498.95 (384.65, 613.25)	438.32 (389.53, 487.12)